# POWER SYSTEMS DEVELOPMENT FACILITY

## TECHNICAL PROGRESS REPORT FOR KELLOGG BROWN & ROOT TRANSPORT REACTOR TRAIN WITH SIEMENS WESTINGHOUSE PARTICULATE CONTROL DEVICE

## **TC03 REPORT: MAY 31 – AUGUST 10, 1998**

DOE Cooperative Agreement Number
DE-FC21-90MC25140

Prepared by:
Southern Company Services, Inc.
Power Systems Development Facility
P.O. Box 1069
Wilsonville, AL 35186

September 1999

DISCLAIMER

This report was prepared as an account of work sponsored by an agency of the United States Government. Neither the United States Government nor any agency thereof, nor any of their employees, nor Southern Company Services, Inc., nor any of its employees, nor any of its subcontractors, makes any warranty, expressed or implied, or assumes any legal liability or responsibility for the accuracy, completeness, or usefulness of any information, apparatus, product, or process disclosed, or represents that its use would not infringe privately owned rights. Reference herein to any specific commercial product, process, or service by trade name, trademark, manufacturer or otherwise, does not necessarily constitute or imply its endorsement, recommendation, or favoring by the United States Government or any agency thereof. The views and opinions of authors expressed herein do not necessarily state or reflect those of the United States Government or any agency thereof.

Available to the public from the National Technical Information Service, U.S. Department of Commerce, 5285 Port Royal Road, Springfield, VA 22161. Phone orders accepted at (703) 487-4650.

# CONTENTS

Section Page

Inside Cover
Disclaimer

Listing of Tables and Figures ..... iv

1.0 EXECUTIVE SUMMARY ..... 1.1-1

1.1 Operation Status ..... 1.1-1
1.1.1 Transport Reactor ..... 1.1-3
1.1.2 Siemens Westinghouse PCD ..... 1.1-4

1.2 PSDF Accomplishments During TC03 ..... 1.2-1
1.2.1 Transport Reactor Train ..... 1.2-1
1.2.2 PCD-Related Systems ..... 1.2-2

1.3 Future Plans ..... 1.3-1

2.0 INTRODUCTION ..... 2.1-1

2.1 The Power Systems Development Facility ..... 2.1-2
2.2 Transport Reactor System Description ..... 2.2-1
2.3 Siemens Westinghouse Particulate Control Device ..... 2.3-1

3.0 PARTICLE FILTER SYSTEM ..... 3.1-1

3.1 PCD Overview ..... 3.1-1
3.1.1 Summary ..... 3.1-1
3.1.2 TC03 Accomplishments ..... 3.1-1
3.1.3 Developmental Areas ..... 3.1-2
3.1.4 Future Plans ..... 3.1-3

3.2 PCD Operation During Test Run TC03 ..... 3.2-1
3.2.1 Run Summary ..... 3.2-1
3.2.2 Test Objectives ..... 3.2-1
3.2.3 Observations/Events ..... 3.2-1
3.2.4 Run Outcome ..... 3.2-2

3.3 TC03 Inspection Report ..... 3.3-1
3.3.1 Summary ..... 3.3-1
3.3.2 PCD Inspection and Dustcake Observations ..... 3.3-1
3.3.3 Inspection Outcome ..... 3.3-2

3.4 TC03 Ash Characteristics and PCD Performance ..... 3.4-1
3.4.1 Measurements of Particulate Mass Loadings ..... 3.4-1
3.4.2 PCD Cut-Size Tests ..... 3.4-3
3.4.3 Chemical Analyses ..... 3.4-5
3.4.4 Measurements of Physical Properties ..... 3.4-8

4.0 TRANSPORT REACTOR LOOP ..... 4.1-1

4.1 TC03 Run Summary ..... 4.1-1

4.2 Heat and Material Balance ..... 4.2-1

4.3 $SO_2$, $SO_3$, and Solids Analyses ..... 4.3-1

4.4 $NO_X$ Emissions ..... 4.4-1

4.5 TC03 Temperature Profile ..... 4.5-1

TERMS ..... PSDF Terms-1

Listing of Tables

Table Page

2.2-1 Major Equipment in the Transport Reactor Train....2.2-3
2.2-2 Major Equipment in the Balance-of-Plant .... 2.2-4

3.2-1 TC03 Run Statistics ....3.2-4
3.2-2 TC03 Major Events ....3.2-5

3.4-1 Summary of Inlet Particulate Loadings Measured During TC03 .... 3.4-13
3.4-2 Summary of Outlet Particulate Loadings Measured During TC03 .... 3.4-14
3.4-3 PCD Particulate Collection Efficiencies for TC03 .... 3.4-14
3.4-4 Chemical Composition of TC03 In situ Samples.... 3.4-15
3.4-5 Chemical Composition of TC03 Hopper Samples .... 3.4-16
3.4-6 Chemical Composition of Dustcake Samples Collected After TC03 .... 3.4-17
3.4-7 Physical Properties of TC03 In situ Samples.... 3.4-18
3.4-8 Physical Properties of TC03 Hopper Samples .... 3.4-19
3.4-9 Physical Properties of Dustcake Samples Collected After TC03.... 3.4-20

4.1-1 TC03 Operating Conditions....4.1-5
4.1-2 Coal Analyses....4.1-5
4.1-3 Sorbent Analyses....4.1-6

4.2-1 Average Reactor Conditions ....4.2-2
4.2-2 Bulk Material Balance....4.2-2
4.2-3 Elemental Material Balances....4.2-2

4.3-1 TC03 Sorbent Compositions....4.3-9
4.3-2 TC03 $SO_2$ and $SO_3$ Data....4.3-9
4.3-3 TC03 $SO_2$ and $SO_3$ Results .... 4.3-10

4.4-1 Reactor Operating Conditions....4.4-4

Listing of Figures

Figure Page

2.2-1 Flow Diagram of the Transport Reactor Train in Combustion Mode of Operation ..... 2.2-7

2.3-1 Siemens Westinghouse PCD ..... 2.3-2

3.2-1 Filter Element Layout for TC03 (Layout No. 9) ..... 3.2-6
3.2-2 TC03 Temperature and Pressure for May 31 Through June 7 ..... 3.2-7
3.2-3 TC03 Back-Pulse Pressure and Face Velocity for May 31 Through June 7 ..... 3.2-8
3.2-4 TC03 Pressure Drop and Permeance for May 31 Through June 7 ..... 3.2-9
3.2-5 TC03 Temperature and Pressure for June 7 Through June 14 ..... 3.2-10
3.2-6 TC03 Back-Pulse Pressure and Face Velocity for June 7 Through June 14 ..... 3.2-11
3.2-7 TC03 Pressure Drop and Permeance for June 7 Through June 14 ..... 3.2-12
3.2-8 TC03 Temperature and Pressure for June 14 Through June 21 ..... 3.2-13
3.2-9 TC03 Back-Pulse Pressure and Face Velocity for June 14 Through June 21 ..... 3.2-14
3.2-10 TC03 Pressure Drop and Permeance for June 14 Through June 21 ..... 3.2-15
3.2-11 TC03 Temperature and Pressure for July 11 Through July 17 ..... 3.2-16
3.2-12 TC03 Back-Pulse Pressure and Face Velocity for July 11 Through July 17 ..... 3.2-17
3.2-13 TC03 Pressure Drop and Permeance for July 11 Through July 17 ..... 3.2-18
3.2-14 TC03 Temperature and Pressure for July 23 Through July 30 ..... 3.2-19
3.2-15 TC03 Back-Pulse Pressure and Face Velocity for July 23 Through July 30 ..... 3.2-20
3.2-16 TC03 Pressure Drop and Permeance for July 23 Through July 30 ..... 3.2-21
3.2-17 TC03 Temperature and Pressure for July 30 Through August 5 ..... 3.2-22
3.2-18 TC03 Back-Pulse Pressure and Face Velocity for July 30 Through August 5 ..... 3.2-23
3.2-19 TC03 Pressure Drop and Permeance for July 30 Through August 5 ..... 3.2-24
3.2-20 TC03 Temperature and Pressure for August 5 Through August 11 ..... 3.2-25
3.2-21 TC03 Back-Pulse Pressure and Face Velocity for August 5 Through August 11 ..... 3.2-26
3.2-22 TC03 Pressure Drop and Permeance for August 5 Through August 11 ..... 3.2-27

3.3-1 Failed Liner Support ..... 3.3-3
3.3-2 Shroud Touching Vessel Liner ..... 3.3-3
3.3-3 Distortion of the Shroud ..... 3.3-4
3.3-4 Upward Cone Liner Growth ..... 3.3-4
3.3-5 Notches in the Shroud ..... 3.3-5
3.3-6 Liner Distortion Near Inlet ..... 3.3-5
3.3-7 Cracked Pulse Pipe ..... 3.3-6

3.3-8 Bottom Plenum After Removal From PCD ..... 3.3-7
3.3-9 Thermocouples on Elements ..... 3.3-8
3.3-10 Installed Blank in Top Plenum ..... 3.3-9
3.3-11 2-Meter Pall 326 Elements (Left) and 3M Oxide Elements (Right) ..... 3.3-10
3.3-12 Element Layout 10 for TC04 ..... 3.3-11

3.4-1 Particle-Size Distributions of Inlet Particulate and Ash Dropout Samples Collected During TC03 Cut-Size Test ..... 3.4-21
3.4-2 Particulate Dropout in PCD as a Function of Particle Size ..... 3.4-22
3.4-3 Drag-Equivalent Diameter Versus BET Surface Area for TC03 In situ Particulate Samples ..... 3.4-23
3.4-4 Drag-Equivalent Diameter Versus BET Surface Area for All TC03 In situ Particulate Samples and Hopper Samples ..... 3.4-24
3.4-5 Drag-Equivalent Diameter Versus Calcium Content of all TC03 In situ Particulate and Hopper Samples ..... 3.4-25
3.4-6 Drag-Equivalent Diameter Versus Calcium Content of all TC03 and TC01 In situ Particulate Samples ..... 3.4-26
3.4-7 Lab-Measured Drag Versus Drag Calculated From Transient Pressure Drop Across PCD ..... 3.4-27

4.1-1 CO0201 System Profile ..... 4.1-7
4.1-2 Start-up Burner Flow/Temperature ..... 4.1-7
4.1-3 System Pressures Downstream of PCD ..... 4.1-7
4.1-4 Total Gas In/Out Flow Rates ..... 4.1-8
4.1-5 Reactor Mixing Zone and Riser Temperature ..... 4.1-8
4.1-6 Standpipe Temperatures ..... 4.1-8
4.1-7 Cyclone Dipleg Temperatures ..... 4.1-9
4.1-8 Temperature Profiles Downstream of Reactor ..... 4.1-9
4.1-9 Reactor Pressure/Riser Differential Pressure Profiles ..... 4.1-9
4.1-10 Standpipe Differential Pressure Profiles ..... 4.1-10
4.1-11 CY0201 Dipleg Differential Pressure Profiles ..... 4.1-10
4.1-12 Coal Feed Rate Based on Gas Analysis ..... 4.1-10
4.1-13 CO0201 System ..... 4.1-11
4.1-14 Start-up Burner Flow/Temperature ..... 4.1-11
4.1-15 System Pressures Downstream of PCD ..... 4.1-11
4.1-16 Total Gas In/Out Flow Rates ..... 4.1-12
4.1-17 Reactor Mixing Zone and Riser Temperature ..... 4.1-12
4.1-18 Standpipe Temperatures ..... 4.1-12
4.1-19 Cyclone Dipleg Temperatures ..... 4.1-13
4.1-20 Temperature Profiles Downstream of Reactor ..... 4.1-13
4.1-21 Reactor Pressure/Riser Differential Pressure Profiles ..... 4.1-13
4.1-22 Standpipe Differential Pressure Profiles ..... 4.1-14
4.1-23 CY0201 Dipleg Differential Pressure Profiles ..... 4.1-14
4.1-24 Coal Feed Rate Based on Gas Analysis ..... 4.1-14

4.3-1 TC03 System Pressure, Standpipe Temperature ....4.3-11
4.3-2 TC03 System Pressure, Standpipe Temperature ....4.3-11
4.3-3 TC03 Coal Feed and $SO_2$ Emissions ....4.3-12
4.3-4 TC03 Coal Feed and $SO_2$ Emissions ....4.3-12
4.3-5 TC03 Coal Sulfur and Ash Contents ....4.3-13
4.3-6 TC03 Coal Sulfur and Ash Contents ....4.3-13
4.3-7 TC03 Coal and Sorbent Particle Size ....4.3-14
4.3-8 TC03 Coal and Sorbent Particle Size ....4.3-14
4.3-9 TC03 Coal and Sorbent Sieve Particle-Size Distribution ....4.3-15
4.3-10 TC03 Sorbent Microtrac Particle-Size Distribution ....4.3-15
4.3-11 TC03 Sorbent $CaCO_3$ and $MgCO_3$ Contents ....4.3-16
4.3-12 TC03 Limestone $CaCO_3$ and $MgCO_3$ Contents ....4.3-16
4.3-13 TC03 PCD Solids Ca/S, Feeds Ca/S, and $SO_2$ Emissions ....4.3-17
4.3-14 TC03 PCD Solids Ca/S, Feeds Ca/S, and $SO_2$ Emissions ....4.3-17
4.3-15 TC03 PCD Solids Ca/S, Feeds Ca/S, and Reactor Solids Ca/S ....4.3-18
4.3-16 TC03 PCD Solids Ca/S, Feeds Ca/S, and Reactor Solids Ca/S ....4.3-18
4.3-17 TC03 PCD and Reactor Particle Sizes ....4.3-19
4.3-18 TC03 PCD and Reactor Particle Sizes ....4.3-19
4.3-19 TC03 Reactor Solids Particle-Size Distribution ....4.3-20
4.3-20 TC03 PCD Solids Particle-Size Distribution ....4.3-20
4.3-21 TC03 PCD and Reactor $CaCO_3$ and $CaSO_4$ Contents ....4.3-21
4.3-22 TC03 PCD and Reactor $CaCO_3$ and $CaSO_4$ Contents ....4.3-21
4.3-23 TC03 PCD and Reactor CaO, CaO•MgO, and MgO Contents ....4.3-22
4.3-24 TC03 PCD and Reactor CaO, CaO•MgO, and MgO Contents ....4.3-22
4.3-25 TC03 PCD and Reactor Inerts Contents ....4.3-23
4.3-26 TC03 PCD and Reactor Inerts Contents ....4.3-23
4.3-27 TC03 PCD and Reactor Unburned Carbon ....4.3-24
4.3-28 TC03 PCD and Reactor Unburned Carbon ....4.3-24
4.3-29 TC03 $SO_2$ Emission and PCD Pressure Drop - August 1, 1998 ....4.3-25
4.3-30 TC03 $SO_3$ Testing, Limestone Off - July 30, 1998 ....4.3-25
4.3-31 TC03 Transition From Ohio to Alabama Limestone - August 3, 1998 ....4.3-26
4.3-32 TC03 Transition From Alabama to Florida Limestone - August 6, 1998 ....4.3-26
4.3-33 TC02 and TC03 $SO_2$-$SO_3$ Equilibrium ....4.3-27

4.4-1 Transport Reactor Train Loop Schematic ....4.4-6
4.4-2 Effect of Different Coal Feeds on $NO_X$ Emissions ....4.4-7
4.4-3 Effect of Different Sorbents on $NO_X$ Emissions ....4.4-7
4.4-4 Effect of Increasing Coal Feed Rate on $NO_X$ Emissions (Data Set G) ....4.4-8
4.4-5 Effect of Reactor Temperature on $NO_X$ Emissions ....4.4-8
4.4-6 Effect of Coal Feed System Cycles on $NO_X$ Emissions (Data Set H) ....4.4-9
4.4-7 Effect of Bucyrus Limestone Feed Rate on $NO_X$ Emissions ....4.4-9
4.4-8 Effect of Longview Limestone Feed Rate on $NO_X$ Emissions ....4.4-10
4.4-9 Effect of Florida Limestone Feed Rate on $NO_X$ Emissions ....4.4-10

4.4-10 Response Time of $NO_X$ Emissions to Increasing Dolomite Feed Rate (Data Set O) ..... 4.4-11
4.4-11 Response Time of $NO_X$ Emissions to Decreasing Bucyrus Limestone Feed Rate and Effect of Sorbent "Blow-Through" on $NO_X$ Emissions (Data Set P) ..... 4.4-11

4.5-1 Mixing Zone Temperature Profile ..... 4.5-2
4.5-2 Standpipe, Dipleg, and HX0203 Temperature Profile ..... 4.5-2
4.5-3 Riser Temperature Profile ..... 4.5-3

# 1.0 EXECUTIVE SUMMARY

## 1.1 OPERATION STATUS

This report discusses test campaign TC03 of the Kellogg Brown & Root transport reactor train with a Siemens Westinghouse Power Corporation (Siemens Westinghouse) particle filter system at the Power Systems Development Facility (PSDF) located in Wilsonville, Alabama. The transport reactor is an advanced circulating fluidized-bed reactor designed to operate as either a combustor or a gasifier using one of two possible particulate control devices (PCDs). The transport reactor was operated as a pressurized combustor during TC03.

The objectives of the PSDF are to:

1. Develop advanced coal-fired power generation technologies through testing and evaluation of hot gas clean-up systems and other major components at the pilot scale.

2. Assess and demonstrate the performance of the components in an integrated mode of operation.

The primary focus of the PSDF project is to demonstrate and evaluate high-temperature PCDs that are the single most important component required for successful development of advanced power generation systems. High-temperature PCDs are a common component of advanced gasification and advanced pressurized fluidized-bed combustion (APFBC) technologies, both of which will be evaluated at the facility. The facility is sized to test the components at capacities that are readily scaleable to commercial systems.

Commissioning activities began in September 1995 and proceeded in parallel with construction activities. Construction of the transport reactor and associated equipment was completed in early summer of 1996. All separate components and subsystems were fully operational by midsummer and commissioning work was focused on integration issues for the entire transport reactor train. The first coal fire was achieved on August 18, 1996. A series of characterization tests was initiated to develop an understanding of reactor system operations.

Test runs CCT1, CCT2, and CCT3 were completed by December 1996. Solids carryover from the reactor to the PCD was found to be excessive during these test runs. A number of start-up and design problems associated with various equipment were successfully addressed.

During 1997, three additional sets of characterization test runs, CCT4, CCT5, and CCT6, and one major test campaign, TC01, were undertaken. The major accomplishments in 1997 included the following:

- Operating the Siemens Westinghouse PCD for over 1,200 hours on coal in combustion mode without ash bridging at PCD inlet temperatures between 1,350 and 1,400°F.

- Demonstrating stable reactor operations by successfully addressing the excessive solids carryover problem.

- Achieving over 1,980 hours on coal and approximately 2,600 hours of solids circulation in 1997.

- Achieving nearly 100-percent on-line availability during the last 12 days of test run TC01.

Excluding the outages caused by the inherent testing nature of the transport reactor and PCD, the on-line availability (based on coal) for the entire TC01 test run was about 71 percent. The major bottleneck for sustained high on-line availability was the unreliability of the coal feed and fine ash removal systems. During the second half of the TC01 test run, modifications were made to the fine ash removal system that significantly increased its availability. Also, modifications made to the coal feed system improved its availability to nearly 100 percent in the last 2 weeks of the test run.

With these achievements, TC02 was planned for reactor parametric testing to better quantify the effect of different variables on reactor operation. Test run TC02 was begun on April 5, 1998, and completed on May 11, 1998. The major accomplishments and observations during TC02 included the following:

1. Higher temperatures were achieved with the start-up burner before feeding coal. The start-up burner firing, originally designed for 3.6 MBtu/hr, was increased to 7.5 MBtu/hr, which resulted in a PCD inlet starting temperature of 920°F and a reactor starting temperature of 1,200 °F.

2. Test run TC02 included the longest continuous trouble-free operations (298 hours). A total of 559 hours on coal feed was accumulated during this run. Through test run TC02, the PSDF had achieved over 2,760 hours of operation on coal feed and about 3,950 hours of solids circulation.

3. Coal feed system modifications were effective and the system operated reliably over a longer period of time.

4. The Siemens Westinghouse PCD operated without ash bridging, with a coal/sorbent combination at PCD inlet temperatures over 1,350°F.

5. Monitoring and controlling ash level in the PCD continued to be successful.

6. The pulse valves supplied with the PCD were modified and the modifications were proven successful.

7. The 3M Company resolved the issue of dust leaking around the 3M elements, an issue due to the filter vessel supplied gasketing scheme, by designing a ceramic insert to allow use of the “standard” gasketing scheme.

Based on TC02 findings, TC03 was planned for additional reactor parametric testing to better quantify the effect of different variables on reactor operation and to evaluate different feedstocks. Test run TC03 was begun on May 31, 1998, and completed on August 10, 1998. The major accomplishments and observations during TC03 included the following:

1. Stable operations were demonstrated using the Eastern Kentucky coal and Plum Run dolomite, Bucyrus limestone, and Longview limestone. There were, however, circulation problems using the Eastern Kentucky coal and Florida Gregg Mine limestone.

2. Test run TC03 included the longest continuous trouble-free operations without any interruption from the coal feed system or any other subsystem (382 hours) to date. A total of 795 hours on coal feed was accumulated during this run. To date, PSDF has achieved over 3,556 hours of operation on coal feed and about 4,840 hours of solids circulation.

3. Nearly 100-percent carbon conversion for Eastern Kentucky coal at 1,500°F reactor temperature was achieved.

4. There was not much observable difference using the Eastern Kentucky coal with limestone or dolomite for sulfur capture.

5. The Siemens Westinghouse PCD was operated for almost 800 hours on coal in combustion without ash bridging and with outlet loadings below 1 ppm.

6. Two coals and four sorbents were used and demonstrated no negative effects on PCD operation.

7. PSDF has successfully demonstrated the operation of the PCD with the design coal and sorbent for the Lakeland CCT project.

8. By the end of TC03, several monolithic silicon carbide filter elements had accumulated over 3,200 hours of exposure. Additionally, the composite filter elements installed in early 1998 had accumulated over 1,350 hours of exposure.

### 1.1.1 Transport Reactor

TC03 was planned as a 500-hour test run for reactor parametric testing to better quantify the effect of different variables on reactor operation and to test different feedstocks. The objectives of test run TC03 for the transport reactor were:

- *Demonstrate stable reactor operations with different feeds.* Demonstrate stable reactor operations using Eastern Kentucky coal with Plum Run dolomite, Bucyrus limestone, Longview limestone, and Gregg Mine limestone.

- *Evaluate effects of reactor conditions on $NO_x$ emissions.* Vary Ca/S molar ratio, excess air, coal feed rate, and operation temperature.

- *Evaluate effects of reactor conditions on $SO_2$ emissions.* Vary Ca/S molar ratio, solids inventory, and operation temperature.

- *Investigate the effects of increasing the mixing zone density.* Decrease various aeration flows and increase solids inventory.

Overall, this test run was successful; however there were circulation problems when using the Eastern Kentucky coal and the Gregg Mine limestone from Florida. A total of 890 hours of solid circulation and 795 hours of coal feed were attained in TC03.

In addition to improved reactor operations, there were several notable findings concerning the $SO_x$ and $NO_x$ emissions. A high-sulfur capture, greater than 97 percent, was achieved using Bucyrus limestone at a Ca/S molar ratio of 1.6. It was observed that immediately after a back-pulse the $SO_2$ increased from 5 to 35 ppm, then gradually decreased back to 5 ppm within 20 to 30 minutes. In most instances, the separate effect of each back-pulse on $SO_2$ was detectable. The $NO_x$ emissions were as low as 0.04 lb/MBtu and varied up to 0.55 lb/MBtu when excess sorbent was added to the system as bed material. The $NO_x$ emissions from the Eastern Kentucky coal and Alabama coal were generally similar, with the $NO_x$ emissions from the Eastern Kentucky coal being lower at times than the Alabama coal. The $NO_x$ emissions with the Florida and Longview limestone were close, ranging from 0.1 to 0.14 lb/MBtu and were slightly higher than the $NO_x$ emissions with the Bucyrus limestone, which ranged from 0.07 to 0.1 lb/MBtu. In addition, it was observed that there was a significant increase in $NO_x$ emissions when sorbent was added to the system for all sorbent types. For example, with Bucyrus limestone, the $NO_x$ emissions increased by 40 percent as the Ca/S molar ratio was increased from 0 to 1.0. Mixing zone operations under both highly reducing and highly oxidizing conditions showed no perceptible change in $NO_x$ formation or $SO_2$ capture. Analysis of both $SO_x$ and $NO_x$ emissions is covered further in sections 4.3 and 4.4, respectively.

### 1.1.2 Siemens Westinghouse PCD

The Siemens Westinghouse particulate control device (PCD) operated for almost 800 hours on coal in TC03. The run was uneventful for the PCD, with no failures or problems during the full length of the run. Two coal types and four types of sorbent were used during the run. Specifically, Eastern Kentucky coal and Gregg limestone, both slated for the Lakeland clean coal technology project, were proven viable. Particulate loadings to the PCD varied significantly during the run, however, no conclusive prediction method for loading, based on the sorbent/coal type was determined. PCD performance was unaffected by varying coal or sorbent.

Southern Research Institute's (SRI) particulate collection system continued to operate reliably. Outlet particulate loadings remained below 0.37 ppmw for the full duration of TC03, maintaining collection efficiencies of 99.9935 percent or greater.

The PCD and auxiliary systems continued to perform well during operation in TC03. No downtime was attributed to the ash removal systems. The newly designed seal material

functioned flawlessly. Problems with the fine ash screw cooler, however, continued to require attention during TC03. Leaking shaft rider seals required additional monitoring by plant personnel. Operation staff continued to monitor ash level in the PCD with success. Rising ash levels became an issue for concern several times during the run, but at no time did the ash level approach the filter elements.

## 1.2 PSDF ACCOMPLISHMENTS DURING TC03

The following information summarizes major accomplishments during the TC03 test run that resulted in improved equipment and process design, higher availability, improved process performance, or better understanding of the transport reactor and PCD operations.

### 1.2.1 Transport Reactor Train

1. Stable operations were demonstrated using the Eastern Kentucky coal and Plum Run dolomite, Bucyrus limestone, and Longview limestone. There were, however, circulation problems using the Eastern Kentucky coal and Florida Gregg Mine limestone.

2. Effective solids circulation and higher disengager/cyclone collection efficiency were achieved, with smaller grind size start-up bed material (~120 µm mmd).

3. Limestone was successfully ground to 15 to 25 µm mmd and was used in the sorbent feed system to feed into the reactor without any problems.

4. Test run TC03 included the longest continuous trouble-free operations, with no interruption from the coal feed system or any other subsystem (382 hours). A total of 795 hours on coal feed was accumulated during this run. To date, PSDF has achieved over 3,556 hours of operation on coal feed and about 4,840 hours of solids circulation.

5. For the entire TC03 test run, with the modifications made to the sealing mechanism on the spheri seal holding plate, the filter ash depressurization and transportation system performed well.

6. The coal feed system operated well during TC03. It was found that operational problems develop when (segregated) fine coal moves through the coal feed system.

7. Nearly 100-percent carbon coversion was achieved for Eastern Kentucky coal at 1,500°F reactor temperature.

8. There was not much observable difference using the Eastern Kentucky coal with either limestone or dolomite for sulfur capture.

9. Lower particle loadings to the PCD were achieved (5,000 to 7,500 ppm).

10. Different legs of an empty reactor loop and combustor heat exchanger were successfully heated to different temperatures, and the PCD was heated to above 800°F before adding sand through the coal feed system at 110 to 135 psig reactor pressure.

11. Smoother operation in the reactor was achieved with lower grind-size material in the reactor.

### 1.2.2 PCD-Related Systems

1. The Siemens Westinghouse PCD was operated for almost 800 hours on coal in combustion without ash bridging.

2. Two coals and four sorbents were used and demonstrated no negative effects on PCD operation.

3. Monitoring and controlling ash level in the PCD continued to be successfully proven.

4. Isokinetic ash samples on both the PCD inlet and outlet continued to be reliably, safely, and routinely taken.

5. The Siemens Westinghouse PCD has successfully operated continuously with outlet loadings below 1 ppm for almost 800 hours.

6. PSDF has successfully demonstrated the operation of the PCD with the design coal and sorbent for the Lakeland CCT project.

7. 3M resolved the gasketing issues with the previous design by designing a ceramic insert to allow use of the “standard” gasketing scheme.

8. A better understanding of what is happening inside the PCD during operation has been developed. This was accomplished through many avenues: on-going FLUENT modeling, which is a cooperative effort between the DOE and PSDF; sampling to determine what fraction of the particulate is being separated prior to reaching the filter elements; and pulse system modeling and optimization.

9. The acoustic detectors were redesigned and installed prior to TC02. However, electrical cross talk between the inlet and outlet probe prevented obtaining meaningful data.

10. By the end of TC03, several monolithic silicon carbide filter elements had accumulated over 3,200 hours of exposure. Additionally, the composite filter elements installed in early 1998 had accumulated over 1,350 hours of exposure.

11. New seal materials with the standard temperature ratings were delivered to the site. They performed remarkably well, with no seal failures.

12. Cut-size tests were performed to help determine the amount of ash removed from the PCD by cyclonic action.

## 1.3 FUTURE PLANS

The plans for the remainder of 1998 and 1999 are shown below.

1. The next test run, TC04, was scheduled for the fourth quarter of 1998.

2. The decision had been made at the time of this writing to stay in combustion on the MWK transport reactor through April 1999. Gasification is scheduled for late summer 1999.

3. A system is planned, to be built essentially identical to FL0301, as the PCD for the Foster Wheeler carbonizer. The request for quotations (RFQ) is out to potential suppliers.

4. Material testing, both destructive and nondestructive, should continue to gain momentum.

5. New filter elements will be introduced into the filter system for the first time at the PSDF. These include elements from Ensto, 2-meter-long 3M oxide elements, 2-meter-long Pall 326 elements, Pall 181 elements, and a new Pall Fe-Al element.

# 2.0 INTRODUCTION

This report provides an account of the TC03 test campaign with the Kellogg Brown & Root Company (KBR) transport reactor and the Siemens Westinghouse Power Corporation (Siemens Westinghouse) filter vessel at the Power Systems Development Facility (PSDF) located in Wilsonville, Alabama, 40 miles southeast of Birmingham. The PSDF is sponsored by the U. S. Department of Energy (DOE) and is an engineering-scale demonstration of two advanced coal-fired power systems. In addition to DOE, Southern Company Services, Inc., (SCS), the Electric Power Research Institute (EPRI), and Peabody Holding Company are cofunders. Other cofunding participants supplying services or equipment include KBR, Foster Wheeler (FW), Siemens Westinghouse, and Combustion Power Company. SCS is responsible for constructing, commissioning, and operating the PSDF.

The transport reactor is an advanced circulating fluidized-bed reactor acting as either a combustor or as a gasifier, using one of two possible hot gas clean-up filter technologies (particulate control devices or PCDs) at a component size readily scaleable to commercial systems. Design and construction of the transport reactor and required associated equipment were completed in early summer of 1996. All separate components and subsystems were fully operational by midsummer and commissioning work focused on integration issues for the entire reactor system. At the same time, the first set of ceramic candles was loaded into the Siemens Westinghouse PCD. Initial operation of the transport reactor as a combustor was completed in late August, with further combustion commissioning tests completed in the last quarter of 1996. Combustion characterization tests were then performed and the first major test campaign, TC01, was completed by the end of 1997. TC01 focused on exposing the PCD candles to process gas for 1,000 hours at temperatures from 1,350 to 1,400°F and to achieving stable reactor operations. The second major test run, TC02, was conducted from April 2 to May 11, 1998. Reactor parametric testing was performed during this test run to better quantify the effect of different variables on reactor and candle filter operation.

With this accomplished, TC03 was planned for additional reactor parametric testing to quantify to an even greater extent the effect of different variables on reactor and candle filter operation and to evaluate different feedstocks. Test run TC03 was begun on May 31, 1998, in combustion mode of operation after the reactor inspections, preventive maintenance activities, and process modifications had been completed. Test run TC03 was completed on August 10, 1998. The objectives of test run TC03 for the transport reactor were:

- *Demonstrate stable reactor operations with different feeds.* Demonstrate stable reactor operations using Eastern Kentucky coal with Plum Run dolomite, Bucyrus limestone, Longview limestone and Gregg Mine limestone.

- *Evaluate effects of reactor conditions on $NO_x$ emissions .* Vary Ca/S molar ratio, excess air, coal feed rate, and operation temperature.

- *Evaluate effects of reactor conditions on $SO_2$ emissions.* Vary Ca/S molar ratio, solids inventory, and operation temperature.

- *Investigate the effect of increasing the mixing zone density*. Decrease various aeration flows and increase solids inventory.

## 2.1 THE POWER SYSTEMS DEVELOPMENT FACILITY

SCS entered into an agreement with DOE/FETC for the design, construction, and operation of a hot gas clean-up test facility for gasification and pressurized combustion. The purpose of the PSDF is to provide a flexible test facility that can be used to develop advanced power system components, evaluate advanced turbine system configurations, and assess the integration and control issues of these advanced power systems. The facility was designed as a resource for rigorous, long-term testing and performance assessment of hot-stream, clean-up devices and other components in an integrated environment.

The PSDF will consist of five modules for systems and component testing. These modules include:

- An advanced pressurized fluidized-bed combustion module (APFBC).
- A transport reactor module.
- A hot-gas, clean-up module.
- A compressor/turbine module.
- A fuel cell module.

The APFBC module consists of FW technology for second-generation PFBC. This module relies on partial conversion of the coal to fuel gas in a carbonizer, with the remaining char converted in a pressurized fluidized-bed combustion (PFBC). Both the fuel gas and PFBC exhaust gas streams are filtered to remove particulates, then combined to fire a combustion turbine. The advanced gasifier module includes KBR transport technology for pressurized combustion and gasification to provide either an oxidizing or reducing gas for parametric testing of hot particulate control devices.

The filter systems that will be tested at PSDF include PCDs supplied by Combustion Power Company from Menlo Park, California, and Siemens Westinghouse filter systems from Pittsburgh, Pennsylvania. An RFP (request for proposal) has been issued for supply of the PCD for treating the carbonizer.

## 2.2 TRANSPORT REACTOR SYSTEM DESCRIPTION

The transport reactor train operating in the combustion mode is shown schematically in Figure 2.2-1. A taglist of all major equipment in the process train and associated balance-of-plant is provided in Tables 2.2-1 and -2. Two PCDs are shown in this flow diagram; however, only one PCD is tested with the transport reactor at a given time during operations. The intent is to be able to install, change out, or provide maintenance on a second PCD while one is being tested. This provides increased flexibility for the test facility and reduces downtime. The facility is sized to process nominally 2 ton/hr of coal. This size generates sufficient gas to test the PCDs at a nominal 1,000 ACFM of gas at the PCD inlet. Indirect cooling of the gas from the transport reactor allows testing of the PCDs with inlet temperatures between 600 and 1,400°F and at pressures ranging from 150 to 305 psia. The PCD in this train receives particulate laden gas from the transport reactor, which can operate in either gasification or combustion mode. In the gasification mode, the gas exiting the PCDs is oxidized, cooled, and filtered in a baghouse before being discharged from a stack. The ash and char produced in the gasification mode are oxidized in a sulfator prior to disposal.

Coal is ground to a nominal average particle diameter of 100 and 200 microns when the transport reactor is operated in gasification mode and combustion mode, respectively. Sorbent is ground to a nomimal average particle diameter of 100 microns. Both coal and sorbent are pneumatically fed by feeders into the transport gasifier/combustor at a continuous, controlled rate.

Air is compressed to about 350 psia in the main air compressor and fed directly to the transport reactor. For start-up purposes, a burner (BR0201) is provided at the reactor mixing zone. Liquefied propane gas (LPG) is used as start-up fuel. Fuel, sorbent, and gas feeds enter a mixing zone at the bottom of the reactor where they mix with recycled solids from the disengager cyclone. Coal conversion begins in this zone; the reaction mixture then flows upward into the more narrow riser section at high velocity, and then flows to the disengager.

The reactor typically operates at temperatures of 1,600 to 1,625°F in combustion mode. Provision is made to inject air at several different points along the riser to control the formation of $NO_X$. Limestone or dolomitic sorbents are fed into the reactor for sulfur capture, therefore eliminating the need for downstream facilities to reduce plant sulfur emissions.

Solids and gases leaving the reactor flow to the disengager for bulk separation of the two phases. Most of the solids collected in the disengager are recycled to the reactor. Coal ash and spent sorbent are discharged from the transport reactor to maintain the solids inventory in the system. In the combustion mode, heat removal from the reactor system is necessary to control the reactor temperature. This is accomplished by removing solids from the disengager, cooling the solids in the combustor heat exchanger (HX0203), and returning the solids to the reactor system.

The gas exiting the disengager still contains a high loading of particulates; it is then sent to a cyclone system for additional solids recovery prior to being fed to the PCDs. This cyclone is provided with spoiling gas to vary the solids loading into the effluent gas. The resulting

conditioned gas next enters the PCD, where essentially all of the remaining particulates in the gas are removed. The cleaned gas leaving the PCD is then sent to a secondary gas cooler (HX0402) and, ultimately, is cooled to about 600°F. All gas stream cooling is accomplished by generating steam. A portion of the cooled gas is then further cooled in the compressor feed cooler (HX0405) and sent to the recycle gas booster compressor (CO0401), where the pressure is increased to about 400 psia. This gas acts as aeration fluidization gas in the combustor heat exchanger.

The main gas stream from the secondary gas cooler is cooled further by dilution air and cleaned of any remaining particulates in a baghouse before being discharged to the atmosphere through a stack.

Table 2.2-1

Major Equipment in the Transport Reactor Train

| TAG NAME | DESCRIPTION |
|---|---|
| BR0201 | Reactor Start-Up Burner |
| BR0401 | Thermal Oxidizer |
| BR0602 | Sulfator Start-Up/PCD Preheat Burner |
| CO0201 | Main Air Compressor |
| CO0401 | Recycle Gas Booster Compressor |
| CO0601 | Sulfator Air Compressor |
| CY0201 | Primary Cyclone in the Reactor Loop |
| CY0207 | Disengager in the Reactor Loop |
| CY0601 | Sulfator Cyclone |
| DR0402 | Steam Drum |
| DY0201 | Feeder System Air Dryer |
| FD0206 | Spent Solids Screw Cooler |
| FD0210 | Coal Feeder System |
| FD0220 | Sorbent Feeder System |
| FD0502 | Fines Screw Cooler |
| FD0510 | Spent Solids Transporter System |
| FD0520 | Fines Transporter System |
| FD0530 | Spent Solids Feeder System |
| FD0602 | Sulfator Solids Screw Cooler |
| FD0610 | Sulfator Sorbent Feeder System |
| FL0301 | PCD — Siemens Westinghouse |
| FL0302 | PCD — Combustion Power |
| FL0401 | Compressor Intake Filter |
| HX0202 | Primary Gas Cooler |
| HX0203 | Combustor Heat Exchanger |
| HX0204 | Transport Air Cooler |
| HX0402 | Secondary Gas Cooler |
| HX0405 | Compressor Feed Cooler |
| HX0601 | Sulfator Heat Recovery Exchanger |
| ME0540 | Heat Transfer Fluid System |
| RX0201 | Transport Reactor |
| SI0602 | Spent Solids Silo |
| SU0601 | Sulfator |

Table 2.2-2 (Page 1 of 3)

Major Equipment in the Balance-of-Plant

| TAG NAME | DESCRIPTION |
|---|---|
| BO2920 | Auxiliary Boiler |
| BO2921 | Auxiliary Boiler - Superheater |
| CL2100 | Cooling Tower |
| CO2201A-D | Service Air Compressor A-D |
| CO2202 | Air-Cooled Service Air Compressor |
| CO2203 | High-Pressure Air Compressor |
| CO2601A-C | Reciprocating $N_2$ Compressor A-C |
| CR0104 | Coal and Sorbent Crusher |
| CV0100 | Crushed Feed Conveyor |
| CV0101 | Crushed Material Conveyor |
| DP2301 | Baghouse Bypass Damper |
| DP2303 | Inlet Damper on Dilution Air Blower |
| DP2304 | Outlet Damper on Dilution Air Blower |
| DY2201A-D | Service Air Dryer A-D |
| DY2202 | Air-Cooled Service Air Compressor Air Dryer |
| DY2203 | High-Pressure Air Compressor Air Dryer |
| FD0104 | MWK Coal Transport System |
| FD0111 | MWK Coal Mill Feeder |
| FD0113 | Sorbent Mill Feeder |
| FD0140 | Coke Breeze and Bed Material Transport System |
| FD0154 | MWK Limestone Transport System |
| FD0810 | Ash Unloading System |
| FD0820 | Baghouse Ash Transport System |
| FL0700 | Baghouse |
| FN0700 | Dilution Air Blower |
| HO0100 | Reclaim Hopper |
| HO0105 | Crushed Material Surge Hopper |
| HO0252 | Coal Surge Hopper |
| HO0253 | Sorbent Surge Hopper |
| HT2101 | MWK Equipment Cooling Water Head Tank |
| HT2103 | SCS Equipment Cooling Water Head Tank |
| HT0399 | 60-Ton Bridge Crane |
| HX2002 | MWK Steam Condenser |
| HX2003 | MWK Feed Water Heater |

Table 2.2-2 (Page 2 of 3)

Major Equipment in the Balance-of-Plant

| TAG NAME | DESCRIPTION |
|---|---|
| HX2004 | MWK Subcooler |
| HX2103A | SCS Cooling Water Heat Exchanger |
| HX2103C | MWK Cooling Water Heat Exchanger |
| LF0300 | Propane Vaporizer |
| MC3001-3017 | MCCs for Various Equipment |
| ME0700 | MWK Stack |
| ME0701 | Flare |
| ME0814 | Dry Ash Unloader for MWK Train |
| ML0111 | Coal Mill for MWK Train |
| ML0113 | Sorbent Mill for Both Trains |
| PG2600 | Nitrogen Plant |
| PU2000A-B | MWK Feed Water Pump A-B |
| PU2100A-B | Raw Water Pump A-B |
| PU2101A-B | Service Water Pump A-B |
| PU2102A-B | Cooling Tower Make-Up Pump A-B |
| PU2103A-D | Circulating Water Pump A-D |
| PU2107 | SCS Cooling Water Make-Up Pump |
| PU2109A-B | SCS Cooling Water Pump A-B |
| PU2111A-B | MWK Cooling Water Pump A-B |
| PU2300 | Propane Pump |
| PU2301 | Diesel Rolling Stock Pump |
| PU2302 | Diesel Generator Transfer Pump |
| PU2303 | Diesel Tank Sump Pump |
| PU2400 | Fire Protection Jockey Pump |
| PU2401 | Diesel Fire Water Pump #1 |
| PU2402 | Diesel Fire Water Pump #2 |
| PU2504A-B | Waste Water Sump Pump A-B |
| PU2507 | Coal and Limestone Storage Sump Pump |
| PU2700A-B | Demineralizer Forwarding Pump A-B |
| PU2701 | SCS Closed-Loop System Make-Up Pump |
| PU2711 | Corrosion Inhibitor Pump |
| PU2713 | Waste Water Alum Pump |
| PU2714 | Waste Water Caustic Pump |
| PU2720 | Acid Pump |
| PU2721 | Waste Water Acid Pump |

Table 2.2-2 (Page 3 of 3)

Major Equipment in the Balance-of-Plant

| TAG NAME | DESCRIPTION |
|---|---|
| PU2730 | MWK Steam System Phosphate Pump |
| PU2740 | Cooling Tower Sodium Bisulfate Pump |
| PU2741 | Cooling Tower Sodium Bisulfate Pump |
| PU2750 | MWK Steam System $O_2$ Scavenger and pH Pump |
| PU2900A-C | Chemical Injection Pump A-C |
| PU2920A-B | Auxiliary Boiler Feed Water Pump A-B |
| SB3001 | 125-V DC Station Battery |
| SB3002 | UPS |
| SC0700 | Baghouse Screw Conveyor |
| SG3000-3005 | 4160-V, 480-V Switchgear Buses |
| SI0101 | MWK Crushed Coal Storage Silo |
| SI0103 | Crushed Sorbent Storage Silo |
| SI0111 | MWK Pulverized Coal Storage Silo |
| SI0113 | MWK Limestone Silo |
| SI0114 | FW Limestone Silo |
| SI0810 | Ash Silo |
| ST2601 | $N_2$ Storage Tube Bank |
| TK2000 | MWK Condensate Storage Tank |
| TK2001 | FW Condensate Tank |
| TK2100 | Raw Water Storage Tank |
| TK2300A-D | Propane Storage Tank A-D |
| TK2301 | Diesel Storage Tank |
| TK2401 | Fire Water Tank |
| XF3000A | 230/4.16-kV Main Power Transformer |
| XF3001B-5B | 4160/480-V SS Transformer No. 1-5 |
| XF3001G | 480/120-V-Miscellaneous Transformer |
| XF3010G | 120/208 Distribution Transformer |
| XF3012G | UPS Isolation Transformer |
| VS2203 | High-Pressure-Air Receiver |

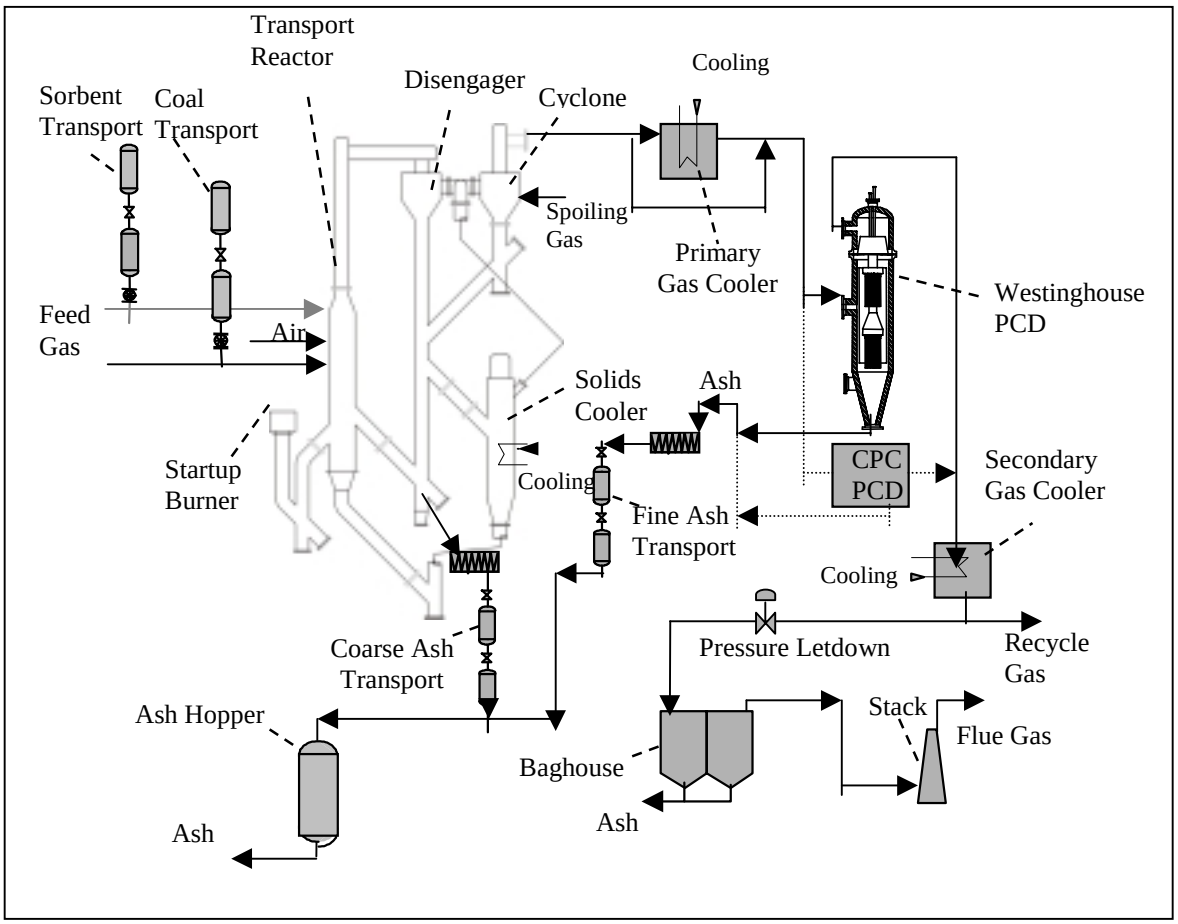


Figure 2.2-1 Flow Diagram of the Transport Reactor Train in Combustion Mode of Operation

## 2.3 SIEMENS WESTINGHOUSE PARTICULATE CONTROL DEVICE

Different PCDs will be evaluated on the transport reactor train. The first PCD that was commissioned in 1996 and has been used in the all of 1997 and 1998 testing was the filter system designed by Siemens Westinghouse. The dirty gas enters the PCD below the tubesheet, flows through the filter elements, and the ash collects on the outside of the filter. The clean gas passes from the plenum/filter element assembly through the plenum pipe to the outlet pipe. As the ash collects on the outside surface of the filter elements, the pressure drop across the filter system gradually increases. The filter cake is periodically dislodged by injecting a high-pressure gas pulse to the clean side of the candles. The cake then falls to the discharge hopper.

To date, the transport reactor has been operated only in the combustion mode. Initially, high-pressure air was used as the pulse gas for the PCD. However, the pulse gas was changed to nitrogen early in 1997. The pulse gas was routed individually to the two-plenum/filter element assemblies via injection tubes mounted on the top head of the PCD vessel. The pulse duration was typically 0.1 to 0.5 seconds.

A sketch of the Siemens Westinghouse PCD is shown in Figure 2.3-1.

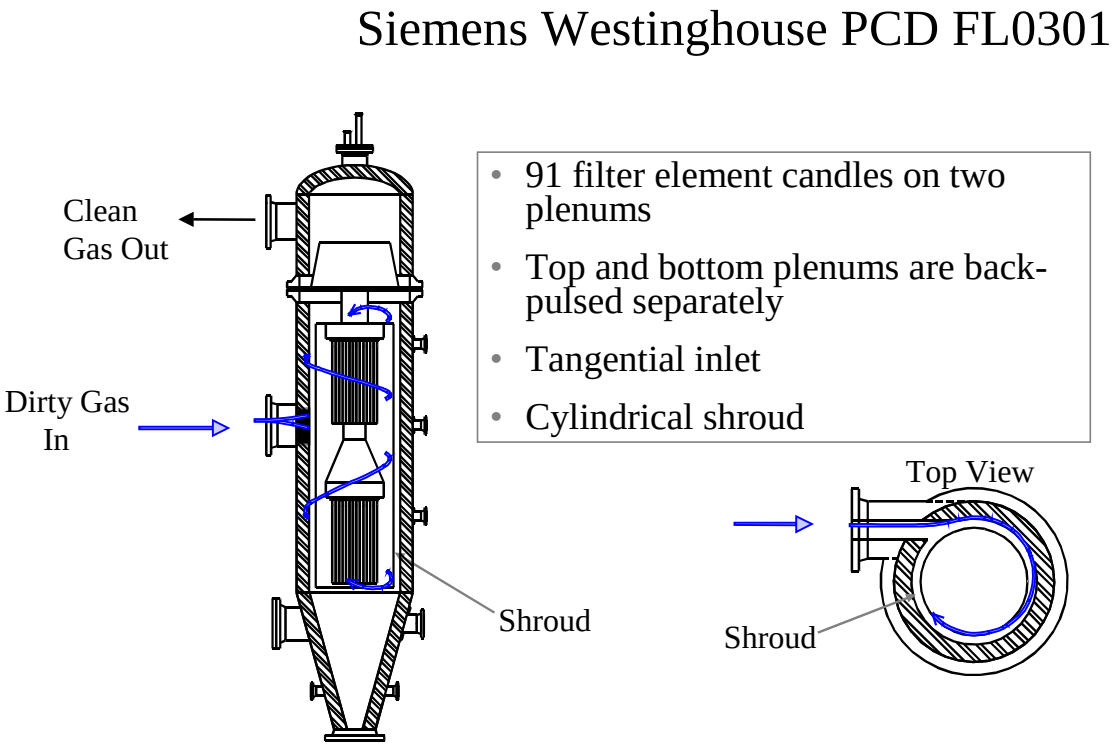


Figure 2.3-1 Siemens Westinghouse PCD

# 3.0 PARTICLE FILTER SYSTEM

## 3.1 PCD OVERVIEW

### 3.1.1 Summary

The Siemens Westinghouse Power Corporation (Siemens Westinghouse ) particulate control device (PCD) operated for almost 800 hours on coal in test run TC03. The run was uneventful for the PCD, with no failures or problems during the full length of the run. Two types of coal and four types of sorbent were used during the run. Specifically, Eastern Kentucky coal and Gregg limestone, both slated for the Lakeland clean coal technology (CCT) project, were proven viable. Particulate loadings to the PCD varied significantly during the run; however, no conclusive prediction method for loading based on the sorbent/coal type was determined. PCD performance was not negatively affected by varying coal or sorbent.

The Southern Research Institute (SRI) particulate collection system continued to operate reliably. Outlet particulate loadings remained below 0.37 ppmw for the duration of TC03, maintaining collection efficiencies of 99.9935 percent or greater.

Operation of the PCD and auxiliary systems continued to perform well during TC03. No downtime was attributed to the ash removal systems. The newly designed seal material functioned flawlessly. Problems with the fine-ash screw cooler, however, continued to require attention during TC03. Leaking shaft rider seals required additional monitoring by plant personnel. Operation staff continued monitoring ash level in the PCD with success. Rising ash levels became an issue for concern several times during the run, but at no time did the ash level approach the filter elements.

### 3.1.2 TC03 Accomplishments

The accomplishments for TC03 include:

- The Siemens Westinghouse PCD was operated for almost 800 hours on coal in combustion without ash bridging.
- Two coals and four sorbents were used and no negative effects on PCD operation were demonstrated.
- Monitoring and controlling ash level in the PCD continued to be successful.
- Isokinetic ash samples, both on the PCD inlet and outlet, continued to be reliably, safely, and routinely taken.
- The Siemens Westinghouse PCD successfully operated continuously with outlet loadings below 1 ppm for almost 800 hours.

- The PSDF has successfully demonstrated the operation of the PCD with the design coal and sorbent for the Lakeland CCT project.

- The 3M Company resolved gasketing issues of the previous design by creating a ceramic insert to allow use of the "standard" gasketing scheme.

- There is a better understanding of what is happening inside the PCD during operation. This has been accomplished through many avenues: 1) on-going FLUENT modeling, which is a cooperative effort between the DOE and PSDF; 2) sampling, to determine what fraction of the particulate is being separated prior to reaching the filter elements; and 3) pulse system modeling and optimization.

- The acoustic detectors were redesigned and installed prior to TC02. However, electrical cross talk between the inlet and outlet probe prevented obtaining meaningful data.

- Several monolithic silicon carbide filter elements had accumulated over 3,200 hours of exposure by the end of TC03. Additionally, the composite filter elements installed in early 1998 had accumulated over 1,350 hours of exposure.

- New seal materials with the standard temperature ratings were delivered to the site and performed remarkably well with no seal failures.

- Cut-size tests were performed to help determine the amount of ash removed from the PCD by cyclonic action.

### 3.1.3 Developmental Areas

The system performed well throughout TC03. The previous elevated outlet loadings had essentially been eliminated, problems with the spent fines removal system were less apparent during the run than ever before, and there were no element failures. However, there are still areas of concern that require further evaluation in the future. These include the following:

- Fail-safe performance and the performance of the filter gaskets continue to need attention. Different gasketing materials for the fail-safe were experimented with during the run. Work continues with Siemens Westinghouse to improve both the design and the installation of the filter gaskets.

- Modifications to the screw cooler are being manufactured for delivery to the plant by the end of 1998.

### 3.1.4 Future Plans

The plans for the remainder of 1998 and for 1999 are shown below.

- Test run TC04 was scheduled for the last quarter of 1998.
- The decision had been made at the time of this writing to remain in combustion on the MWK transport reactor through April 1999. Gasification is scheduled for late summer 1999.
- A system essentially identical to FL0301 is planned and will be built as the PCD for the Foster Wheeler carbonizer. The request for quotations (RFQ) is out to potential suppliers.
- Material testing, both destructive and nondestructive, should continue to gain momentum.
- New filter elements will be introduced into the filter system for the first time at the PSDF. These include elements from Ensto, 2-meter long 3M oxide elements, 2-meter long Pall 326 elements, Pall 181 elements, and a new Pall Fe-Al element.

## 3.2 PCD OPERATION DURING TEST RUN TC03

### 3.2.1 Run Summary

Test campaign TC03 was started on the afternoon of May 31, 1998, for the purpose of evaluating the transport reactor performance. Clyde proprietary seals were installed in the spent fines transport system (FD0520) for this run.

This was an uneventful run for the particulate control device (PCD), with no problems for the duration of the run. Tests were also completed during TC03 on use of eastern Kentucky coal that is being considered for the Lakeland project. Additionally, Gregg limestone, which is also being considered for the Lakeland Clean Coal Technology Project, was used. Various other types of limestone were also tried during the run. Particulate loadings to the PCD were different during these trials; however, no conclusive prediction method for loading and sorbent/coal type was determined. Operational changes in the transport reactor, differing feed requirements for type of sorbent materials, and variations in the compositions of the coal are just a few of the factors attributed to some of these variations. Regardless, PCD performance was not negatively affected by varying coal and sorbent material. Using limestone as a sorbent, however, posed new operational challenges for the transport reactor. Clinker formation in the reactor complicated the operation. In an effort to alleviate some of the clinker problems, the inlet temperature to the PCD was set to average slightly below 1,350°F (732.2°C). The run ended on August 10, 1998.

### 3.2.2 Test Objectives

The primary objective of test run TC03 was to characterize reactor performance using new types of sorbent and coal feed. The main objective for the PCD was to support this primary objective and observe any changes in PCD operation relating to the different types of sorbent and coal feed.

### 3.2.3 Observations/Events

A. Test Started-May 31 at 19:16. The main air compressor (MAC) was started May 31, 1998, to begin TC03.

B. Coal Feed Began-June 2 at 10:25.

C. Coal Feed Interrupted-June 2 at 13:15. Coal feed was stopped to inspect the coal rotofeeder.

D. Coal Feed Began-June 3 at 12:00.

E. Solids Sent to PCD-June 3 at 15:00.

F. Cut-Size Testing Began-June 5 at 13:20. Samplings of ash from FD0520 were selectively timed to characterize particle separation in the PCD.

G. Cut-Size Testing Stopped-June 5 at 14:39.

H. Dipleg Upset. Solids Sent to PCD-June 5 at 15:45.

I. FD0502 Leaking Problems-June 7 at 14:00. The shaft rider seal had to be adjusted to remedy leaking process gas.

J. Lost Coal Feed-June 14 at 14:00.

K. Coal Feed Resumed-June 14 at 22:32.

L. Difficult Reactor Operation. Many Upsets-June 15 through June 16. Reactor operations were extremely unstable and there were many upsets during this time that carried solids over to the PCD.

M. Lost Coal Feed-June 18 at 13:00.

N. Reactor Shut Down-June 19 at 07:04. Clinker formation in the reactor forced the unit off-line.

O. Coal Feed Resumed-July 13 at 22:10.

P. Reactor Shut Down-July 15 at 20:00. Clinker formation in the reactor forced the unit off-line.

Q. Coal Feed Resumed-July 25 at 21:23.

R. Plant Information System Down-July 27 at 12:58. The data acquisition system was off-line for approximately 24 minutes.

S. Run Ended-August 10 at 21:37.

### 3.2.4 Run Outcome

FL0301

Operation of the PCD was flawless during TC03. No significant problems occurred and outlet particle loadings were less than 1ppmw for over 800 hours of operation. The installation of filter elements into the plenum for TC04 was completed at the beginning of October. However, it was noticed when the vessel head was removed for installation of the plenum that the bottom of the shroud was “square” instead of round. Upon inspection, it was discovered that the supports for the bottom cone liner had failed to the extent that they were distorting the shroud. A detailed account of this incident is reported in section 3.3.

FD0502/FD0520

Attention was still focused during the run on leakage around the shaft rider seal packing glands on the fine ash removal screw cooler (FD0502). The severity of the leakage was much less than on the previous run and care was taken to watch the seal during the run. The new seal material for the Clyde system (FD0520) performed remarkably well. No seal failures or wear were observed during the run. Modifications to the seal support ring, however, were made during the run to remedy some leakage there that had been observed.

Table 3.2-1

TC03 Run Statistics

| | |
|---|---|
| Start Time: | 5/31/98 at 19:16 |
| End Time: | 8/10/98 at 21:37 |
| | |
| Coals: | Calumet Alabama Bituminous<br>Eastern Kentucky |
| Hours on Coal: | 795 |
| Sorbents: | Plum Run Dolomite<br>Florida Greg Mine Limestone<br>Ohio Bucyrus Limestone<br>Alabama Longview Limestone |
| | |
| Number of Filter Elements: | 88 |
| Filter Element Layout No.: | 9 (Figure 3.2-4) |
| Filtration Area: | 240.7 $ft^2$ (22.4 $m^2$) |
| | |
| Pulse Valve Open Time: | 0.2 sec. |
| Pulse Time Trigger: | 20 to 40 min |
| Pulse Pressure: | 250 to 450 psig (17 to 31 bar,g) |
| Pulse DP Trigger: | 140 to 200 inWG (349-498 mbar) |

Table 3.2-2

TC03 Major Events

| Event | Description | Date at Time |
|---|---|---|
| A | Test Started | May 31 at 19:16 |
| B | Coal Feed Began | June 2 at 10:25 |
| C | Coal Feed Interrupted | June 2 at 13:15 |
| D | Coal Feed Began | June 3 at 12:00 |
| E | Solids Sent to PCD | June 3 at 15:00 |
| F | Cut Size Testing Began | June 5 at 13:20 |
| G | Cut Size Testing Stopped | June 5 at 14:39 |
| H | Dipleg Upset; Solids Sent to PCD | June 5 at 15:45 |
| I | FD0502 Leaking Problems | June 7 at 14:00 |
| J | Lost Coal Feed | June 14 at 14:00 |
| K | Coal Feed Resumed | June 14 at 22:32 |
| L | Difficult Reactor Operation; Many Upsets | June 15 through June 16 |
| M | Lost Coal Feed | June 18 at 13:00 |
| N | Reactor Shut Down | June 19 at 07:04 |
| O | Coal Feed Resumed | July 13 at 22:10 |
| P | Reactor Shut Down | July 15 at 20:00 |
| Q | Coal Feed Resumed | July 25 at 21:23 |
| R | Plant Information System Down About 24 Minutes | July 27 at 12:58 |
| S | Run Ended | August 10 at 21:37 |

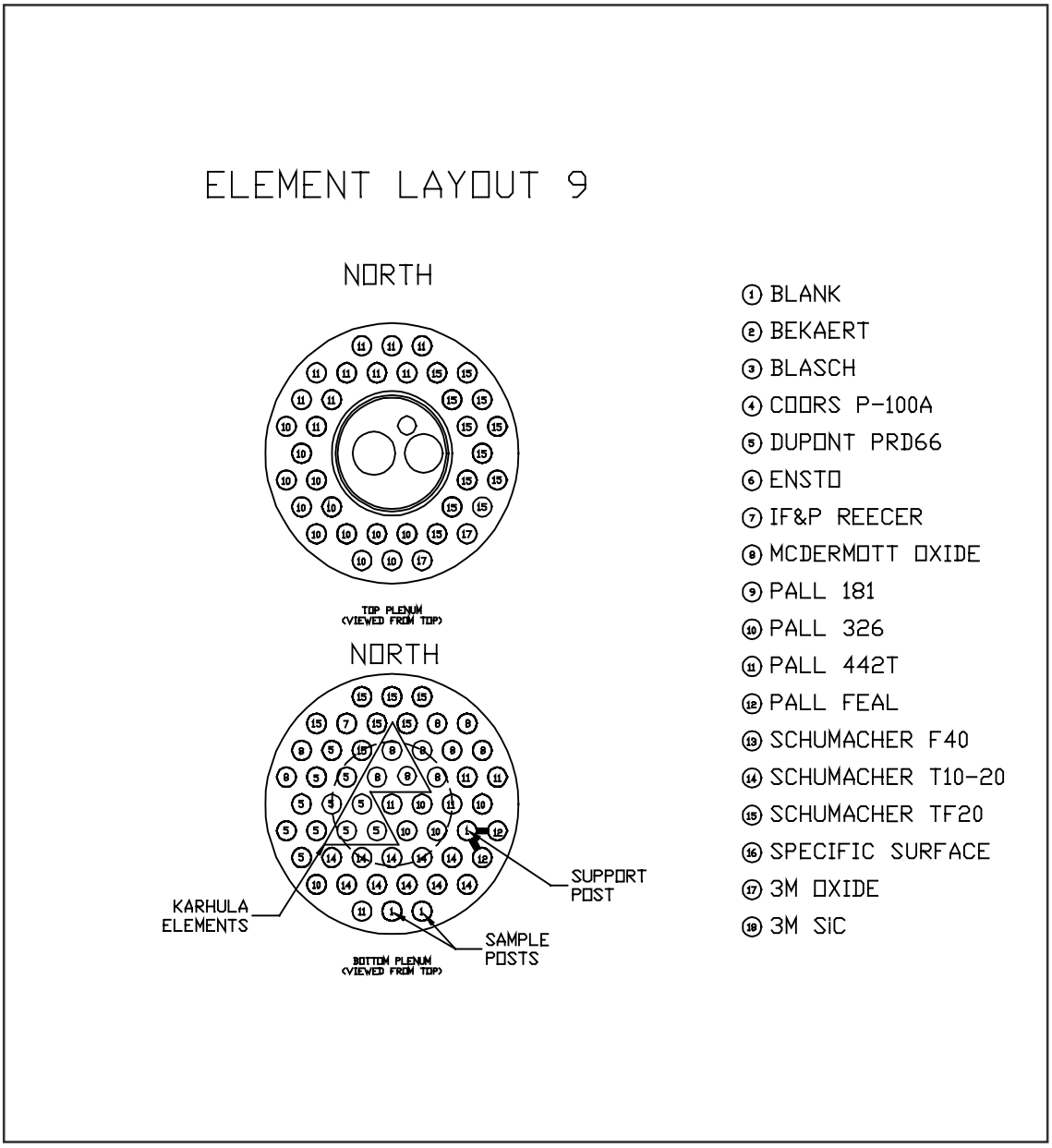


Figure 3.2-1 Filter Element Layout for TC03 (Layout No. 9)

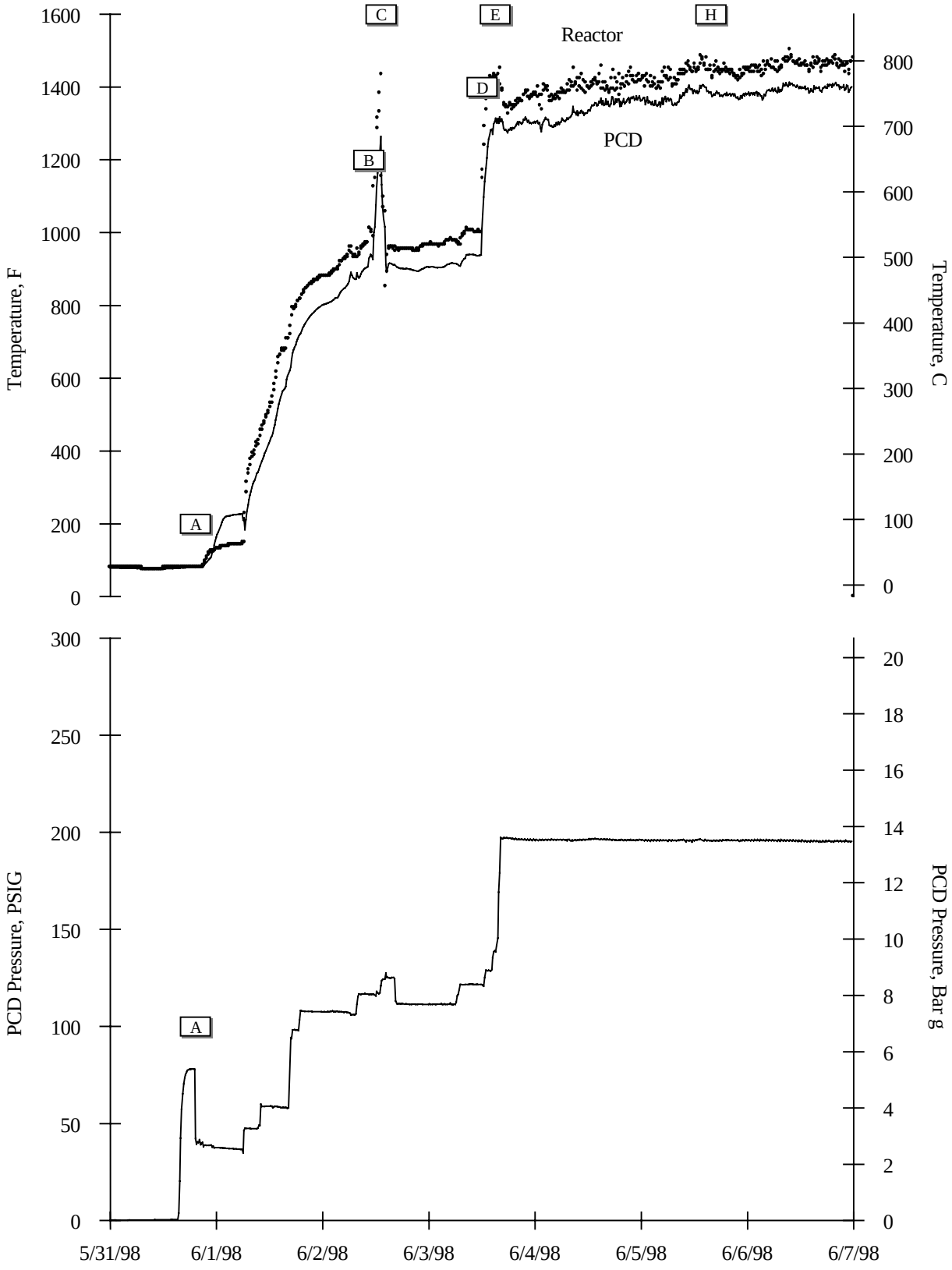


Figure 3.2-2 TC03 Temperature and Pressure for May 31 Through June 7

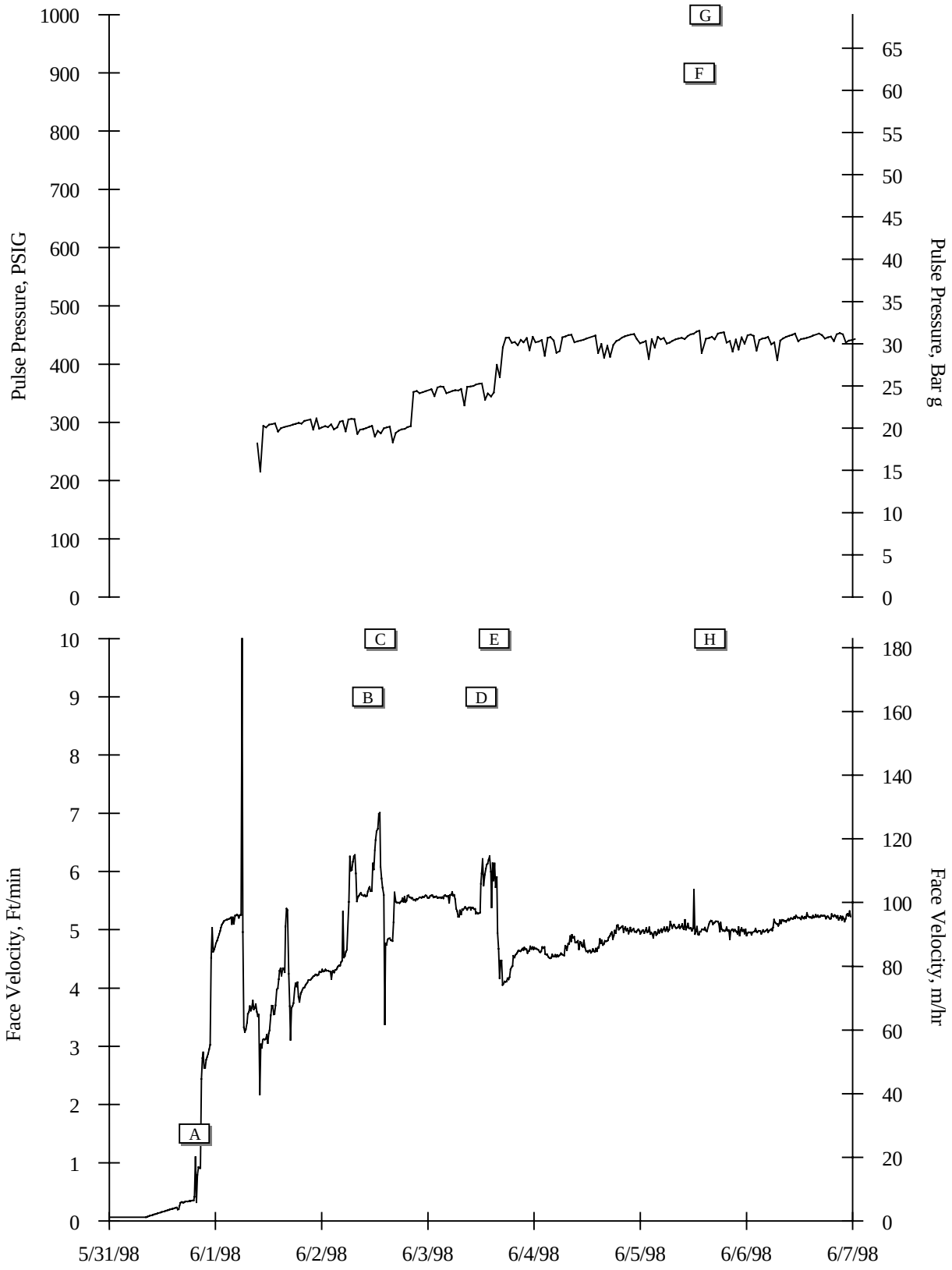


Figure 3.2-3 TC03 Back-Pulse Pressure and Face Velocity for May 31 Through June 7

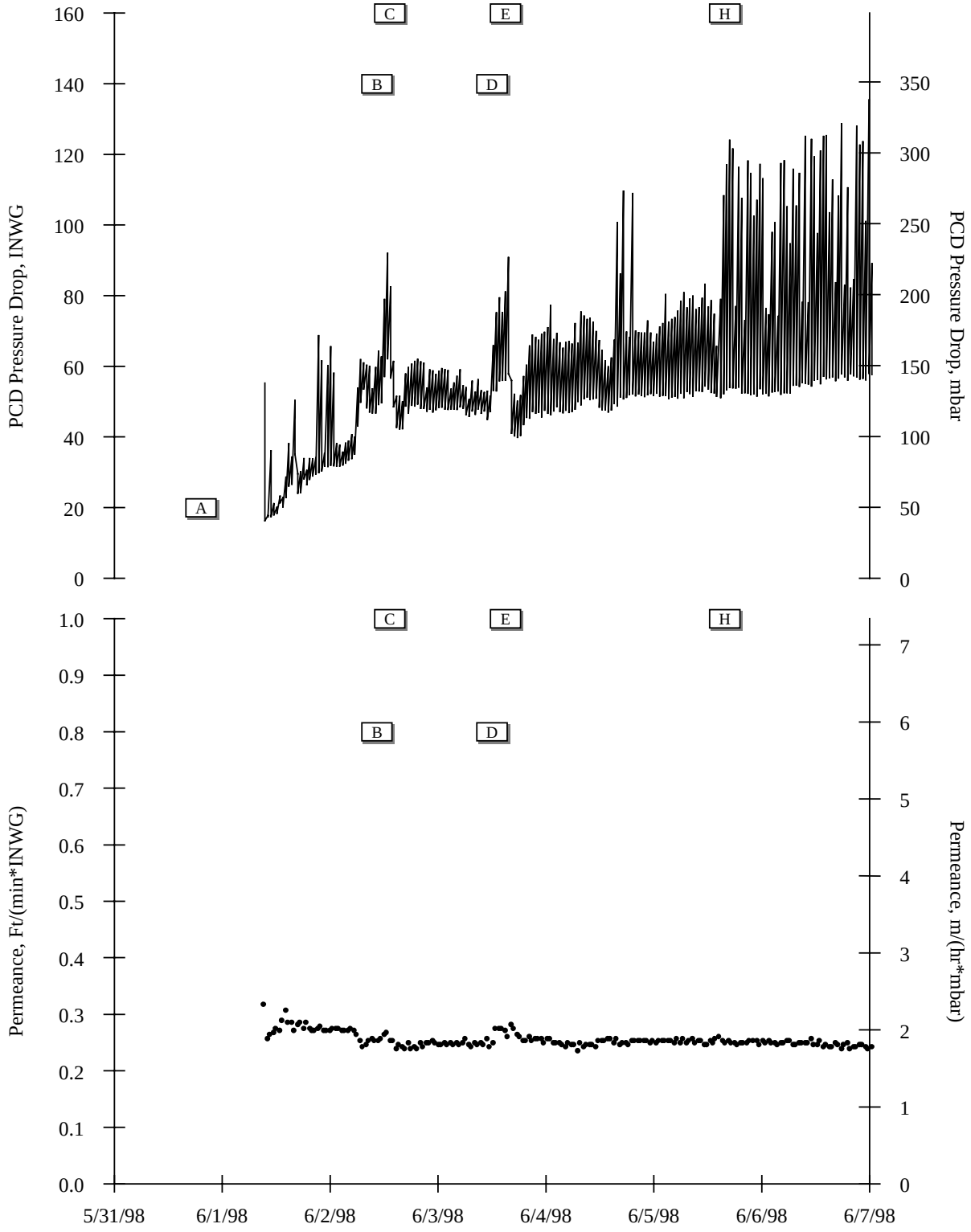


Figure 3.2-4 TC03 Pressure Drop and Permeance for May 31 Through June 7

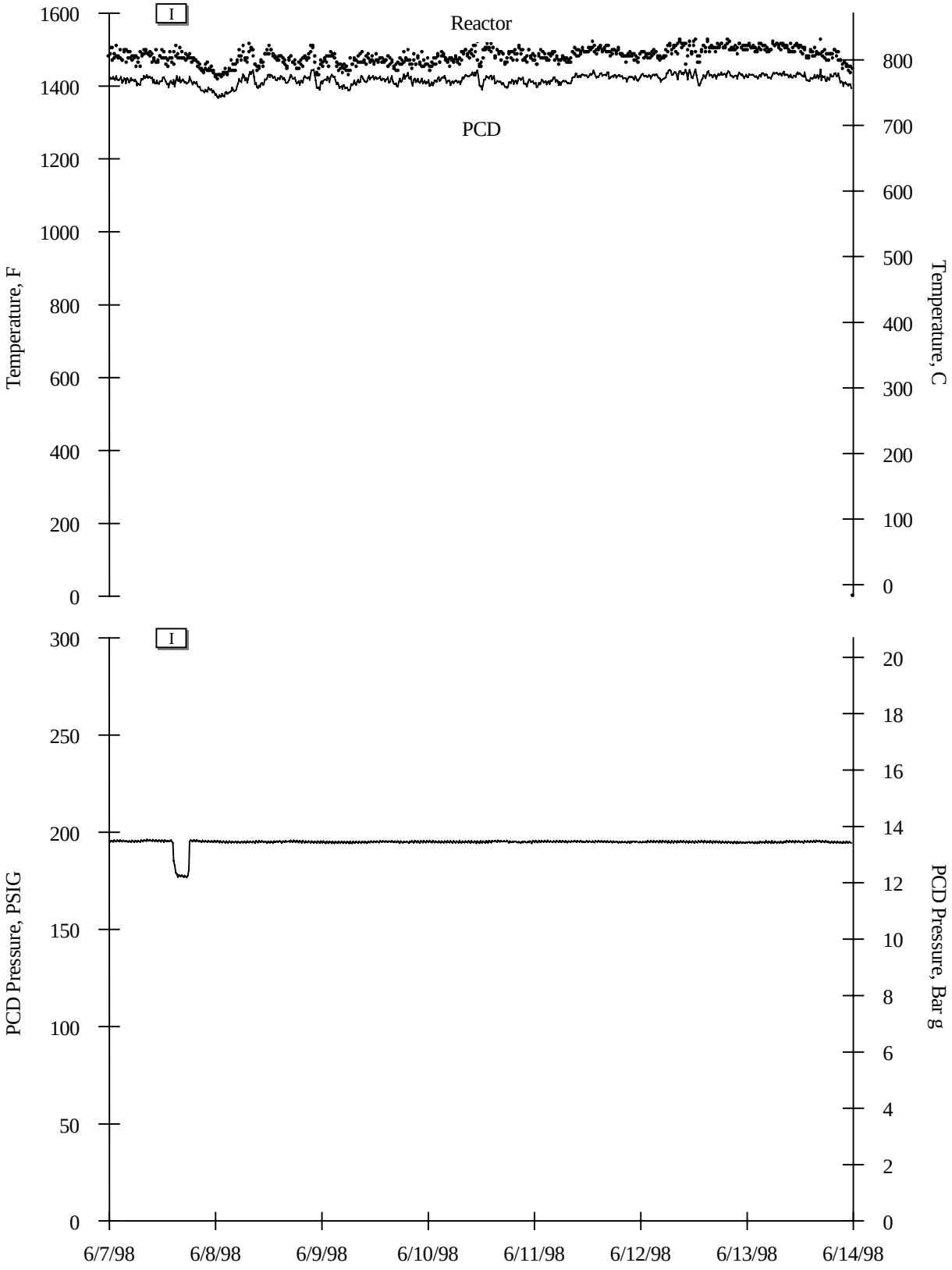


Figure 3.2-5 TC03 Temperature and Pressure for June 7 Through June 14

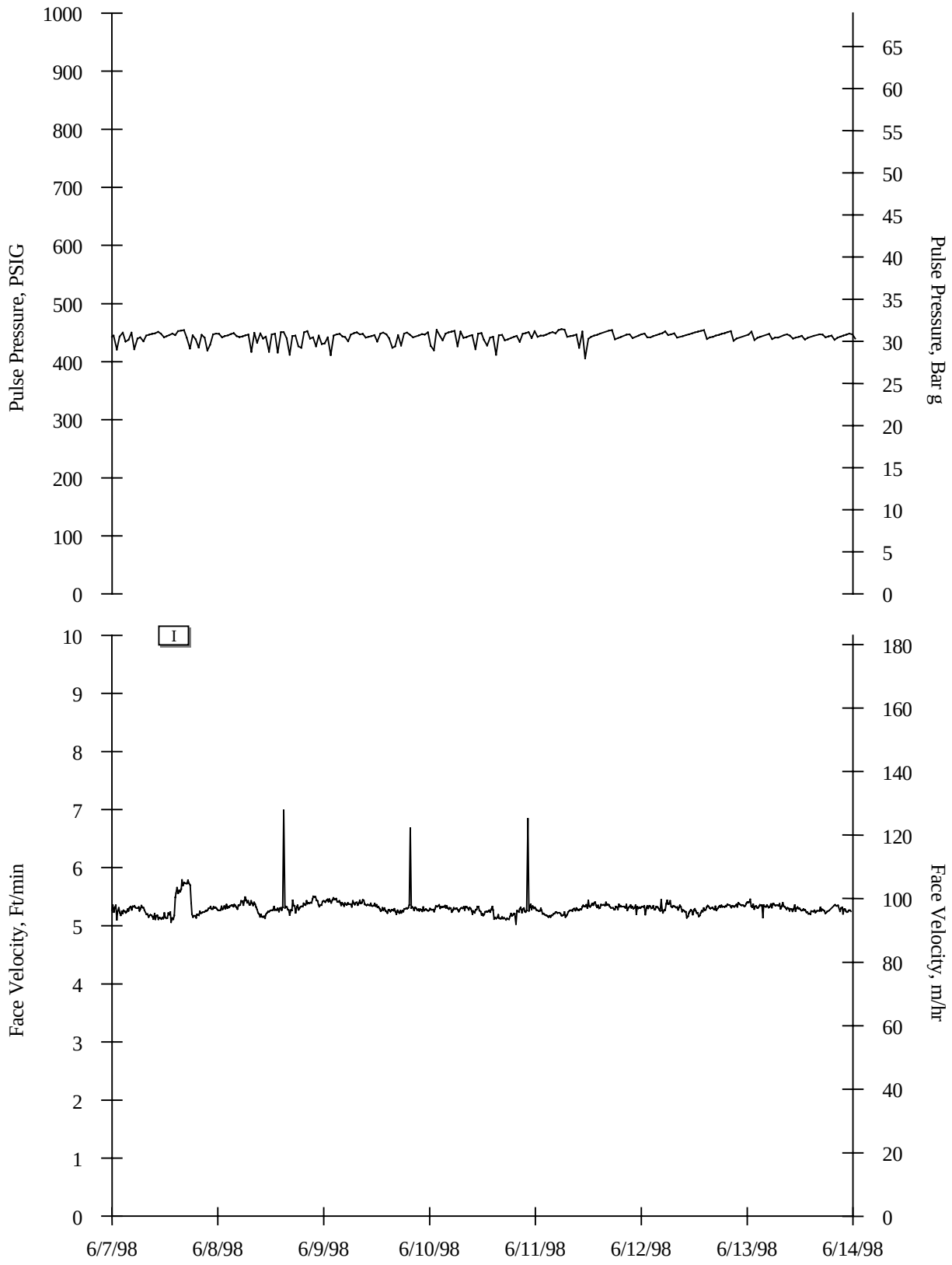


Figure 3.2-6 TC03 Back-Pulse Pressure and Face Velocity for June 7 Through June 14

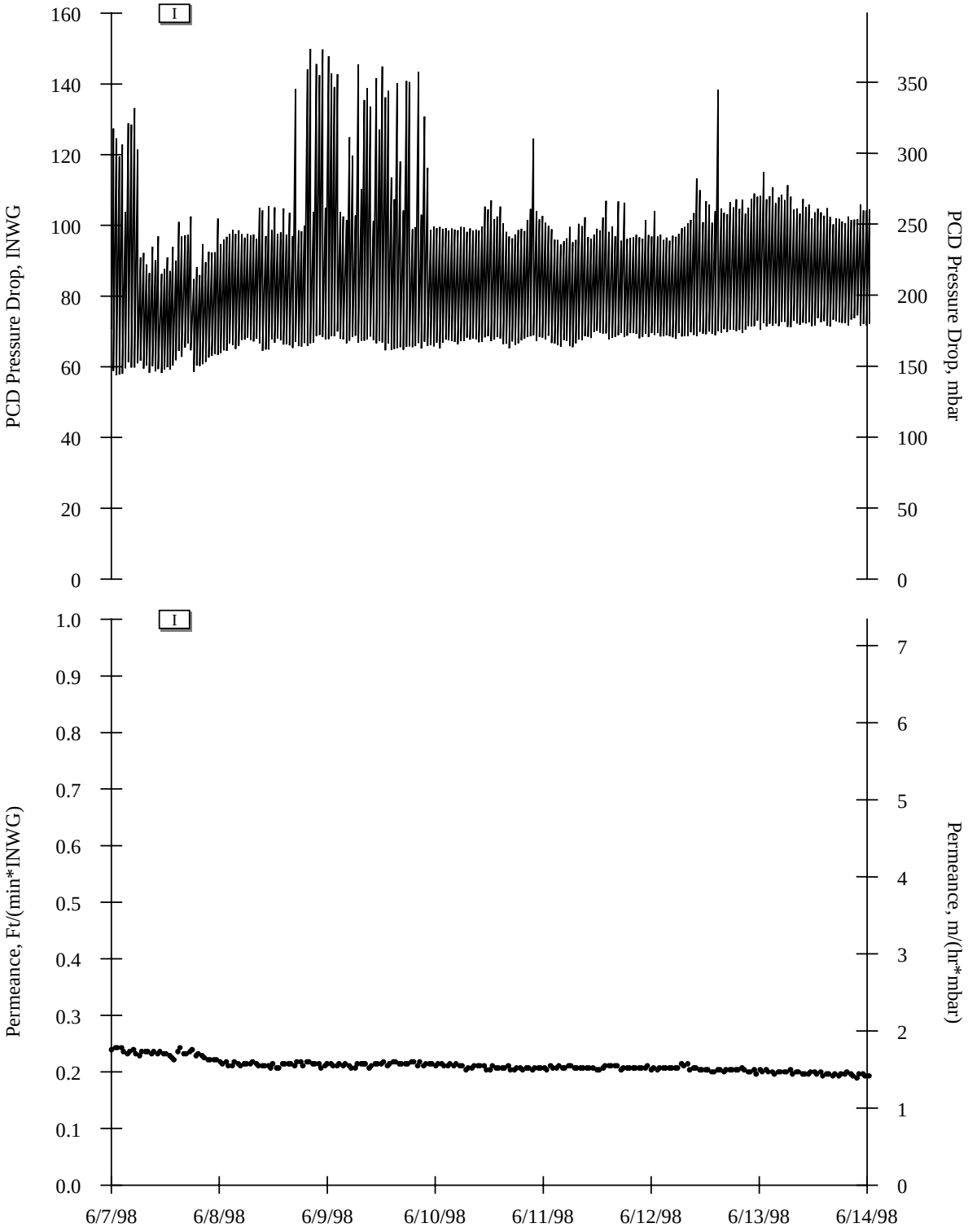


Figure 3.2-7 TC03 Pressure Drop and Permeance for June 7 Through June 14

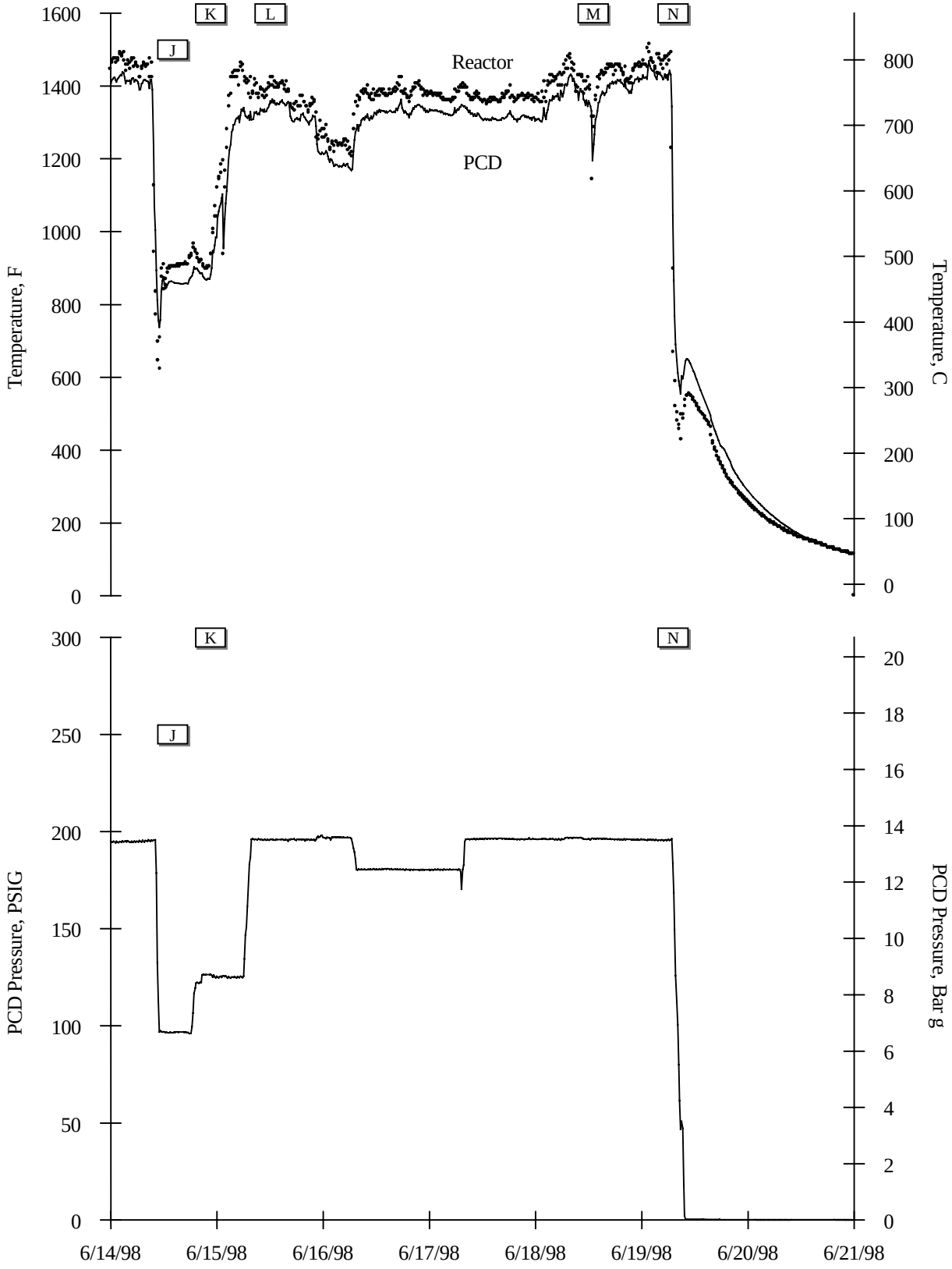


Figure 3.2-8 TC03 Temperature and Pressure for June 14 Through June 21

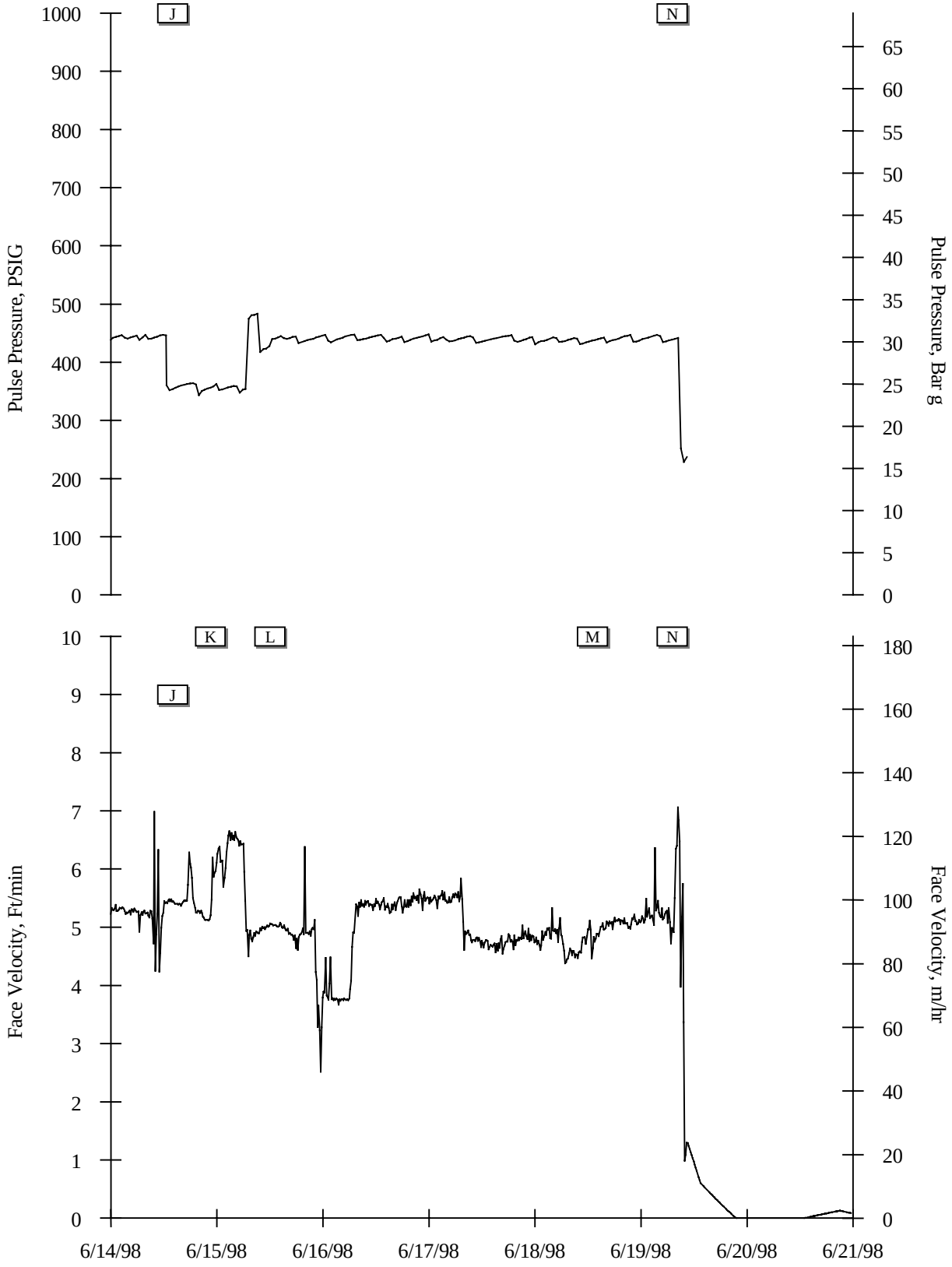


Figure 3.2-9 TC03 Back-Pulse Pressure and Face Velocity for June 14 Through June 21

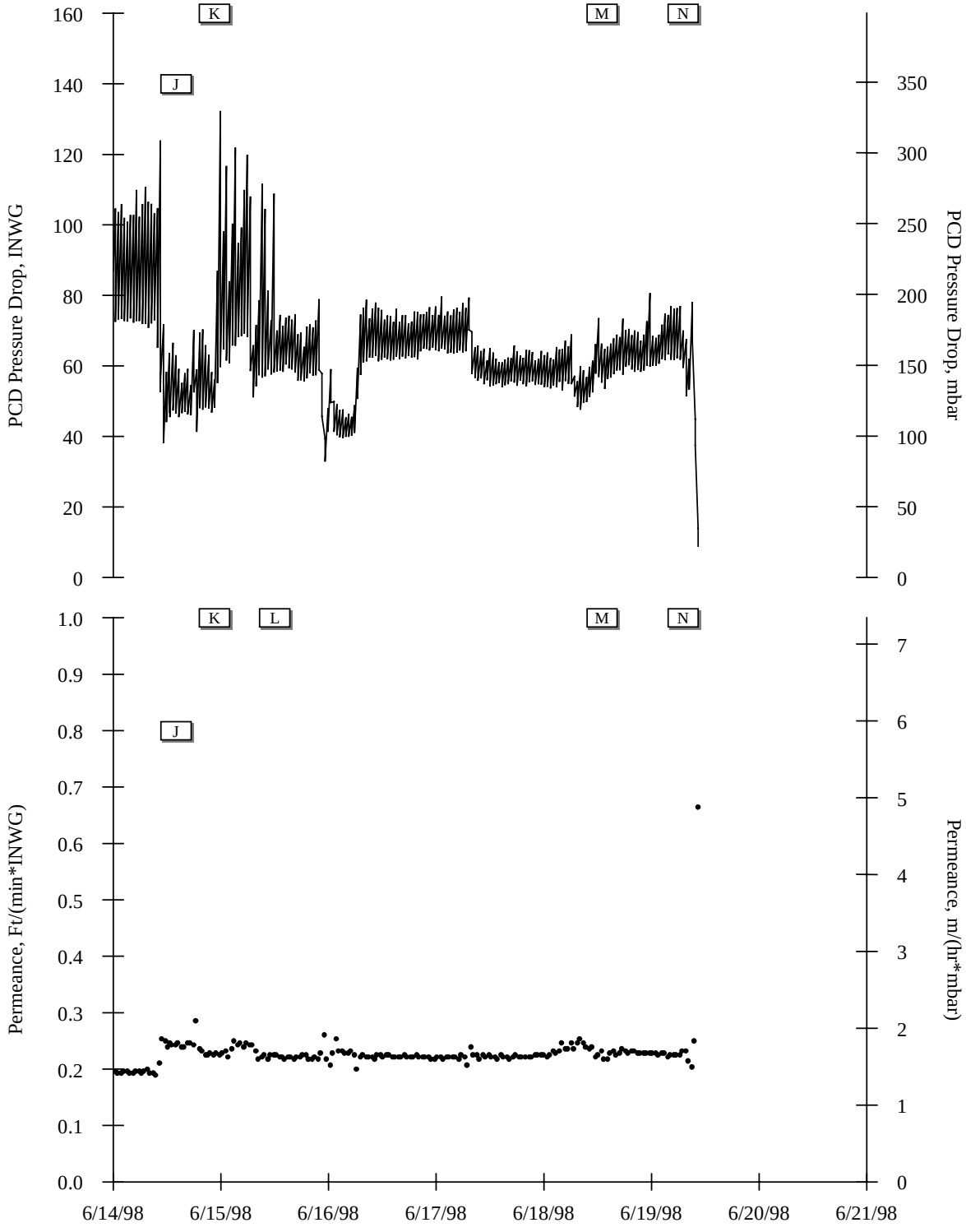


Figure 3.2-10 TC03 Pressure Drop and Permeance for June 14 Through June 21

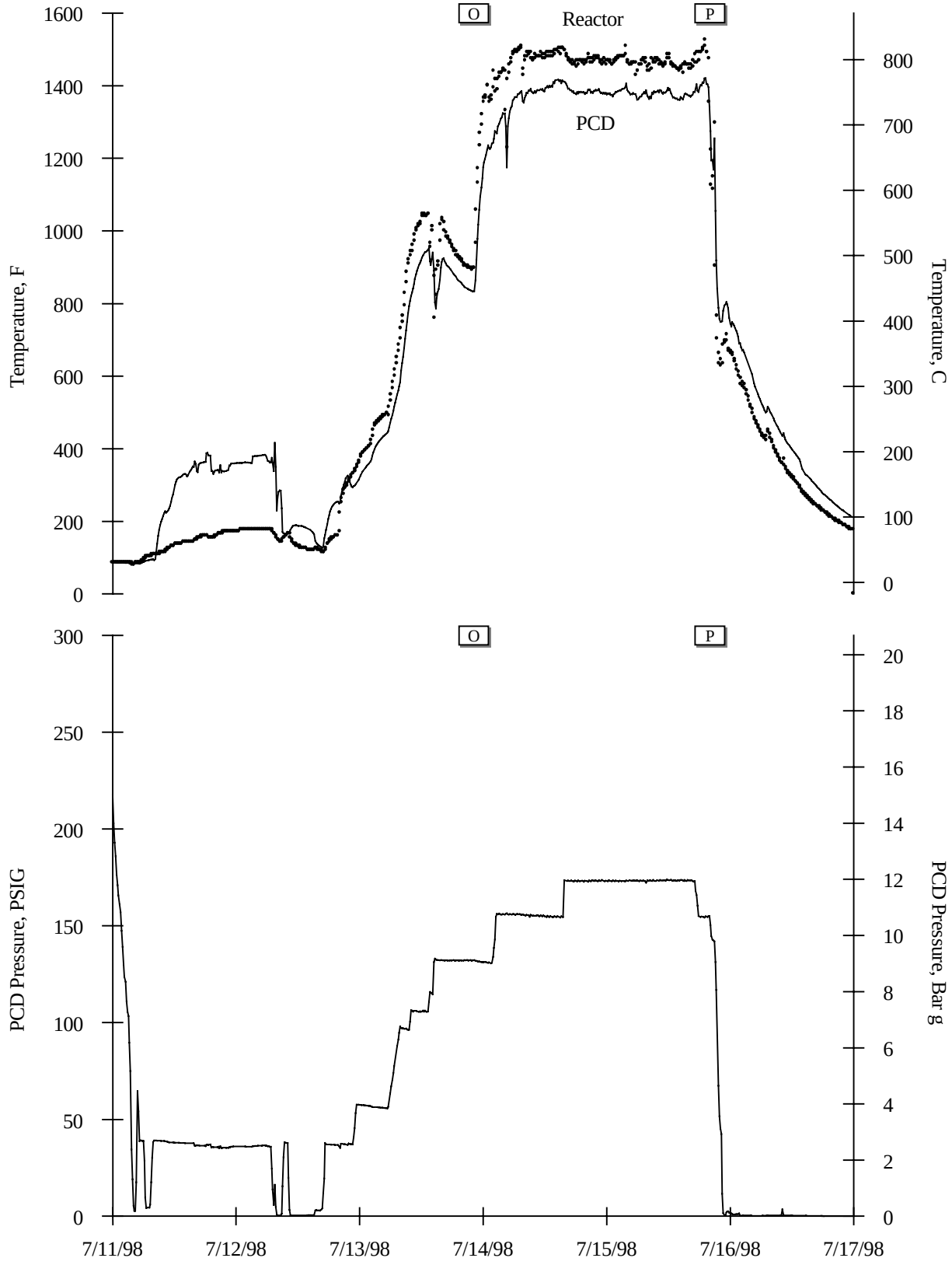


Figure 3.2-11 TC03 Temperature and Pressure for July 11 Through July 17

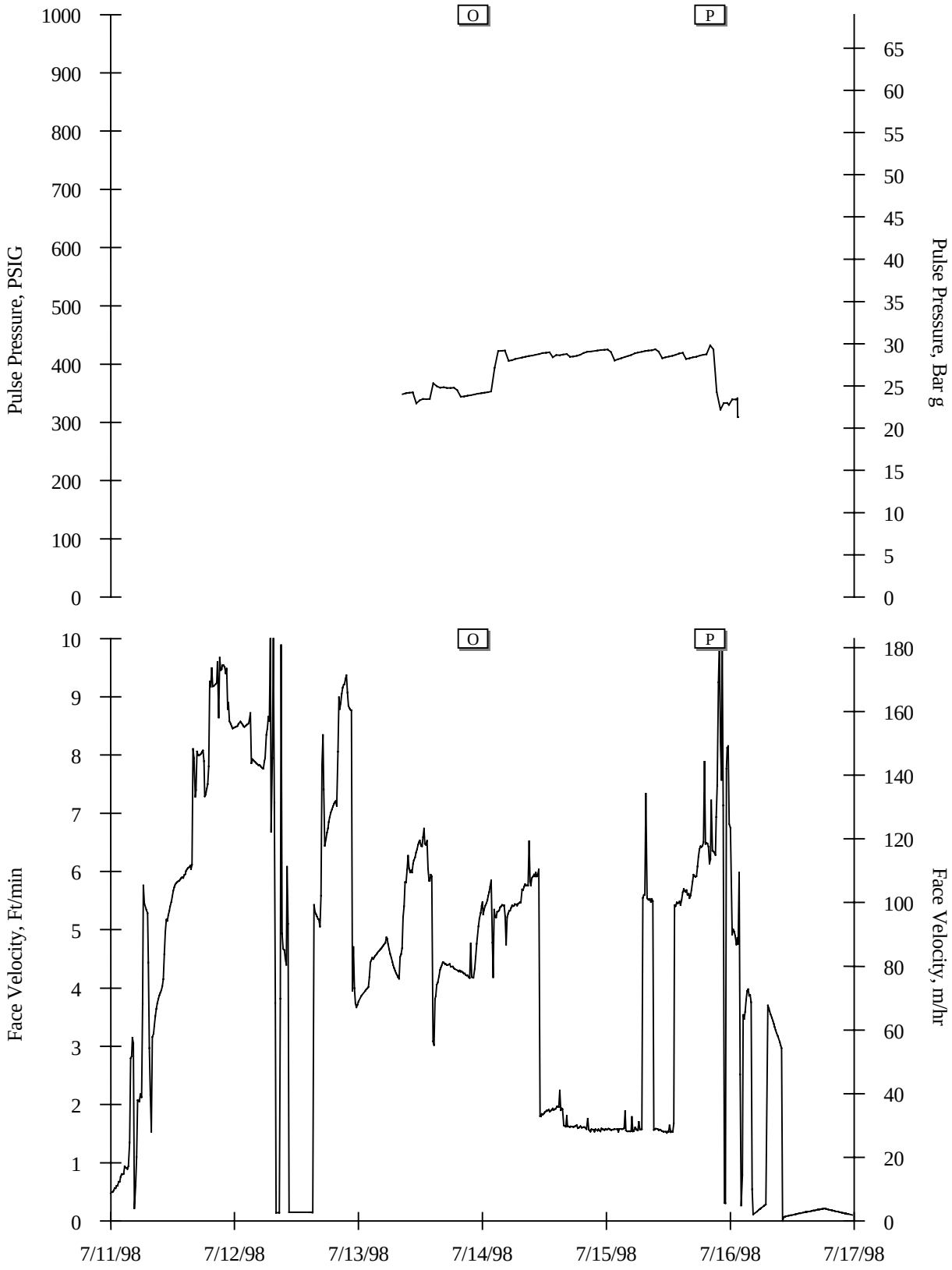


Figure 3.2-12 TC03 Back-Pulse Pressure and Face Velocity for July 11 Through July 17

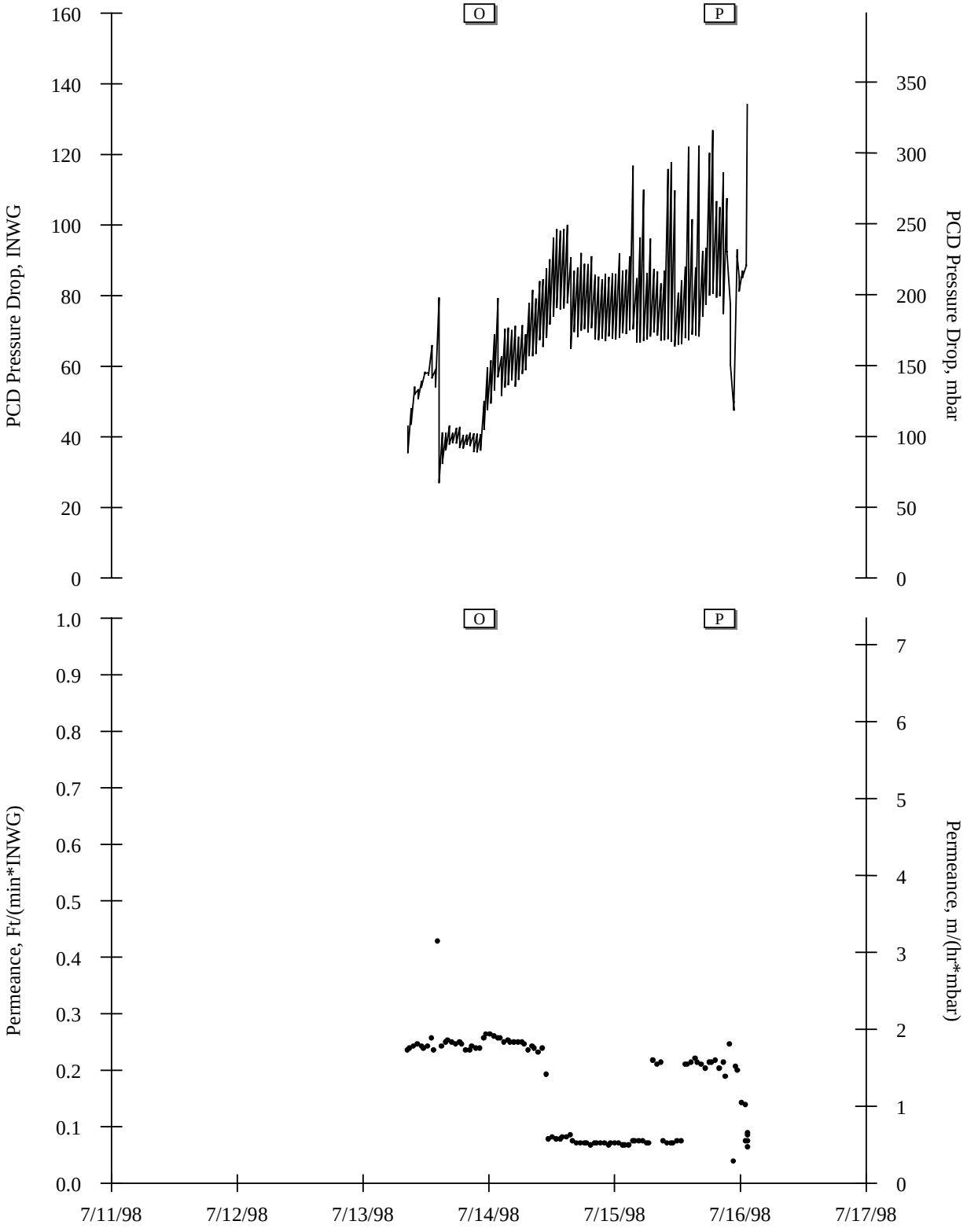


Figure 3.2-13 TC03 Pressure Drop and Permeance for July 11 Through July 17

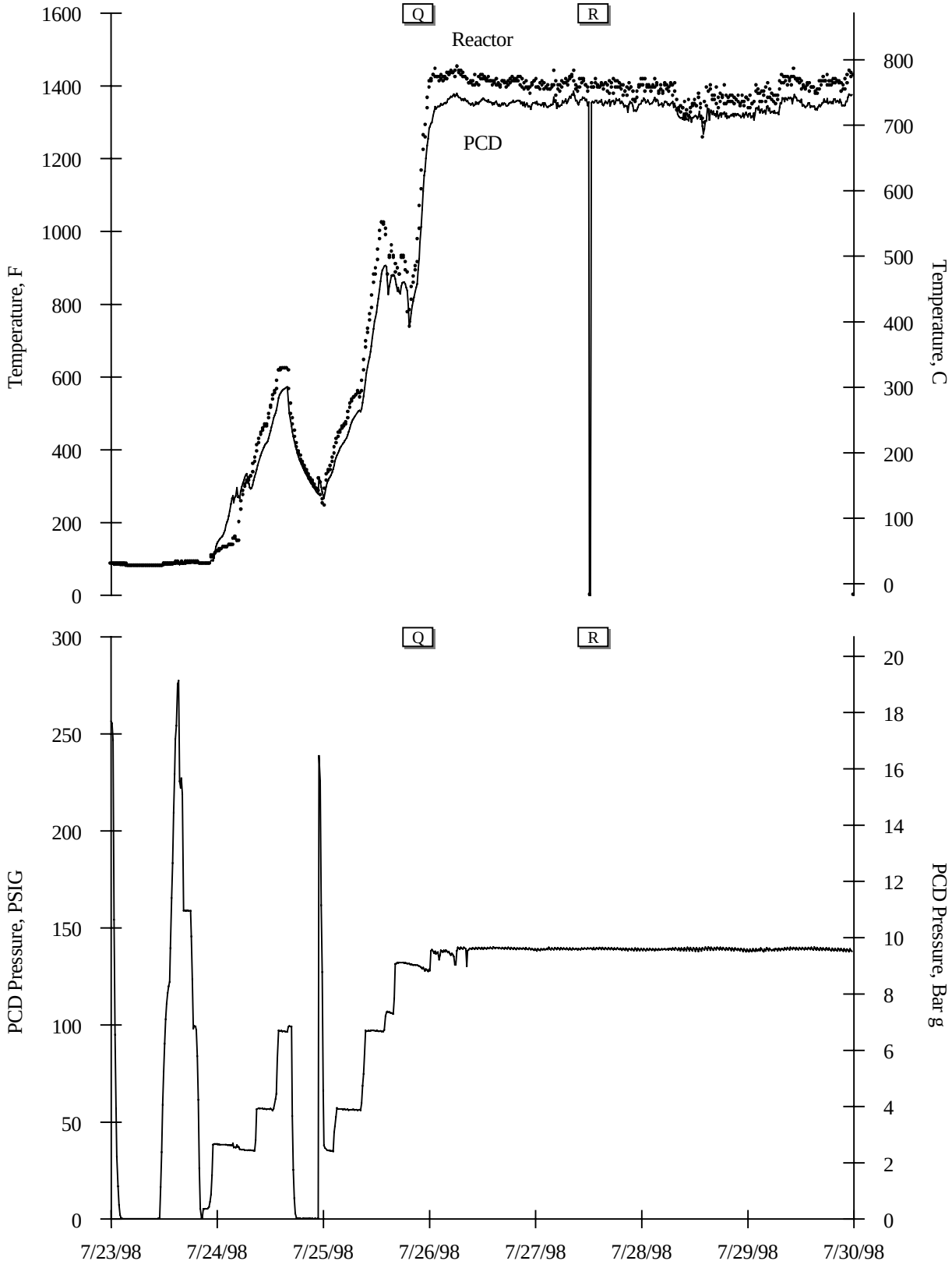


Figure 3.2-14 TC03 Temperature and Pressure for July 23 Through July 30

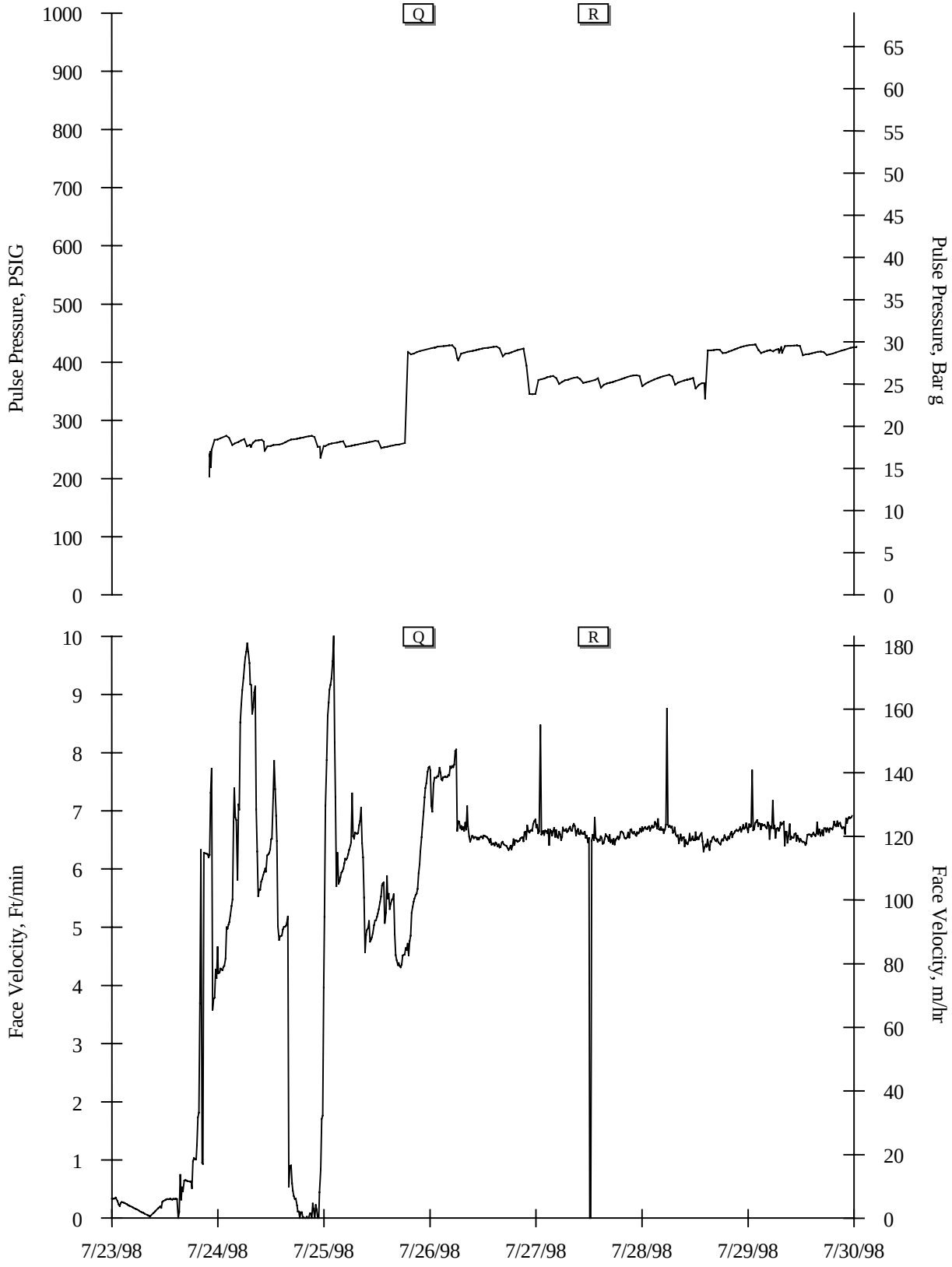


Figure 3.2-15 TC03 Back-Pulse Pressure and Face Velocity for July 23 Through July 30

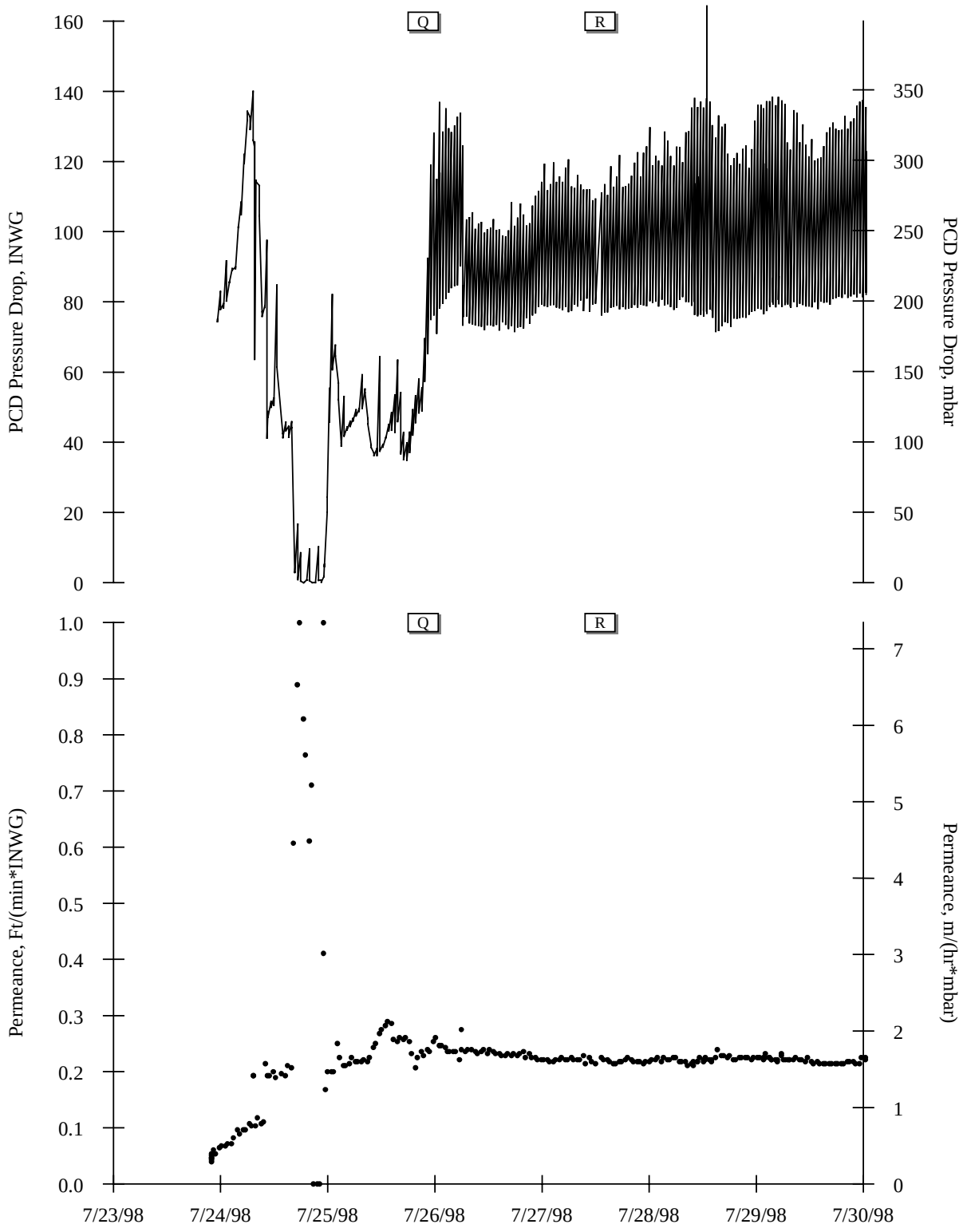


Figure 3.2-16 TC03 Pressure Drop and Permeance for July 23 Through July 30

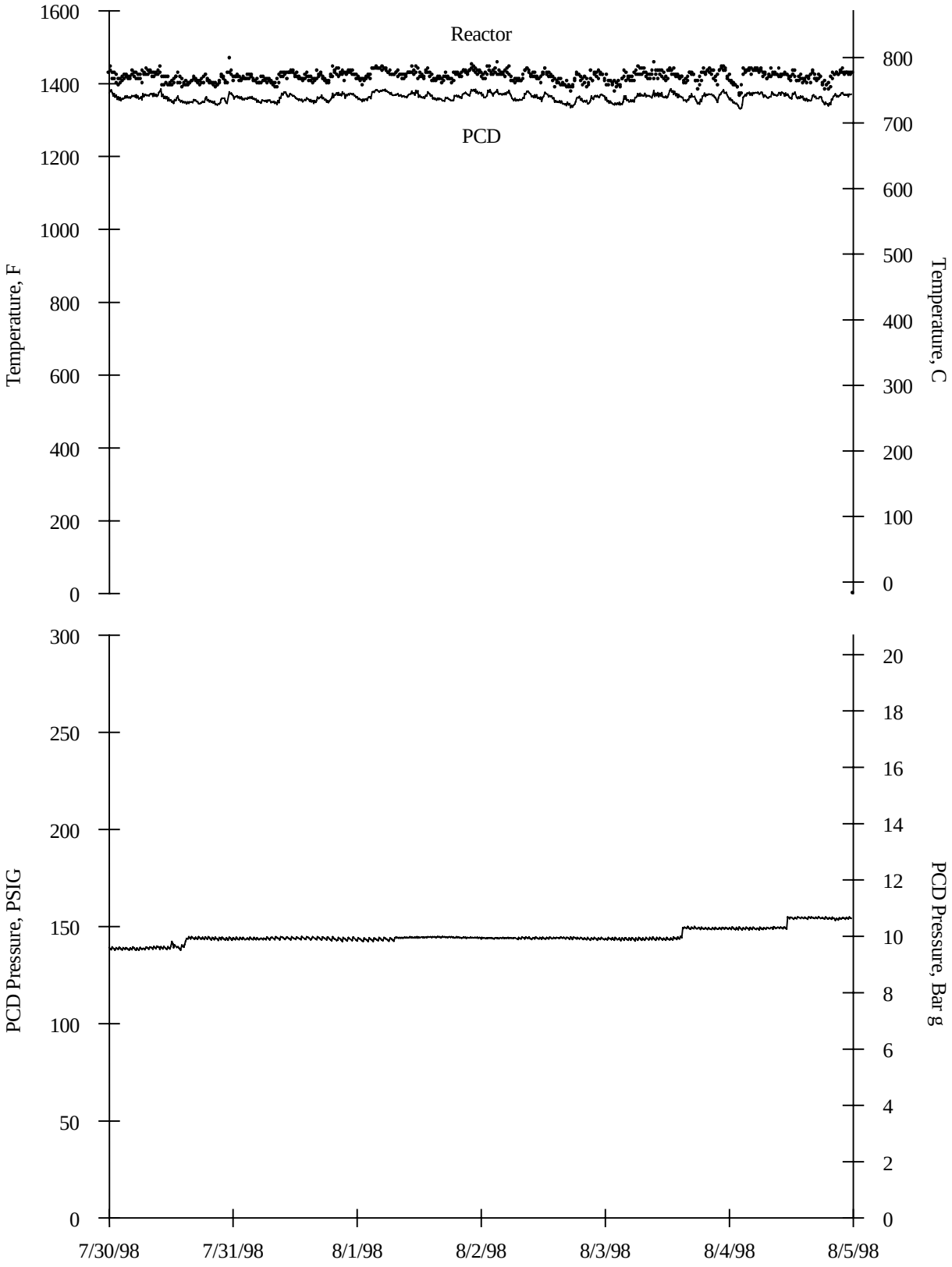


Figure 3.2-17 TC03 Temperature and Pressure for July 30 Through August 5

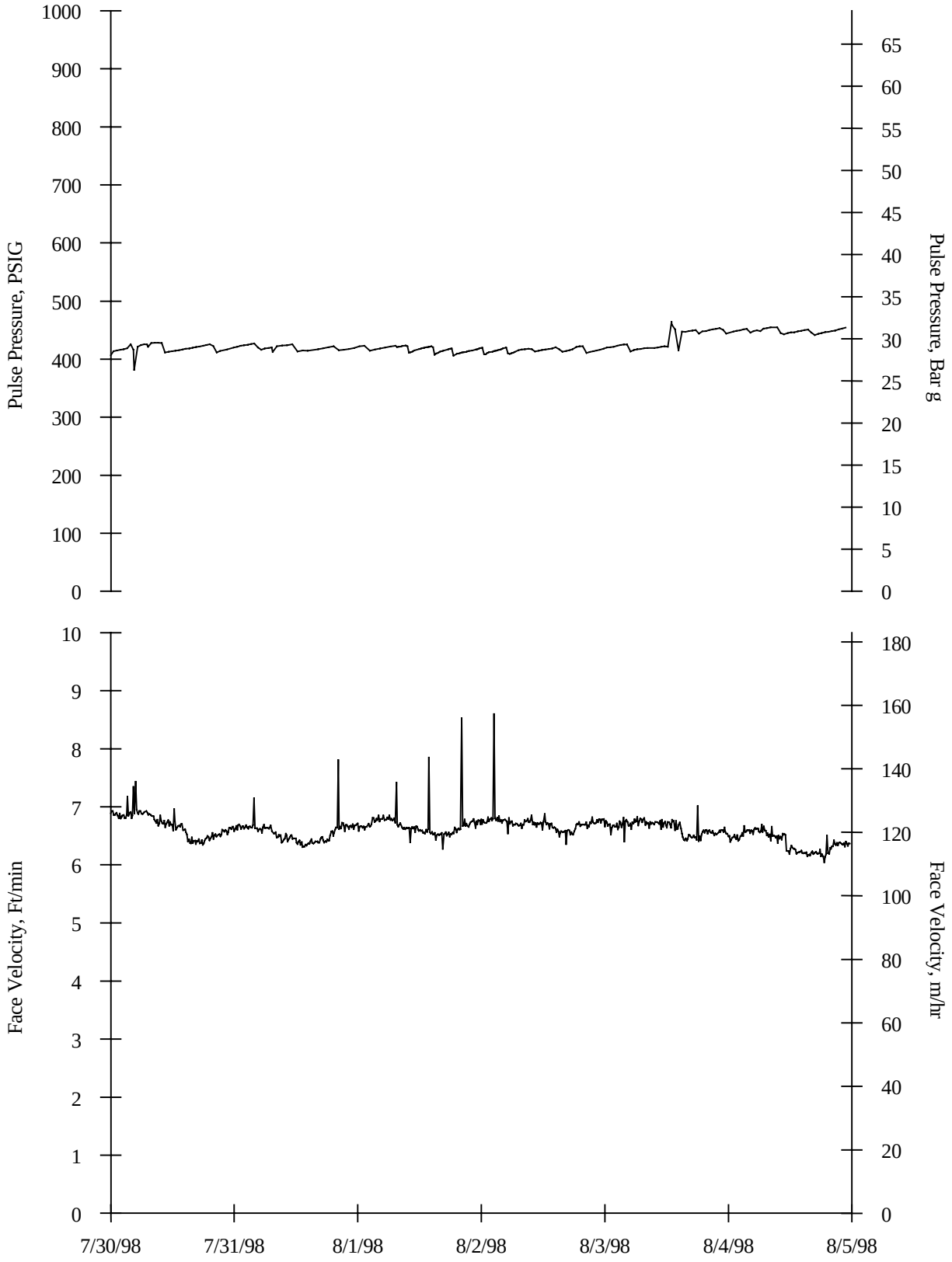


Figure 3.2-18 TC03 Back-Pulse Pressure and Face Velocity for July 30 Through August 5

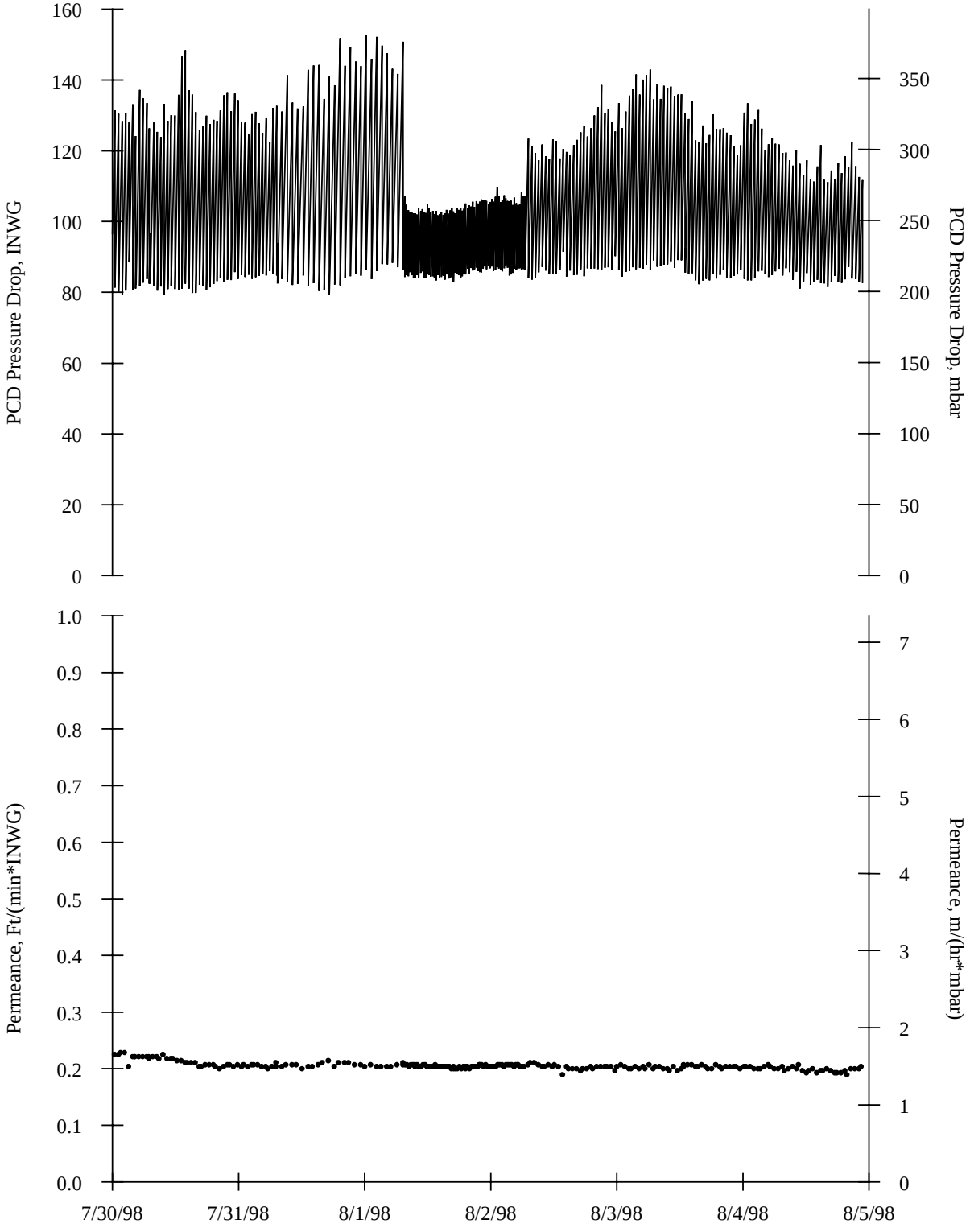


Figure 3.2-19 TC03 Pressure Drop and Permeance for July 30 Through August 5

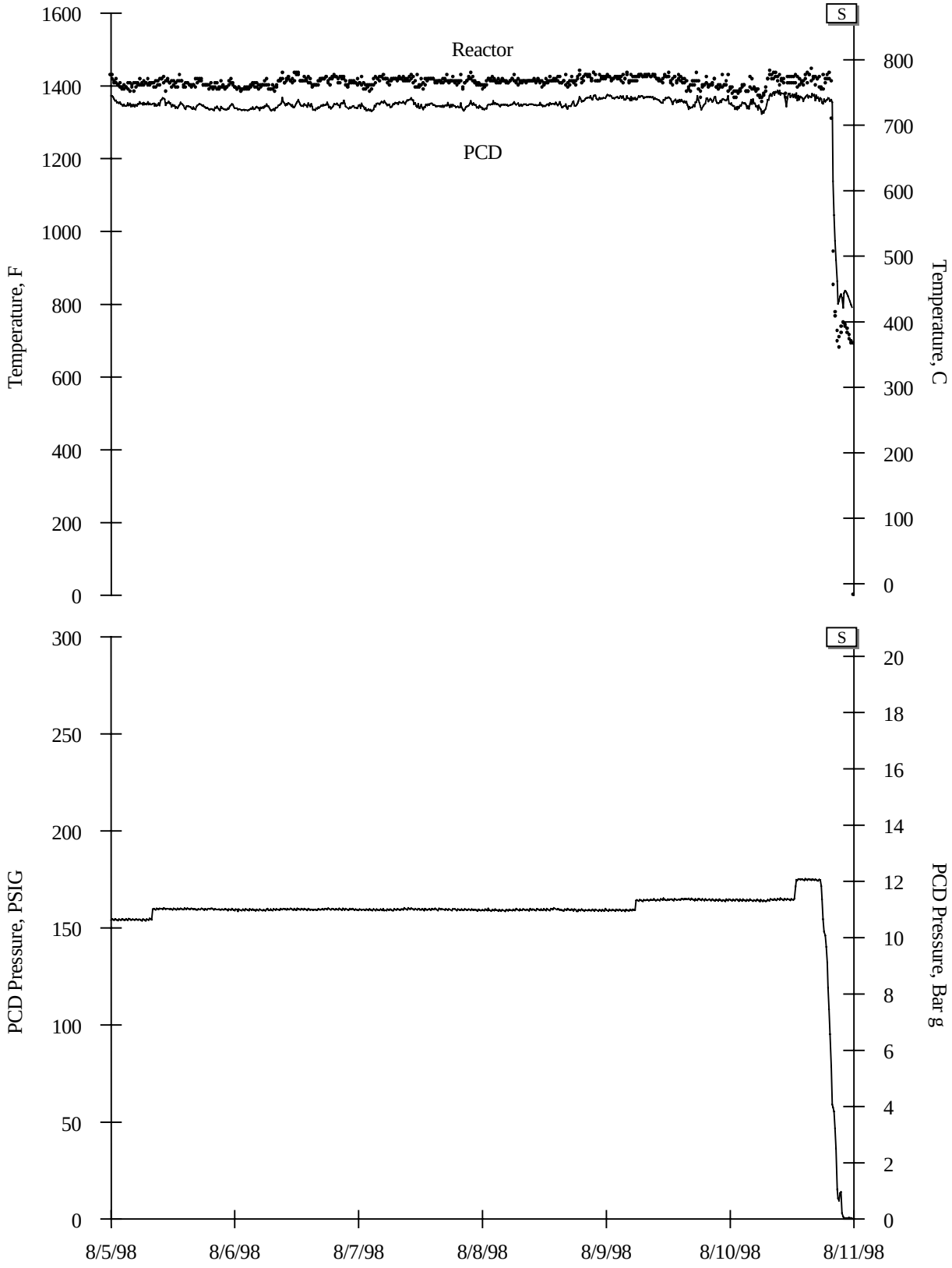


Figure 3.2-20 TC03 Temperature and Pressure for August 5 Through August 11

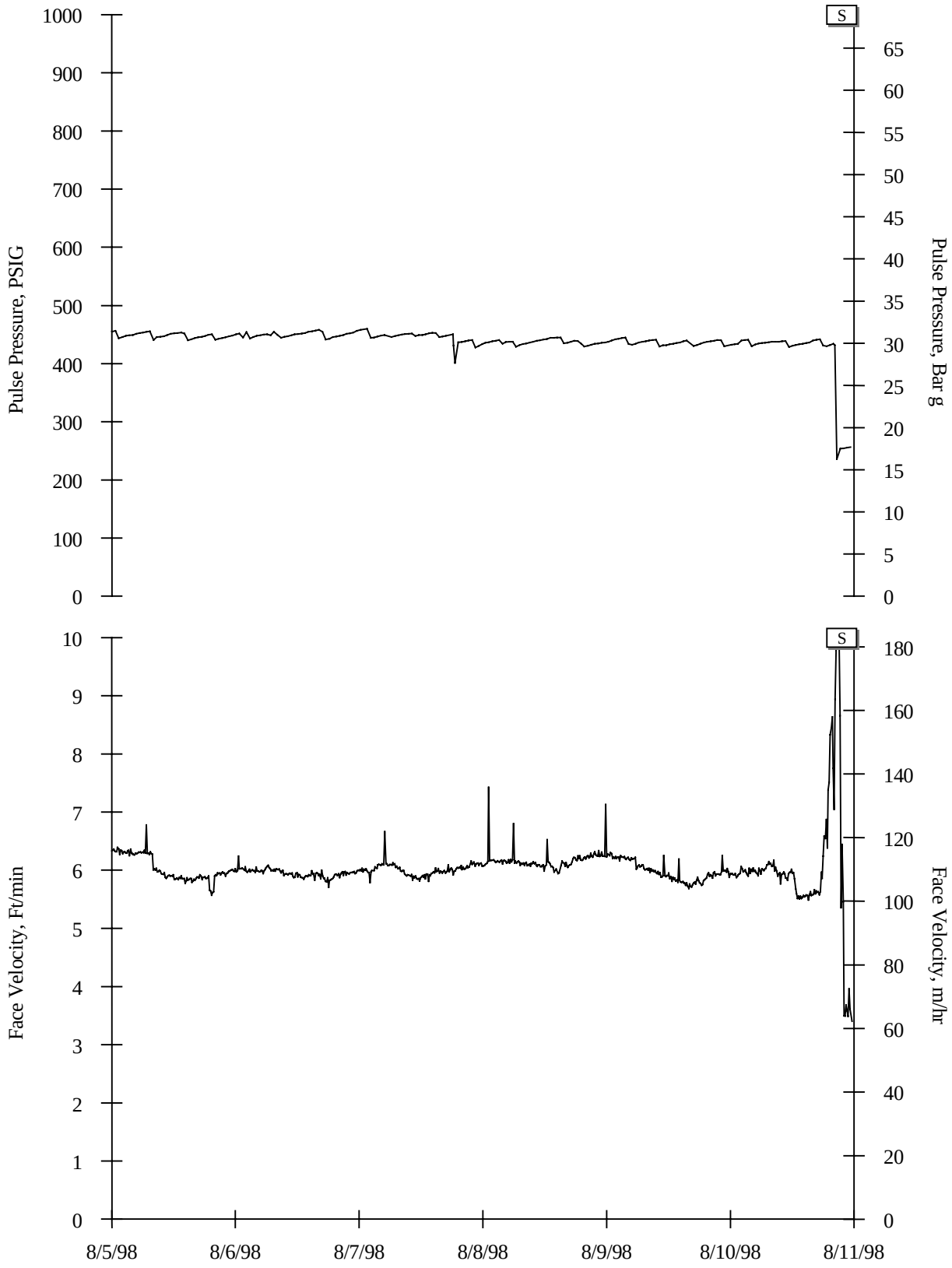


Figure 3.2-21 TC03 Back-Pulse Pressure and Face Velocity for August 5 Through August 11

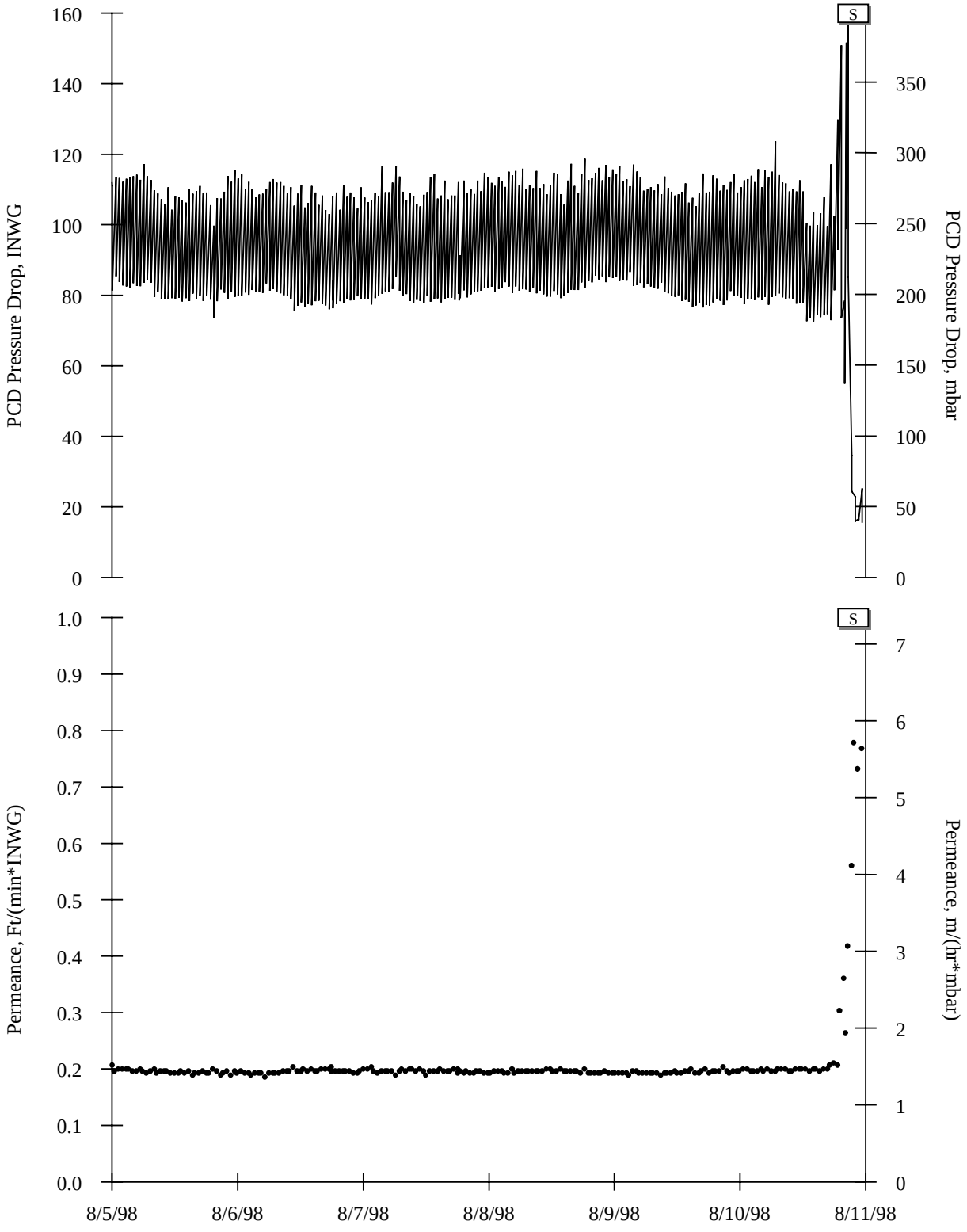


Figure 3.2-22 TC03 Pressure Drop and Permeance for August 5 Through August 11

## 3.3 TC03 INSPECTION REPORT

### 3.3.1 Summary

Test campaign TC03 ended on August 10, 1998, as a part of a controlled shutdown. Once the PCD tubesheet and elements were lifted from the vessel and placed in the maintenance bay, inspection of the exposed elements and installation of the new elements began. The inspection revealed no bridging, no evidence of leaking gaskets, no broken filter elements, and normal accumulation of ash around the filter holders. The particulate control device (PCD) had performed well with no problems.

### 3.3.2 PCD Inspection and Dustcake Observations

Installation of filter elements into the plenum for TC04 was completed at the beginning of October. However, it was noticed when the vessel head was removed for installation of the plenum that the bottom of the shroud was slightly out of round. Upon inspection, it was discovered that the supports for the cone liner had failed to the extent that they were distorting the shroud. Figure 3.3-1 shows one of these failed liner supports. Figure 3.3-2 shows the shroud opposite the failure being pushed to the side of the liner. Figure 3.3-3 shows the shroud distortion from the top. The reason for the failure appears to be ash accumulating between the cone liner and the refractory in the cone. Due to the liner design, there is no way to remove this ash, neither during operation nor during an inspection. The fiberfrax between the liner and the refractory prevents the ash from draining out. The cone liner under normal operating conditions grows down with heating. This downward growth is not possible with the accumulation of ash between the liner and the refractory, so the cone liner grows upwards instead. Figure 3.3-4 shows evidence of this upward growth relative to a stationary thermocouple located in the cone. This upward growth sheared off all four supports and caused several supports to kick out, catch the lip of the shroud, and cause the distortion. The liner supports had become caught on the stiffening ring of the shroud, and to remove the shroud and repair the liner, the shroud had to be notched at the bottom, as shown in Figure 3.3-5.

A solution has not been determined, but several options have been discussed with Siemens Westinghouse. In the meantime, the supports for the cone liner were removed, the cone liner was modified near the thermocouples to prevent additional binding of the liner.

It was also discovered during the inspection that the middle section of the liner, which includes the tangential inlet, was heavily distorted. The worst area of distortion was at the inlet nozzle and at places where the liner was in contact with the shroud. This distortion is undoubtedly disrupting the gas distribution in the vessel, but it is not possible to quantify the effect of the disruption at this time. Figure 3.3-6 shows this distortion.

Additionally, the pulse pipes showed substantial deterioration primarily at the cold end. Figure 3.3-7 shows the condition of the pulse pipes after removal. After monitoring the progress of this deterioration over several previous test runs, it was decided to replace the top portion (the part with the most corrosion and cracking) of the pulse pipes.

Figure 3.3-8 shows the bottom plenum as removed from the PCD. The PCD had been back-pulsed prior to this inspection and extensively during and after the TC03 shutdown. There was only a very thin dustcake (thickness < 0.1 in.) remaining on any of the filter elements.

### 3.3.3 Inspection Outcome

Most of the inspection centered on preparation for TC04, since there were no issues to address from TC03. Three new Pall 326 elements (two on the bottom plenum and one on the top plenum) and two fail-safes (one on bottom plenum and one on top plenum) with thermocouples were installed in the vessel for TC04. Figure 3.3-9 shows an element with thermocouples installed. Additionally, only 57 elements were installed for TC04 so that the face velocity for the elements could be raised to 7 ft/min. Figure 3.3-10 shows the blanks as installed in the plenum. Among the elements installed for TC04 were: a pair of 2-meter 3M oxide elements and a pair of 2-meter Pall 326 elements. Figure 3.3-11 shows the 2-meter 3M oxide elements and the 2-meter Pall 326 elements. Figure 3.3-12 shows the final arrangement as installed for TC04.

Figure 3.3-1 Failed Liner Support

Figure 3.3-2 Shroud Touching Vessel Liner

Figure 3.3-3 Distortion of the Shroud

Figure 3.3-4 Upward Cone Liner Growth

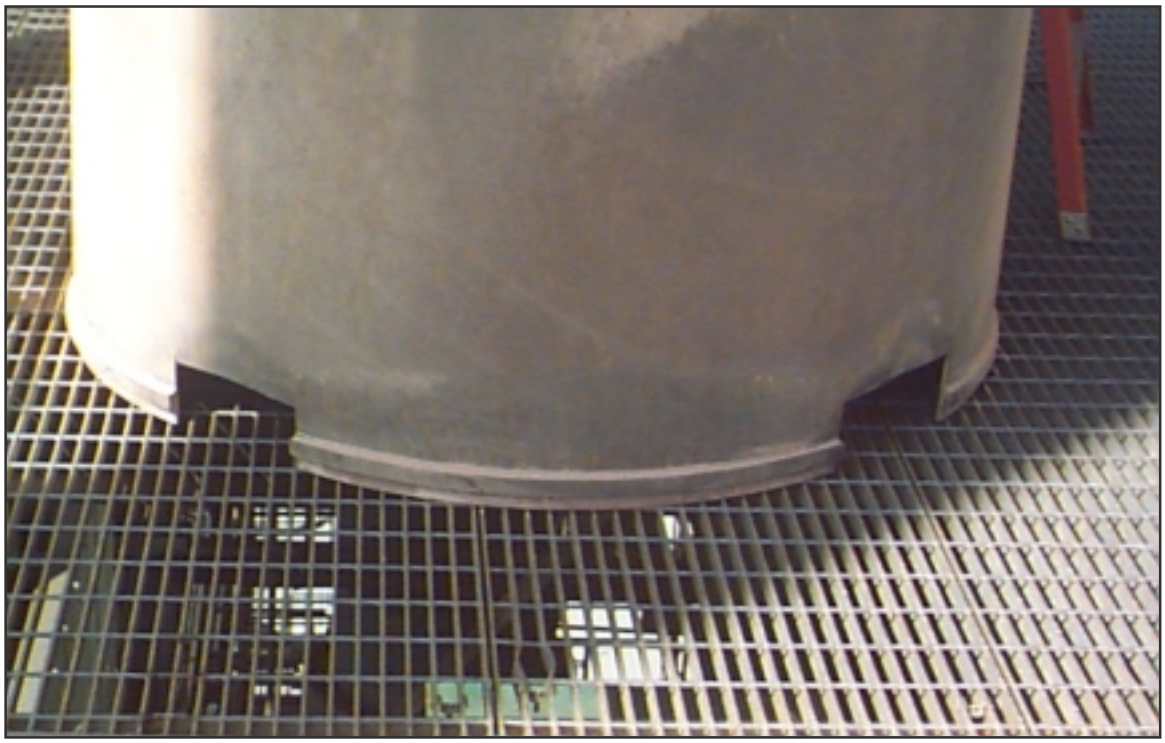

Figure 3.3-5 Notches in the Shroud

Figure 3.3-6 Liner Distortion Near Inlet

Figure 3.3-7 Cracked Pulse Pipe

Figure 3.3-8 Bottom Plenum After Removal From PCD

Figure 3.3-9 Thermocouples on Element

Figure 3.3-10 Installed Blank in Top Plenum

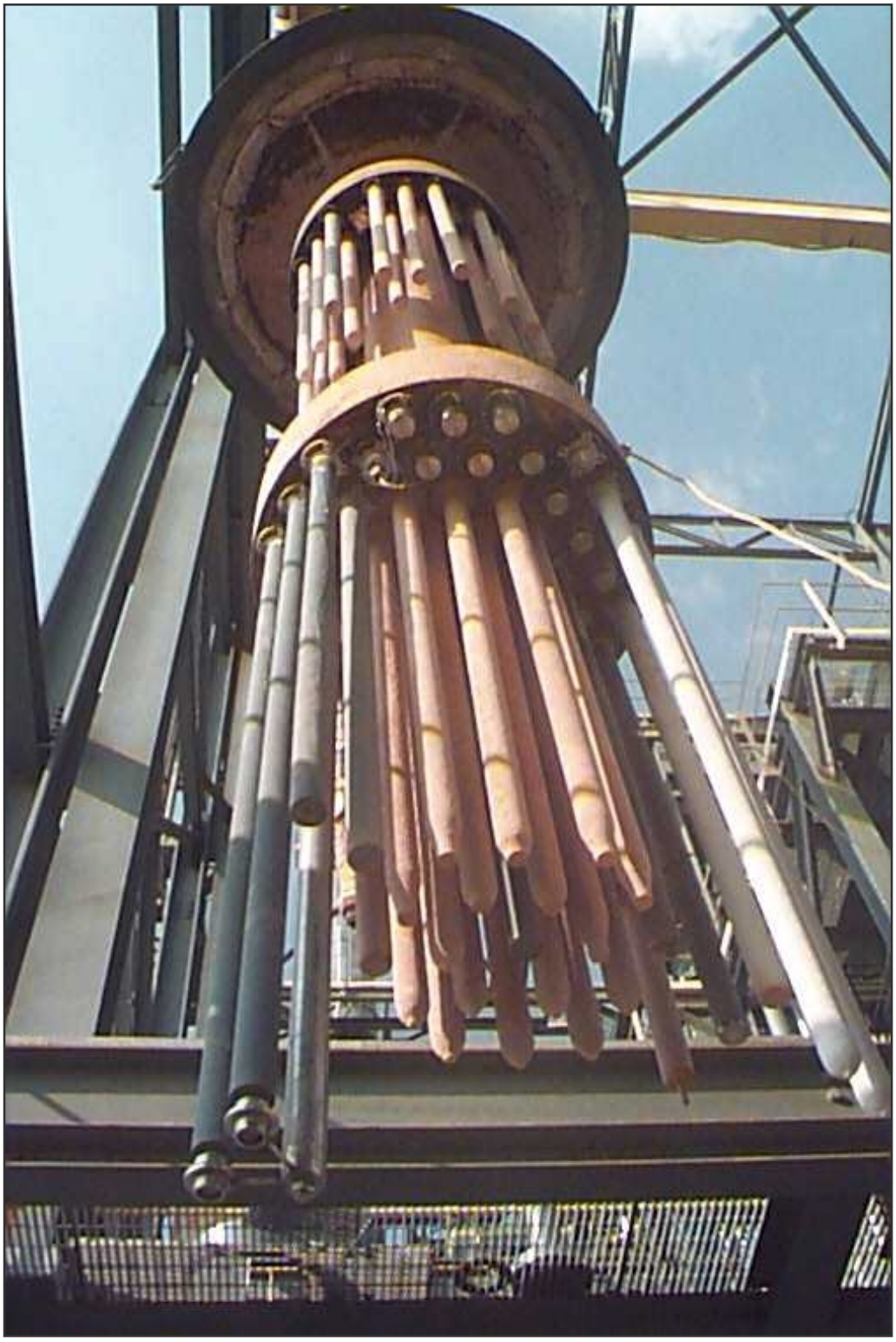

Figure 3.3-11 2-Meter Pall 326 Elements (Left) and 3M Oxide Elements (Right)

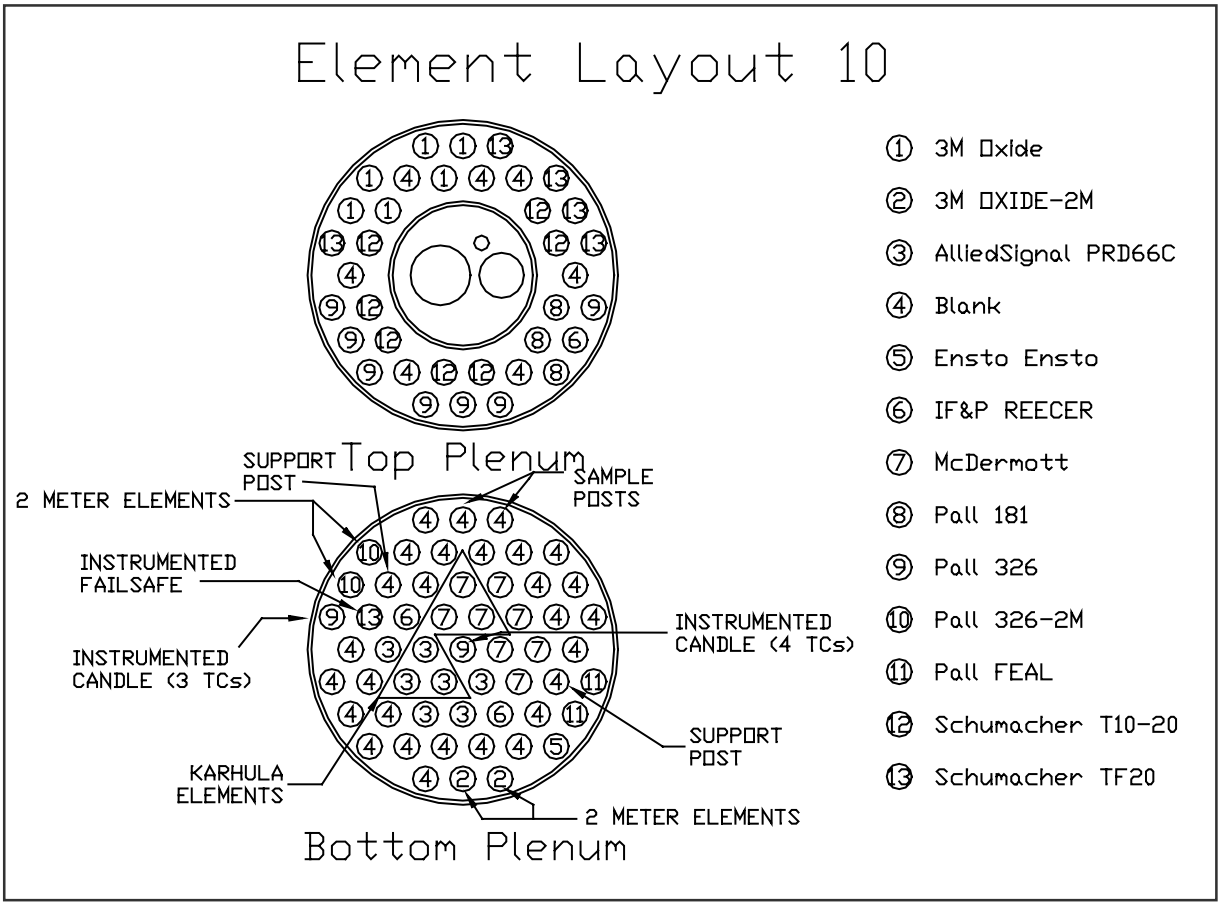


Figure 3.3-12 Element Layout 10 for TC04

## 3.4 TC03 ASH CHARACTERISTICS AND PCD PERFORMANCE

In situ particulate sampling runs were performed during TC03 on a regular basis at the PCD inlet and outlet. There were 17 samples taken of the particulate mass entering the PCD and 10 samples were taken of the particulate mass exiting the PCD. All of the samples collected at the PCD inlet and outlet were total particulate mass samples collected on a single filter (mass samples). No cascade impactor samples were collected because the outlet particulate loadings were too low for accurate particle-size discrimination. Initial sampling runs performed at the PCD inlet were directed at quantifying the particulate loadings produced with the Alabama coal and Plum Run dolomite used in previous tests. In subsequent runs, the Alabama coal was replaced with an Eastern Kentucky coal having a lower ash content. To quantify the effect of the sorbent addition on the inlet particulate loading, tests were performed with the Plum Run dolomite, three different types of limestone, and with no sorbent addition. The sampling effort included three PCD cut-size tests (i.e., measurements to quantify the fraction of solids that drop out ahead of the filter elements).

This report summarizes the particulate mass loadings determined from the TC03 sampling runs and PCD collection efficiencies calculated from the inlet and outlet loadings. Particle-size distributions determined by particle-size analysis in the laboratory are discussed and compared to particle-size measurements from previous test series. Significant physical and chemical characteristics of the in situ samples are presented and compared to the characteristics of ash samples taken from the PCD hopper and of dustcake samples taken from the filter elements after the TC03 shutdown. To investigate the usefulness of the laboratory characterization tests, flow-resistance (drag) measurements made on the in situ ash samples are compared to the transient drag across the PCD during the time interval when the in situ sample was collected.

### 3.4.1 Measurements of Particulate Mass Loadings

Inlet Measurements

Table 3.4-1 provides a summary of the inlet particulate loadings measured during TC03. The first three measurements (TC03IMT-01, -02, and -03) were made with the Alabama coal and Plum Run dolomite that were used in previous testing. These runs yielded particulate loadings of 8,300 to 8,600 ppmw, which were slightly lower than the particulate loadings measured during TC02 (9,100 to 11,100 ppmw). The lower loadings were attributed to higher flue gas velocities through the primary cyclone, which produced higher cyclone collection efficiencies and lower particulate loadings to the PCD.

All subsequent TC03 sampling runs were done with the Eastern Kentucky coal, which is being considered for the Lakeland clean coal technology project. Lower particulate loadings were expected with the Eastern Kentucky coal because the ash content of the Eastern Kentucky coal is significantly lower than the ash content of the Alabama coal. Contrary to this expectation, the single sampling run performed with the Eastern Kentucky coal and Plum Run dolomite (TC03IMT-04) yielded a loading that was similar to those measured with the Alabama coal and the Plum Run dolomite (9,200 ppmw versus 8,300 to 8,600 ppmw). The effect of the lower ash content may not have been evident in the measured particulate loadings because the incremental decrease in solids flow was very small compared to the total solids circulation rate. (The

difference in ash content would account for an incremental decrease in solids input on the order of 100 lb/hr out of a total solids circulation rate on the order of 50,000 lb/hr. Because of the dynamics of the transport reactor system, it would probably take several days for the effect of the reduced solids input to be seen at the PCD inlet.)

The next step in the TC03 test plan, after establishing stable transport reactor operation with the Eastern Kentucky coal and Plum Run dolomite, called for gradual replacement of the dolomite with Gregg limestone. This is the limestone being considered for the Lakeland clean coal technology project. Unfortunately, an increase in solids carryover caused the last batch of dolomite to be consumed more rapidly than expected, resulting in a relatively quick build up of the solids level in the bed using the Gregg limestone. Transport reactor operation became unstable during this sudden transition to limestone and resulted in unusually high levels of particulate carryover, as indicated in the results of runs TC03IMT-05 and -06. As expected, the particulate loadings measured during the unstable operation were relatively high (30,900 and 12,900 ppmw). Unstable operation may have contributed to the formation of a clinker in the transport reactor loop that forced a plant shutdown in mid-June.

After removing the clinker, the transport reactor system was restarted in July and stable operation was established with the Eastern Kentucky coal and Gregg limestone. Two sampling runs (TC03IMT-07 and -08) were performed and yielded particulate loadings of 5,100 and 6,500 ppmw. These lower loadings may be partially attributable to the lower ash content of the Eastern Kentucky coal and the lower mass feed rate of sorbent associated with the use of limestone instead of dolomite. However, velocities through the primary cyclone were higher during the limestone addition than they were during the dolomite addition. The higher cyclone velocities resulted in higher cyclone collection efficiencies, which also helps to explain the lower particulate loadings obtained with limestone.

All of the subsequent TC03 testing was done with Eastern Kentucky coal and with several different types of limestone (Gregg, Bucyrus, and Longview) as shown in Table 3.4-1. The results obtained from the Eastern Kentucky coal with the various sorbents are summarized below.

| Sorbent | Loading, ppmw |
|---|---|
| Plum Run dolomite | 9,200 |
| Gregg limestone | 5,100 to 6,800 |
| Bucyrus limestone | 6,200 to 8,500 |
| Longview limestone | 5,700 to 7,700 |

Particulate loadings generated with the various types of limestone were generally lower than the particulate loadings generated with dolomite. This result is to be expected because about 184 lb of dolomite is required to supply one lb-mole of calcium, while only about 100 lb of limestone is required to supply the same amount of calcium. The higher cyclone velocities mentioned earlier were also partly responsible for the reduced particulate loadings obtained during limestone addition.

Outlet Measurements

Table 3.4-2 provides a summary of the outlet particulate loadings measured during TC03. This information shows that outlet particulate loading varied from 0.03 to 0.37 ppmw. Also included in the table are the corresponding blank values for each run. The blank values indicate the magnitude of the error associated with flue gas interaction with the filter material, weighing errors, and any other problems that may have occurred in handling the substrates. The measured loadings in all but one case were at least 60 percent greater than the corresponding blank values, suggesting that there was a very low, but measurable, concentration of dust in the flue gas. The TC03 outlet loadings were significantly lower than the 5- to 12-ppmw outlet loadings obtained during TC02, when there was some leakage caused by an inadequate sealing arrangement between the 3M filter elements and the tubesheet. This problem was solved prior to TC03 by the use of a 3M-designed insert that facilitated a positive seal in the area of the element flange, fail-safe, and tubesheet.

Collection Efficiency

PCD collection efficiencies shown in Table 3.4-3 were calculated using corresponding inlet and outlet loadings measured on the same day. These collection efficiencies are quite high compared to those obtained with control technologies that are currently in service at conventional coal-fired power plants. Collection efficiencies reported here confirm that there was essentially no particulate penetration through the PCD during any segment of TC03. Outlet loadings as high as 12 ppmw had been measured during TC02. As mentioned above, the source of this particle penetration was traced to a sealing problem between the 3M filter elements and their fail-safe devices that allowed particles to penetrate between the tubesheet and the element/fail-safe assembly. Ceramic inserts designed by 3M were placed in the 3M filter elements to address this problem and, therefore, ensure a positive seal between the components in question. The outlet loadings measured during TC03 confirm that the ceramic inserts were effective in eliminating the leakage that had previously occurred.

### 3.4.2 PCD Cut-Size Tests

As discussed in previous reports, any meaningful analysis of PCD performance must take into account the particulate dropout that occurs within the PCD vessel. SRI performed several series of PCD cut-size tests, where ash that is dropped out between PCD back-pulses is segregated within the ash discharge system and collected separately in order to quantify the fraction of the inlet particulate matter that drops out ahead of the filter elements. In each cut-size test, the collection of the dropout ash is coordinated with an inlet particulate sampling run. In theory, this procedure should make it possible to measure, within the same time interval, the total particulate mass entering the PCD and the mass of particles dropping out. In actual practice, however, the performance of these tests is complicated by the holdup of ash within the ash discharge system and the possibility of contamination of the dropout ash with ash that is back-pulsed off the filter elements. The effect of these problems on the test results can be minimized by paying close attention to the timing of the sample collection and by carefully monitoring thermocouples in the ash discharge system. The PCD hopper was fluffed with nitrogen and the ash transport system was cleared of all solids prior to beginning the collection of samples in order to help clear out any old ash deposits. Three PCD cut-size tests were performed during

test TC02, but two of the tests were unsuccessful because of contamination of the dropout sample with back-pulsed ash. Based on the single successful test, the particulate dropout was estimated to be 28 percent.

Since only one successful cut-size test was completed during TC02, the test was repeated in TC03. The TC03 cut-size test was coordinated with the first TC03 in situ sampling run (TC03IMT-1). This run was done with Alabama coal and Plum Run dolomite, the same type coal and sorbent used in TC02. The results of the TC03 cut-size test indicated that about 26 percent of the particulate mass entering the PCD dropped out before reaching the filter elements, which almost matches the 28-percent dropout measured during TC02. It is important to note that this degree of dropout applies only to this particular combination of coal and sorbent and to these particular operating conditions. Since particle settling is a function of particle size, particle density, and gas velocity, the degree of particulate dropout may vary with changes in the type of coal and sorbent and with differing operating conditions (e.g., changes in the efficiency of the cyclone upstream of the PCD and changes in the gas velocity between the PCD vessel wall and the shroud).

The effect of particle size on ash dropout in the PCD is illustrated in Figure 3.4-1. This figure shows the particle-size distributions of the inlet particulate sample and of the dropout material collected between PCD back-pulses. The size distributions are compared on the basis of differential mass to allow a direct comparison of the inlet particulate mass and the dropout mass in a given particle-size interval. For particle sizes smaller than about 2.5 μm, the inlet particulate mass is about 2 orders of magnitude higher than the dropout mass in the same size interval. At 4 μm, the inlet mass has a factor of 16 times higher than the dropout mass. The factor is reduced to about 9 at a particle size of 10 μm, to about 4 at a particle size of 25 μm, and to a factor of 1 at particle sizes above 80 μm. These results confirm that the particle dropout in the PCD is a strong function of particle size, as illustrated in Figure 3.4-2. This figure shows the particle removal efficiency calculated from the size distributions of the inlet ash and of the dropout ash. As expected, almost all of the very large particles ($D_p$ > 100 μm) drop out in the hopper, while almost none of the very small particles ($D_p$ < 2.5 μm) drop out.

Over the particle-size range of 2.5 μm to about 40 μm, the particle dropout efficiency apparently varies from about 1 to about 30 percent. Generally lower dropout efficiencies were expected over this size range because the gravitational settling velocities of these particles are in the range of 0.0007 to 0.15 ft/sec. The most likely explanation for the unexpectedly high dropout in this size range is that these smaller particles were actually removed as part of larger agglomerates, which were subsequently broken apart during the laboratory particle sizing. (The laboratory particle-size analysis procedures include ultrasonic dispersal of the particles, which could break apart fragile agglomerates.)

As indicated previously, the total particulate dropout in the PCD was determined to be about 26 percent based on the total masses of inlet dust and dropout dust collected. Based on the measured-size distribution of the inlet dust, 26 percent of the inlet particulate would include all particles larger than about 45 μm. This suggests that there was very little dropout of particles smaller than 45 μm and that the dropout of particles smaller than about 45 μm contributes very little to the total mass of dropout ash collected between back-pulses, as would be expected based on the settling velocities of these particles.

### 3.4.3 Chemical Analyses

Table 3.4-4 summarizes the chemical composition of selected in situ particulate samples collected during TC03. Samples from runs TC03IMT-5 to -8 were not analyzed because process conditions were not stable during these runs. Table 3.4-5 shows the same compositional information for the hopper samples and Table 3.4-6 contains comparable data for the dustcake samples taken from the PCD filter elements during the post-TC03 PCD inspection. All of the analytical results are reported as the element, on an ignited basis. The elemental concentrations are not reported in their oxide forms, since calcium is predominantly present in the form of the sulfate and carbonate, and other ash constituents may be present as sulfates, carbonates, silicates, aluminosilicates, halides, and sulfides. The procedures used to convert the elemental analysis into chemical composition ($CaCO_3$, $CaSO_4$, etc.) have been described in previous reports. The same procedures were followed with the TC03 ash samples, except that CaO•MgO was not an allowed species when the sorbent was limestone rather than dolomite. All calcium in the samples generated during limestone addition that was not accounted for as $CaCO_3$ or as $CaSO_4$ was assumed to be present as CaO.

In situ Samples

Analyses reported in Table 3.4-4 show that calcium utilization (i.e., the percentage of the calcium that is converted to calcium sulfate on a molar basis) varied from about 49 to 78 percent, depending on the test conditions and the amount of dolomite or limestone being added. The values of calcium utilization were generally in the range expected, based on the observed $SO_2$ removals and the amount of sorbent injected. The calculated chemical compositions of the TC03 in situ samples are summarized below and compared to those calculated for the TC02 in situ samples. Comparisons with TC01 in situ samples could not be made because sulfur and carbonate were not measured on the TC01 samples.

The TC03 in situ sample information listed below shows that samples collected during sorbent addition generally contained more $CaSO_4$ and less ash/sand than did the TC02 in situ samples. Nevertheless, the average calcium utilizations were in the same range for both sets of in situ samples.

Chemical Compositions of In situ Samples From TC03

| Test | TC02 | TC03 | TC03 | TC03 | TC03 |
|---|---|---|---|---|---|
| Coal | Alabama | Alabama | East KY | East KY | East KY |
| Sorbent | Dolomite | Dolomite | Dolomite | Limestone | None |
| % $CaSO_4$ | 13 to 16 | 17 to 31 | 30 | 19 to 29 | 8 |
| % CaO•MgO | 1 to 9 | 5 to 11 | 6 | 0 | 0 |
| % CaO | 0 | 0 | 0 | 1 to 5 | 0.5 |
| % $CaCO_3$ | 1 to 4 | 1 to 4 | 1 | 4 to 15 | 0.2 |
| % MgO | 2 to 5 | 6 to 9 | 9 | 1 to 4 | 2 |
| % Ash/Sand | 69 to 81 | 54 to 64 | 50 | 55 to 75 | 90 |

As indicated above, the levels of $CaSO_4$ in the samples generated from the Eastern Kentucky coal and limestone were lower than the levels of $CaSO_4$ in samples generated from the Eastern Kentucky coal but with dolomite. This result may reflect a difference in the reactivity of these two types of sorbent. Perhaps the most surprising result of the chemical analysis is the level of $CaSO_4$ in the sample collected in the absence of sorbent addition (8 percent). Even if all of the naturally occurring calcium in the coal fly ash were converted to $CaSO_4$, the level of $CaSO_4$ in the solids should be no higher than 3 percent. Therefore, over half of this $CaSO_4$ must have come from reacted sorbent material that was still being carried out of the transport reactor system during this test, even though the sorbent addition had been terminated about 8 hours earlier. This effect should be kept in mind when comparing chemical compositions (and other properties) of solids generated under varying test conditions.

Hopper Samples

Ash chemistry is usually determined in a typical power plant environment from grab samples collected from the hopper of the PCD. Transport reactor operators at the PSDF routinely collect PCD hopper samples once per shift. These samples are typically collected (integrated) over a short period of time, and no substantial efforts are made to clear the hopper or transport system prior to collection. Therefore, these samples have the potential to be unrepresentative of long-term operating conditions. However, because of the pervasiveness of this type of sampling, hopper samples were collected for comparison to the more carefully collected in situ samples.

Elemental analyses and calculated chemical compositions for the TC03 hopper samples are summarized in Table 3.4-5. Calcium utilizations calculated for these samples tended to be slightly higher than the utilizations calculated for the in situ samples, possibly due to the additional uptake of sulfur that occurs while the ash resides on the filter elements. The chemical compositions of the TC03 hopper samples are compared to those of the TC02 hopper samples in the following information.

Chemical Compositions of Hopper Samples

| Test | TC02 | TC03 | TC03 | TC03 | TC03 |
|---|---|---|---|---|---|
| Coal | Alabama | Alabama | East KY | East KY | East KY |
| Sorbent | Dolomite | Dolomite | Dolomite | Limestone | None |
| % $CaSO_4$ | 11 to 17 | 17 to 28 | 30 | 24 to 28 | 24 |
| % CaO•MgO | 4 to 9 | 8 to 9 | 8 to 12 | 0 | 0 |
| % CaO | 0 | 0 | 0 | 0.4 to 5 | 0 |
| % $CaCO_3$ | 2 to 8 | 0.5 to 3 | 0.9 | 4 to 6 | 5 |
| % MgO | 3 to 7 | 6 to 8 | 9 | 0 | 0 |
| % Ash/Sand | 67 to 75 | 56 to 65 | 48 | 59 to 71 | 71 |

The hopper samples and the in situ samples from TC03 are both characterized by higher levels of $CaSO_4$ and lower levels of ash/sand than the levels in the TC02 hopper samples. The relatively low concentration of ash/sand materials in the TC03 samples compared to the TC02 samples could be a result of improved control of bed material carryover and/or generally higher rates of sorbent addition (see listing above). The level of $CaSO_4$ in the hopper sample collected when the sorbent was turned off is obviously much higher than expected (24 percent). This

level of $CaSO_4$ is 3 times the level found in the corresponding in situ sample and 8 times the level that could be produced by complete sulfation of the calcium in the coal ash. In fact, the composition of the no-sorbent hopper sample is quite similar to the composition of the preceding hopper sample, which was collected during limestone addition.

The results shown above cast strong doubt on the reliability of hopper samples as indicators of process performance or as indicators of the actual ash composition associated with a given test segment (see Chemical Compositions of Hopper Samples, on previous page). This doubt shows that analyses of PCD performance should not be based on hopper grab samples, but on the composition and physical properties of the in situ samples, dustcake samples, or hopper samples collected over long periods of time.

Dustcake Samples

Table 3.4-6 summarizes the chemical composition of dustcake samples removed during the PCD inspection at the end of TC03. Prior to this inspection, the PCD had been back-pulsed extensively during and following the TC03 shutdown. There was only a very thin dustcake (thickness < 0.1 in.) remaining on any of the filter elements. Since there was so little dustcake left on the elements, it was necessary to combine dustcake samples from several filter elements to obtain enough sample for permeability tests, chemical analyses, and other characterization tests. The composite samples for these tests were created by combining dustcake samples taken from adjacent filter elements of the same type (see Table 3.4-6). One sample, which was not actually a dustcake, was taken from the top of the filter plenum as noted.

Chemical Compositions of Dustcake Samples and Plenum Ash Sample

| Sample | TC03 Dustcake | TC03 Plenum | TC02 Dustcake | TC01 Dustcake |
|---|---|---|---|---|
| % $CaSO_4$ | 35 to 40 | 28 | 14 to 27 | 4 to 12 |
| % CaO•MgO | 0 to 2.5 | 14 | 0 to 1.6 | 2 to 4 |
| % $CaCO_3$ | 4.5 to 8 | 6 | 0.8 to 5 | 0.6 to 1 |
| % CaO | 0 | 0 | 0 | 0 |
| % MgO | 3 to 4 | 0 | 6 to 8 | 3 to 6 |
| % Ash/Sand | 50 to 55 | 52 | 64 to 76 | 79 to 89 |

The information listed above shows that calculated compositions of the dustcakes varied slightly, but the composition of the ash removed from the top of the plenum was markedly different from that of the dustcakes. The results were not sufficient to reveal any systematic variation in chemical composition as a function of the type of filter element on which the dustcake was collected. As with the in situ and hopper samples discussed earlier, the dustcake compositions for TC02 and TC03 show a progression toward lower levels of ash/sand and higher levels of sorbent reaction products. This suggests a general trend toward reduced carryover of bed material and better utilization of sorbents. TC03 dustcake samples, as in previous test programs, contain more $CaSO_4$ (35 to 40 percent) than either the in situ samples (8 to 31 percent) or the hopper samples (17 to 30 percent). This is the result expected, considering the prolonged exposure of the residual dustcake to $SO_2$.

The ash sample taken from the top of the plenum contained less $CaSO_4$ than any of the dustcake samples, probably because the plenum sample is composed of large particles that settled onto the plenum surface. These large particles contain less $CaSO_4$ than do smaller particles, since the extent of the sulfation reaction generally decreases with increasing particle size.

### 3.4.4 Measurements of Physical Properties

Tables 3.4-7, -8, and -9 are summaries of physical measurements made on the TC03 in situ samples, hopper samples, and dustcake samples. The measured parameters include:

- Bulk density.
- True (skeletal-particle) density.
- Uncompacted bulk porosity (UBP).
- BET surface area.
- Mass-median diameter (MMD).
- Drag-equivalent diameter (DED).

As discussed in previous reports, the DED is not a physical size, but rather is a fitted parameter that can be used to rank the characteristic gas flow resistance of ashes at equal porosities. Increasing values of DED indicate lower resistance to gas flow (less drag) at a given porosity.

Bulk density was determined, as in previous tests, by measuring the volume of a known weight of ash. True density measurements were made by helium pycnometry using a Quantachrome Model 1000 ultrapycnometer and UBP was calculated from the bulk density and true density. Specific surface area was determined by the BET method using a Micromeritics FloSorb-II analyzer and the MMD was based on particle-size analysis on a Leeds & Northrup Microtrac X-100 analyzer.

In situ Samples

Table 3.4-7 contains the physical properties measured for in situ samples collected during TC03. The table shows that the first four samples collected during dolomite addition had higher MMDs and DEDs than did any of the other samples collected during limestone addition. As noted earlier, the particulate loadings measured during dolomite addition were also higher than those measured during limestone addition. A change in the transport reactor cyclone velocity was at least partially responsible for the reduction in mass loading and particle size when the sorbent was switched from dolomite to limestone. However, it is important to note that equally significant variations in the MMD, BET surface area, and DED were seen with various given sorbents, as shown in the information listed below.

Physical Properties of TC03 In situ Samples

| Sorbent | Dolomite | Bucyrus Limestone | Longview Limestone | Gregg Limestone |
|---|---|---|---|---|
| UBP(%) | 76 to 80 | 78 | 76 to 81 | 77 to 79 |
| BET ($m^2/g$) | 1.8 to 2.7 | 3.3 to 3.7 | 2.7 to 3.9 | 2.4 to 3.0 |
| MMD (μm) | 19 to 23 | 10 to 16 | 9 to 15 | 9 to 13 |
| DED (μm) | 2.8 to 4.5 | 2.5 to 3.2 | 2.6 to 3.9 | 3.3 to 3.7 |

Based on these results, it is clear that finer particle sizes were produced during the limestone addition, but the effect on drag is not clear due the variation in DED obtained with a given sorbent. It is interesting to note that the Bucyrus and Longview limestones appear to produce higher BET surface areas than do the Gregg limestone and dolomite. The higher surface area might be expected to result in better $SO_2$ removal if all other factors were equal, but there is too much variation in the calcium utilizations calculated from the chemical analyses to confirm this assertion (59 to 73 percent with Bucyrus limestone, 49 to 54 percent with Longview limestone, 59 percent with Gregg limestone, and 45 to 73 percent with dolomite).

Hopper Samples

Physical properties of selected TC03 hopper samples are summarized in Table 3.4-8. The variations in physical properties with sorbent type that were evident in the in situ samples are not apparent in the hopper samples. As noted in the discussion of ash chemistry, the failure of the hopper samples to reflect the changes in sorbent type strongly suggests that hopper grab samples are not reliable indicators of process operations. The MMD of the hopper samples are generally larger than those of the corresponding in situ samples, although the DED of the two types of samples is not significantly different. Again, these apparent anomalies suggest that the hopper samples are not reliable. The same conclusion has been supported in previous tests where the properties of hopper samples did not reflect changes in operating conditions and feedstocks. Possible explanations include holdup of material in the PCD hopper and ash discharge system and cross-contamination of hopper samples in the sample collection process. In any case, results of TC03 as well as previous tests strongly suggest that hopper samples are not appropriate samples for analyzing the effects of changing operating conditions.

Dustcake Samples

Dustcake properties summarized in Table 3.4-9 show that the dustcake samples taken from the two types of Pall filter elements had lower MMD, lower DED, and lower surface areas than did the dustcake samples taken from the other types of elements (Schumacher and 3M). Since the Pall elements have higher permeabilities than the other types of elements, the dustcakes on the Pall elements would probably be subjected to higher face velocities during most, if not all, of the filtration cycle. All other factors being equal, the higher gas velocity through the Pall dustcakes should create more drag and more compaction of the cake. The higher gas flow through the Pall elements would also tend to modify the flow field in the vicinity of these elements, producing flow effects that could alter the size-distribution of the particles reaching the elements. This effect could explain the observed difference in MMD (7.7 μm for the Pall

dustcakes versus 11 μm for the Schumacher and 3M dustcakes). Of course, it is important to note that various particle-size-fractionation mechanisms (i.e., swirl effects and settling) are at work throughout the filter vessel. Therefore, it is reasonable to expect that particle sizes may vary with location in the vessel. These particle-size differences could also produce corresponding differences in the dustcakes formed in different areas of the PCD. Settling of particles on inactive surfaces within the PCD would be expected to produce deposits containing predominantly large particles, as seen in the plenum sample (MMD = 25 μm versus 7.7 to 11 μm for the dustcakes).

The reports from TC01, TC02, and TC03 all show that work is continuing on developing a better understanding of how flow resistance (DED) varies with various parameters. As discussed in the TC01 report, a reasonably good correlation between DED and BET surface area was developed with TC01 in situ samples. The same type of correlation was applied to the TC03 in situ samples and the results, shown in Figure 3.4-3, indicate a definite trend, although the linear correlation coefficient was lower than that obtained with the TC01 data ($r^2 = 0.80$ for TC03 in situ data versus $r^2 = 0.88$ for TC01 in situ data). The correlation became much worse when the hopper samples were included in the analysis, as shown in Figure 3.4-4. However, as already discussed, the hopper samples are not representative and are an unreliable source of data on DED and BET surface area. Therefore, it is not surprising that inclusion of the hopper samples in the analysis would degrade the correlation.

Previous studies of fly ash from conventional pc-fired power plants have shown a good correlation between DED and BET surface area (Bush, et al., *JAPCA*, Vol. 39, pp. 228-237, 1989). The fly ash from conventional pc-fired boilers is predominantly composed of fused, spherical ash particles with little or no internal porosity (i.e., no internal surface area). Since almost all of the surface area is external, almost all of the surface area contributes to dustcake drag. Therefore, it is not at all surprising that there is a good correlation between the DED and BET surface area of conventional fly ash. However, it is important to note that this rationale does not necessarily apply to the TC03 ash samples because the ash generated in the transport reactor is not fused and is not spherical. The BET surface area of the TC03 ash is about 30 to 50 percent higher than the surface area calculated from the particle-size distribution of this ash, assuming the ash particles are spherical. This difference in surface areas suggests that the TC03 ash contains additional surface area in the form of internal surface area and in the form of irregular surface features. Therefore, it is somewhat surprising that there is apparently a reasonably good correlation between the DED and the BET surface area of the TC03 ash.

An analysis of dustcake DED versus calcium content that was presented in the TC02 report showed a reasonably well defined trend with a correlation coefficient ($r^2$) of 0.79. This trend toward increasing DED (decreasing drag) with increasing calcium content was not discernible in the measurements made on the TC03 in situ and hopper samples with a correlation coefficient ($r^2$) of 0.21 (see Figure 3.4-5). The type of DED-versus-calcium trend that was evident in the TC02 dustcake data could not be substantiated in TC03 because of the limited DED data on the TC03 dustcakes (see Table 3.4-9). Again, the failure to see these types of trends in hopper data may simply reflect the fact that these samples are not representative and that future analyses should focus on the in situ samples and dustcake samples. To determine whether a better correlation could be achieved with in situ samples, the DED and calcium contents of these samples were correlated using all of the TC01 and TC03 data. No data were available for TC02

in situ samples because all of TC02 in situ samples were consumed by other tests before the permeability measurements could be made. The results for the TC01 and TC03 in situ samples are illustrated in Figure 3.4-6. Although the correlation coefficient is relatively poor ($r^2 = 0.61$), the graph definitely reveals a trend toward higher DED values at higher values of calcium content (i.e., the presence of the sorbent appears to reduce the dustcake flow resistance). This type of result is not too surprising, since the sorbent does not form any ultrafine aerosols of the type that are formed by the vaporization and condensation of certain ash components. If the coal and sorbent have similar grind sizes, the char fragmentation and ash volatilization/condensation that occur during coal combustion should cause the particulate matter generated from the coal to be finer than that generated from the sorbent.

Of course, all of the foregoing analyses are useful only if the drag measurments that are made in the laboratory can be related to the PCD pressure drop observed in the field. To determine whether there could be a direct correspondence between the laboratory measurements and actual PCD operation, the transient pressure drop across the PCD was monitored during each of the TC03 in situ sampling runs. The transient pressure drop was recorded during each run and was then converted into an equivalent transient dustcake drag using the procedure described below.

- First, the amount of dust deposited on the filter during a given filtration cycle was calculated from:
  - The measured inlet particulate loading (from the corresponding in situ sampling run).
  - The fraction of ash that drops out (from the PCD cut-size tests).
  - The duration of the filtration cycle (40 minutes).
- Second, this mass of dust was converted into an equivalent areal loading based on the known surface area of the filter elements.
- Third, the transient drag was calculated by dividing the pressure drop accumulated during the filtration cycle (transient pressure drop) by the areal loading and by the face velocity.

This actual value of transient dustcake drag was then compared to the drag measured in the laboratory using the dust sample from the corresponding sampling run after it was sieved to simulate the effect of the ash dropout ahead of the filter elements. The lab-measured drag was corrected from ambient temperature to process temperature (1,400°F) by making the appropriate adjustment for gas viscosity. A comparison of the resulting values of laboratory-measured drag to the corresponding values of actual PCD transient drag are shown in Figure 3.4-7. As shown in the figure, the laboratory drag measurements are not in perfect agreement with the values of the actual PCD transient drag. In fact, in all cases the laboratory drag estimates are lower than the actual PCD drag.

Laboratory drag values are a strong function of the porosity at which the measurement is made. The laboratory drag values that were used in this analysis are the values corresponding to the

uncompacted bulk porosity (UBP) of each sample. The value of UBP may or may not be a good indicator of the actual dustcake porosity, and the difference between UBP and the actual dustcake porosity may partly explain the difference between the lab drag measurements and the PCD transient drag values. In fact, in this case, calculation of laboratory drag at a porosity which is 93 percent of UBP does a reasonably good job of matching the PCD drag values. However, the use of a constant correction may not work for other dusts. This sort of adjustment will be investigated in future test campaigns with other fuels and sorbents.

Clearly, there is a need to develop a means for predicting or simulating the true porosity of the dustcake as it exists on the filter elements during PCD operation. One means of addressing this issue is through the use of a modified permeability test procedure in which the dust sample is entrained in air and deposited onto a filter at the same face velocity used in the PCD. A permeability test procedure of this type has been used routinely by Schumacher, and SRI is now putting together a similar apparatus for use at the PSDF. It is hoped, that by building the dustcake in a manner that more closely approximates the formation of the dustcake in the PCD, this new permeability test apparatus will provide an even better means of evaluating and ultimately predicting filter pressure drop.

Table 3.4-1

Summary of Inlet Particulate Loadings Measured During TC03

| SRI Run No. | Date | Start Time | End Time | Coal | Sorbent | Test Condition | PCD Pulse | Loading, ppmw |
|---|---|---|---|---|---|---|---|---|
| TC03IMT-01 | 6/05/98 | 14:01 | 14:21 | Alabama | Plum Run Dolomite | Stable | No | 8,600 |
| TC03IMT-02 | 6/08/98 | 10:25 | 10:55 | Alabama | Plum Run Dolomite | Stable | No | 8,500 |
| TC03IMT-03 | 6/10/98 | 9:50 | 10:20 | Alabama | Plum Run Dolomite | Stable | No | 8,300 |
| TC03IMT-04 | 6/12/98 | 10:30 | 11:00 | East Kentucky | Plum Run Dolomite | Stable | No | 9,200 |
| TC03IMT-05 | 6/17/98 | 9:25 | 9:55 | East Kentucky | Gregg Limestone | Unstable | No | 30,900 |
| TC03IMT-06 | 6/18/98 | 9:25 | 9:55 | East Kentucky | Gregg Limestone | Unstable | No | 12,900 |
| TC03IMT-07 | 7/14/98 | 13:50 | 14:20 | East Kentucky | Gregg Limestone | Stable | No | 5,100 |
| TC03IMT-08 | 7/15/98 | 11:18 | 11:43 | East Kentucky | Gregg Limestone | Stable | No | 6,500 |
| TC03IMT-09 | 7/28/98 | 9:50 | 10:20 | East Kentucky | Bucyrus Limestone | Stable | No | 7,500 |
| TC03IMT-10 | 7/29/98 | 9:15 | 9:45 | East Kentucky | Bucyrus Limestone | Stable | No | 8,500 |
| TC03IMT-11 | 7/30/98 | 9:55 | 10:25 | East Kentucky | None | Stable | No | 6,300 |
| TC03IMT-12 | 7/31/98 | 9:42 | 10:11 | East Kentucky | Bucyrus Limestone | Stable | No | 6,200 |
| TC03IMT-13 | 8/03/98 | 12:45 | 13:15 | East Kentucky | Longview Limestone | Stable | No | 7,700 |
| TC03IMT-14 | 8/04/98 | 10:07 | 10:37 | East Kentucky | Longview Limestone | Stable | No | 5,900 |
| TC03IMT-15 | 8/05/98 | 10:07 | 10:37 | East Kentucky | Longview Limestone | Stable | No | 5,700 |
| TC03IMT-16 | 8/07/98 | 9:35 | 10:05 | East Kentucky | Gregg Limestone | Stable | No | 6,200 |
| TC03IMT-17 | 8/10/98 | 9:45 | 10:15 | East Kentucky | Gregg Limestone | Stable | Yes | 6,800 |

Table 3.4-2

Summary of Outlet Particulate Loadings Measured During TC03

| SRI Run No. | Date | Start Time | End Time | Loading (ppmw) | Blank (ppmw) |
|---|---|---|---|---|---|
| TC03OMT-01 | 6/05/98 | 10:05 | 14:06 | 0.15 | 0.09 |
| TC03OMT-02 | 6/08/98 | 9:30 | 14:00 | 0.13 | 0.08 |
| TC03OMT-03 | 6/10/98 | 8:50 | 13:50 | 0.17 | 0.05 |
| TC03OMT-04 | 6/12/98 | 9:25 | 13:35 | 0.27 | 0.27 |
| TC03OMT-05 | 7/29/98 | 9:05 | 13:05 | 0.03 | -0.14 |
| TC03OMT-06 | 7/31/98 | 9:05 | 14:05 | 0.18 | 0.03 |
| TC03OMT-07 | 8/03/98 | 10:25 | 14:25 | 0.32 | 0.13 |
| TC03OMT-08 | 8/05/98 | 9:50 | 14:00 | 0.37 | 0.12 |
| TC03OMT-09 | 8/07/98 | 7:32 | 14:32 | 0.21 | 0.08 |
| TC03OMT-10 | 8/10/98 | 9:35 | 14:37 | 0.22 | 0.10 |

Table 3.4-3

PCD Particulate Collection Efficiencies for TC03

| SRI Run No | Outlet Run Date | Outlet Run Time | | Loadings, ppmw | | Efficiency (%) | Penetration (%) |
|---|---|---|---|---|---|---|---|
| | | Start | End | Inlet | Outlet | | |
| TC03OMT-01 | 6/05/98 | 10:05 | 14:06 | 8,600 | 0.15 | 99.9982 | 0.0018 |
| TC03OMT-02 | 6/08/98 | 9:30 | 14:00 | 8,500 | 0.13 | 99.9985 | 0.0015 |
| TC03OMT-03 | 6/10/98 | 8:50 | 13:50 | 8,300 | 0.17 | 99.9980 | 0.0020 |
| TC03OMT-04 | 6/12/98 | 9:25 | 13:35 | 9,200 | 0.27 | 99.9971 | 0.0029 |
| TC03OMT-05 | 7/29/98 | 9:05 | 13:05 | 8,500 | 0.03 | 99.9996 | 0.0004 |
| TC03OMT-06 | 7/31/98 | 9:05 | 14:05 | 6,200 | 0.18 | 99.9971 | 0.0029 |
| TC03OMT-07 | 8/03/98 | 10:25 | 14:25 | 7,700 | 0.32 | 99.9959 | 0.0041 |
| TC03OMT-08 | 8/05/98 | 9:50 | 14:00 | 5,700 | 0.37 | 99.9935 | 0.0065 |
| TC03OMT-09 | 8/07/98 | 7:32 | 14:32 | 6,200 | 0.21 | 99.9966 | 0.0034 |
| TC03OMT-10 | 8/10/98 | 9:35 | 14:37 | 6,800 | 0.22 | 99.9968 | 0.0032 |

# Table 3.4-4

## Chemical Composition of TC03 In situ Samples

| Run No. TC03IMT- | Date | $CO_2$, Dry Basis (Wt%) | Si, Ignited Basis (Wt%) | Al, Ignited Basis (Wt%) | Ti, Ignited Basis (Wt%) | Fe, Ignited Basis (Wt%) | Ca, Ignited Basis (Wt%) | Mg, Ignited Basis (Wt%) | K, Ignited Basis (Wt%) | Na, Ignited Basis (Wt%) | P, Ignited Basis (Wt%) | S, Ignited Basis (Wt%) |
|---|---|---|---|---|---|---|---|---|---|---|---|---|
| 1 | 06/05/98 | 1.71 | 16.14 | 7.11 | 0.44 | 2.90 | 10.96 | 6.35 | 1.46 | 1.34 | 0.14 | 3.96 |
| 2 | 06/08/98 | 0.40 | 17.50 | 7.78 | 0.48 | 3.71 | 9.20 | 5.44 | 1.42 | 1.21 | 0.18 | 5.36 |
| 3 | 06/10/98 | 0.25 | 13.77 | 6.14 | 0.39 | 4.38 | 11.64 | 6.72 | 1.22 | 1.30 | 0.08 | 7.30 |
| 4 | 06/12/98 | 0.58 | 11.41 | 5.47 | 0.37 | 4.01 | 13.00 | 7.77 | 1.05 | 1.19 | 0.06 | 7.15 |
| 9 | 07/28/98 | 3.07 | 20.46 | 10.32 | 0.49 | 4.84 | 10.87 | 2.42 | 1.87 | 0.51 | 0.14 | 5.14 |
| 10 | 07/29/98 | 1.72 | 22.96 | 9.93 | 0.17 | 3.73 | 8.72 | 1.87 | 1.11 | 0.56 | 0.17 | 4.50 |
| 11 | 07/30/98 | 0.10 | 28.18 | 13.89 | 0.74 | 4.37 | 2.71 | 0.97 | 1.99 | 0.65 | 0.21 | 1.82 |
| 12 | 07/31/98 | 2.44 | 20.60 | 8.69 | 0.45 | 4.26 | 11.06 | 2.26 | 1.19 | 0.68 | 0.16 | 6.44 |
| 13 | 08/03/98 | 2.88 | 20.42 | 11.26 | 0.55 | 4.31 | 11.40 | 1.38 | 1.70 | 0.66 | 0.17 | 4.99 |
| 14 | 08/04/98 | 4.31 | 17.39 | 9.41 | 0.46 | 4.27 | 15.26 | 1.13 | 1.23 | 0.75 | 0.53 | 6.73 |
| 15 | 08/05/98 | 3.21 | 17.83 | 9.40 | 0.47 | 4.97 | 14.10 | 1.11 | 2.49 | 0.68 | 0.02 | 6.62 |
| 16 | 08/07/98 | 4.37 | 16.88 | 9.01 | 0.45 | 4.70 | 15.61 | 0.70 | 1.15 | 0.77 | 0.20 | 6.45 |
| 17 | 08/10/98 | 6.71 | 16.24 | 8.86 | 0.42 | 3.90 | 15.06 | 1.48 | 1.29 | 2.67 | 0.21 | 5.94 |

Calculated Parameters

| Run No. TC03IMT- | Date | CaCO3 (Wt%) | CaSO4 (Wt%) | CaO·MgO (Wt%) | CaO (Wt%) | MgO (Wt%) | Ash/Sand (Wt%) | Ca Utilization | Ca/S Ratio |
|---|---|---|---|---|---|---|---|---|---|
| 1 | 06/05/98 | 3.89 | 16.83 | 10.73 | 0.00 | 6.04 | 62.51 | 45.16 | 2.21 |
| 2 | 06/08/98 | 0.91 | 22.78 | 5.14 | 0.00 | 6.87 | 64.30 | 72.83 | 1.37 |
| 3 | 06/10/98 | 0.57 | 31.03 | 5.51 | 0.00 | 8.84 | 54.06 | 78.39 | 1.28 |
| 4 | 06/12/98 | 1.32 | 30.39 | 8.51 | 0.00 | 9.32 | 50.46 | 68.75 | 1.45 |
| 9 | 07/28/98 | 6.98 | 21.85 | 0.00 | 2.32 | 0.00 | 68.86 | 59.11 | 1.69 |
| 10 | 07/29/98 | 3.91 | 19.13 | 0.00 | 2.14 | 0.00 | 74.82 | 64.51 | 1.55 |
| 11 | 07/30/98 | 0.23 | 7.74 | 0.00 | 0.48 | 0.00 | 91.56 | 83.95 | 1.19 |
| 12 | 07/31/98 | 5.55 | 27.37 | 0.00 | 1.11 | 0.00 | 65.98 | 72.78 | 1.37 |
| 13 | 08/03/98 | 6.55 | 21.21 | 0.00 | 3.56 | 0.00 | 68.69 | 54.71 | 1.83 |
| 14 | 08/04/98 | 9.93 | 27.41 | 0.00 | 4.10 | 0.00 | 58.55 | 51.65 | 1.94 |
| 15 | 08/05/98 | 15.25 | 25.25 | 0.00 | 4.07 | 0.00 | 55.44 | 49.30 | 2.03 |
| 16 | 08/07/98 | 7.30 | 28.14 | 0.00 | 5.00 | 0.00 | 59.56 | 58.69 | 1.70 |
| 17 | 08/10/98 | 9.80 | 28.60 | 0.00 | 2.15 | 0.00 | 59.45 | 55.13 | 1.81 |

## Table 3.4-5

## Chemical Composition of TC03 Hopper Samples

| Sample ID | Date | Coal/Sorbent | $CO_2$, Dry Basis (Wt%) | Si, Ignited Basis (Wt%) | Al, Ignited Basis (Wt%) | Ti, Ignited Basis (Wt%) | Fe, Ignited Basis (Wt%) | Ca, Ignited Basis (Wt%) | Mg, Ignited Basis (Wt%) | K, Ignited Basis (Wt%) | Na, Ignited Basis (Wt%) | P, Ignited Basis (Wt%) | S, Ignited Basis (Wt%) |
|---|---|---|---|---|---|---|---|---|---|---|---|---|---|
| AB03229 | 06/05/98 | Ala/Dolomite | 1.13 | 20.36 | 8.41 | 0.48 | 2.99 | 9.85 | 5.76 | 0.83 | 2.13 | 0.34 | 4.05 |
| AB03236 | 06/08/98 | Ala/Dolomite | 0.29 | 22.58 | 9.61 | 0.48 | 3.64 | 9.02 | 5.40 | 0.56 | 0.84 | 0.16 | N.R.[1] |
| AB03289 | 06/10/98 | Ala/Dolomite | 0.21 | 15.86 | 8.78 | 0.47 | 4.87 | 11.60 | 6.89 | 0.18 | 0.57 | 0.15 | 6.48 |
| AB03332 | 06/12/98 | E. Ky/Dolomite | 0.38 | 14.53 | 7.78 | 0.40 | 4.78 | 14.35 | 8.44 | 0.12 | 0.32 | 0.11 | 7.11 |
| AB03608 | 07/28/98 | E. Ky/Bucyrus LS | 2.30 | 18.21 | 7.13 | 0.34 | 4.80 | 11.01 | 2.59 | 1.47 | 0.87 | 0.27 | 5.87 |
| AB03627 | 07/29/98 | E. Ky/Bucyrus LS | 2.21 | 18.73 | 7.05 | 0.39 | 4.34 | 10.38 | 2.19 | 1.50 | 0.94 | 0.09 | 6.47 |
| AB03642 | 07/30/98 | E. Ky/None | 2.11 | 18.58 | 8.34 | 0.44 | 4.97 | 6.48 | 1.86 | 1.47 | 0.51 | 0.10 | 5.70 |
| AB03662 | 07/31/98 | E. Ky/Bucyrus LS | 1.92 | 15.25 | 11.17 | 0.17 | 7.54 | 9.27 | 1.10 | 1.68 | 0.46 | 0.37 | 5.81 |
| AB03703 | 08/03/98 | E. Ky/Longview LS | 2.67 | 15.44 | 8.51 | 0.42 | 4.14 | 11.90 | 2.41 | 1.23 | 0.66 | 0.12 | 6.43 |
| AB03705 | 08/04/98 | E. Ky/Longview LS | 2.33 | 19.23 | 8.99 | 0.43 | 3.84 | 11.20 | 1.47 | 1.23 | 0.73 | 0.07 | 5.59 |
| AB03752 | 08/05/98 | E. Ky/Longview LS | 1.65 | 21.79 | 9.25 | 0.47 | 4.88 | 12.26 | 1.55 | 1.32 | 0.87 | 0.09 | 6.00 |
| AB03769 | 08/07/98 | E. Ky/Gregg LS | 1.93 | 20.80 | 8.07 | 0.42 | 4.28 | 11.57 | 1.52 | 1.20 | 0.88 | 0.09 | 5.72 |
| AB03794 | 08/10/98 | E. Ky/Gregg LS | 3.75 | 15.94 | 7.15 | 0.45 | 4.88 | 15.06 | 0.71 | 1.45 | 1.14 | 0.09 | 6.50 |

Calculated Parameters

| Sample ID | Date | Coal/Sorbent | CaCO3 (Wt%) | CaSO4 (Wt%) | CaO·MgO (Wt%) | CaO (Wt%) | MgO (Wt%) | Ash/Sand (Wt%) | Ca Utilization | Ca/S Ratio |
|---|---|---|---|---|---|---|---|---|---|---|
| AB03229 | 06/05/98 | Ala/Dolomite | 2.57 | 17.21 | 9.05 | 0.00 | 5.76 | 65.40 | 51.40 | 1.95 |
| AB03236 | 06/08/98 | Ala/Dolomite | 0.66 | N.R.[1] | N.R.[1] | 0.00 | N.R.[1] | N.R.[1] | N.R.[1] | N.R.[1] |
| AB03289 | 06/10/98 | Ala/Dolomite | 0.48 | 27.54 | 7.97 | 0.00 | 8.09 | 55.92 | 69.83 | 1.43 |
| AB03332 | 06/12/98 | E. Ky/Dolomite | 0.86 | 30.22 | 12.32 | 0.00 | 8.84 | 47.76 | 61.93 | 1.61 |
| AB03608 | 07/28/98 | E. Ky/Bucyrus LS | 5.23 | 24.95 | 0.00 | 2.21 | 0.00 | 67.61 | 66.64 | 1.50 |
| AB03627 | 07/29/98 | E. Ky/Bucyrus LS | 5.02 | 27.50 | 0.00 | 0.40 | 0.00 | 67.08 | 77.91 | 1.28 |
| AB03642 | 07/30/98 | E. Ky/None | 4.80 | 24.23 | 0.00 | 0.00 | 0.00 | 70.98 | 109.95 | 0.91 |
| AB03662 | 07/31/98 | E. Ky/Bucyrus LS | 4.36 | 24.69 | 0.00 | 0.37 | 0.00 | 70.58 | 78.34 | 1.28 |
| AB03703 | 08/03/98 | E. Ky/Longview LS | 6.07 | 27.33 | 0.00 | 2.01 | 0.00 | 64.60 | 67.54 | 1.48 |
| AB03705 | 08/04/98 | E. Ky/Longview LS | 5.30 | 23.76 | 0.00 | 2.93 | 0.00 | 68.02 | 62.39 | 1.60 |
| AB03752 | 08/05/98 | E. Ky/Longview LS | 3.75 | 25.50 | 0.00 | 4.56 | 0.00 | 66.19 | 61.17 | 1.63 |
| AB03769 | 08/07/98 | E. Ky/Gregg LS | 4.39 | 24.31 | 0.00 | 3.73 | 0.00 | 67.57 | 61.80 | 1.62 |
| AB03794 | 08/10/98 | E. Ky/Gregg LS | 8.52 | 27.63 | 0.00 | 4.94 | 0.00 | 58.92 | 53.95 | 1.85 |

1. Not reported because of error in analysis.

# Table 3.4-6

## Chemical Composition of Dustcake Samples Collected After TC03

| Sample ID | Filter Element Locations | Type of Filter Element | $CO_2$, Dry Basis (Wt%) | Si, Ignited Basis (Wt%) | Al, Ignited Basis (Wt%) | Ti, Ignited Basis (Wt%) | Fe, Ignited Basis (Wt%) | Ca, Ignited Basis (Wt%) | Mg, Ignited Basis (Wt%) | K, Ignited Basis (Wt%) | Na, Ignited Basis (Wt%) | P, Ignited Basis (Wt%) | S, Ignited Basis (Wt%) |
|---|---|---|---|---|---|---|---|---|---|---|---|---|---|
| AB03954 | T1, T2, T17, T18 | Pall 442-T | 2.95 | 14.05 | 7.75 | 0.47 | 3.07 | 11.88 | 1.63 | 1.82 | 0.84 | 0.08 | 8.33 |
| AB03955 | T3, T4, T5, T6, T7, T24 | Schumacher TF-20 | 2.48 | 13.89 | 7.16 | 0.45 | 2.98 | 12.94 | 2.36 | 1.22 | 0.75 | 0.10 | 8.97 |
| AB03956 | T8, T9 | 3M Oxide | 1.99 | 15.26 | 7.64 | 0.50 | 3.49 | 14.60 | 2.61 | 1.56 | 0.93 | 0.10 | 9.42 |
| AB03957 | T10, T11, T12, T13, T30 | Pall 326 | 3.35 | 15.33 | 7.62 | 0.51 | 3.35 | 14.14 | 1.83 | 1.67 | 0.94 | 0.10 | 8.66 |
| AB03958 | Top of Plenum | None | 2.70 | 15.92 | 6.38 | 0.31 | 3.47 | 16.48 | 2.99 | 1.71 | 0.94 | 0.09 | 6.49 |

Calculated Parameters

| Sample ID | Filter Element Locations | Type of Filter Element | CaCO3 (Wt%) | CaSO4 (Wt%) | CaO·MgO (Wt%) | CaO (Wt%) | MgO (Wt%) | Ash/Sand (Wt%) | Ca Utilization | Ca/S Ratio |
|---|---|---|---|---|---|---|---|---|---|---|
| AB03954 | T1, T2, T17, T18 | Pall 442-T | 6.70 | 35.40 | 0.00 | 0.00 | 2.70 | 55.19 | 87.65 | 1.14 |
| AB03955 | T3, T4, T5, T6, T7, T24 | Schumacher TF-20 | 5.64 | 38.12 | 0.00 | 0.00 | 3.91 | 52.33 | 86.65 | 1.15 |
| AB03956 | T8, T9 | 3M Oxide | 4.52 | 40.04 | 2.45 | 0.00 | 3.30 | 49.69 | 80.65 | 1.24 |
| AB03957 | T10, T11, T12, T13, T30 | Pall 326 | 7.61 | 36.81 | 0.65 | 0.00 | 2.76 | 52.17 | 76.56 | 1.31 |
| AB03958 | Top of Plenum | None | 6.14 | 27.58 | 14.24 | 0.00 | 0.00 | 52.05 | 49.23 | 2.03 |

Table 3.4-7

Physical Properties of TC03 In situ Samples

| Run Number | Date | Coal | Sorbent | Bulk Density ($g/cm^3$) | True Density ($g/cm^3$) | UBP[1], (%) | BET Surface Area ($m^2/g$) | MMD[2] (µm) | DED[3] (µm) |
|---|---|---|---|---|---|---|---|---|---|
| TC03IMT-1 | 06/05/98 | Alabama | Dolomite | 0.58 | 2.70 | 78.5 | 1.78 | 18.5 | 4.5 |
| TC03IMT-2 | 06/08/98 | Alabama | Dolomite | 0.56 | 2.75 | 79.6 | 2.66 | 20.2 | 2.8 |
| TC03IMT-3 | 06/10/98 | Alabama | Dolomite | 0.69 | 2.92 | 76.4 | 2.27 | 22.8 | 3.5 |
| TC03IMT-4 | 06/12/98 | E. Ky | Dolomite | 0.67 | 2.96 | 77.4 | 2.37 | 19.7 | 3.8 |
| TC03IMT-9 | 07/28/98 | E. Ky | Bucyrus Limestone | 0.58 | 2.69 | 78.4 | 3.65 | 10.1 | 2.5 |
| TC03IMT-10 | 07/29/98 | E. Ky | Bucyrus Limestone | 0.60 | 2.72 | 77.9 | 3.32 | 12.0 | 2.6 |
| TC03IMT-11 | 07/30/98 | E. Ky | None | 0.45 | 2.58 | 82.6 | 4.64 | 15.3 | 1.9 |
| TC03IMT-12 | 07/31/98 | E. Ky | Bucyrus Limestone | 0.59 | 2.73 | 78.4 | 3.54 | 16.1 | 3.2 |
| TC03IMT-13 | 08/03/98 | E. Ky | Longview Limestone | 0.52 | 2.69 | 80.7 | 3.87 | 15.2 | 2.6 |
| TC03IMT-14 | 08/04/98 | E. Ky | Longview Limestone | 0.61 | 2.76 | 77.9 | 3.37 | 14.5 | 3.0 |
| TC03IMT-15 | 08/05/98 | E. Ky | Longview Limestone | 0.66 | 2.72 | 75.7 | 2.70 | 9.2 | 3.9 |
| TC03IMT-16 | 08/07/98 | E. Ky | Gregg Limestone | 0.57 | 2.77 | 79.4 | 2.96 | 12.8 | 3.3 |
| TC03IMT-17 | 08/10/98 | E. Ky | Gregg Limestone | 0.64 | 2.72 | 76.5 | 2.42 | 9.3 | 3.7 |

1. UBP = uncompacted bulk porosity
2. MMD = mass median diameter
3. DED = drag-equivalent diameter

Table 3.4-8

Physical Properties of TC03 Hopper Samples

| Sample ID | Date | Coal | Sorbent | Bulk Density ($g/cm^3$) | True Density ($g/cm^3$) | UBP[1], (%) | BET Surface Area ($m^2/g$) | MMD[2] (µm) | DED[3] (µm) |
|---|---|---|---|---|---|---|---|---|---|
| AB03229 | 06/05/98 | Alabama | Dolomite | 0.65 | 2.67 | 75.7 | 2.25 | 18.0 | 2.8 |
| AB03236 | 06/08/98 | Alabama | Dolomite | 0.59 | 2.70 | 78.1 | 2.38 | 20.6 | 2.8 |
| AB03289 | 06/10/98 | Alabama | Dolomite | 0.63 | 2.80 | 77.5 | 2.77 | 27.3 | 2.9 |
| AB03332 | 06/12/98 | E. Ky | Dolomite | 0.79 | 2.88 | 72.6 | 2.07 | 29.7 | 4.7 |
| AB03608 | 07/28/98 | E. Ky | Bucyrus Limestone | 0.67 | 2.60 | 74.2 | 1.56 | 20.0 | 3.9 |
| AB03627 | 07/29/98 | E. Ky | Bucyrus Limestone | 0.58 | 2.62 | 77.9 | 3.24 | 11.4 | 2.5 |
| AB03642 | 07/30/98 | E. Ky | None | 0.59 | 2.60 | 77.3 | 3.30 | 16.7 | 2.8 |
| AB03662 | 07/31/98 | E. Ky | Bucyrus Limestone | 0.66 | 2.63 | 74.9 | 2.73 | 26.5 | 3.9 |
| AB03703 | 08/03/98 | E. Ky | Longview Limestone | 0.66 | 2.66 | 75.2 | 2.79 | 24.5 | 3.5 |
| AB03705 | 08/04/98 | E. Ky | Longview Limestone | 0.69 | 2.64 | 73.9 | 2.40 | 34.1 | 4.0 |
| AB03752 | 08/05/98 | E. Ky | Longview Limestone | 0.73 | 2.66 | 72.6 | 2.14 | 26.2 | 4.1 |
| AB03769 | 08/07/98 | E. Ky | Gregg Limestone | 0.76 | 2.71 | 72.0 | 1.65 | 21.0 | 4.8 |
| AB03794 | 08/10/98 | E. Ky | Gregg Limestone | 0.64 | 2.81 | 77.2 | 2.06 | 11.7 | 2.7 |

1. UBP = uncompacted bulk porosity
2. MMD = mass median diameter
3. DED = drag-equivalent diameter

Table 3.4-9

Physical Properties of Dustcake Samples Collected After TC03

| Sample ID | Filter Element Locations[1] | Type of Filter Element | General Location in PCD | Bulk Density ($g/cm^3$) | True Density ($g/cm^3$) | UBP[2], (%) | BET Surface Area ($m^2/g$) | MMD[3] (µm) | DED[4] (µm) |
|---|---|---|---|---|---|---|---|---|---|
| AB03954 | T1, T2, T17, T18 | Pall 442-T | North | 0.49 | 2.71 | 81.9 | 3.32 | 7.7 | 2.0 |
| AB03955 | T3, T4, T5, T6, T7, T24 | Schumacher TF-20 | East | 0.53 | 2.64 | 79.9 | 4.31 | 10.8 | 2.7 |
| AB03956 | T8, T9 | 3M Oxide | Southeast | 0.51 | 2.66 | 80.8 | 4.15 | 10.5 | 2.7 |
| AB03957 | T10, T11, T12, T13, T30 | Pall 326 | Southwest | 0.52 | 2.74 | 81.0 | 3.54 | 7.7 | 1.9 |
| AB03958 | Top of Plenum | None | West | 0.51 | 2.79 | 81.7 | 2.56 | 25.3 | 11.0 |

1. T1 through T18 are in outer circle of filter elements in top cluster. T24 and T30 are in inner circle of filter elements in top cluster.
2. UBP = uncompacted bulk porosity
3. MMD = mass median diameter
4. DED = drag-equivalent diameter

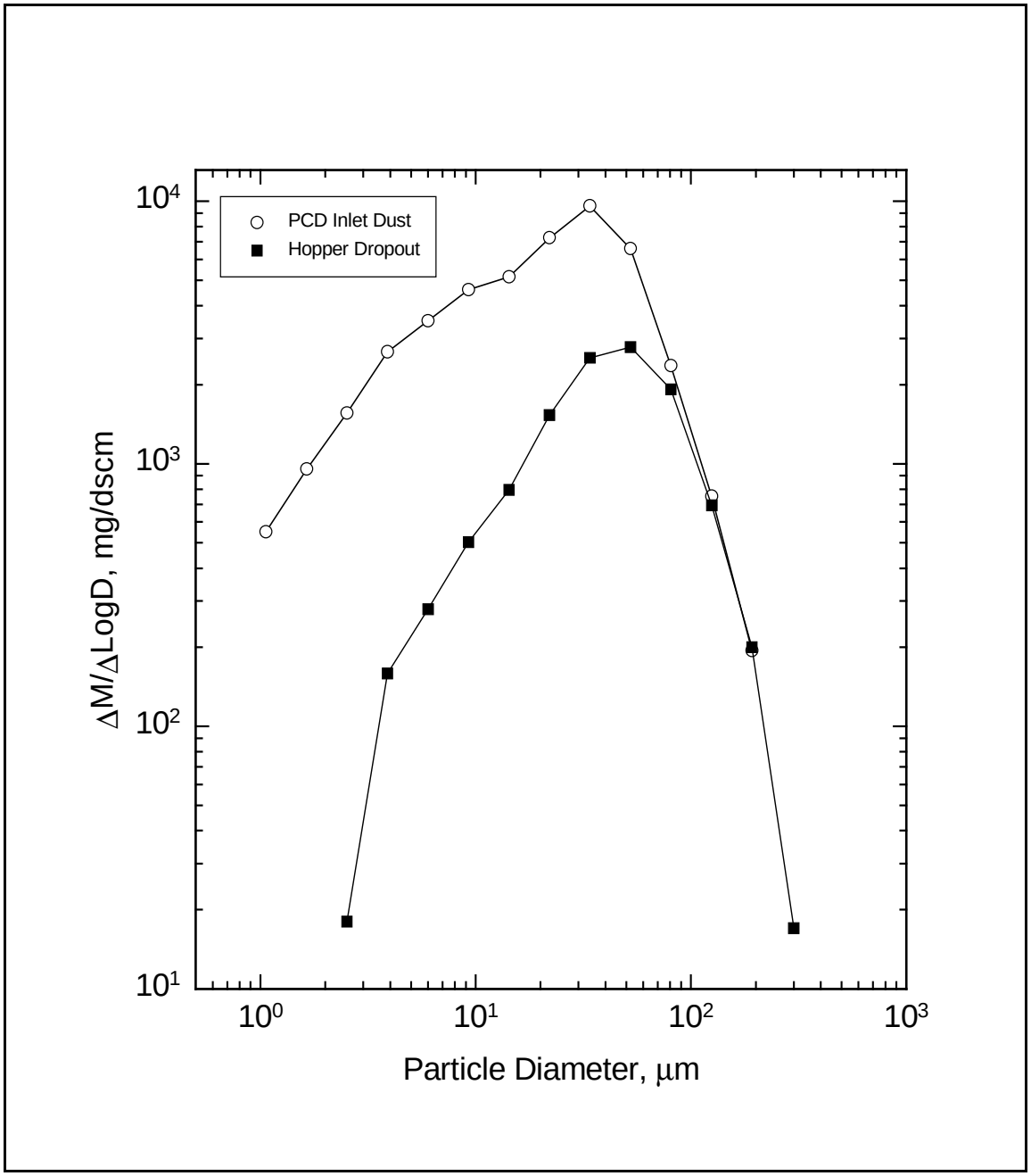


Figure 3.4-1 Particle-Size Distributions of Inlet Particulate and Ash Dropout Samples Collected During TC03 Cut-Size Test

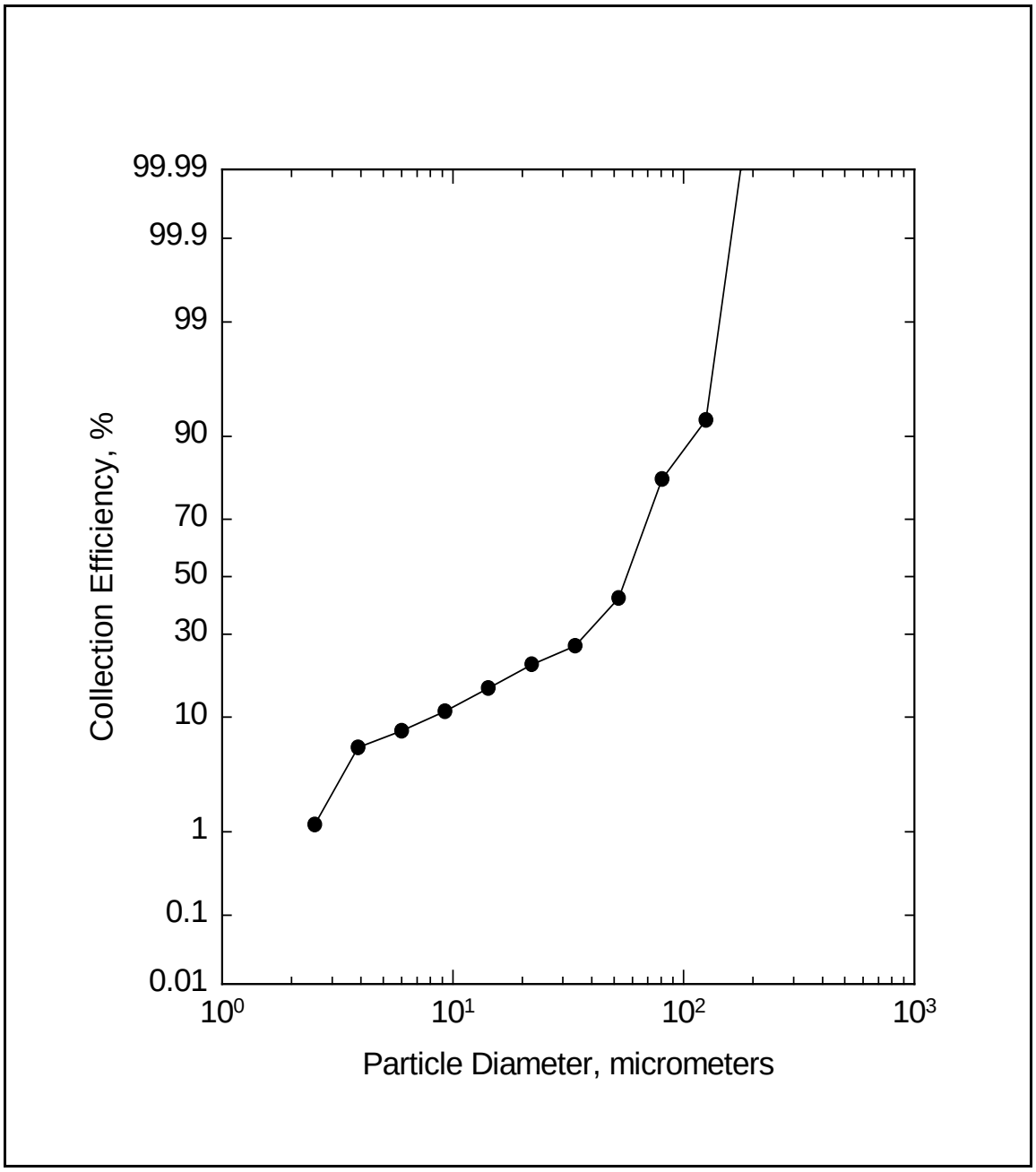


Figure 3.4-2 Particulate Dropout in PCD as a Function of Particle Size

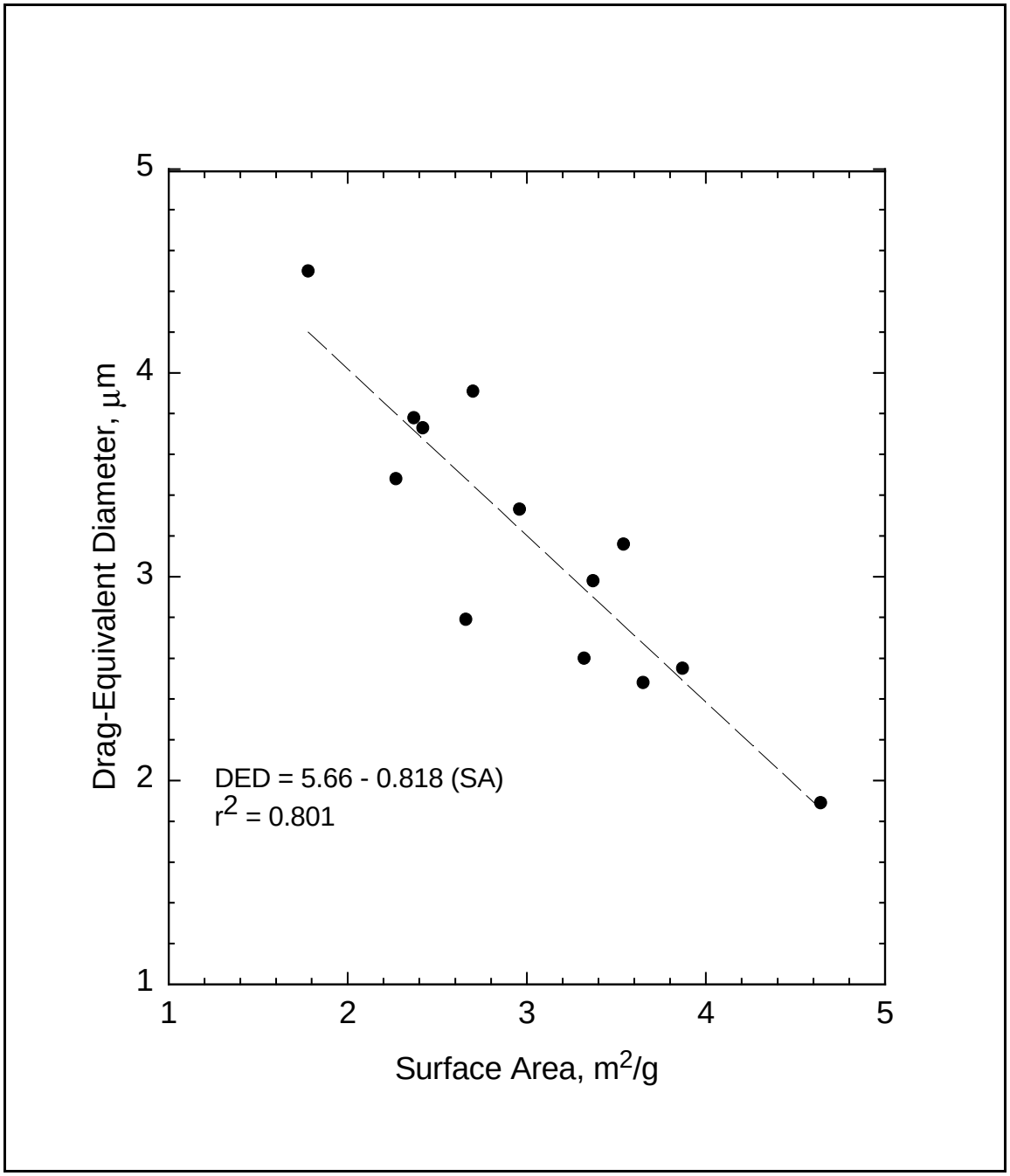


Figure 3.4-3 Drag-Equivalent Diameter Versus BET Surface Area for TC03 In situ Particulate Samples

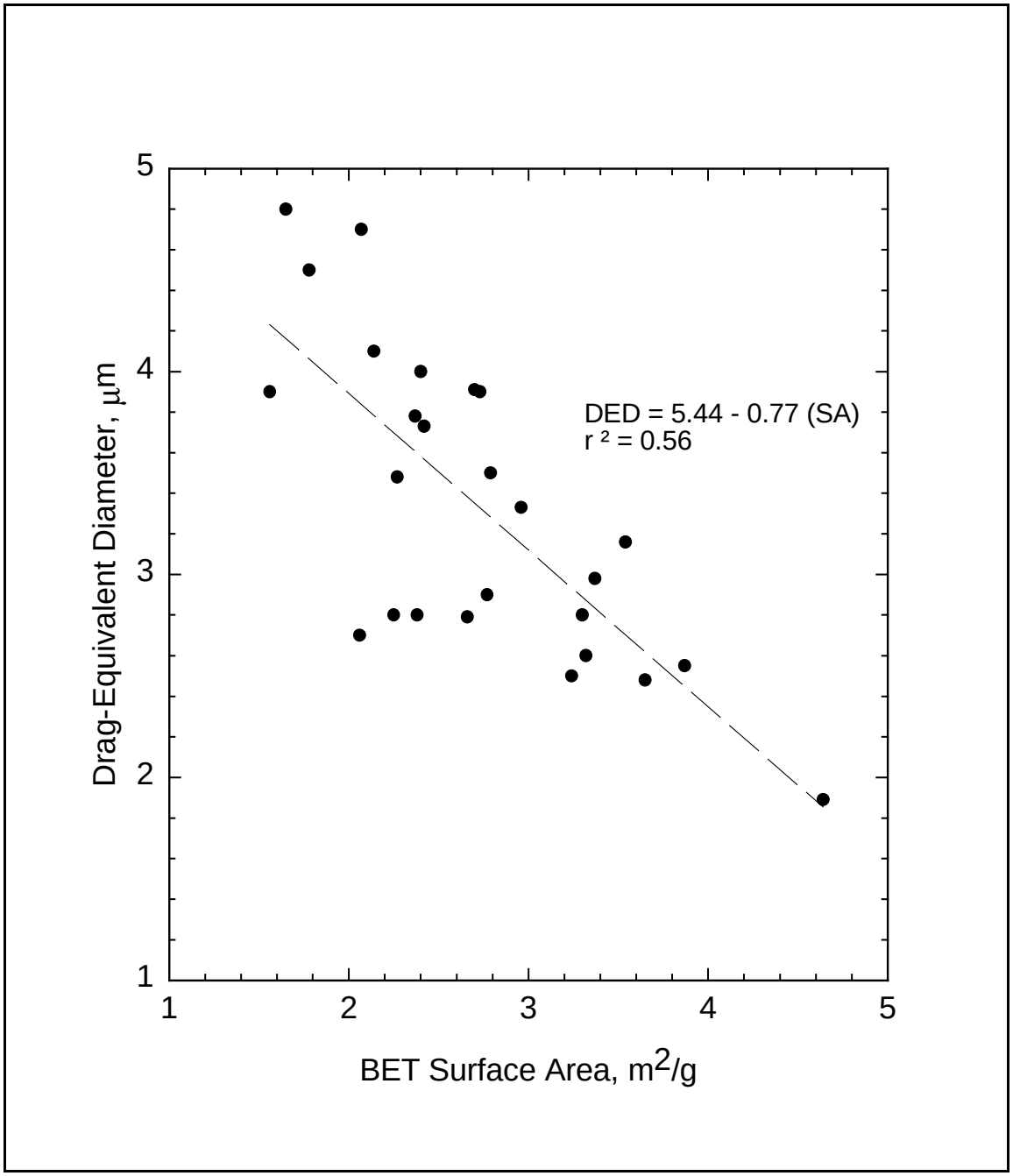


Figure 3.4-4 Drag-Equivalent Diameter Versus BET Surface Area for All TC03 In situ Particulate Samples and Hopper Samples

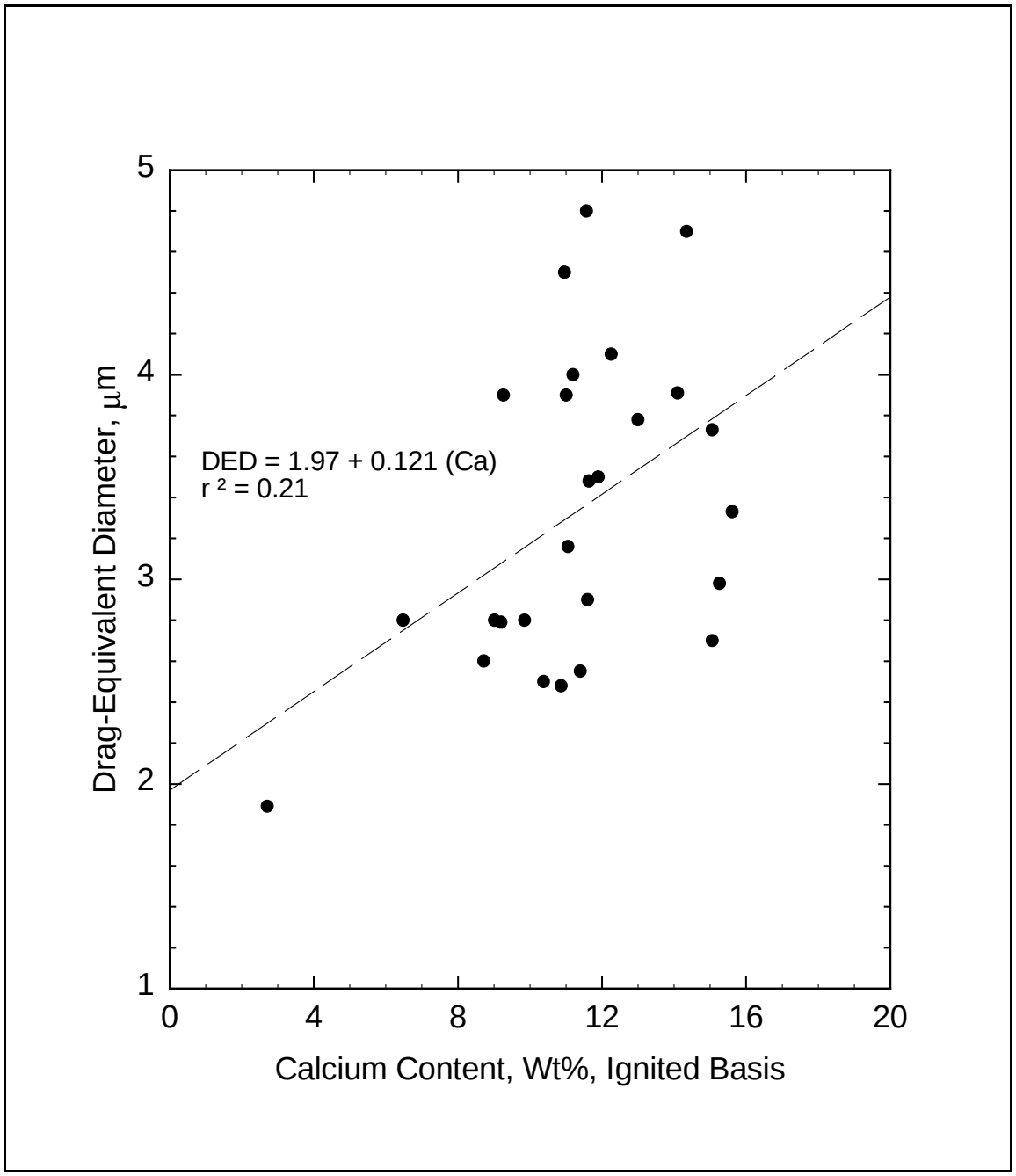


Figure 3.4-5 Drag-Equivalent Diameter Versus Calcium Content of all TC03 In situ Particulate and Hopper Samples

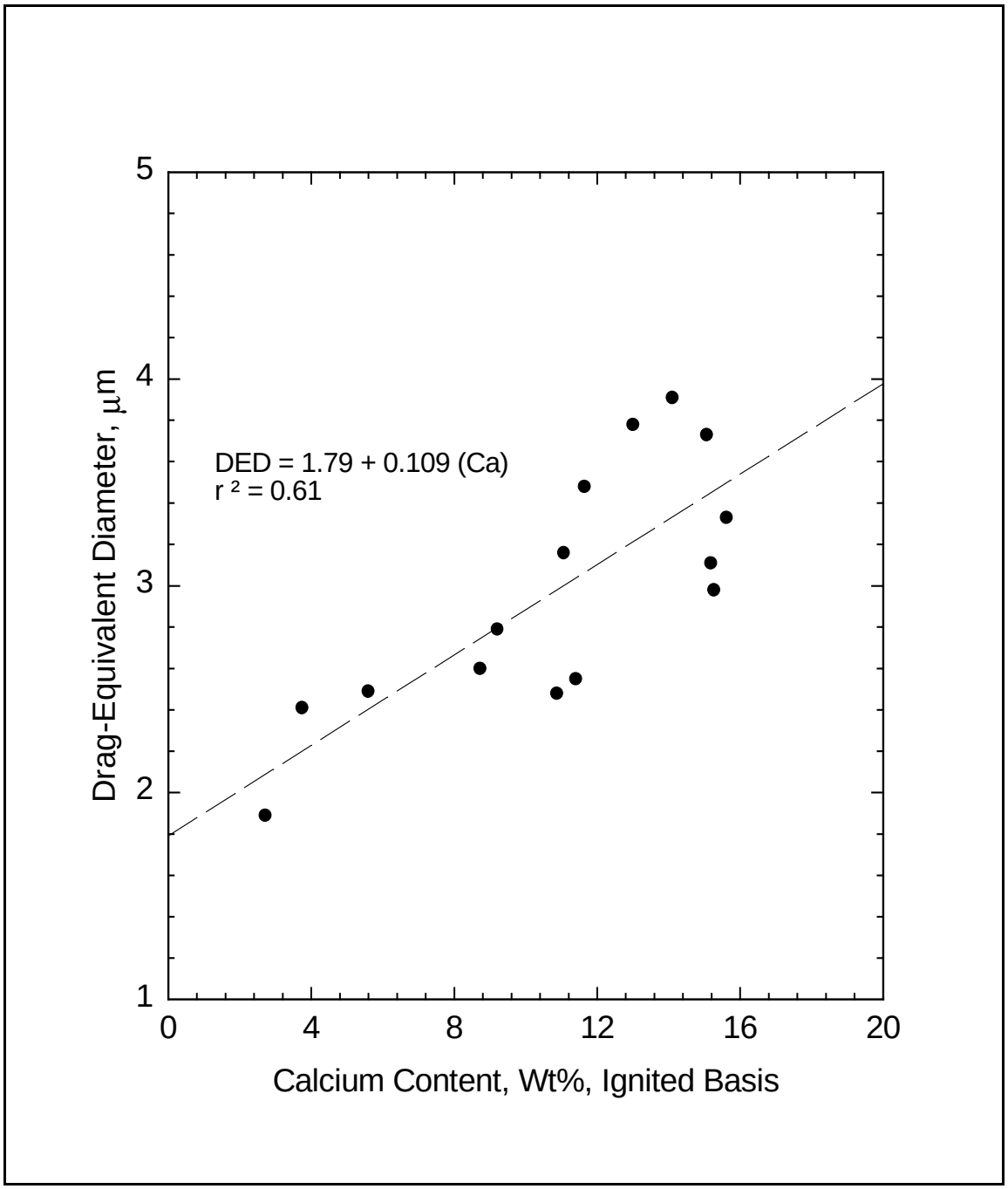


Figure 3.4-6 Drag-Equivalent Diameter Versus Calcium Content of all TC03 and TC01 In situ Particulate Samples

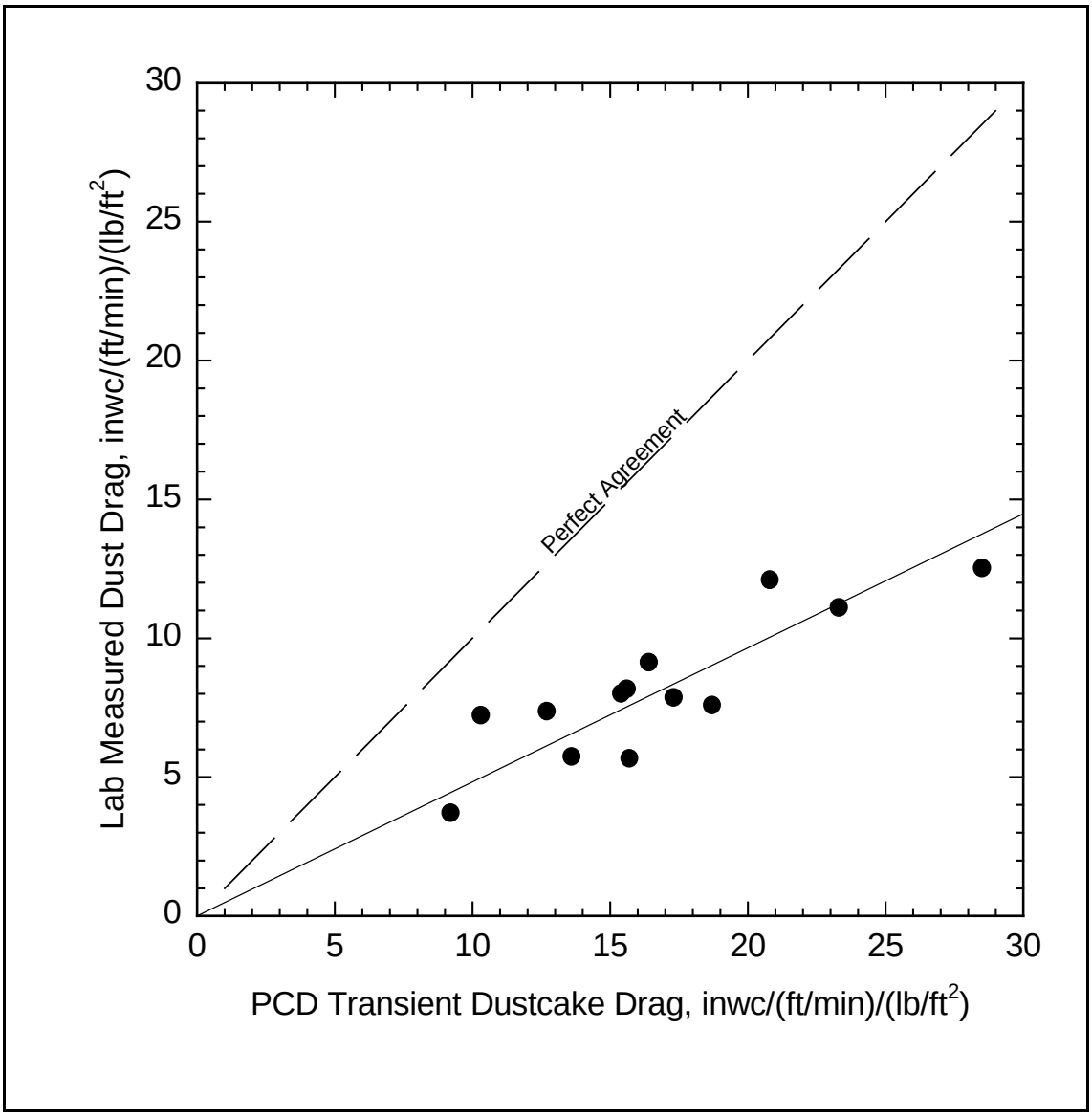


Figure 3.4-7 Lab-Measured Drag Versus Drag Calculated From Transient Pressure Drop Across PCD

# 4.0 TRANSPORT REACTOR

## 4.1 TC03 RUN SUMMARY

Test run TC03 was started on May 31, 1998, in combustion mode of operation after reactor and PCD inspections were completed. The previous test run (TC02) was focused on parametric testing of the transport reactor. TC03 was planned for additional parametric testing to better quantify the effects of different variables on reactor operation. Eastern Kentucky coal from Hazard County mine no. 4 and Gregg Mine limestone from Florida, proposed feedstocks for the city of Lakeland clean coal demonstration project, were chosen for testing. (See Table 4.1-1 for TC03 operating conditions.) The objectives of test run TC03 for the transport reactor were to:

- *Demonstrate stable reactor operations with different feeds.* Demonstrate stable reactor operations using Eastern Kentucky coal with Plum Run dolomite, Bucyrus limestone, Longview limestone, and Gregg Mine limestone.

- *Evaluate effects of reactor conditions on $NO_x$ emissions.* Vary Ca/S molar ratio, excess air, coal feed rate, and operation temperature.

- *Evaluate effects of reactor conditions on $SO_2$ emissions.* Vary Ca/S molar ratio, solids inventory, and operation temperature.

- *Investigate the effect of increasing the mixing zone density.* Decrease various aeration flows and increase solids inventory.

Coal feed was established on June 2, 1998, after the ancillary equipment was started. Coal feed was stopped within 2 hours due to problems with the coal feeder system. The top of the rotor was scoring the bottom of the top plate. The clearance was increased and coal feed resumed on June 3, 1998. Stable reactor operation was established with no problems using the Alabama coal and Plum Run dolomite. Excess dolomite was added to the system for bed material makeup. The Ca/S molar ratio was then varied to determine its effect on the $NO_X$ emissions. Operations continued to be smooth for the next week except for some minor problems with plugging in the spent solids removal system. The coal feed rate was gradually increased as the heat exchanger level increased and the ash content of the bed increased.

The coal feed was changed on-line to the Eastern Kentucky coal on June 11, 1998, after establishing steady operations. The expected changes in reactor operation due to the higher heating value and lower ash content appeared to cause no operational problems. The analyses of the Alabama and Eastern Kentucky coals are listed in Table 4.1-2. Operations continued to be smooth until June 14, 1998, when there was a coal stoppage due to bridging in the coal feeder system. Coal feed was restarted within the day.

On June 15, 1998, the sorbent was changed on-line to the Gregg Mine limestone from Florida. The dipleg was unstable, causing a considerable amount of solids to be carried to the PCD. Since the reactor solids inventory was low, large amounts of limestone were added to increase the solids inventory. The large amount of limestone in the bed hindered circulation in the

reactor significantly and dipleg operations continued to be unstable. The mixing zone density increased and there were several temperature excursions in the mixing zone due to poor solids circulation. The reactor was shutdown and inspected on June 19, 1998.

Inspection revealed significant clinker formation in the mixing zone. The mixing zone was nearly completely blocked by a large deposit that extended from below the coal feed nozzle to nearly the top of the mixing zone. The bend from the crossover to the disengager was partially blocked by another deposit. There was also a bridge of loose material blocking the top of the dipleg. The inspection also revealed that the bed material in the combustor heat exchanger had not drained from the bottom of the heat exchanger when the reactor was emptied of solids. This material was drained, the clinkers were removed, and the reactor system was prepared for start-up.

After a smaller-grind-size sand (~ 120 micron mmd) was added for bed material, coal feed was started on July 13, 1998, with the Eastern Kentucky coal and Florida limestone ground to a smaller size (=150 micron mmd). No excess limestone was added in this case for bed material. The process conditions were similar to previous runs. Operations were smooth for 2 days, except for a momentary loss of coal feed on July 14, 1998. The mixing zone density started increasing within 2 days and solid circulation rate started decreasing. Again, the reactor was shut down and inspected.

Inspection again revealed clinker formation in the mixing zone. These clinkers were in the same location as before—just under the coal inlet nozzle; however, the clinker that was found was much smaller—perhaps 1 to 2 feet in height—and was more easily removed. Some minor inspections and changes to the dense-phase transport systems were done and an additional gas sample nozzle was fabricated and installed. The fine ash screw cooler seals were adjusted, but otherwise undisturbed. The reactor was cleaned and returned to service.

Due to the continued operational problems, the following operating parameters were changed:

- Smaller limestone grind size: 15 to 30 μm mmd.
- No air flow through upper level of primary air.
- No staging air flow.
- Higher gas flow through bottom of mixing zone.
- Higher gas flow through burner leg.
- Lower operating pressure: 145 to 180 psig.
- Lower standpipe and heat exchanger levels.
- Lower operating temperature: 1,400 to 1,550°F.
- Different limestones.
- Higher mixing zone velocity.
- Higher coal conveying gas velocity.

Coal feed was started on July 25, 1998, using the Eastern Kentucky coal and Bucyrus limestone from Ohio. Operations were stable at the moderate operating conditions with the exception of unsteady dipleg operation at times. Dipleg operations became more stable as more experience

was gained on the proper aeration required. The Ca/S molar ratio was varied to study its effect on sulfur capture and $NO_X$ emissions.

On August 3, 1998, the feedstock was changed to the Longview limestone from Alabama. Operations continued to be smooth. The Ca/S molar ratio was varied to study its effect on sulfur capture and $NO_X$ emissions. The sorbent was changed on August 6, 1998, to the Florida Gregg Mine limestone after several days of steady operation. Operations were smooth for several days. On August 9, 1998, process conditions were varied to evaluate the potential for clinker formation. The mixing zone density began to increase within a day and the solids circulation rate dropped. The transport reactor was shut down and inspected.

Reactor inspection again revealed the mixing zone blocked with solids. Nearly 1 month of work was required to remove this clinker. About 25 percent of the circumference of the mixing zone above the clinker was covered in lumpy deposits described to look like an egg carton or fish scales. These deposits extended from the top of the clinker to the top of the mixing zone. For this inspection, the secondary crossover was removed to allow for inspection of the disengager and cyclone. The refractory attached to the disengager roof was damaged. In most areas, the refractory anchor bolts were clearly visible in the top of the disengager. The disengager exit also showed signs of wear. The cyclone was found to be in better shape than was expected. Some minor cracks were visible, but overall the cyclone has not yet experienced the damage seen in the disengager. There was only one anchor bolt visible in the cyclone and there was some damage to the refractory poured on site to modify the cyclone inlet from circular to a restricted rectangular cross-section. The rest of the reactor inspection revealed no problems.

There were 890 hours of solid circulation and 795 hours of coal feed attained in TC03. Overall, this test run was successful. Stable operations were demonstrated using the Eastern Kentucky coal and Plum Run dolomite, Bucyrus limestone, and Longview limestone. There were, however, circulation problems using the Eastern Kentucky coal and Florida limestone. Mixing zone density increased and reactor circulation decreased that could not be increased by any means. In the first incident of circulation problems, a disproportionately large amount of limestone was added to increase the solids inventory in the reactor. In the second incident, only the minimum needed for high sulfur capture (Ca/S molar ratio 1.5 to 2.0) was added. In the third incident, operating parameters were being changed from the moderate set. The average operating conditions for the run are shown in Table 4.1-1 and operating plots in Figures 4.1-1 to -24. The analyses for the four different sorbents are given in Table 4.1-3.

Other accomplishments include:

- Achieved effective solids circulation and higher disengager/cyclone collection efficiency with smaller-grind-size start-up bed material (~120 μm mmd).
- Successfully ground limestone to 15 to 25 μm mmd and used the sorbent feed system to feed into the reactor without any problems.
- Completed the longest continuous test run (382 hours) without any interruption from the coal feed system or any other subsystem.

- Experienced good performance from the filter ash depressurization and transportation systems for the entire TC03 test run after modifications made to the sealing mechanism on the spheri seal holding plate.
- Experienced smooth coal feed system operation during TC03; however, operational problems develop when (segregated) fine coal moves through the coal feed system.
- Achieved nearly 100-percent carbon conversion for Eastern Kentucky coal at 1,500°F reactor temperature.
- Perceived little observable difference using the Eastern Kentucky coal with limestone or dolomite for sulfur capture.
- Achieved lower particle loadings to the PCD (5,000 to 7,500 ppm).
- Successfully heated different legs of an empty reactor loop and combustor heat exchanger to different temperatures and the PCD to above 800°F before adding sand through the coal feed system at 110 to 135 psig reactor pressure.
- Achieved smoother operation with lower-grind-size material in the reactor.

There were several notable observations concerning the $SO_2$ and $NO_X$ emissions. A high-sulfur capture (greater than 97 percent) was achieved using Bucyrus limestone at a Ca/S molar ratio of 1.6. It was observed that immediately after a back-pulse the $SO_2$ increased from 5 to 35 ppm and then gradually decreased back to 5 ppm within 20 to 30 minutes. In some instances the separate effect of each back-pulse on $SO_2$ was detectable. The $NO_X$ emissions were as low as 0.04 and varied up to 0.55 lb/MBtu when excess sorbent was added to the system as bed material. The $NO_X$ emissions with the Eastern Kentucky coal and Alabama coal were similar, with the Eastern Kentucky coal $NO_X$ emissions lower at times than the Alabama coal. The $NO_X$ emissions with the Florida and Longview limestone were similar (ranging from 0.1 to 0.14 lb/MBtu) and were slightly higher than the $NO_X$ emissions with the Bucyrus limestone, which ranged from 0.07 to 0.1 lb/MBtu. In addition, there was a significant increase in $NO_X$ emissions when sorbent was added to the system for all sorbent types. For example, with the addition of Bucyrus limestone there was an increase of 40 percent in $NO_X$ emissions, while the Ca/S molar ratio increased from 0 to 1.0. Mixing zone operations under both highly reducing and highly oxidizing conditions showed no perceptible change in $NO_X$ formation or $SO_2$ capture. Analysis of both $SO_2$ and $NO_X$ emissions is further noted in sections 4.3 and 4.4, respectively.

Table 4.1-1

TC03 Operating Conditions

| | |
|---|---|
| Start-up Bed Material | 120 to 200 μm Silica Sand |
| Coals | Alabama Bituminous<br>Eastern Kentucky Bituminous |
| Coal Grind-Particle Size | 250 to 350 μm |
| Average Coal Feed Rate | 800 to1,600 lb/hr |
| Sorbents | Plum Run Dolomite<br>Florida Limestone<br>Bucyrus Ohio Limestone<br>Longview Limestone |
| Sorbent Grind-Particle Size | 15 to 250 μm |
| Ca/S Molar Ratio | 0 to 2.5 |
| Reactor Temperature | 1,400 to 1,625°F |
| Reactor Pressure | 145 to 200 psig |
| HX0203 Inventory | Nearly Full |

Table 4.1-2

Coal Analyses

| Wt (%) | Alabama | E. Kentucky |
|---|---|---|
| Moisture | 2.2 | 1.8 |
| Ash | 16.9 | 10.0 |
| Sulfur | 0.9 | 1.3 |
| Carbon | 66.5 | 73.9 |
| Hydrogen | 4.3 | 4.8 |
| Nitrogen | 1.6 | 1.6 |
| Oxygen | 7.8 | 6.6 |
| Vol | 31.2 | 36.1 |
| Fix C | 49.5 | 52.1 |
| Heat Value (Btu/lb) | 11,798 | 13,482 |

Table 4.1-3

Sorbent Analyses

| | Plum Run Dolomite From Ohio | Gregg Mine Limestone From Florida | Bucyrus Limestone From Ohio | Longview Limestone From Alabama |
|---|---|---|---|---|
| $CaCO_3$ (wt %) | 51.1 | 90.4 | 73.0 | 88.7 |
| $MgCO_3$ (wt %) | 40.7 | 1.1 | 15.8 | 5.5 |
| Inerts (wt %) | 8.2 | 8.5 | 11.2 | 5.8 |

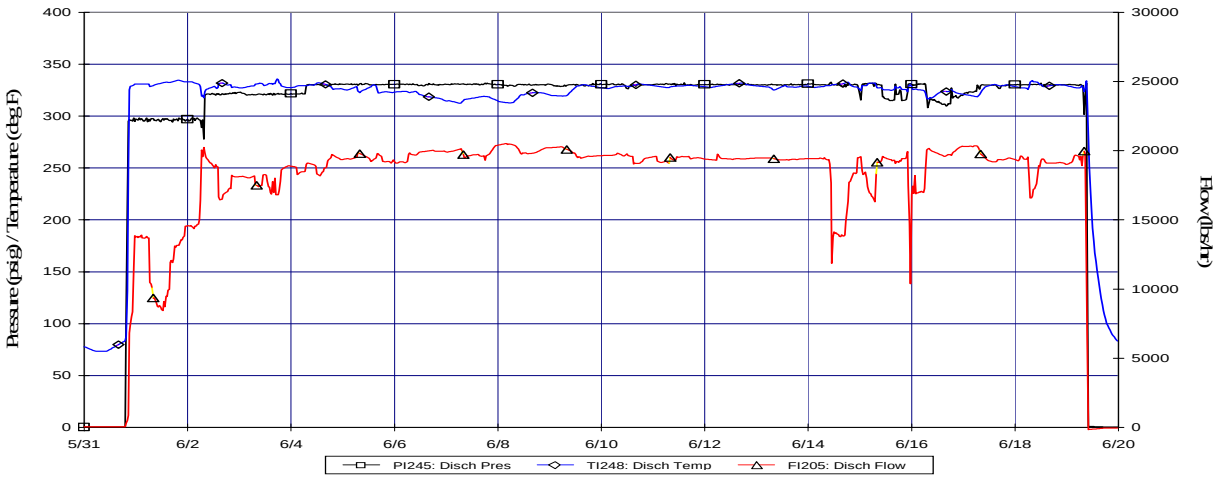


Figure 4.1-1 CO0201 System Profile

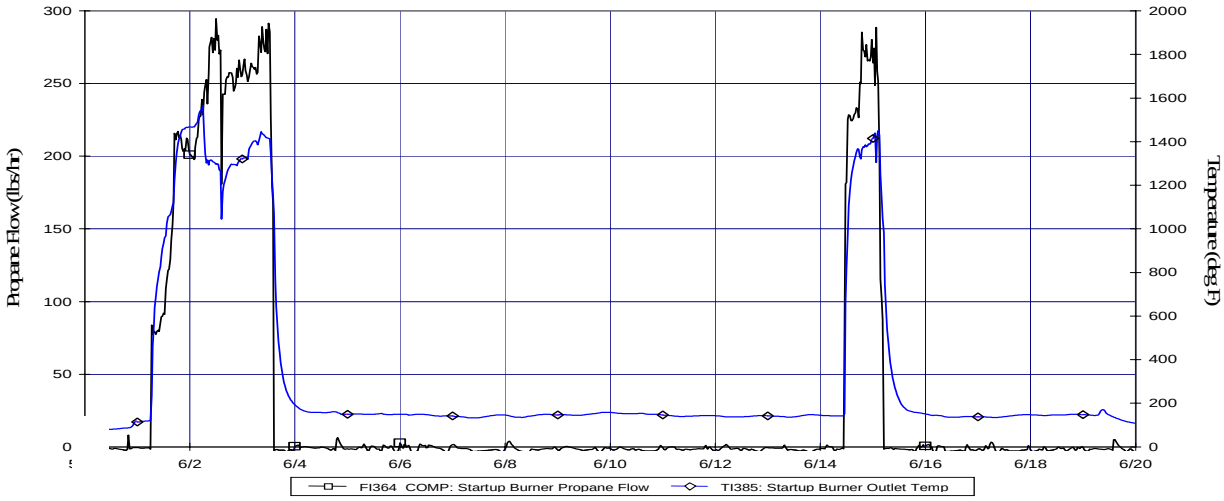


Figure 4.1-2 Start-up Burner Flow/Temperature

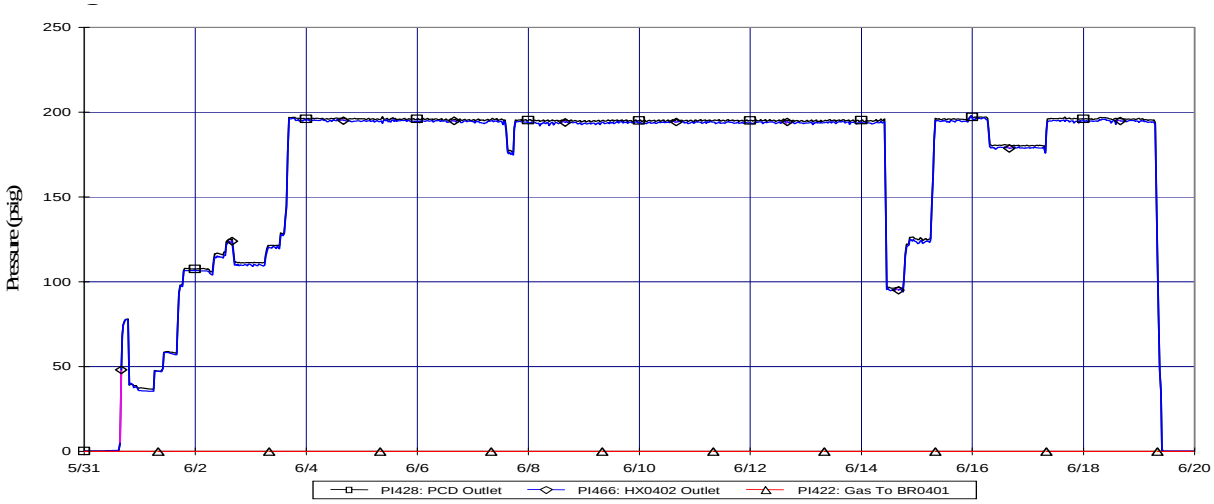


Figure 4.1-3 System Pressures Downstream of PCD

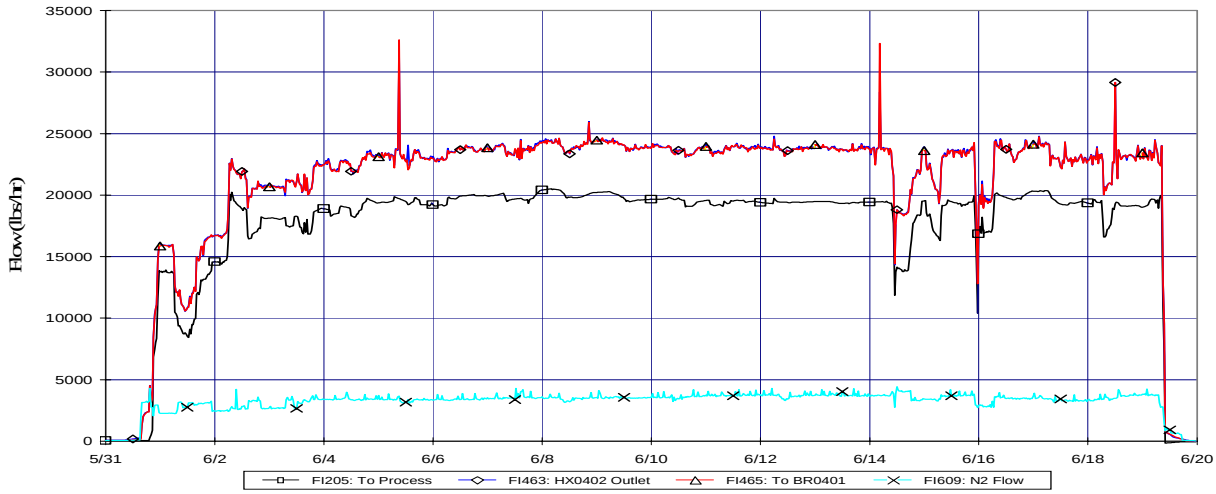


Figure 4.1-4 Total Gas In/Out Flow Rates

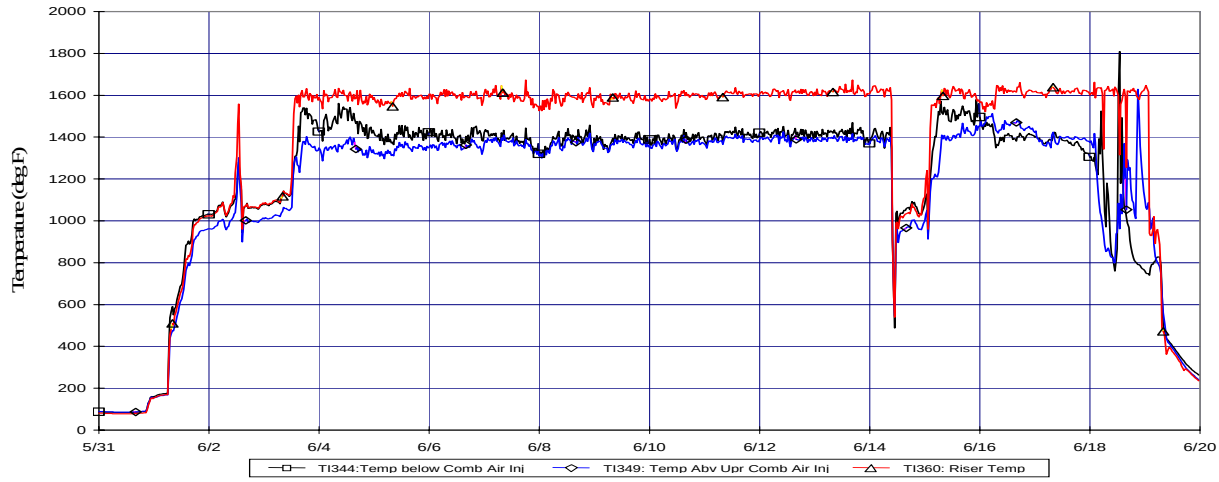


Figure 4.1-5 Reactor Mixing Zone and Riser Temperature

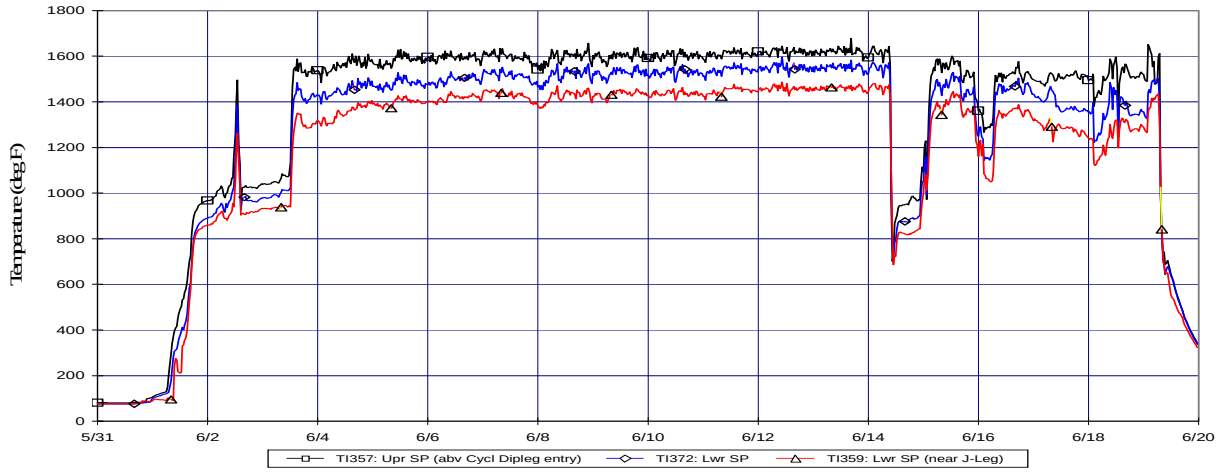


Figure 4.1-6 Standpipe Temperatures

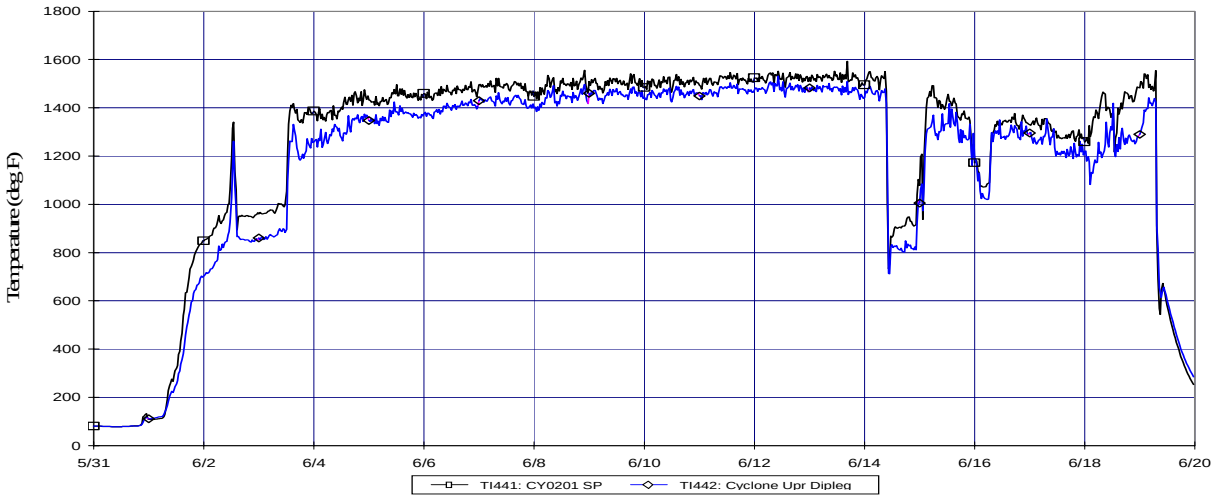


Figure 4.1-7 Cyclone Dipleg Temperatures

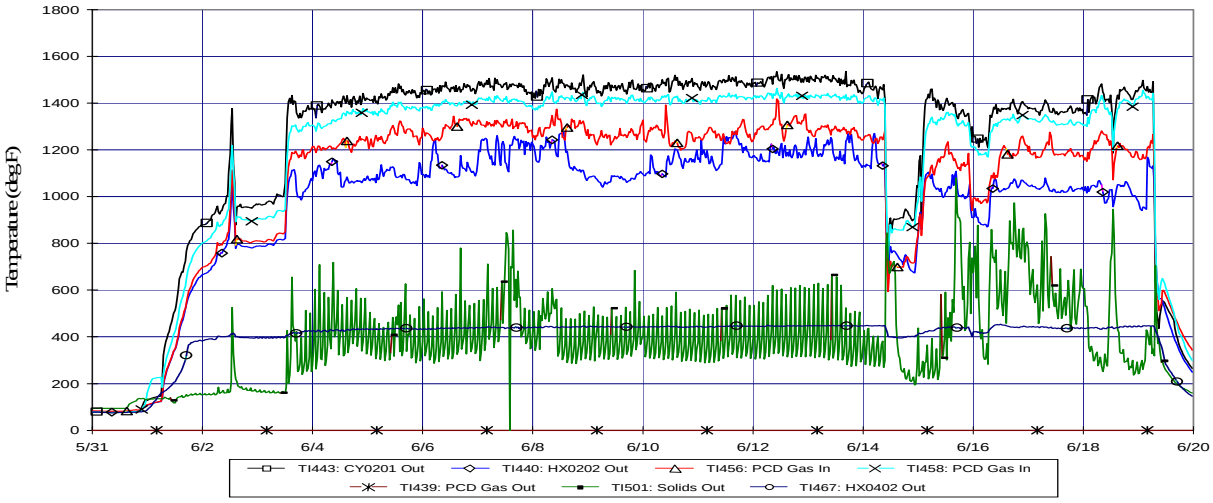


Figure 4.1-8 Temperature Profiles Downstream of Reactor

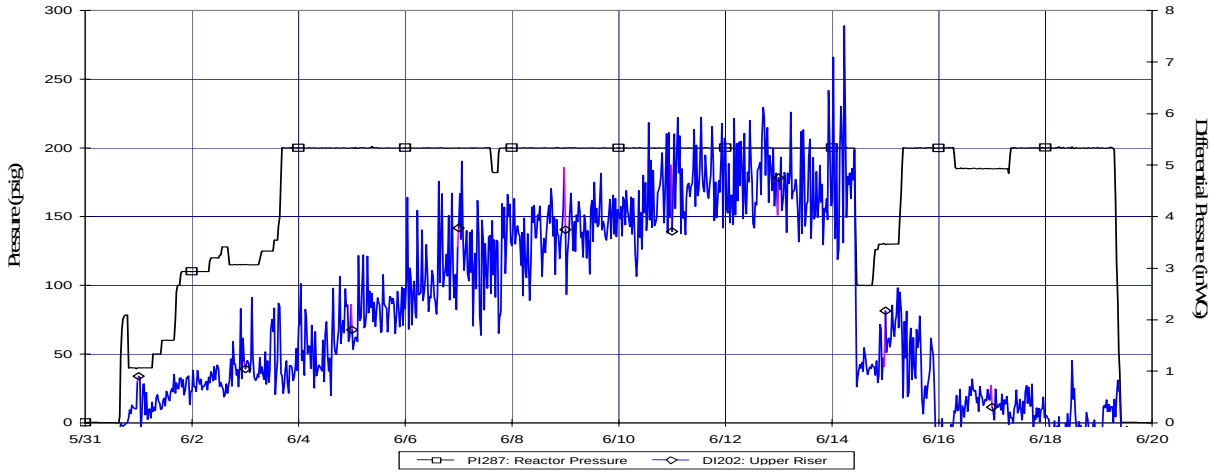


Figure 4.1-9 Reactor Pressure/Riser Differential Pressure Profiles

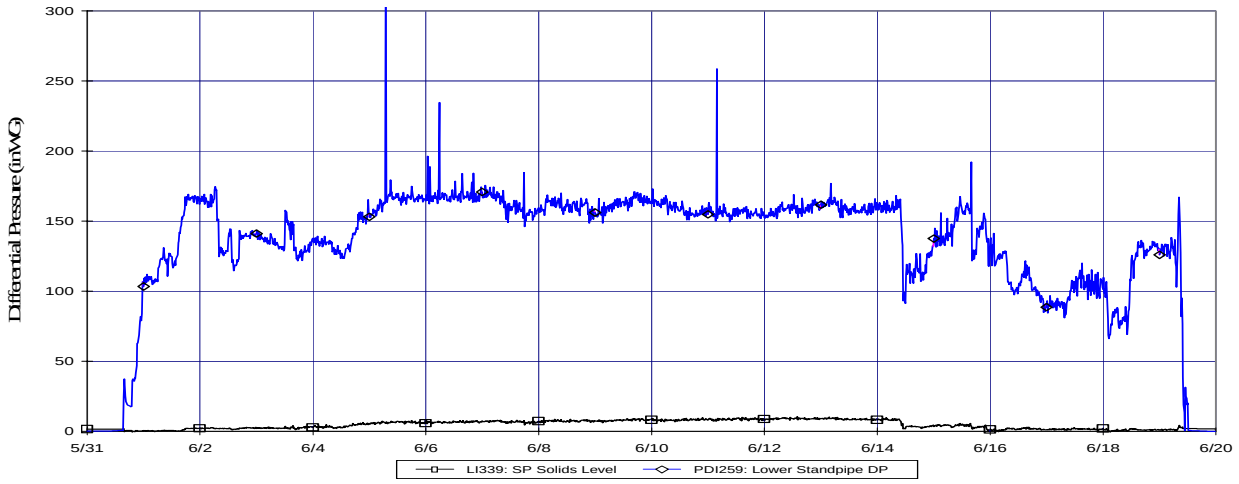


Figure 4.1-10 Standpipe Differential Pressure Profiles

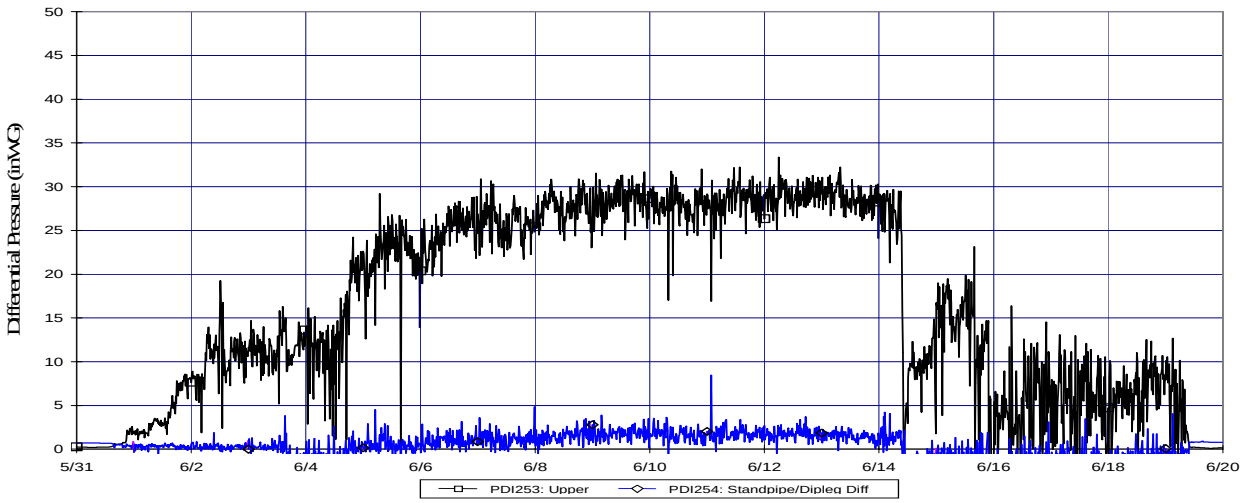


Figure 4.1-11 CY0201 Dipleg Differential Pressure Profiles

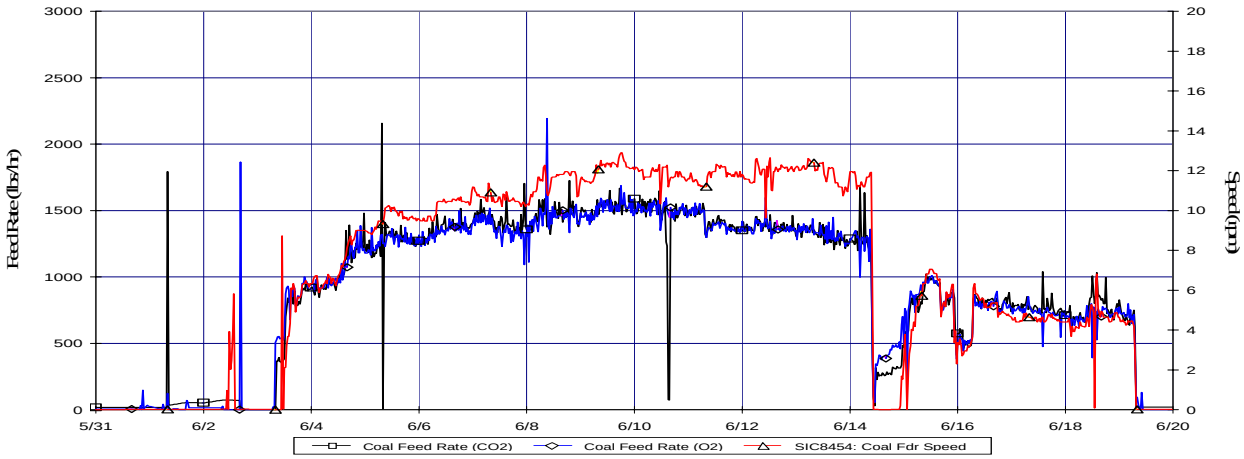


Figure 4.1-12 Coal Feed Rate Based on Gas Analysis

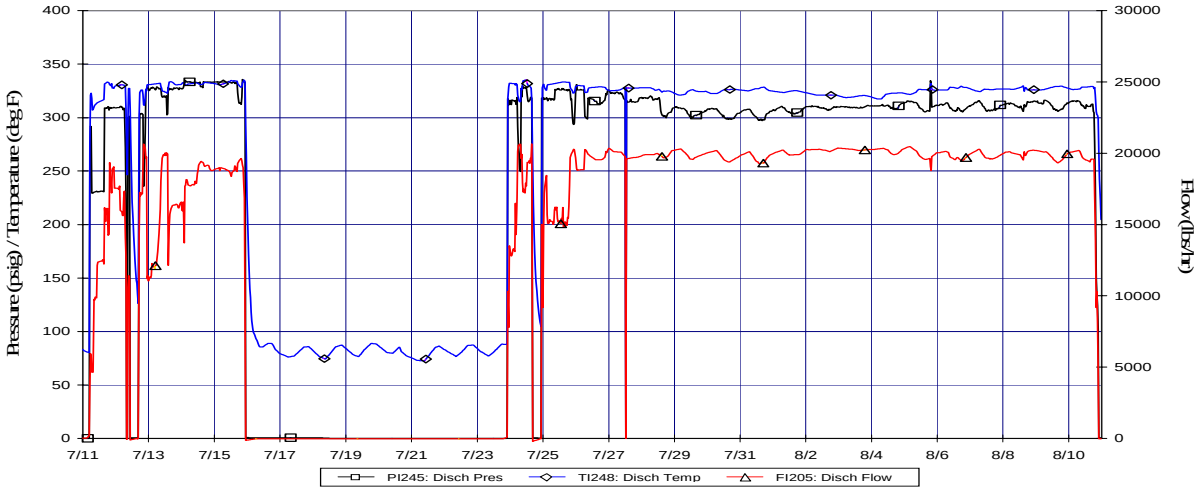


Figure 4.1-13 CO0201 System

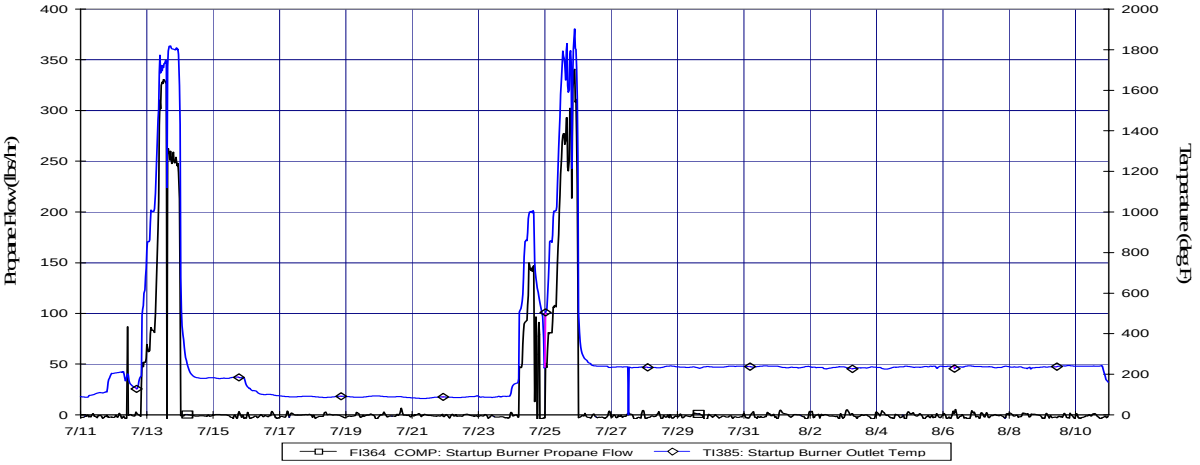


Figure 4.1-14 Start-up Burner Flow/Temperature

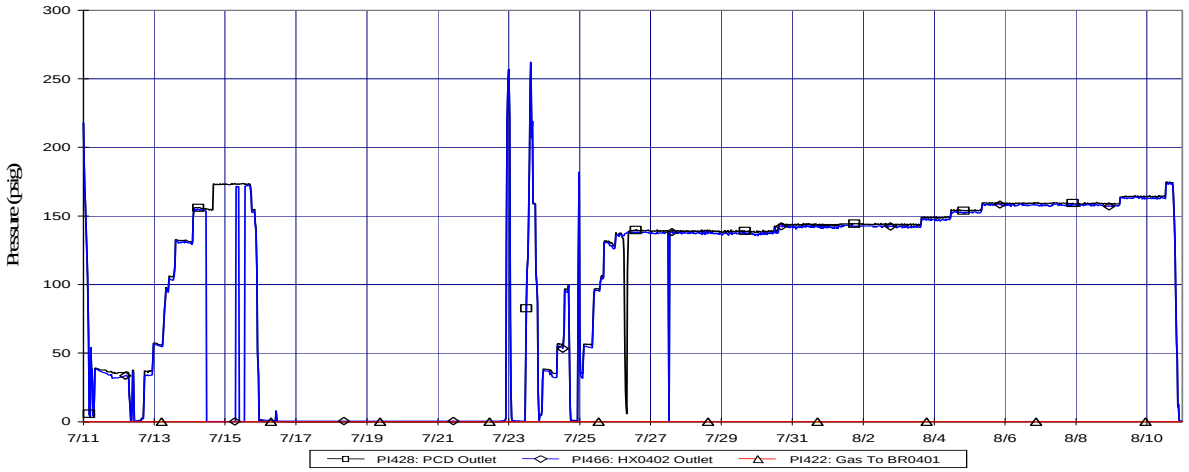


Figure 4.1-15 System Pressures Downstream of PCD

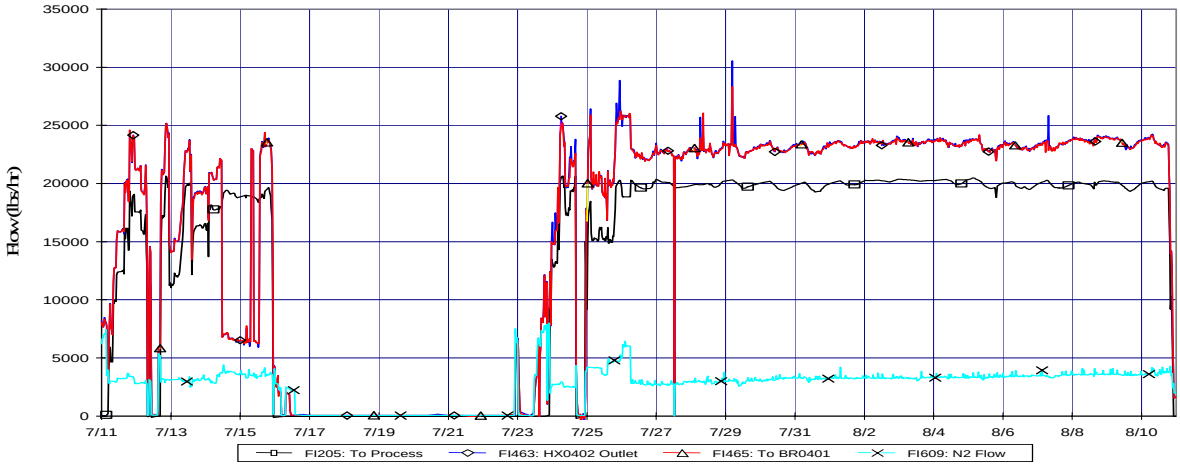


Figure 4.1-16 Total Gas In/Out Flow Rates

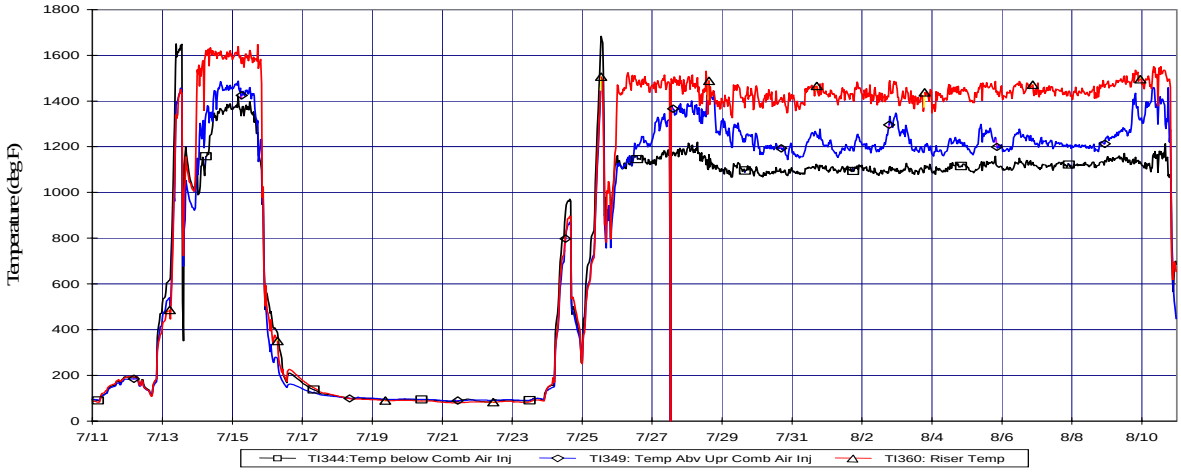


Figure 4.1-17 Reactor Mixing Zone and Riser Temperature

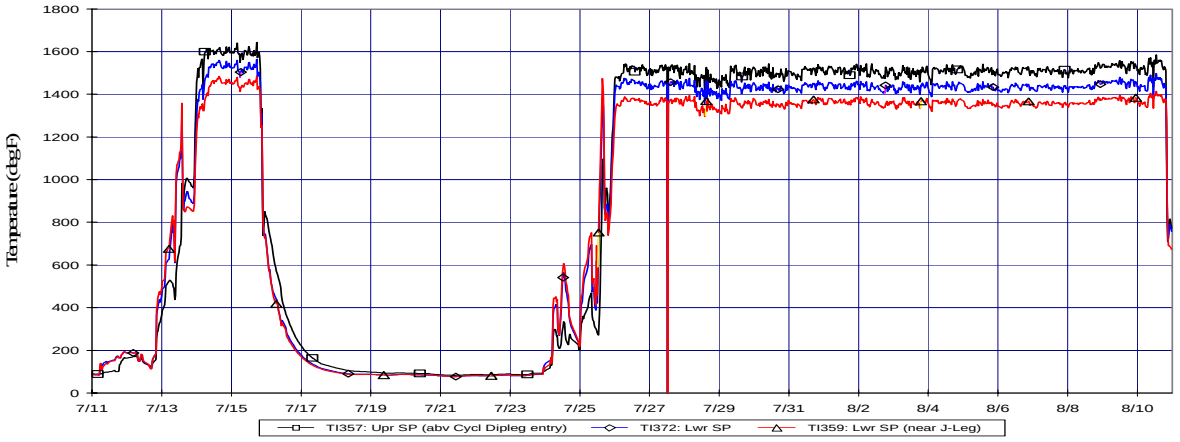


Figure 4.1-18 Standpipe Temperatures

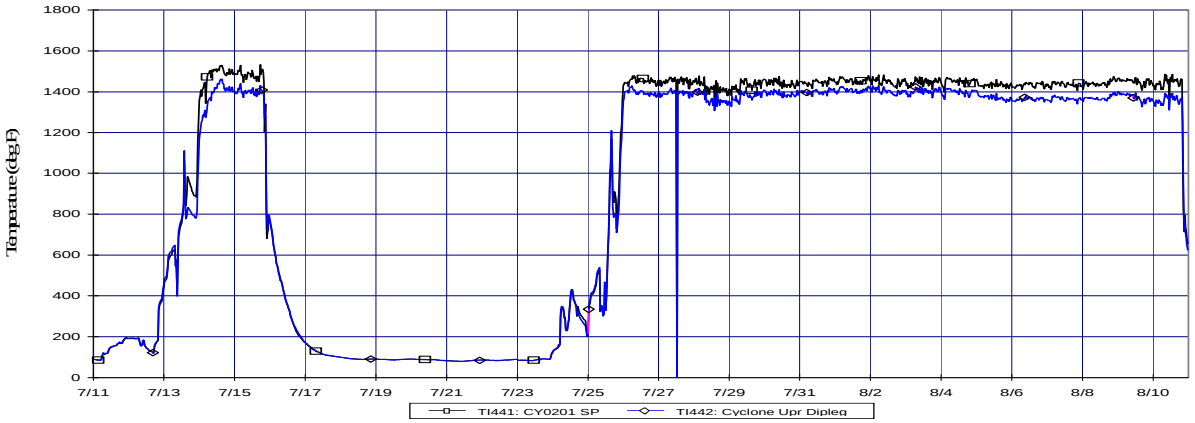


Figure 4.1-19 Cyclone Dipleg Temperatures

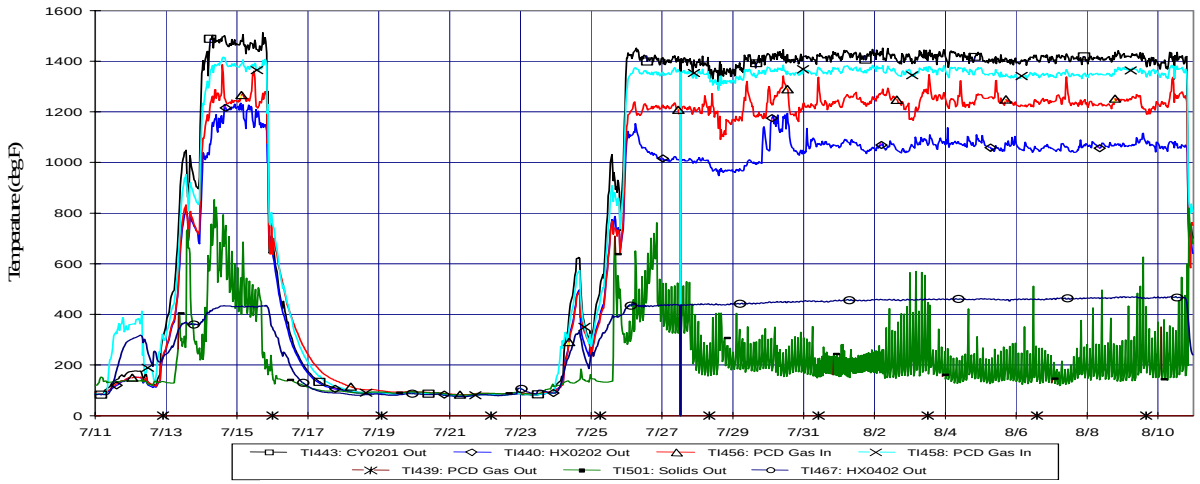


Figure 4.1-20 Temperature Profiles Downstream of Reactor

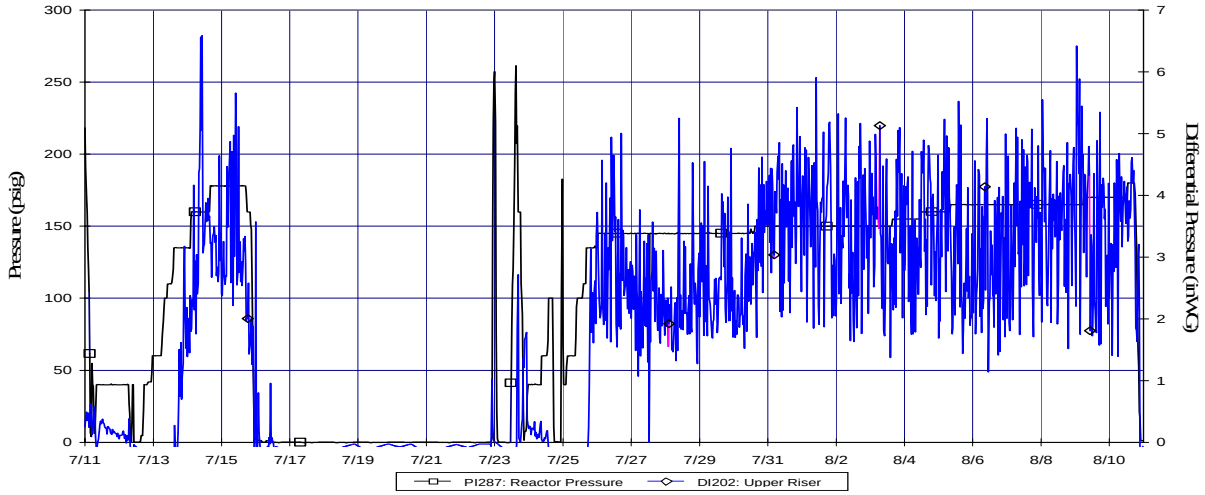


Figure 4.1-21 Reactor Pressure/Riser Differential Pressure Profiles

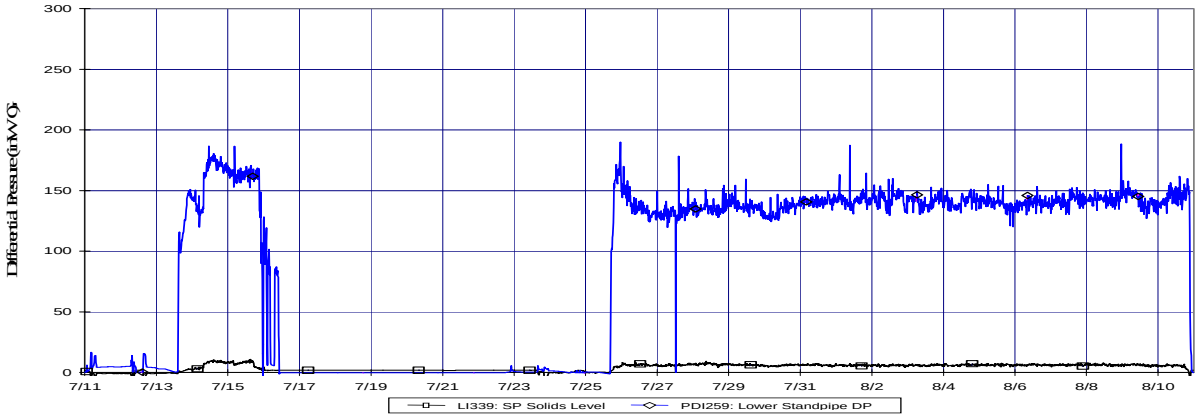


Figure 4.1-22 Standpipe Differential Pressure Profiles

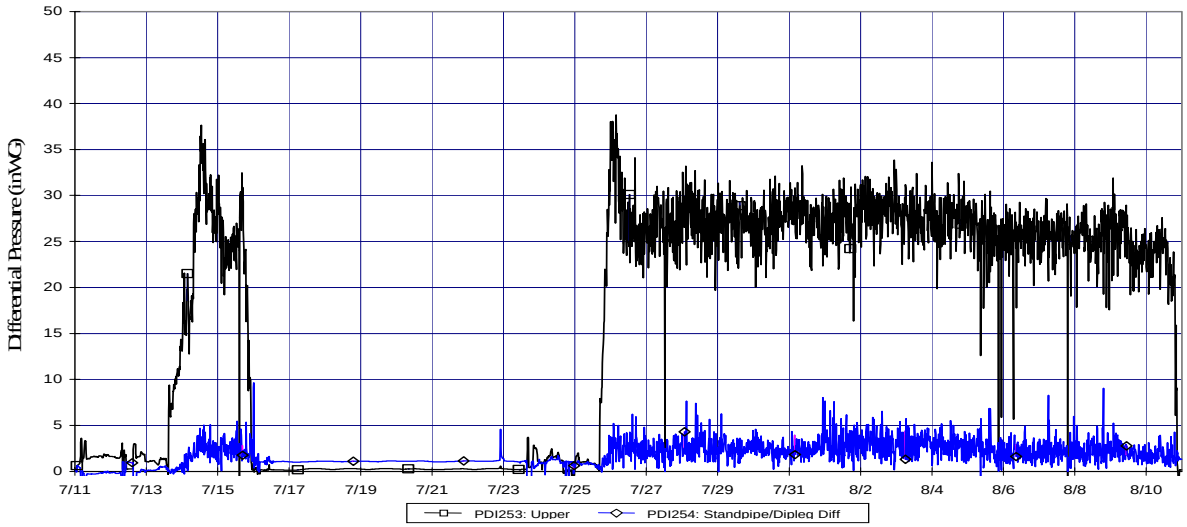


Figure 4.1-23 CY0201 Dipleg Differential Pressure Profiles

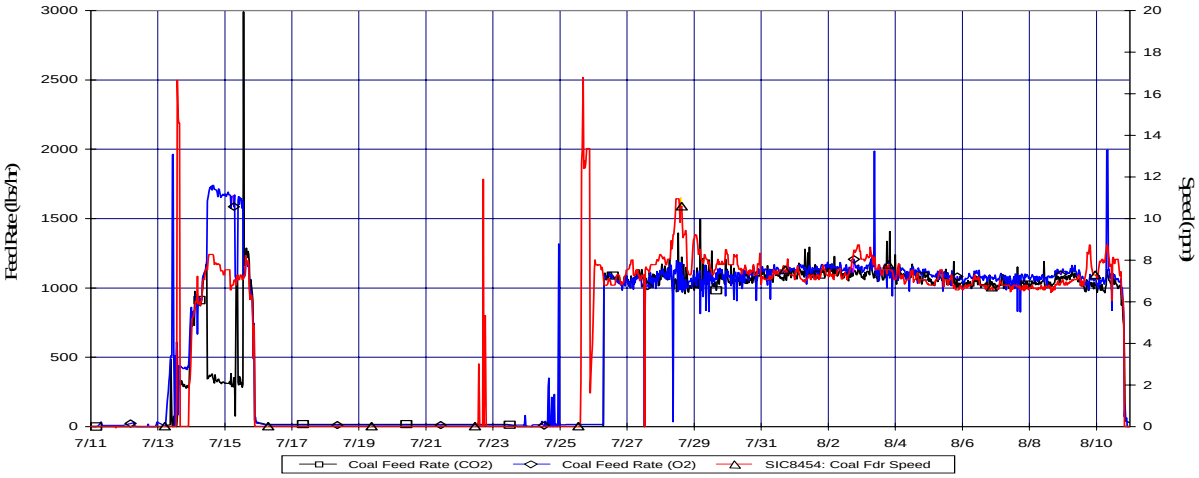


Figure 4.1-24 Coal Feed Rate Based on Gas Analysis

## 4.2 HEAT AND MATERIAL BALANCE

Transport reactor data gathered from 8:00 a.m. on June 13 to 8:00 a.m. on June 14, 1998, was used to perform a heat and material balance. The results are listed below.

The average reactor conditions for this time are summarized in Table 4.2-1. The transport reactor had been operated at very stable conditions for several days leading up to the balance period. During the period, the solids levels in the reactor, the aeration rates, and the solids feed rates were held very steady.

The bulk material balance on the transport reactor closed to within a 2-percent difference (see Table 4.2-2). This difference is typical of the percent error in material balances for the transport reactor. The solids flow rates were determined predominantly with weigh cells. The coal feed rate was back calculated using both the $CO_2$ and the $O_2$ in the flue gas. The three methods gave calculated coal feed rates within 0.5 percent of the average value.

The elemental balances produced low-percent errors for species mainly in the gas phase and higher errors for species predominantly in the solid phase. This is due to the difficulty in measuring solids flow rates and especially the flow of ash. Several of the elemental balances are shown in Table 4.2-3. The gas composition was corrected for moisture in the flue gas.

The material balances also provided transport reactor performance data during this time. The sulfur capture was approximately 99 percent at a Ca/S ratio of 1.3. The reactor produced only 0.08 lb $NO_X$/MBtu. The unburned carbon in the solids removed from the reactor and the CO in the flue gas yields a carbon conversion of 99.9 percent.

Table 4.2-1

Average Reactor Conditions

| | |
|---|---|
| Pressure | 200 psig |
| Riser Temperature | 1,582°F |

Table 4.2-2

Bulk Material Balance

| Feeds | (lb/hr) |
|---|---|
| Coal | 1,295 |
| Dolomite | 134 |
| Air | 19,391 |
| Nitrogen | 3,755 |
| Total | 24,575 |

| Products | (lb/hr) |
|---|---|
| Coarse Ash | 100 |
| Fine Ash | 200 |
| Flue Gas | 23,770 |
| Accumulation | -5 |
| Total | 24,065 |

Table 4.2-3

Elemental Material Balances

| Species | Feed (lb/hr) | Products (lb/hr) | Ratio |
|---|---|---|---|
| Carbon | 967 | 972 | 0.99 |
| Nitrogen | 18,649 | 18,505 | 1.01 |
| Oxygen | 4,607 | 4,591 | 1.00 |
| Sulfur | 17.7 | 18.1 | 0.98 |
| Calcium | 26.7 | 36.1 | 0.74 |
| Magnesium | 16.2 | 20.3 | 0.80 |

## 4.3 $SO_2$, $SO_3$, AND SOLIDS ANALYSES

During TC03 solids were collected from the coal feed system (FD0210), the sorbent feed system (FD0220), the standpipe spent solids transport system (FD0510), and the Particulate Control Device (PCD) fine solids transport system (FD0520). These solids were analyzed for chemical composition and particle size. The $SO_2$ emissions were also continuously measured and recorded by the plant information system (PI). This section utilizes the chemical analysis and $SO_2$ emissions data to show:

- Process and chemical composition changes during a test.
- Effects of sorbent on sulfur dioxide removal.
- Particle size changes during a test.
- Sulfur and calcium balances.
- Thermodynamic equilibrium in the sulfur dioxide - sulfur trioxide system.
- Levels of unburned carbon - combustion efficiency.
- Sulfur trioxide emissions.

Run TC03 began on June 3, 1998, and consisted of the following three separate periods:

1. June 3 to 19, 1998, lasted 16 days. The period started operation on Alabama Calumet Mine bituminous coal and Plum Run dolomite. During this period, the coal was switched to an Eastern Kentucky coal and the sorbent was switched to Gregg Mine, Florida limestone. There was a brief coal outage the night of June 14, 1998.

2. July 13 to 15, 1998, lasted 3 days. The period started operation on Eastern Kentucky coal and Gregg Mine Florida limestone.

3. July 25 to August 19, 1998, lasted 17 days. The period started operation on Eastern Kentucky coal and Ohio Bucyrus limestone. During the period the limestone was first switched to Alabama Longview limestone and then switched to Gregg Mine Florida limestone.

All three periods were terminated due to plugging of the mixing zone. The first and third periods were of a long enough duration to be characteristic of steady-state operation. The second period did not result in steady-state operation and will be excluded from most $SO_X$ and solids analysis. Figures 4.3-1 and -2 show the daily (24-hour) averages of system pressure and upper standpipe (SP) temperature for the first and third periods, June 3 through 19, 1998 and July 26 to August 19, 1998. The periods of operation with different coals and sorbents are shown on the figures. Dolomite operation was generally at 1,600°F and 200 psig, while limestone operation was at 1,500°F and pressures from 145 to 170 psig.

The daily averages for the coal feed rate (by $CO_2$) and the $SO_2$ PCD exit concentrations are given in Figures 4.3-3 and -4. The coal feed rate is calculated from the flue gas rate, $CO_2$ content of the flue gas and the carbon content of the coal. The coal rate increased from June 3 to June 9 as the combustion heat exchanger inventory increased and the solids circulation rate increased.

The period of June 9 to June 13 was characterized by steady operation and slowly decreasing coal feed rate. The transition from Alabama to Eastern Kentucky coal was smooth and uneventful. The coal feed rate was decreased after the addition of Florida limestone due to the difficulty in maintaining circulation, cyclone dipleg level, and heat exchanger level. $SO_2$ emission levels were very low during the June 3 to 18 period.

The coal rate from July 26 to August 10 was nearly constant at about 1,100 pounds per hour. The $SO_2$ concentration increased to 15 ppm, as expected for operation on limestone. The $SO_2$ averaged 90 ppm on July 30 when the limestone was turned off for $SO_3$ testing, which is discussed in detail later this section.

The coals used during TC03 were Alabama Calumet Mine bituminous and Eastern Kentucky bituminous. Figures 4.3-5 and -6 show the coal sulfur and ash as sampled from the coal feed system during TC03. Figure 4.3-5 shows the transition from Alabama Calumet Mine bituminous to Eastern Kentucky, which was gradual due to back mixing in the coal feed system. The sulfur increased during the coal transition, from 0.9-percent sulfur to nearly 1.4-percent sulfur and the ash decreased from 15 to about 10 percent. Figure 4.3-6 shows variations of the Eastern Kentucky coal in sulfur and ash content.

The Sauter mean diameter of the coal sampled from the coal feeder and sorbent sampled from the sorbent feeder is plotted on Figures 4.3-7 and -8. The coal grind size was fairly consistent during TC03, with an average particle-size mass mean diameter of about 300 microns. The coal grind size was kept constant during the entire run.

The sorbent particle size was intentionally decreased after June 20. From June 4 to 20, the sorbent particle size was between 100 to 175 microns, while from July 25 to August 11 the sorbent particle size was below 25 microns.

Typical coal and sorbent particle-size distributions are given on Figures 4.3-9 (sieve analyses) and -10 (Microtrac).

Compositions of the four sorbents used in TC03 are given in Table 4.3-1. Several analyses for the Florida limestone and dolomite were rejected because they were inconsistent or were a mixture of limestone and dolomite. The three limestones were noticeably different from each other in their $MgCO_3$ contents.

Figures 4.3-11 and -12 show the $CaCO_3$ and $MgCO_3$ content of the sorbents during TC03. The magnesium content of the sorbent clearly shows when sorbents were changed. The change from dolomite to Florida limestone was done gradually with the Florida limestone placed over the dolomite in the feed bin. The sample on June 12 was probably a mixture of dolomite and limestone. The transition between the Ohio and Alabama limestone on August 3 was cleaner in that the Ohio limestone was allowed to run out of the feed system before the Alabama limestone was added. Note that the August 3 concentration at 04:00 is typical of the higher magnesium Ohio limestone. The transition between Alabama limestone and Florida limestone on August 6 was done the same way.

The molar ratio of calcium to sulfur (Ca/S) was calculated for each sample from the fine ash system (FD0520) and the reactor solids from the standpipe (FD0510). For dolomite addition, the Ca/S ratio is the measure of excess sorbent required for sulfur removal, according to the equation:

$$SO_2 + CaCO_3 \bullet MgCO_3 + (1/2)O_2 \rightarrow CaSO_4 + 2CO_2 + MgO \tag{1}$$

While for limestone addition, the equation is:

$$SO_2 + CaCO_3 + (1/2)O_2 \rightarrow CaSO_4 + CO_2 \tag{2}$$

To react, all the dolomite or limestone requires an equal molar amount of sorbent and $SO_2$, which would result in the same molar amount of calcium in the solids as sulfur (Ca/S = 1.0). Solids with the minimum amount of sorbent required would then have calcium only present as $CaSO_4$ and there would be neither $CaCO_3$ nor CaO•MgO present. The higher the Ca/S ratio, the more excess sorbent is used than theoretically required for 100-percent $SO_2$ capture.

In Figures 4.3-13 and -14, the PCD exit $SO_2$ concentrations (8-hour averages) are plotted with the spent solids analysis Ca/S molar ratio and the Ca/S ratio based on the coal and sorbent feed rates. The figures note when different sorbents are used. The feed coal sulfur and the coal calcium are calculated from the coal feed rate and coal analysis. The sorbent feed rate is determined from a correlation between sorbent weight cell readings and sorbent feeder speed. The sorbent calcium feed rate is then determined from the sorbent feed rate and the amount of calcium in the sorbent.

At the start of TC03, the dolomite feed rate was high and then reduced to a feed Ca/S of 1.5. The solids Ca/S decreased to below 2.0 on June 5. Except for a few outliers of solids Ca/S, both the solids Ca/S and the Ca/S by the feeds were in agreement between 1.4 and 2.0 from June 7 to June 15. On June 15, when the Florida limestone replaced the dolomite, the limestone feed rate was increased (in an attempt to maintain bed height) and the Ca/S ratios by the feeds were very large and off-scale as seen on Figure 4.3-13. The Ca/S by solids followed the Ca/S ratio by feeds off scale after June 15. Both continued off scale until shut-down on June 19. The $SO_2$ concentration was very low (less than 10 ppm $SO_2$) during the period from June 3 to June 19, with dolomite Ca/S ratios of 1.5 to 2.0 and very high-limestone Ca/S ratios.

After start-up on July 25 on Ohio limestone, the Ca/S ratio by both the feeds and solids agreed with one another from late July 26 to July 30. The $SO_2$ outlet was at 20 ppm during this period. The limestone feed was stopped on July 30 to take $SO_3$ and $SO_2$ measurements and the solids Ca/S decreased to less than 1.0, while the $SO_2$ concentrations increased to 120 ppm. This period is discussed in more detail later in this section. After the limestone feed was resumed at 13:00 on July 30, the feed and PCD solids Ca/S were consistent with each other (at about 1.5) from July 30 to August 2 until the transition from Ohio to Alabama limestone.

The limestone feed was turned off on August 3 when the Alabama limestone replaced the Ohio limestone to ensure a clean break between the two. Note the step changes in feed limestone

$CaCO_3$ and $MgC0_3$ weight percents on August 3 in Figure 4.3-12. The $SO_2$ concentration did not show any change due to limestone feed being turned off in Figure 4.3-14 because the $SO_2$ concentrations were 8-hour averages. The effect is shown in Figure 4.3-31 with an expanded time scale.

After August 4, the Ca/S ratio by solids and feeds leveled off at different values for the remainder of the run, with the Ca/S ratio by solids about 0.3 lower than the Ca/S ratio by the feeds. The Ca/S ratio by solids was about 1.5 to 1.8 from August 4 to August 10, while the Ca/S ratio by feeds was 1.8 to 2.3. At this period, the $SO_2$ concentration was generally less than 20 ppm.

The reactor bed solids Ca/S ratio removed by the FD0510 system are plotted in Figures 4.3-15 and -16 and compared with the Ca/S ratios from the PCD solids and feeds, which are replotted from Figures 4.3-13 and -14. The reactor solids slowly decreased from high-Ca/S values after start-up to near the feeds and PCD solids ratios (about 2.0) on June 13. No reactor solids samples were taken after June 14 because the FD0510 system was operated sparingly from June 14 to June 19.

The reactor solids Ca/S ratio again decreased after start-up from July 26 to August 1 and approached the Ca/S ratio of the feeds and the PCD solids of about 1.5 on August 1. The FD0510 system was operated during this time more than in previous runs. The reactor solids Ca/S ratio increased to around 2.5 after the limestone was turned off during the transition from Ohio to Alabama limestone and are consistent with the high-feed Ca/S. On August 7, the reactor solids Ca/S ratio decreased to 2.0 and was consistent with the feeds Ca/S ratio until shutdown on August 10.

The Sauter mean-particle sizes of the reactor bed solids taken from the standpipe using the spent solids transport system FD0510 and of the solids collected by the PCD and sampled from the fine solids transport system FD0520 are given in Figures 4.3-17 and -18. The reactor Sauter mean diameter decreased from around 250 to 150 microns on June 14 as the test progressed and the start-up sand was purged from the bed. The PCD solids quickly decreased to 20 microns and remained quite constant until the feed coal was switched to Eastern Kentucky coal. The particle sizes of both the PCD and reactor solids increased when the Florida limestone was used, probably due to the unstable reactor operation. When operating on dolomite prior to the addition of Florida limestone, the reactor particle size was larger than the PCD solids, indicating that the cyclone was retaining larger particles in the reactor.

In the period from July 26 to August 11, the reactor solids averaged from 140 to 160 microns. Except for several outliers, the PCD solids were about 20 microns or below for the entire run and similar to the June operation. Again, the reactor solids, as expected, were larger than the PCD solids. A typical particle-size distribution is shown in Figure 4.3-19 for the reactor solids and a typical particle size distribution for the PCD solids in Figure 4.3-20.

The solid compounds produced by the reactor were determined using the solids analysis and several assumptions. The assumptions were different for the dolomite and limestone sorbent operation.

1. All carbon dioxide measured came from $CaCO_3$, hence moles $CO_2$ = moles $CaCO_3$.
2. All sulfur measured came from $CaSO_4$, hence moles sulfur = moles $CaSO_4$.
3. All calcium not taken by $CaSO_4$ and $CaCO_3$ came from CaO•MgO for dolomite. All calcium not taken by $CaSO_4$ and $CaCO_3$ came from CaO for limestone.
4. All remaining magnesium not taken by CaO•MgO came from MgO for dolomite. All magnesium in the sample came from MgO for limestone.
5. All carbon dioxide measured was also measured as carbon, hence unburned carbon in the solids is moles measured carbon minus moles measured $CO_2$.

Figures 4.3-21 and -22 plot the weight percent of $CaCO_3$ and $CaSO_4$ in the PCD solids and reactor solids against time. Another way of looking at these plots is that the $CaCO_3$ is determined by the amount of $CO_2$ in the solids and the $CaSO_4$ is determined by the amount of sulfur in the solids. The PCD $CaCO_3$ weight percent is fairly constant at around 1.0-weight percent for dolomite operation and around 5 percent for July and August limestone operation. The reactor $CaCO_3$ weight percent was constant at 5 percent during the dolomite testing and was constant at 2 percent during the July and August limestone testing. The reactor $CaCO_3$ was higher than the PCD $CaCO_3$ during the dolomite testing, but lower than the PCD $CaCO_3$ during July and August testing.

Both the PCD and reactor $CaSO_4$ weight percent slowly climbed to 30 and 18 weight percent, respectively, during the dolomite testing. During the July and August limestone testing the PCD $CaSO_4$ quickly increased to 20 to 30 percent and stayed in that range for rest of the run. The reactor $CaSO_4$ continually increased during the July and August limestone testing and ended the run at 20 percent. The PCD $CaSO_4$ weight percent was always higher than the reactor $CaSO_4$ weight percent.

Figures 4.3-23 and -24 plot the weight percent of CaO•MgO, CaO, and MgO for the PCD and reactor solids. The CaO•MgO weight percents for both the PCD and reactor were about the same during the dolomite runs, varying between 8 and 15 weight percent. The MgO weight percent for both the PCD and reactor solids also were about the same for the dolomite runs, about 3 to 8 percent. The CaO weight percent rapidly increased during the Florida limestone run from June 14 to June 19 due to the large addition of limestone as an attempt to increase the reactor inventory. No reactor solids were analyzed during this period.

The stable limestone runs from July 25 to August 11 had very low CaO and MgO contents, generally less than 6 percent. The highest CaO content was between the Ohio and Alabama limestone runs on August 3 when the limestone was turned off.

Figures 4.3-25 and -26 plot the weight percent inerts for both the PCD and reactor solids against time. The inerts are defined as a mixture of sand, coal ash, and sorbent inerts and are any bed compounds not containing calcium, magnesium, or sulfur. During the dolomite tests, the PCD inerts started at about 85 percent and then decreased to about 60 percent as the start-up sand was purged from the reactor. The reactor had a slightly higher percent inerts indicating that the inerts tended to be of larger particle size. The PCD inerts decreased drastically as large amounts of limestone were added to the bed during the June Florida limestone test.

The PCD inerts content was fairly constant for the period July 26 to August 11 at 60 to 70 percent except for when the limestone was turned off on August 3 and the PCD inerts content dropped to below 50 percent. For the same period, the reactor inerts slowly decreased to 80 percent as the start-up sand was purged from the bed. The reactor inerts calculated for two samples on July 27 indicated greater than 100-percent inerts due to random errors in analysis and indicates that the bed was all sand at the start of the run.

The laboratory reported carbon in two forms: elemental carbon and carbon dioxide ($CO_2$). The measured elemental carbon is the total carbon in the sample and includes unburned carbon and carbon dioxide. The actual elemental carbon in the solids is the difference between the measured elemental carbon and the measured carbon dioxide. The elemental carbon in the solids is a measure of combustion efficiency. Zero carbon in the solids would indicate 100-percent combustion efficiency. The carbon content of the solids is calculated as the difference of two small numbers that are typically close to each other in value. Hence, there is a lot of relative variation in the carbon content of the solids. Sometimes the $CO_2$ content of solids is larger than the total carbon, resulting in a "negative" unburned carbon.

The unburned carbon contents for both the PCD and reactor solids are plotted in Figures 4.3-27 and -28 as the difference between the elemental carbon and the carbon dioxide of the solids. All unburned carbons are at a very low level, which indicates about 99.9-percent combustion efficiency. There are a few outlier points indicating either high- or low-unburned carbons.

During the limestone sorbent tests, the $SO_2$ emissions had a "sawtooth" pattern with time that was similar to the PCD back-pulse cycle. This is shown on Figure 4.3-29 for two back-pulse cycles. Note that the PCD pressure drop and $SO_2$ concentrations have the same frequency. A high-PCD-pressure drop is synchronous with low-$SO_2$ emissions. The reason for this pattern is that as the dust layer on the candles builds up (increasing the candle pressure drop), the increased amount of dust (which contains some reactive sorbent) removes additional $SO_2$. Note in Figure 4.3-29 that when the PCD back-pulsed at 01:15 and 02:13 the $SO_2$ emissions increased because the PCD back-pulse knocked the reactive dust off the candles.

Southern Research Institute (SRI) obtained both $SO_2$ and $SO_3$ data from the cyclone outlet (PCD inlet). SRI used extractive and wet chemical techniques to obtain $SO_2$ and $SO_3$ concentrations. During TC03, six extractive $SO_2/SO_3$ tests were done (see Table 4.3-2). All but the August 30 tests were done at operating conditions that produced low-$SO_2$ analyzer readings. The tests of August 30 were done after the sorbent had been turned off the day before and while there were measurable $SO_2$ readings and a visible plume coming out of the PSDF stack for 4 to 6 hours (see Figure 4.3-30).

Table 4.3-2 compares the extractive $SO_2$ and $SO_3$ data taken during TC03. The average extractive $SO_2$ and $SO_3$ data are shown as well as the average $SO_2$ gas analyzer data. Both $SO_2$ and $SO_3$ are expressed as measured and as 6-percent $O_2$. The $SO_X$ emissions in pounds of $SO_X$ per million Btu fired and $SO_X$ removal, based on the calculated $SO_X$ from the coal sulfur are given. The Ca/S ratios are taken from Figures 4.3-13 and -14. There was excellent agreement between the extractive and analyzer $SO_2$ readings. All of the $SO_3$ values were fairly close to the $SO_2$ values.

Figure 4.3-30 shows the plots of the online $SO_2$ analyzer readings (hourly averages) and extractive $SO_3$ results for the period before the limestone was stopped on July 29 until after the limestone feed was resumed on July 30. The calculated $SO_X$ is based on the sulfur content in the coal. The difference between the sulfur in the coal and the measured $SO_2$ and $SO_3$ is probably due to sulfur capture by residual limestone in the reactor. Figure 4.3-31 shows the plots of the online $SO_2$ analyzer readings for the change in sorbent between Alabama limestone and Florida limestone on August 3 when the limestone feeder had been emptied to clearly mark the boundary between the use of Florida and Alabama limestone. The same technique was used for the transition between Alabama and Florida limestone on August 6 (see Figure 4.3-32).

The high-$SO_3$ values that were measured are consistent with both thermodynamics and previous results of burning coal in pressurized fluid bed combustors with sorbent as bed material. Two papers from the literature give high measured values of $SO_3$ from PFBC (Wheeldon, et al., 1985 and Burdett, et al., 1983).

A useful way to analyze $SO_2/SO_3$ data is to look at the thermodynamics of the $SO_2$ to $SO_3$ reaction:

$$SO_2 + (1/2)O_2 \leftrightarrow SO_3 \tag{3}$$

Higher pressure and oxygen concentrations will lead to higher $SO_3$ concentrations. Equation (3) leads to the equilibrium constant, which combines the effects of pressure, sulfur oxide concentration, and oxygen concentration. The equilibrium constant $K_P$ is defined as:

$$K_P = \frac{SO_3}{SO_2\sqrt{P(O_2)}} \tag{4}$$

The concentrations $SO_3$ and $SO_2$ are in ppm and $P(O_2)$ is the partial pressure of oxygen in atmospheres.

The measured $K_P$ for the six TC03 $SO_3$ data points is shown in Table 4.3-3. From thermodynamic data, the temperature at which the measured concentrations are at thermodynamic equilibrium can be determined is reported in Table 4.3-3. The equilibrium temperature can be compared to the measured temperature and the difference is called the approach to equilibrium, which is a measure of how close the system is to thermodynamic equilibrium. The lower the approach temperature, the closer the system temperature is to the equilibrium temperature and the closer the system is to thermodynamic equilibrium.

The equilibrium constant is a function of temperature. Wheeldon, et al., 1985 used the equation:

$$K_P = 2.1\text{x}10^{-5}\exp(20520/T) \tag{5}$$

The temperature (T) is in degrees Rankine. According to this equation, plotting the logarithm of the equilibrium constant against reciprocal temperature will result in a straight line. At high temperatures, the formation of $SO_2$ is favored, while at low temperatures the formation of $SO_3$ is favored. Equilibrium constants for TC02 and TC03, both measured and theoretical, are shown in the plots in Figure 4.3-33. TC03 data are grouped together near the equilibrium line and are consistent with one of the TC02 data points.

References

Burdett, B. J., B. J. Glidden, R. C. Hotchkiss, and R. T. Squires, "$SO_3$ in coal-fired fluidized bed combustor," Journal of the Institute of Energy, v. 56 (September 1983) pp. 119 - 124.

Wheeldon, J. M., N. A. Burdett, M. A. Freidman, and J. E. Stantan, "$SO_3$ measurements at the Grimethorpe PFBC," Proceeding of the Eighth International Conference on Fluidized-Bed Combustion, Vol. II, July 1985, p. 715.

Table 4.3-1

TC03 Sorbent Compositions

| Sorbent | Plum Run Dolomite | Gregg Mine Limestone Florida | Bucyrus Limestone Ohio | Longview Limestone Alabama |
|---|---|---|---|---|
| Samples Analyzed | 9 | 15 | 6 | 2 |
| Samples Used | 5 | 9 | 6 | 2 |
| | Wt % | Wt % | Wt % | Wt % |
| $CaCO_3$ | 51.1 | 90.4 | 73.0 | 88.7 |
| $MgCO_3$ | 40.7 | 1.1 | 15.8 | 5.5 |
| Inerts | 8.2 | 8.5 | 11.2 | 5.8 |
| Total | 100.0 | 100.0 | 100.0 | 100.0 |

Table 4.3-2

TC03 $SO_2$ and $SO_3$ Data

| Date | 7/14/98 | 7/15/98 | 7/28/98 | 7/30/98 | 8/4/98 | 8/7/98 |
|---|---|---|---|---|---|---|
| Extractive Data Points | 4 | 4 | 6 | 6 | 4 | 6 |
| Extractive $SO_3$ (ppm) | 31 | 6 | 26 | 136 | 15 | 14 |
| Extractive $SO_2$ (ppm) | 35 | 6 | 35 | 179 | 11 | 11 |
| Analyzer $SO_2$ (ppm) | 34 | 5 | 21 | 175 | 11 | 8 |
| Extractive $SO_3$ (6% $O_2$) (ppm) | 32 | 7 | 31 | 159 | 17 | 17 |
| Extractive $SO_2$ (6% $O_2$) (ppm) | 35 | 6 | 43 | 210 | 13 | 14 |
| Analyzer $SO_2$ (6% $O_2$) (ppm) | 35 | 5 | 26 | 205 | 13 | 10 |
| $SO_X$ From Coal (ppm) | 723 | 1,519 | 524 | 503 | 457 | 446 |
| $SO_X$ Emissions (lb/MBtu) | 0.18 | 0.01 | 0.17 | 1.12 | 0.09 | 0.09 |
| $SO_X$ Removal (%) | 91.0 | 99.3 | 91.1 | 38.2 | 94.5 | 95.0 |
| Feed Solids Ca/S Ratio | 1.5 | 1.7 | 1.4 | — | 1.6 | 1.8 |
| PCD Solids Ca/S Ratio | 1.8 | 1.7 | 1.2 | 0.9 | 1.6 | 1.6 |
| Limestone Used | FL | FL | OH | OH | AL | FL |

Notes:
1. Extractive data collected by Southern Research Institute for about10 minutes.
2. All data taken with E. Kentucky coal.

Table 4.3-3

TC03 $SO_2$ and $SO_3$ Results

| Date | 7/14/98 | 7/15/98 | 7/28/98 | 7/30/98 | 8/4/98 | 8/7/98 |
|---|---|---|---|---|---|---|
| Extractive $SO_3$ (ppm) | 31 | 6 | 26 | 136 | 15 | 14 |
| Extractive $SO_2$ (ppm) | 35 | 6 | 35 | 179 | 11 | 11 |
| PCD Outlet Temp. (°F) | 1,355 | 1,330 | 1,286 | 1,304 | 1,316 | 1,307 |
| Pressure (psig) | 160 | 178 | 145 | 145 | 155 | 165 |
| $O_2$ (%) | 6.3 | 7.4 | 8.7 | 8.2 | 8.3 | 8.6 |
| $K_P$ ($atm^{-0.5}$) | 1.041 | 1.13 | 0.748 | 0.804 | 1.418 | 1.439 |
| Equilibrium Temp. (°F) | 1,055 | 1,048 | 1,088 | 1,081 | 1,026 | 1,029 |
| Approach to Eqm. (°F) | 83 | 98 | 231 | 181 | 71 | 85 |

Notes:
1. $K_P$ is defined in Equation (4).
2. Approach to equilibrium temperature is the difference between equilibrium temperature and actual temperature.

.

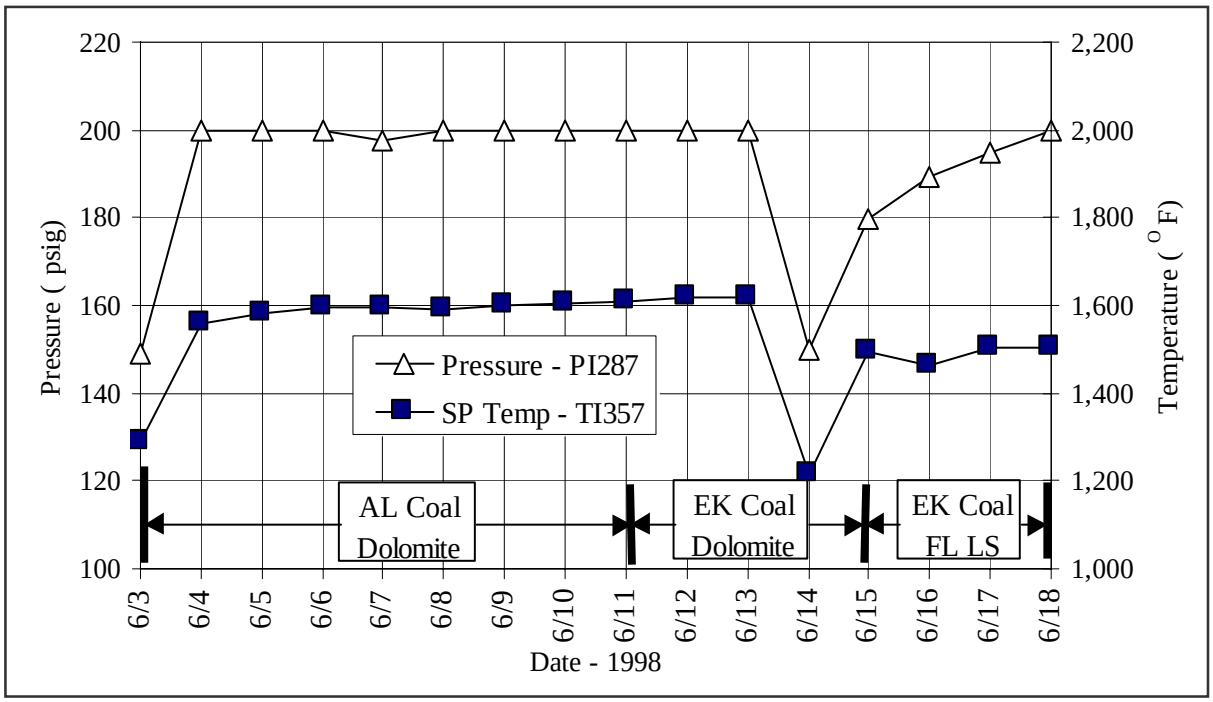


Figure 4.3-1 TC03 System Pressure, Standpipe Temperature

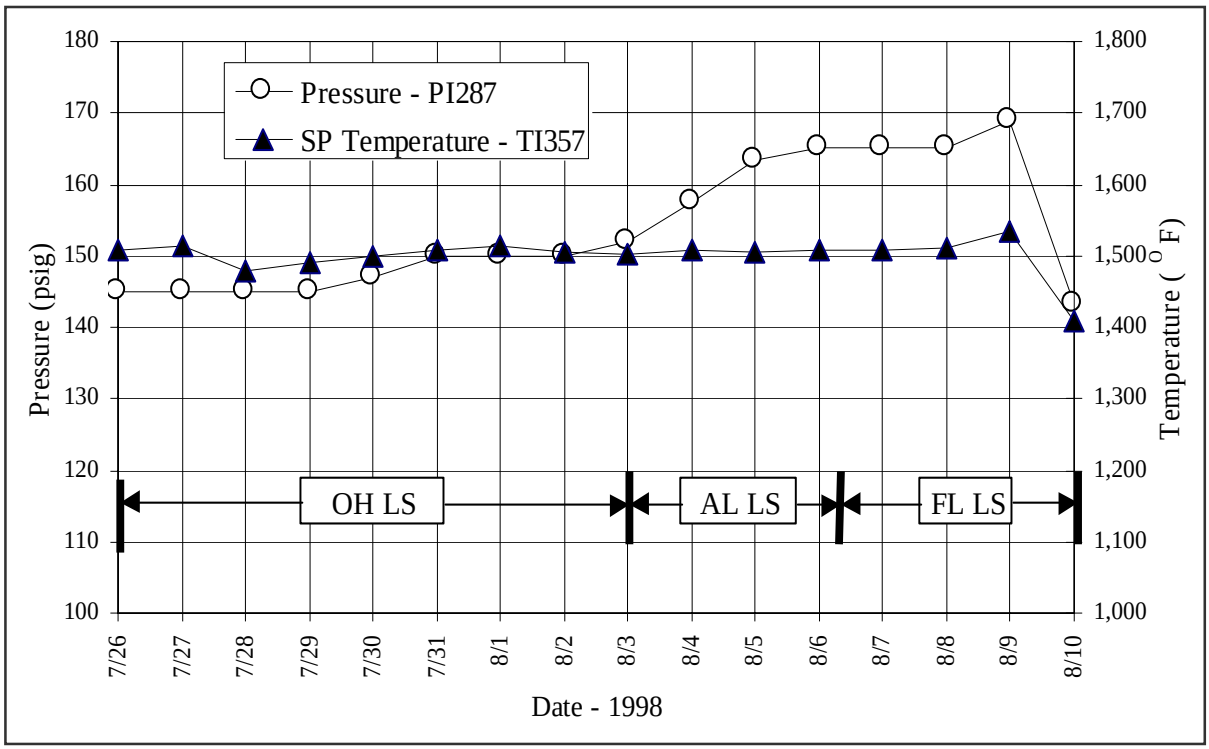


Figure 4.3-2 TC03 System Pressure, Standpipe Temperature

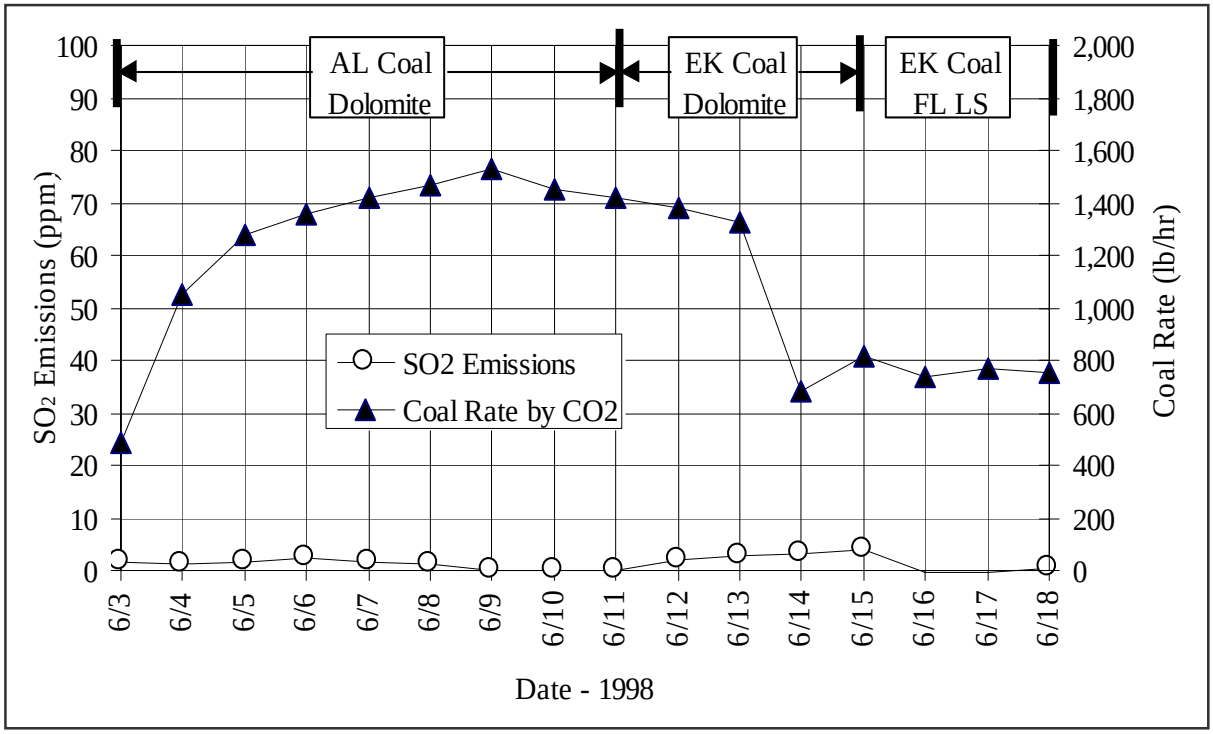


Figure 4.3-3 TC03 Coal Feed and $SO_2$ Emissions

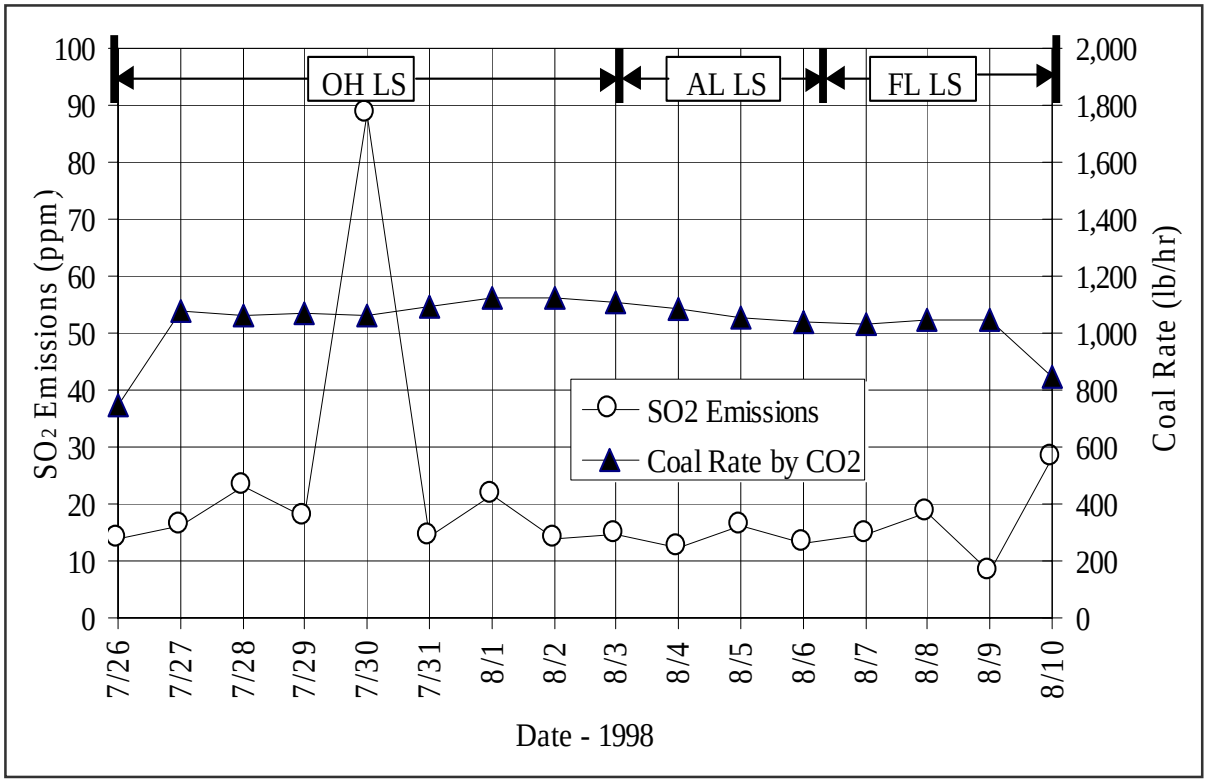


Figure 4.3-4 TC03 Coal Feed and $SO_2$ Emissions

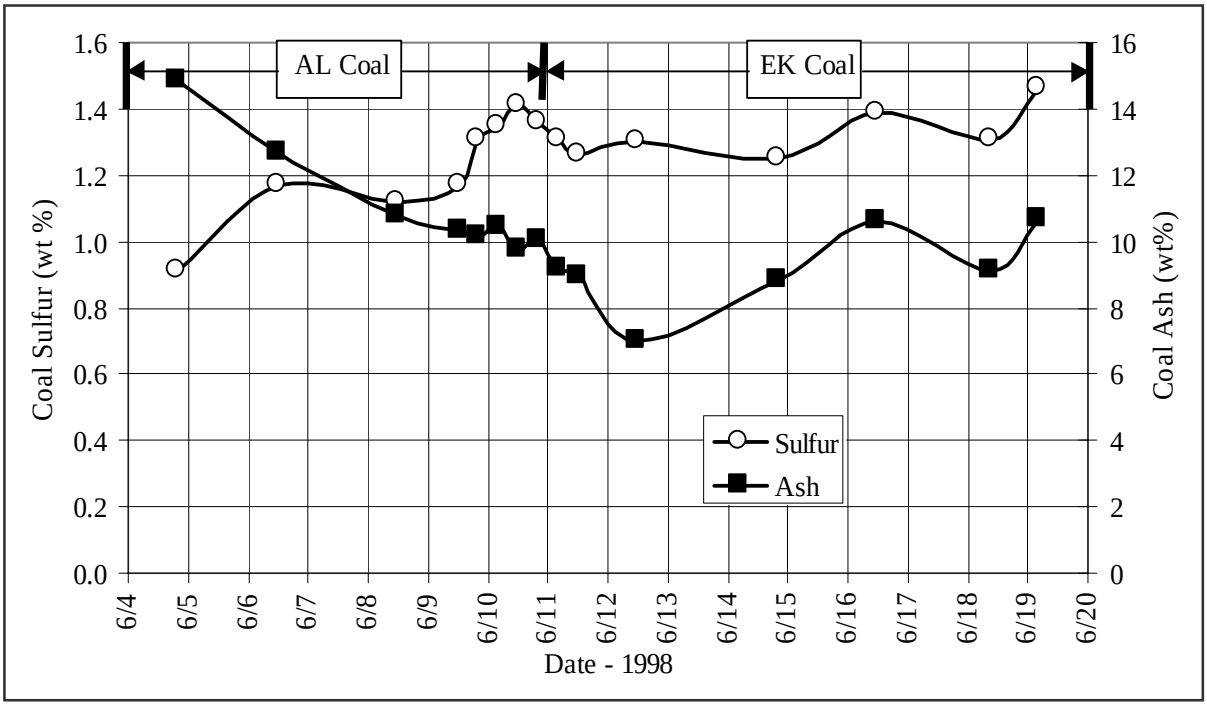


Figure 4.3-5 TC03 Coal Sulfur and Ash Contents

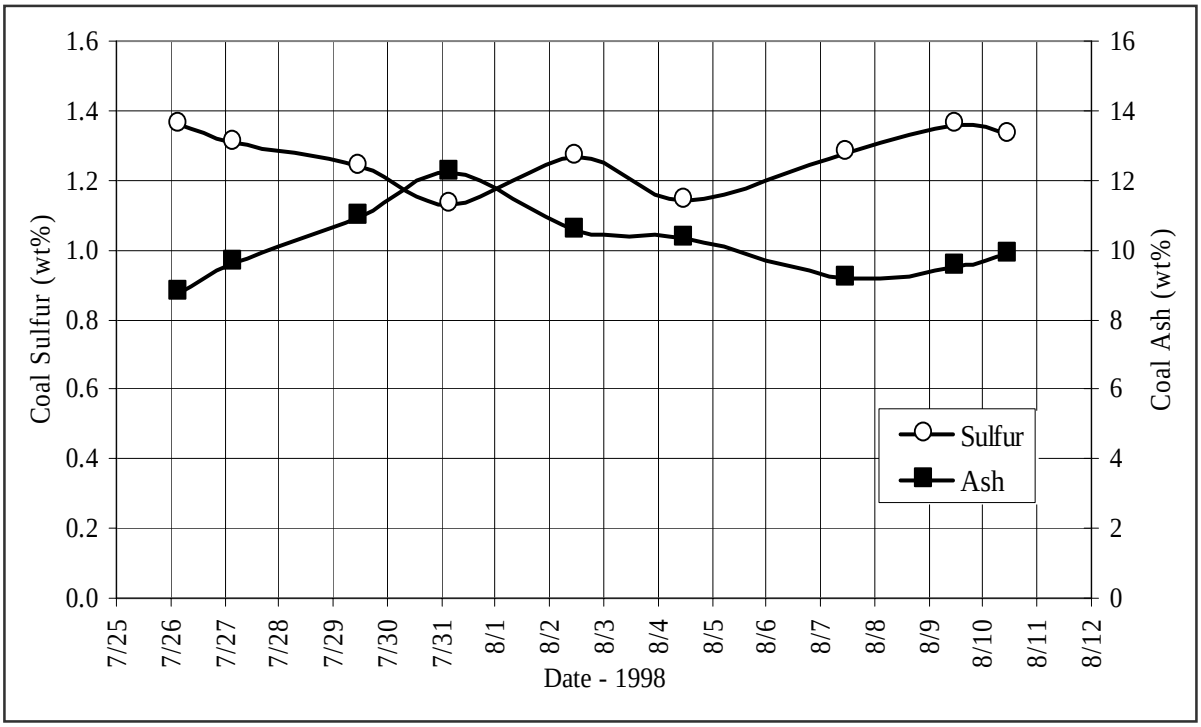


Figure 4.3-6 TC03 Coal Sulfur and Ash Contents

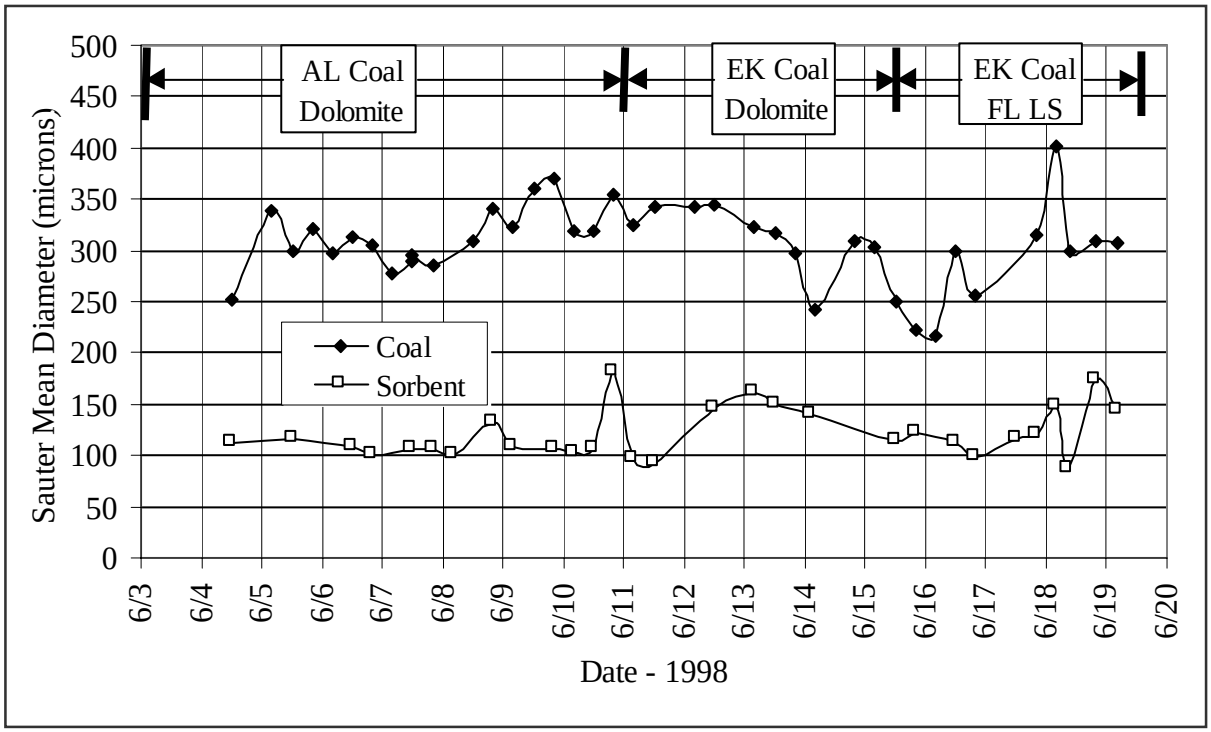


Figure 4.3-7 TC03 Coal and Sorbent Particle Size

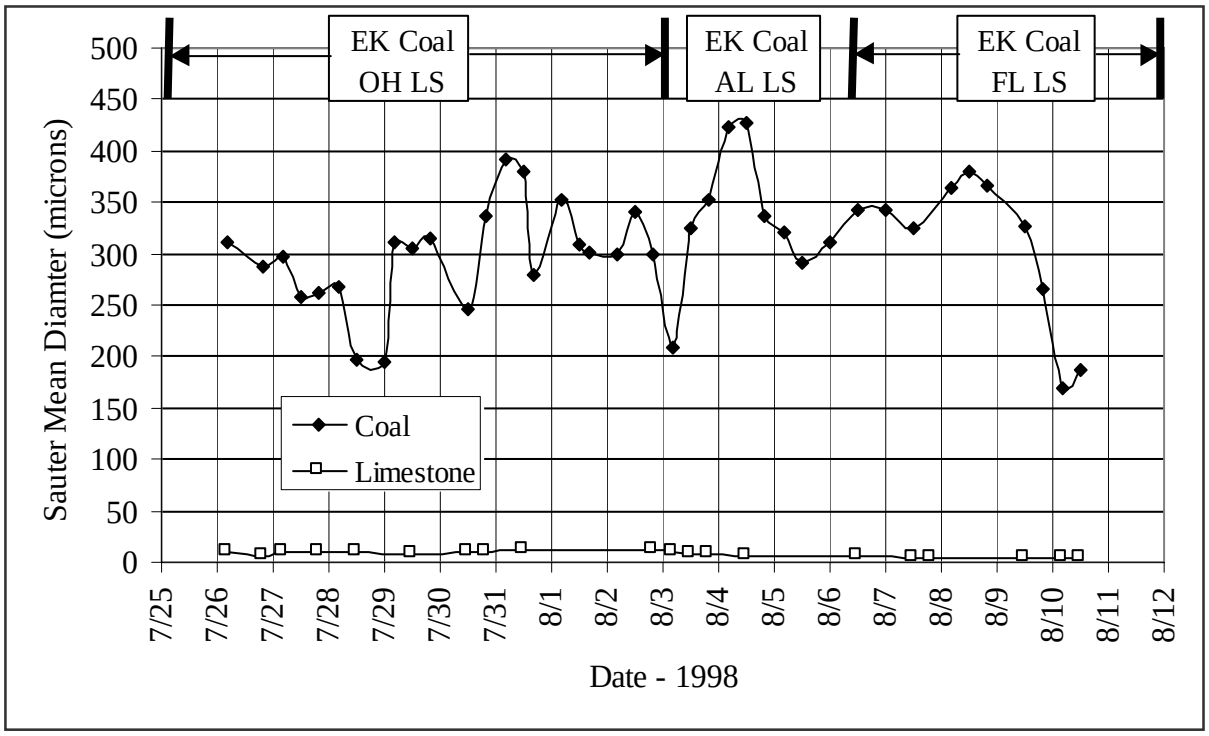


Figure 4.3-8 TC03 Coal and Sorbent Particle Size

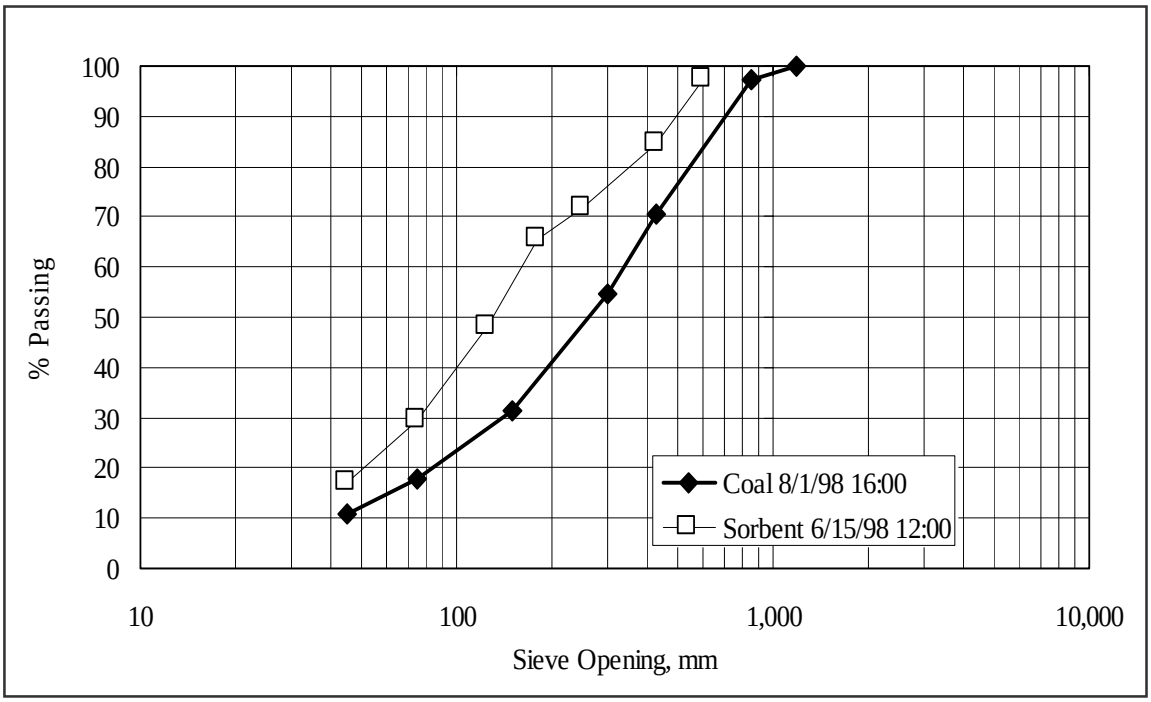


Figure 4.3-9 TC03 Coal and Sorbent Sieve Particle-Size Distribution

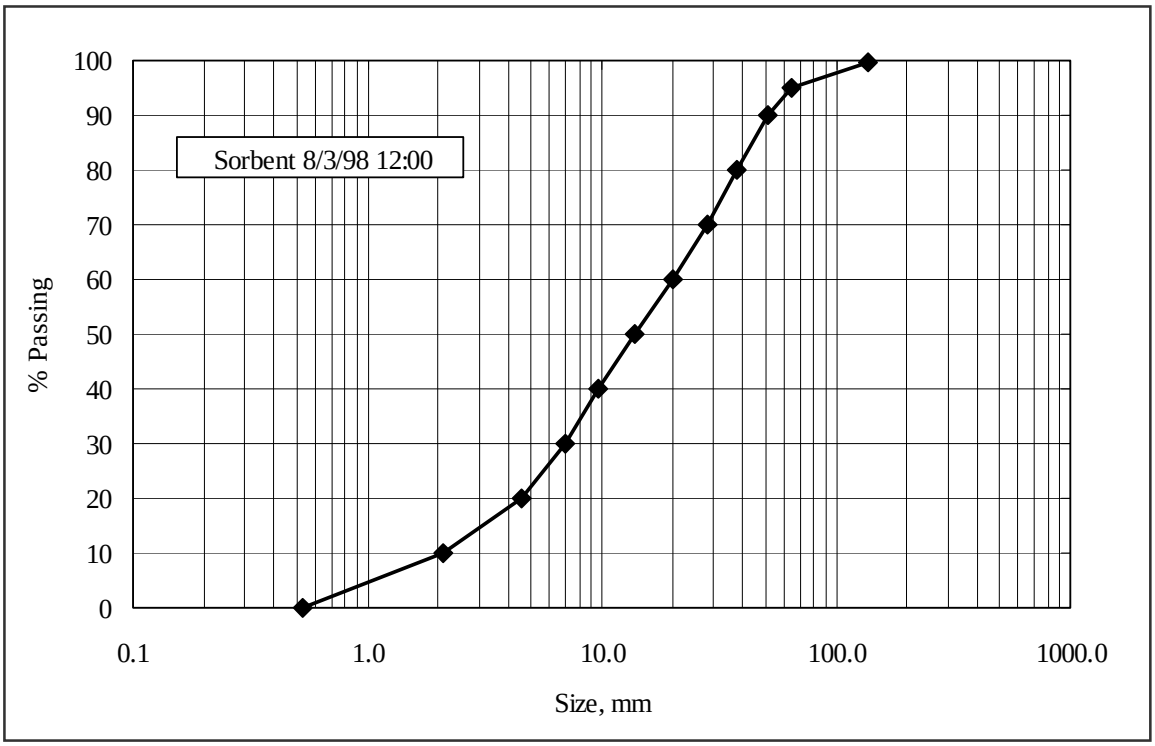


Figure 4.3-10 TC03 Sorbent Microtrac Particle-Size Distribution

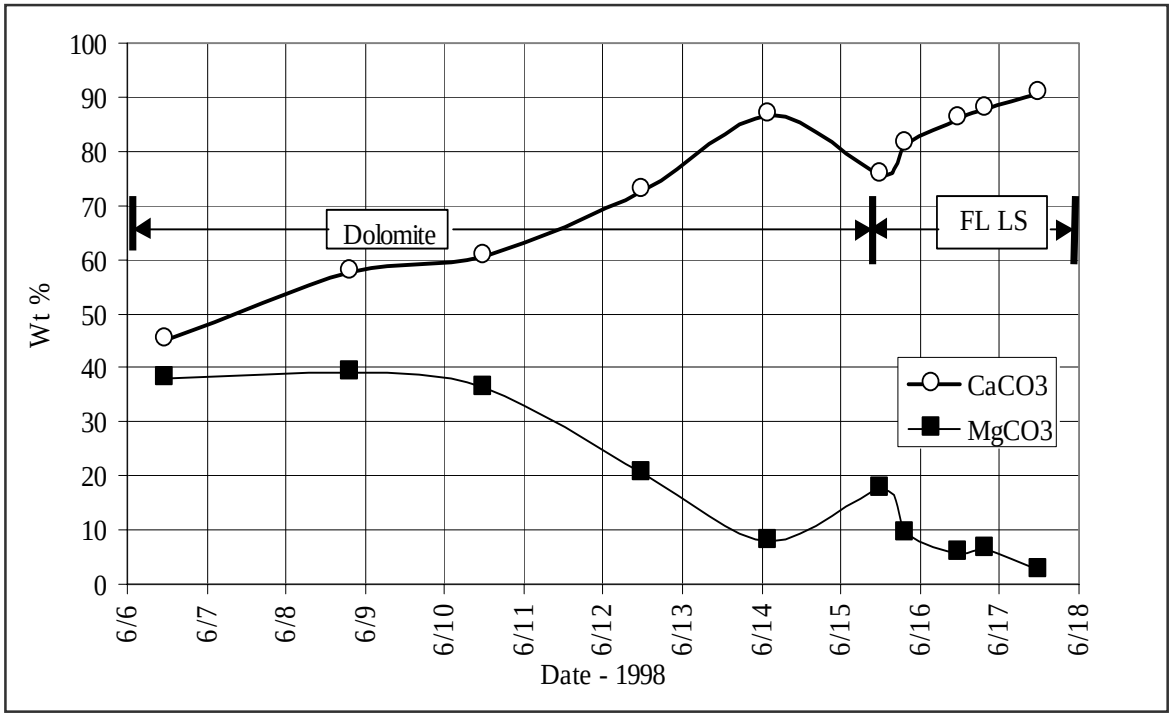


Figure 4.3-11 TC03 Sorbent $CaCO_3$ and $MgCO_3$ Contents

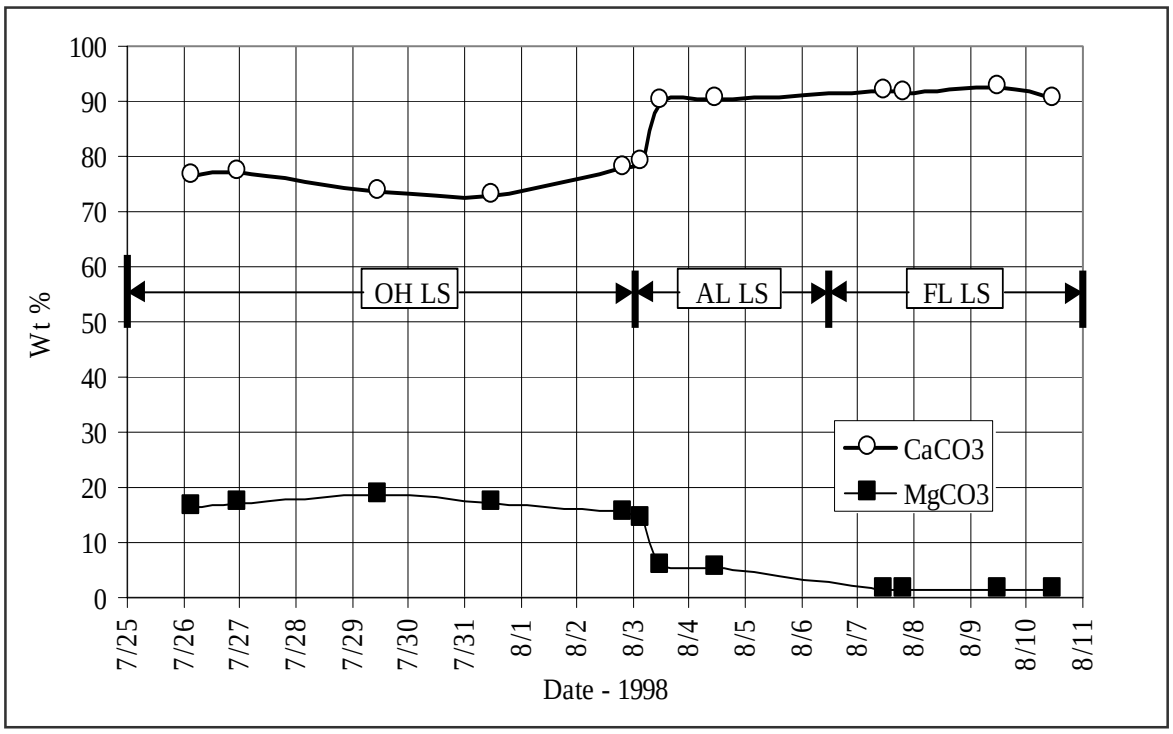


Figure 4.3-12 TC03 Limestone $CaCO_3$ and $MgCO_3$ Contents

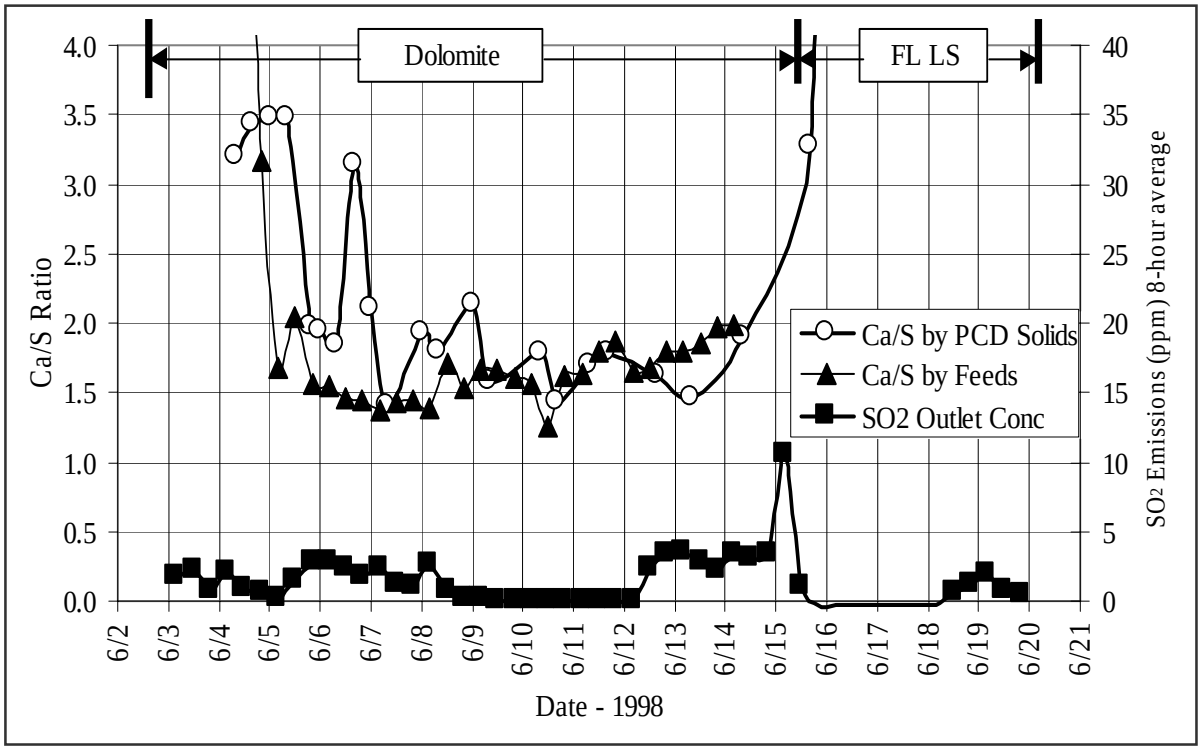


Figure 4.3-13 TC03 PCD Solids Ca/S, Feeds Ca/S, and $SO_2$ Emissions

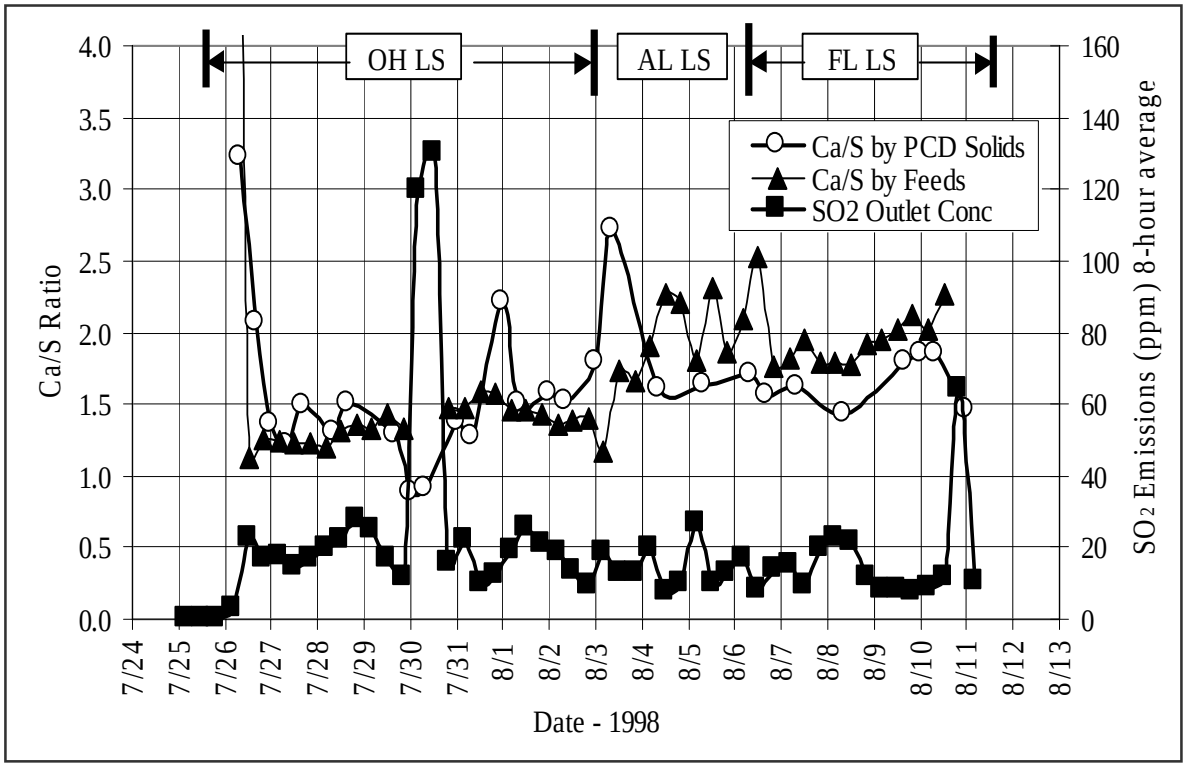


Figure 4.3-14 TC03 PCD Solids Ca/S, Feeds Ca/S, and $SO_2$ Emissions

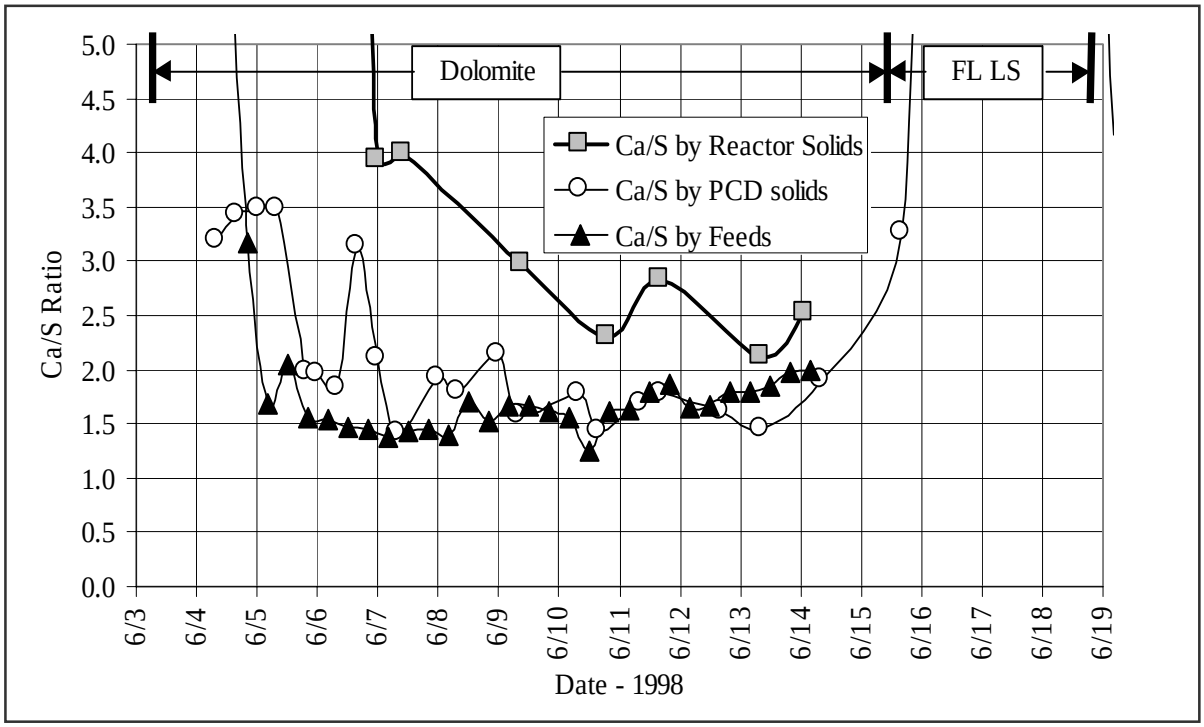


Figure 4.3-15 TC03 PCD Solids Ca/S, Feeds Ca/S, and Reactor Solids Ca/S

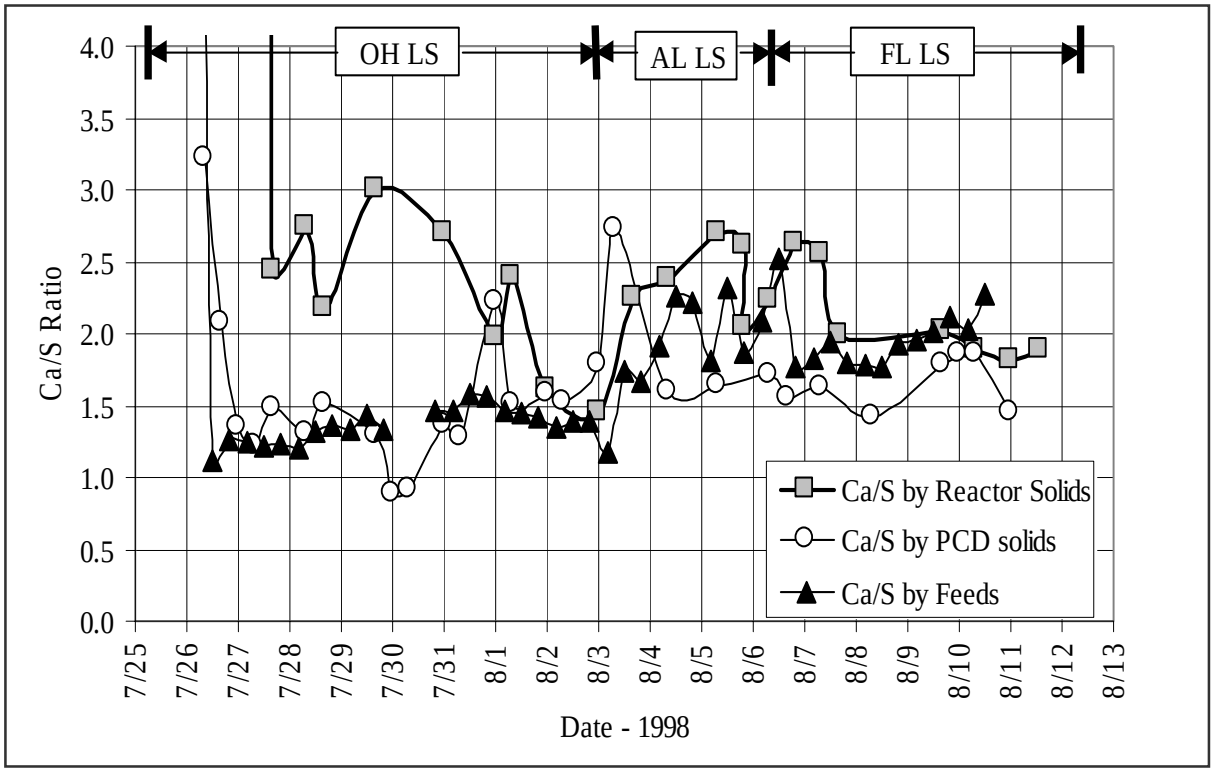


Figure 4.3-16 TC03 PCD Solids Ca/S, Feeds Ca/S, and Reactor Solids Ca/S

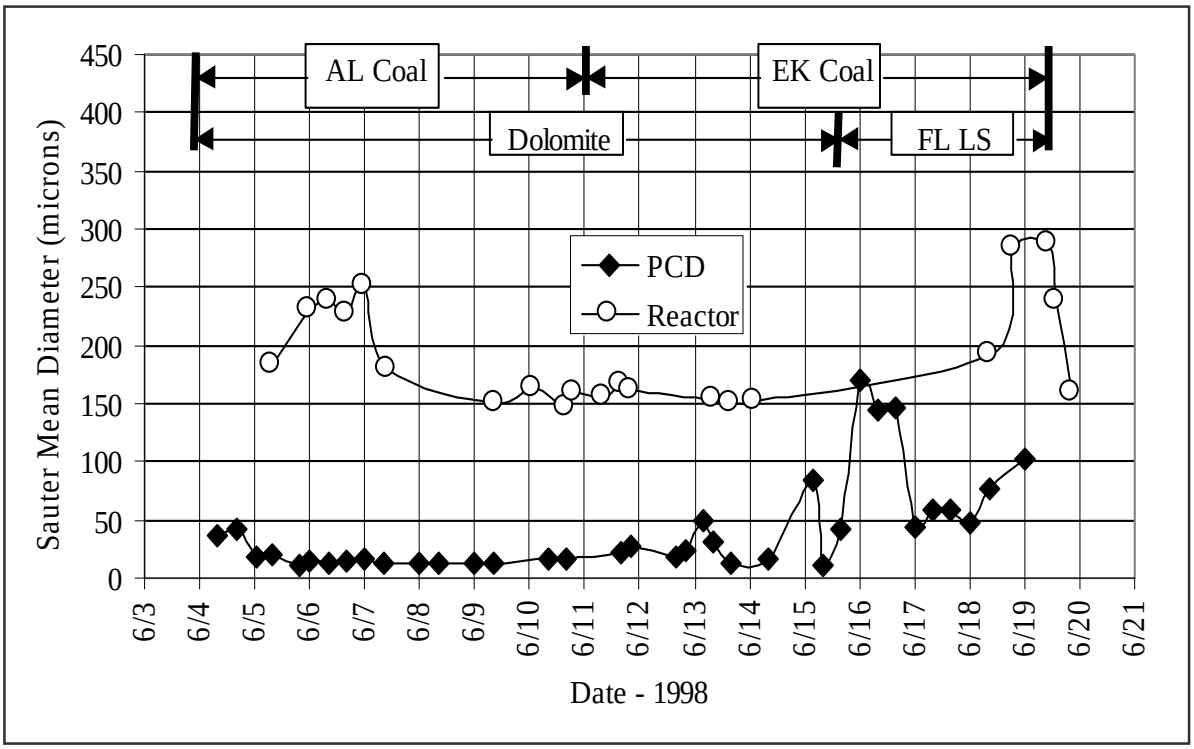


Figure 4.3-17 TC03 PCD and Reactor Particle Sizes

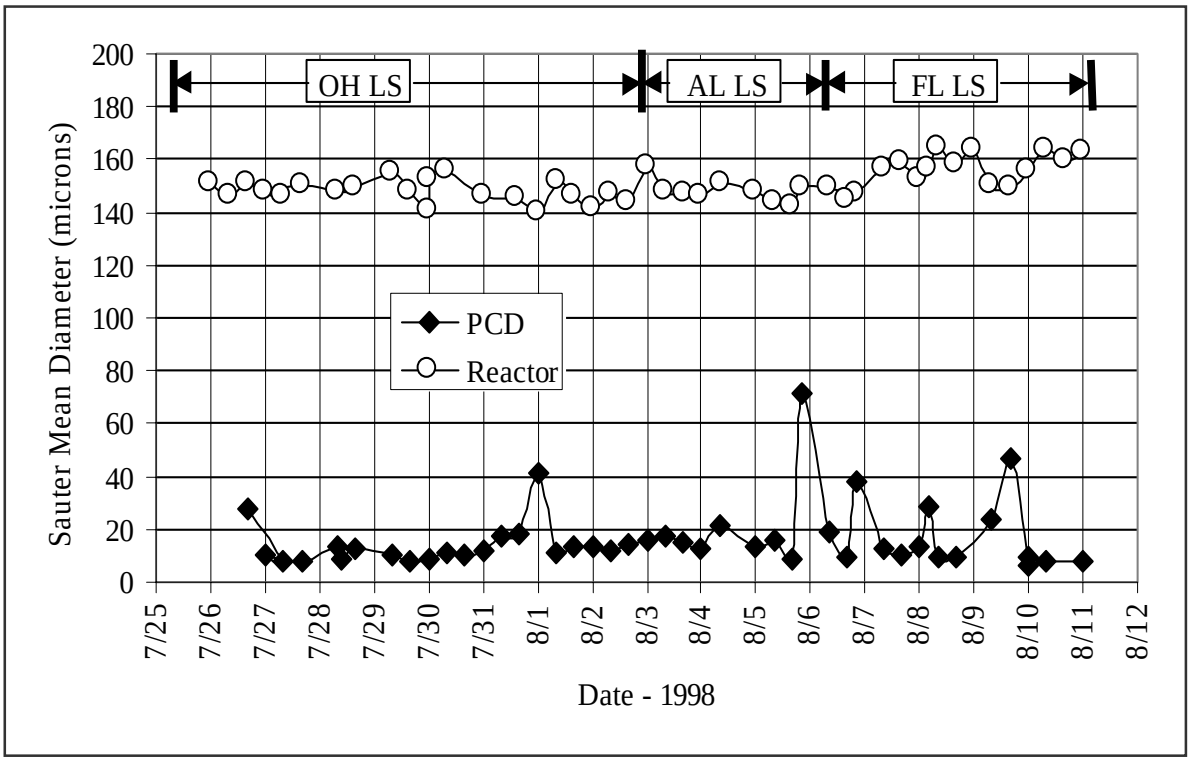


Figure 4.3-18 TC03 PCD and Reactor Particle Sizes

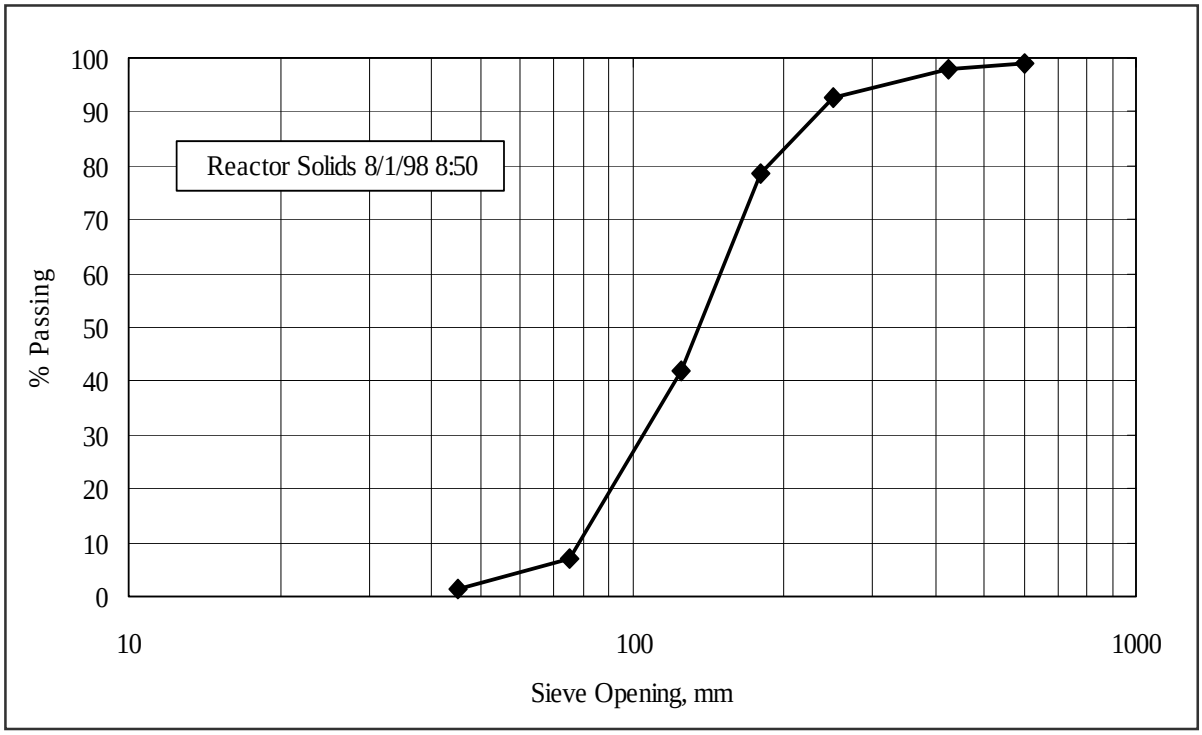


Figure 4.3-19 TC03 Reactor Solids Particle-Size Distribution

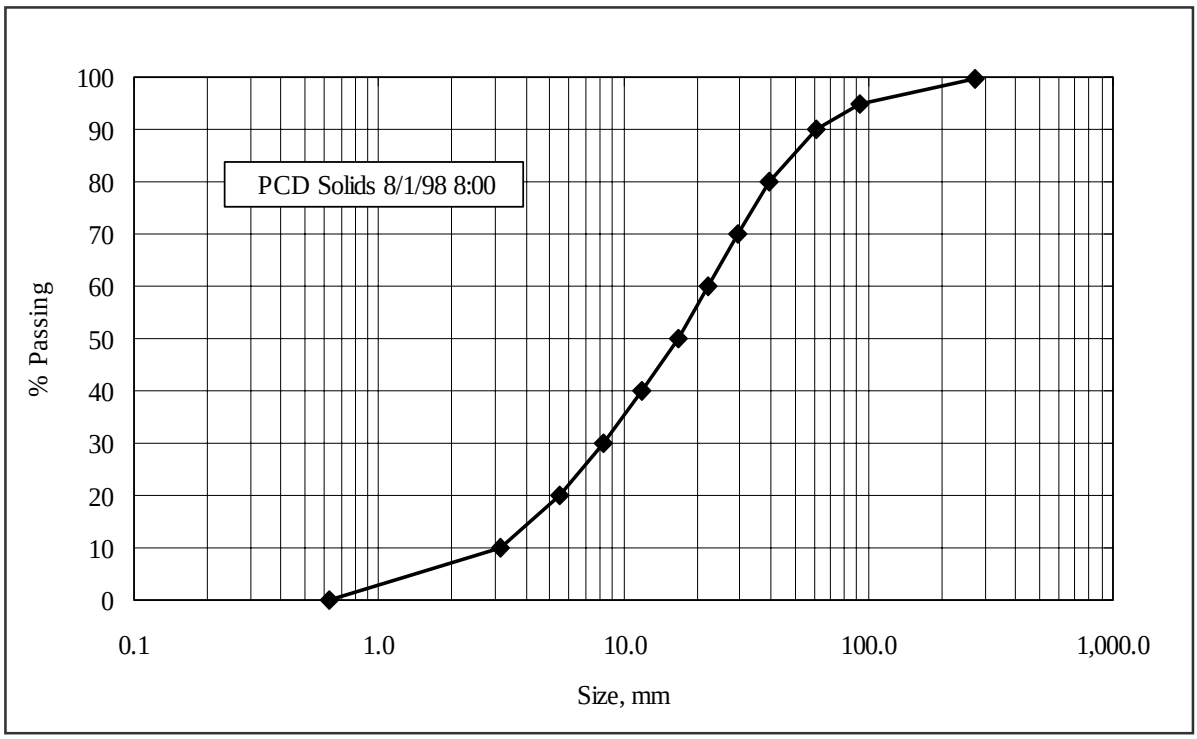


Figure 4.3-20 TC03 PCD Solids Particle-Size Distribution

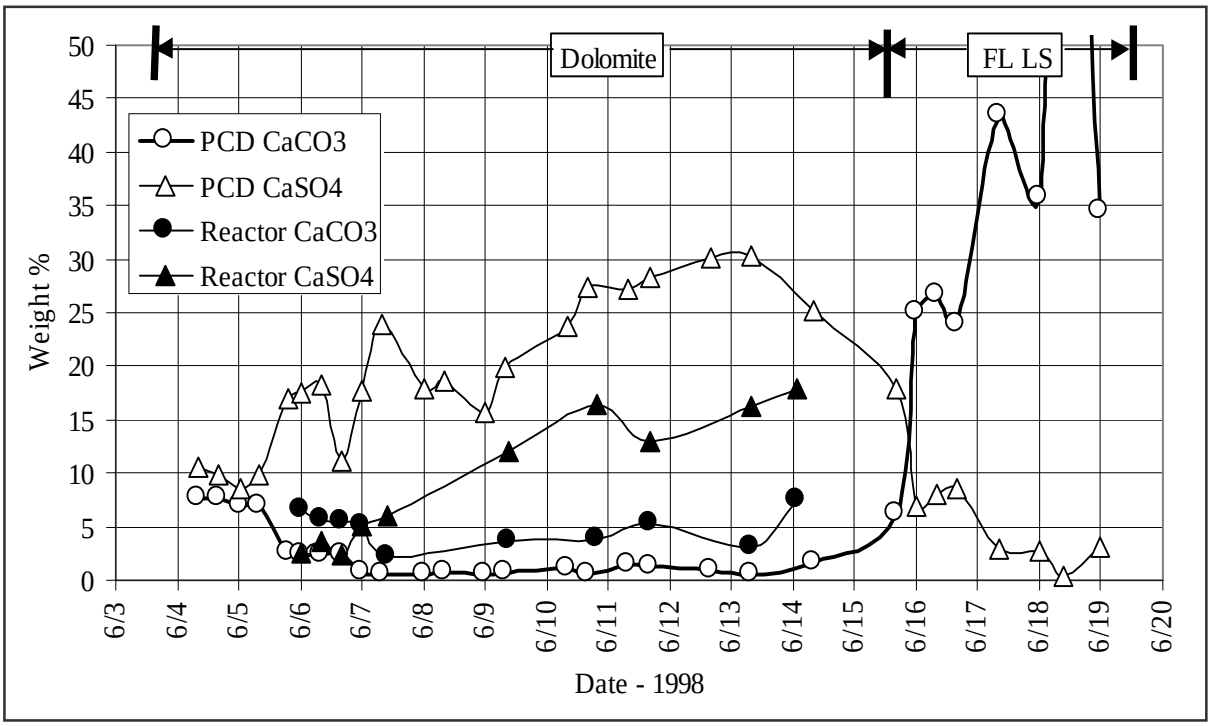


Figure 4.3-21 TC03 PCD and Reactor $CaCO_3$ and $CaSO_4$ Contents

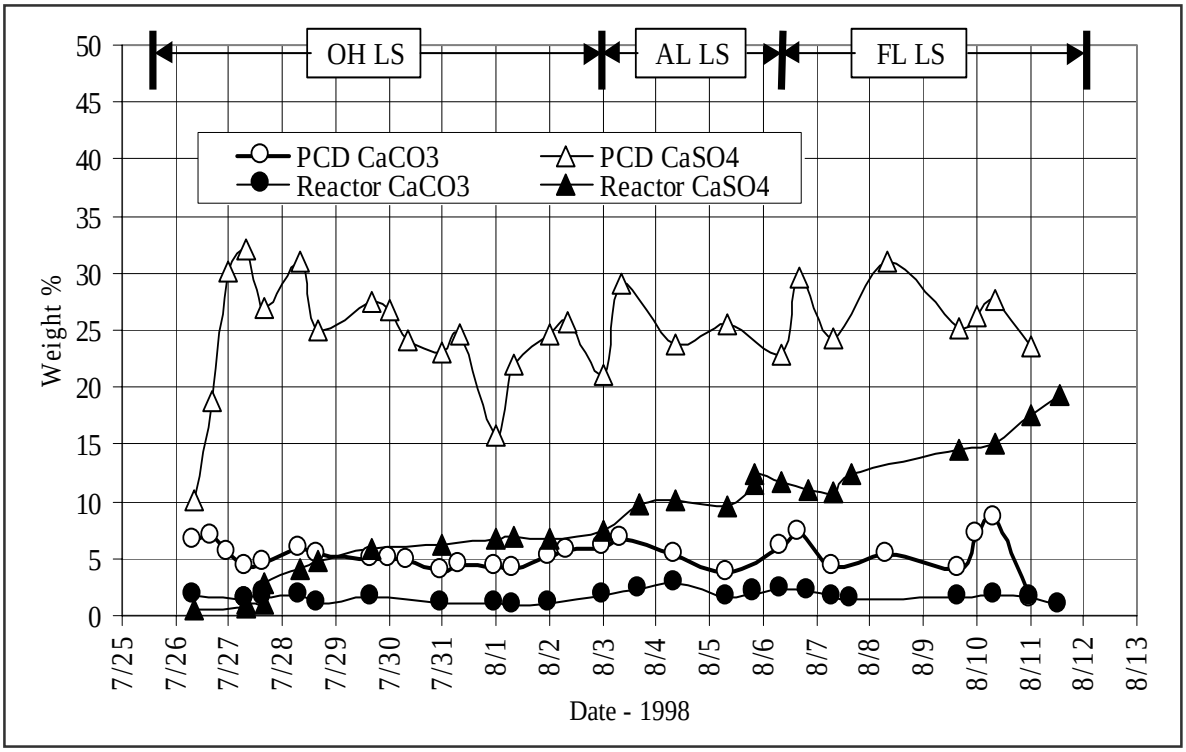


Figure 4.3-22 TC03 PCD and Reactor $CaCO_3$ and $CaSO_4$ Contents

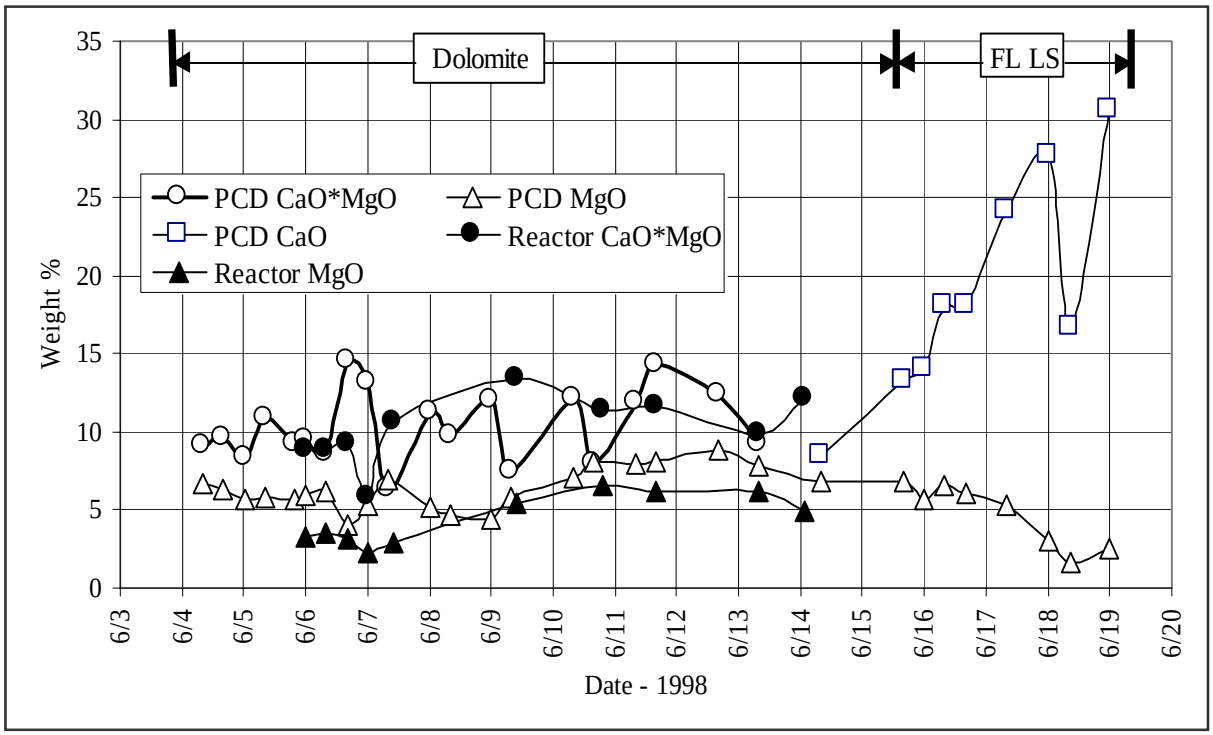


Figure 4.3-23 TC03 PCD and Reactor CaO, CaO•MgO, and MgO Contents

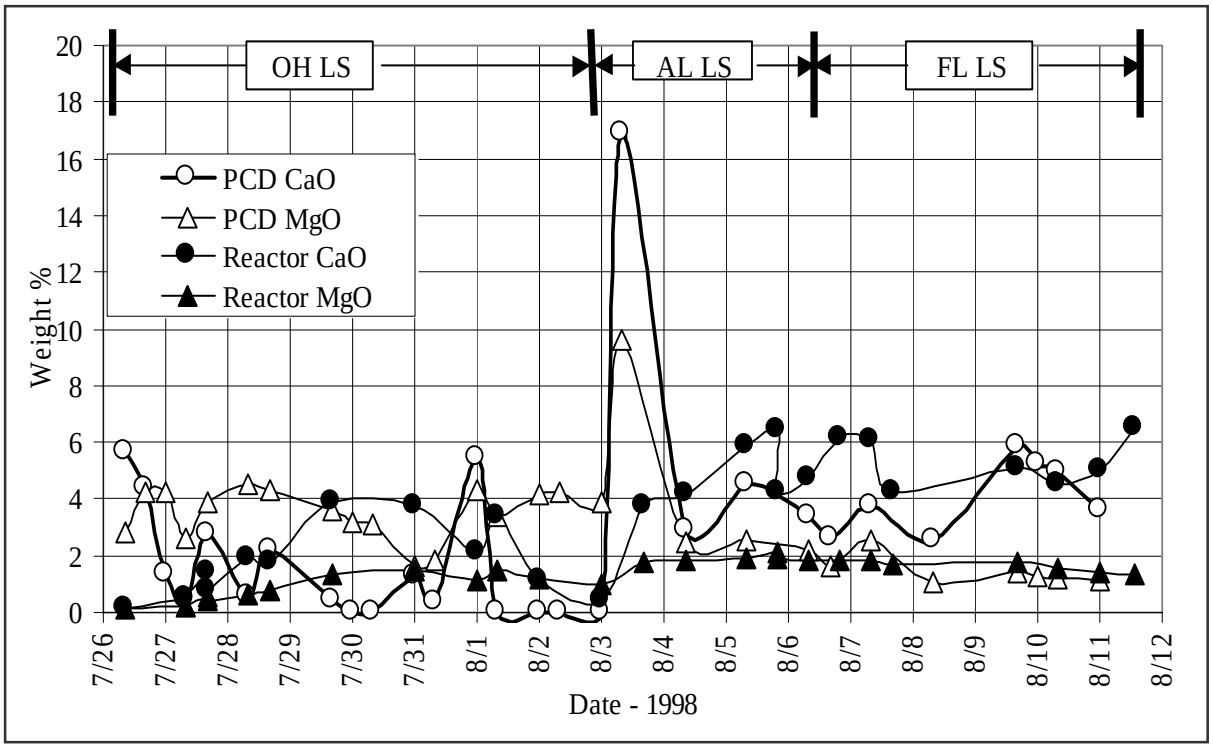


Figure 4.3-24 TC03 PCD and Reactor CaO, CaO•MgO, and MgO Contents

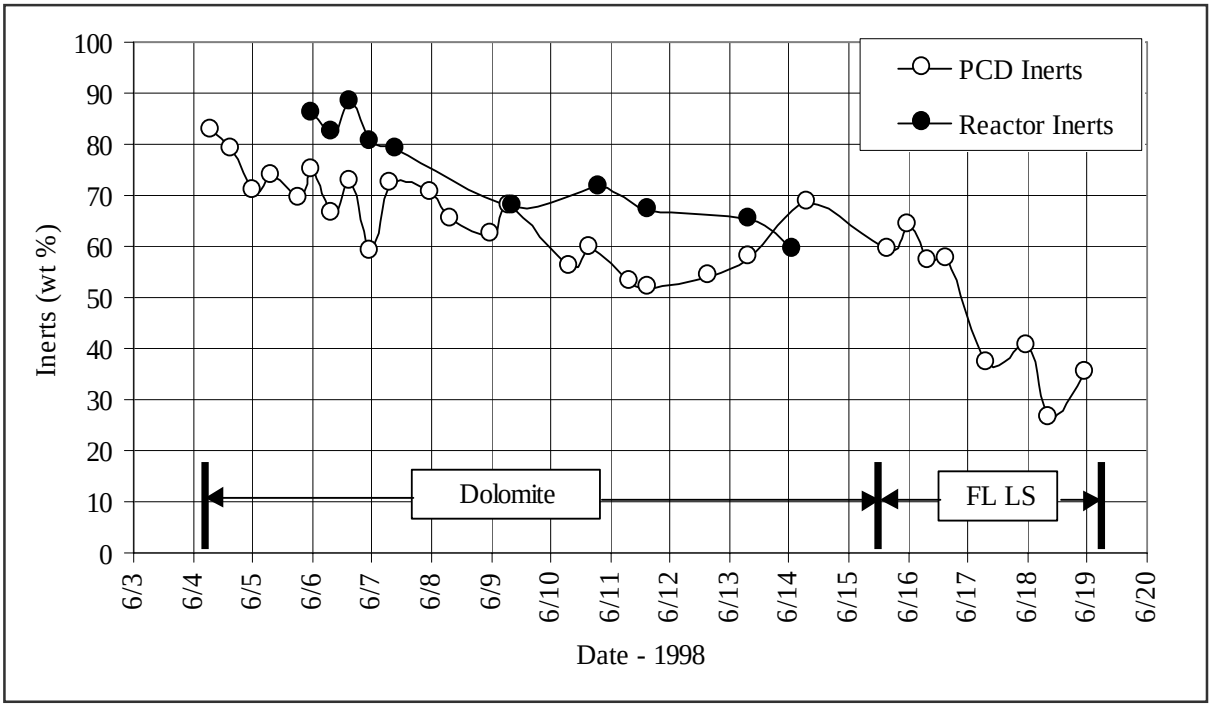


Figure 4.3-25 TC03 PCD and Reactor Inerts Contents

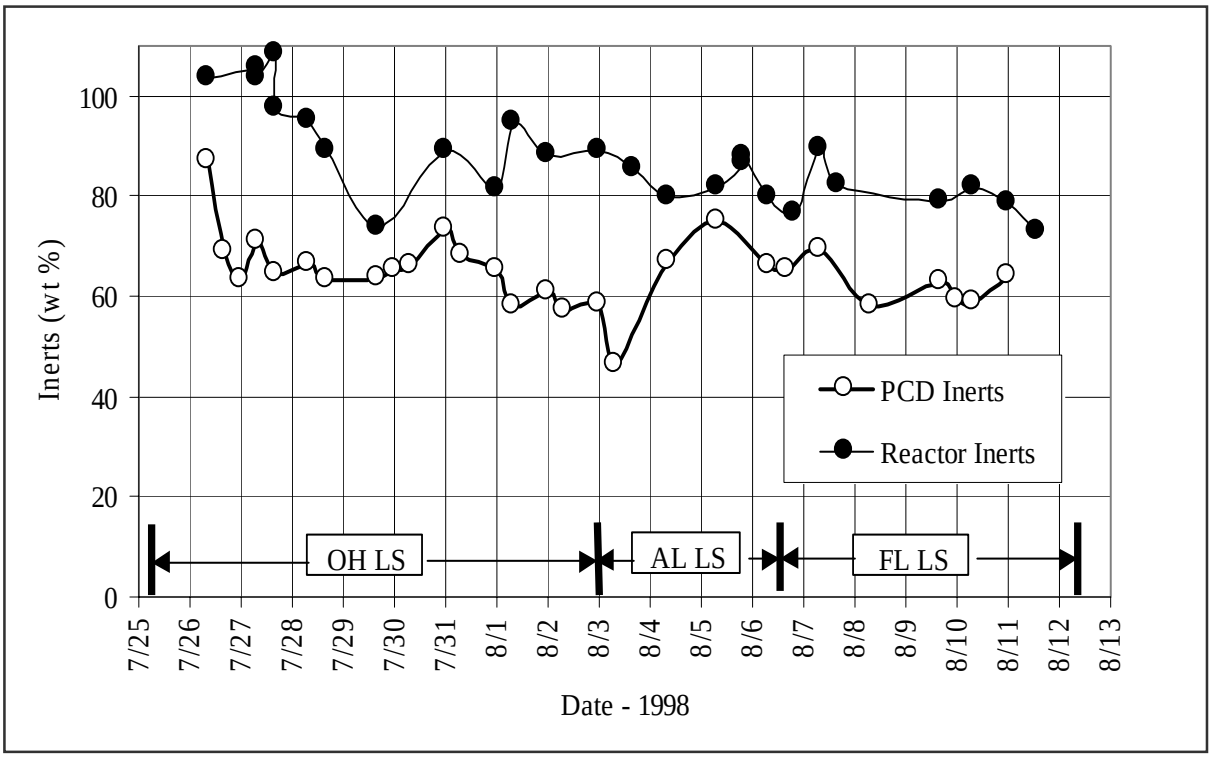


Figure 4.3-26 TC03 PCD and Reactor Inerts Contents

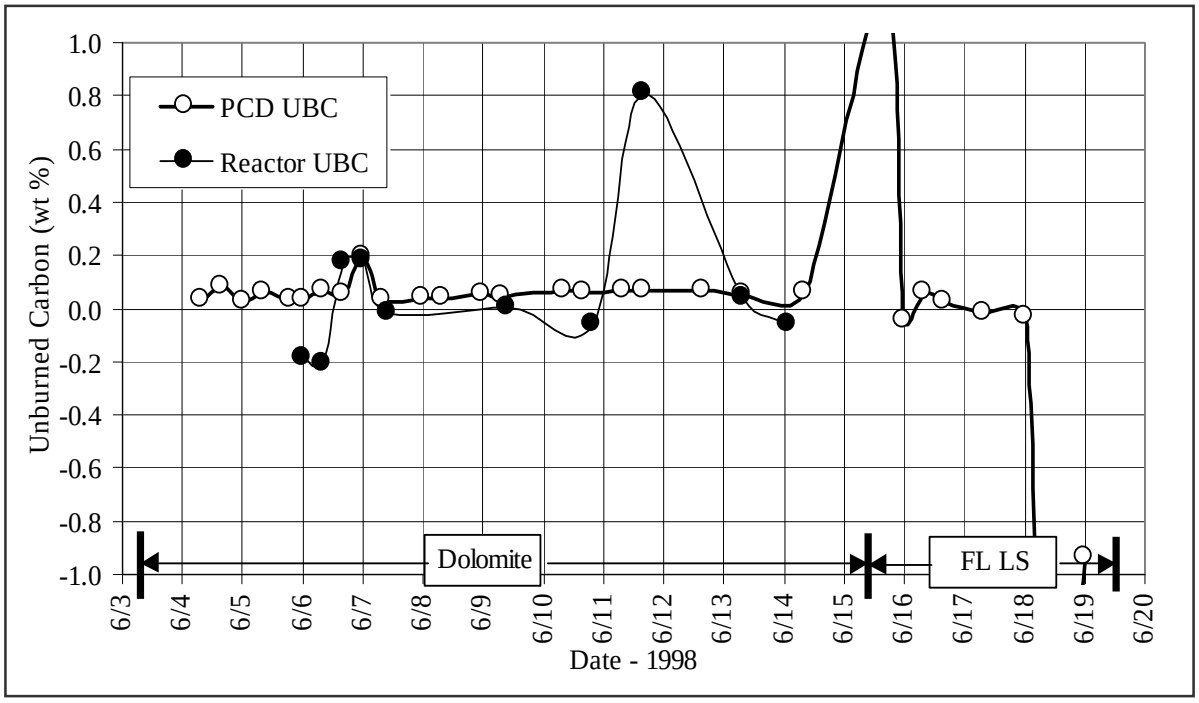


Figure 4.3-27 TC03 PCD and Reactor Unburned Carbon

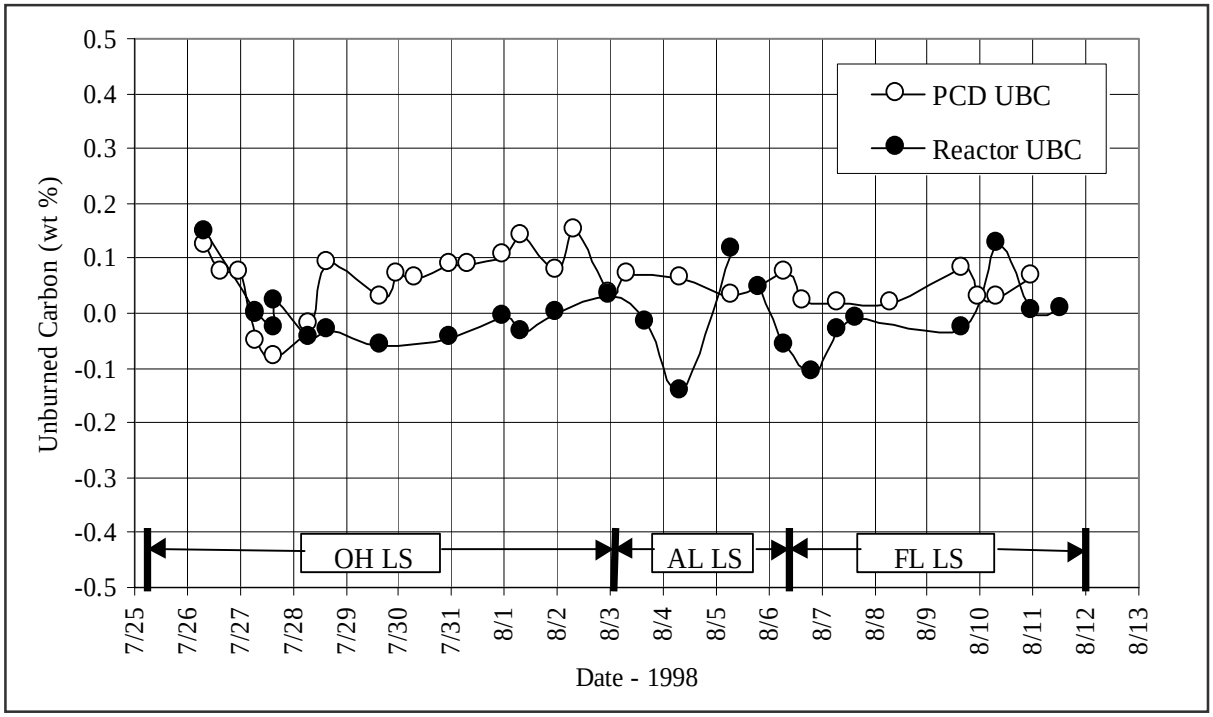


Figure 4.3-28 TC03 PCD and Reactor Unburned Carbon

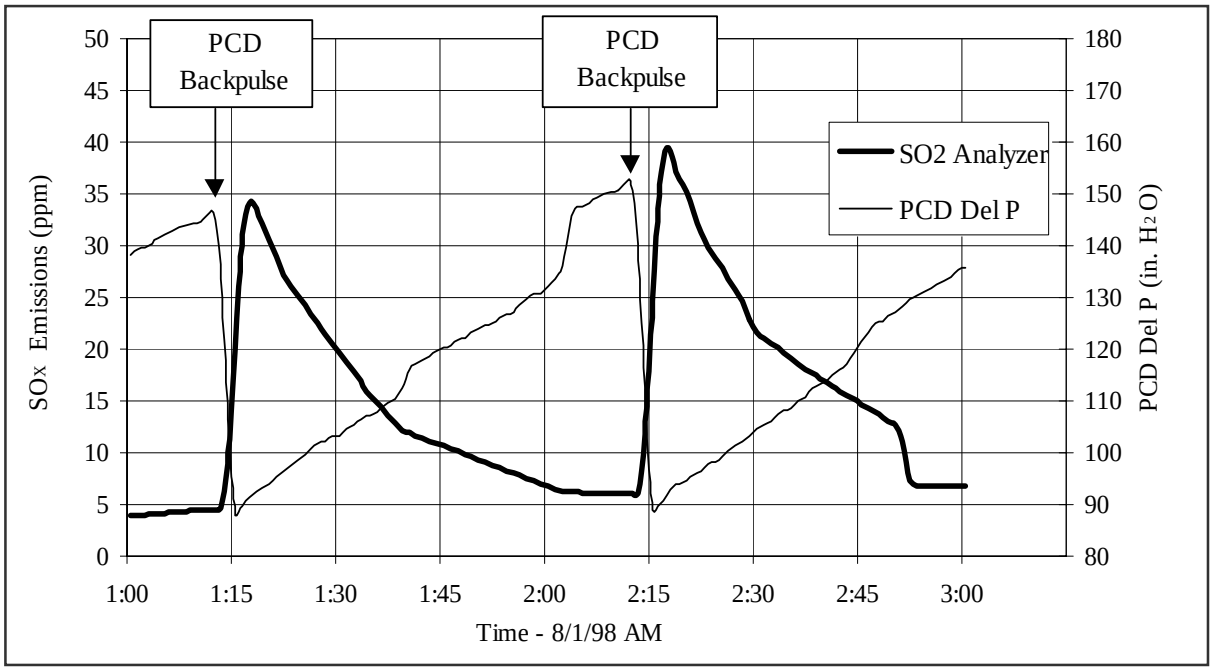


Figure 4.3-29 TC03 $SO_2$ Emission and PCD Pressure Drop - August 1, 1998

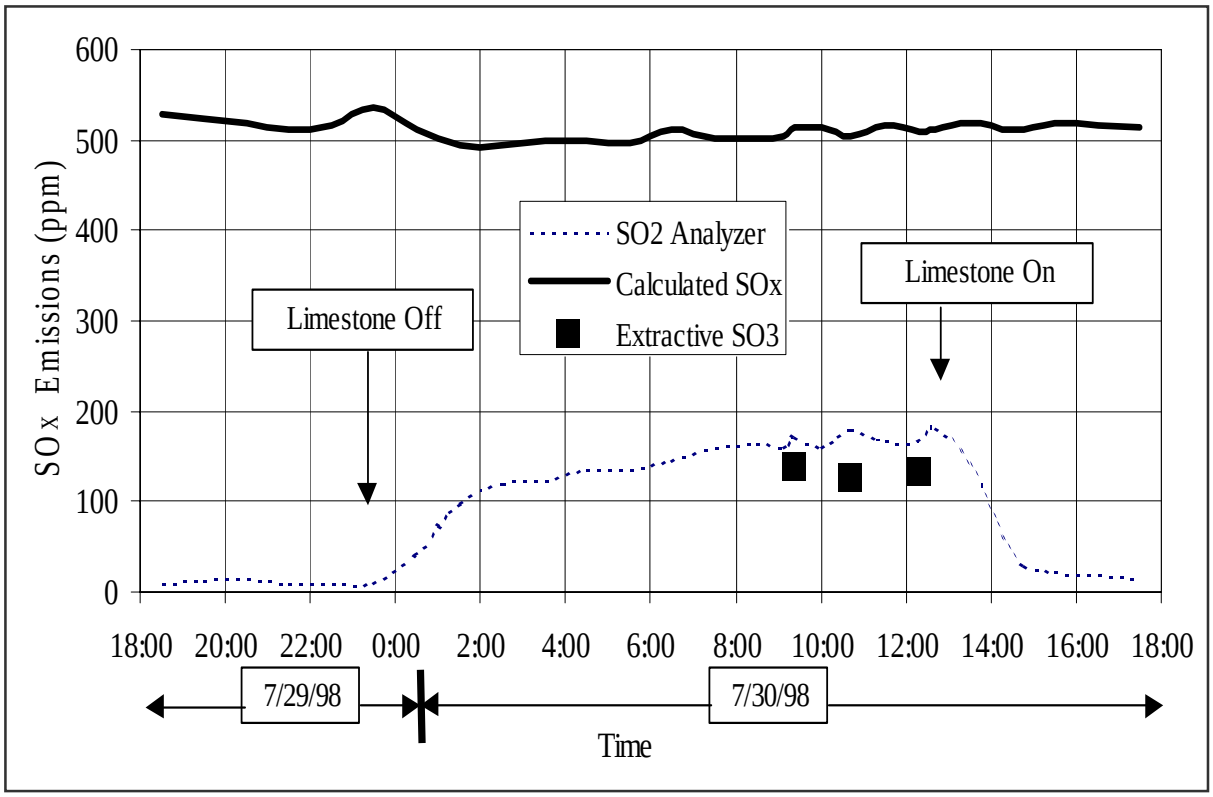


Figure 4.3-30 TC03 $SO_3$ Testing, Limestone Off - July 30, 1998

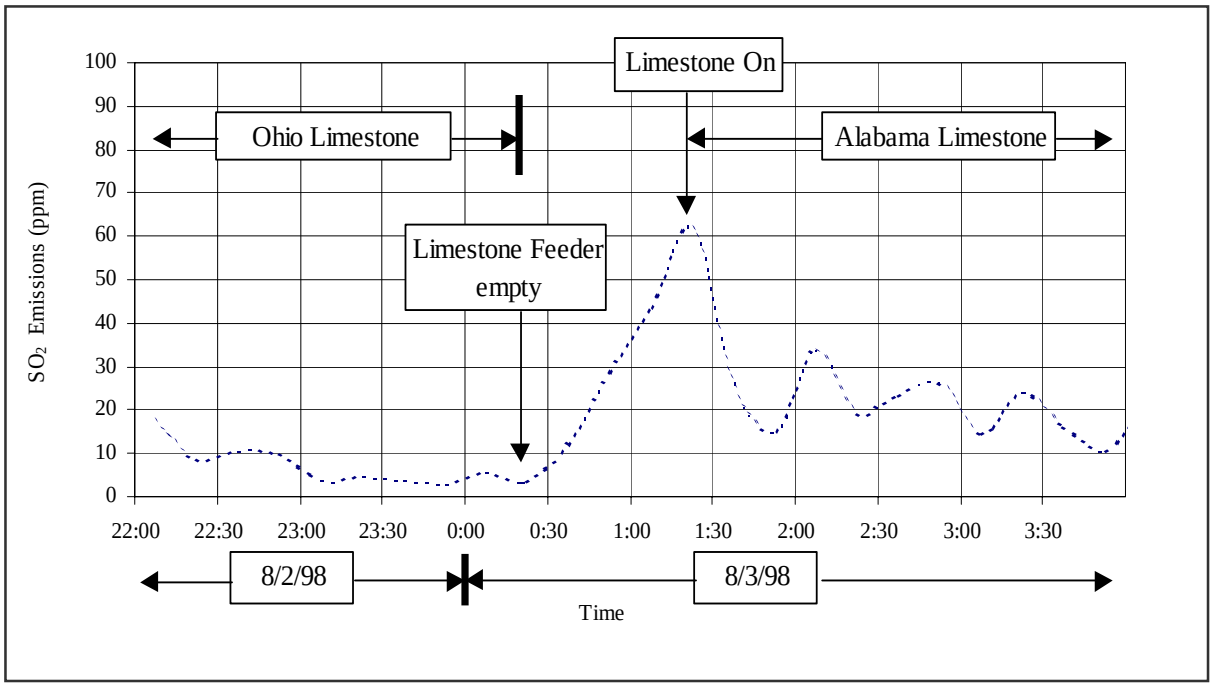


Figure 4.3-31 TC03 Transition From Ohio to Alabama Limestone - August 3, 1998

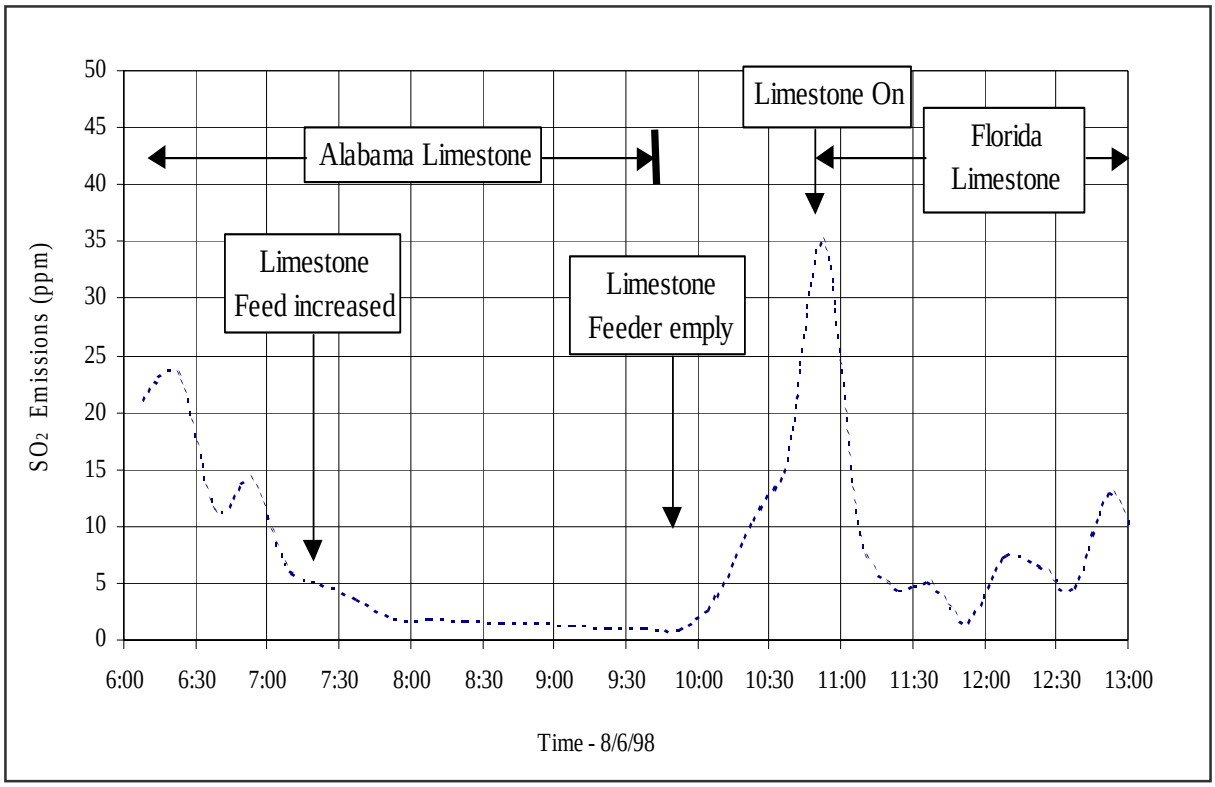


Figure 4.3-32 TC03 Transition From Alabama to Florida Limestone - August 6, 1998

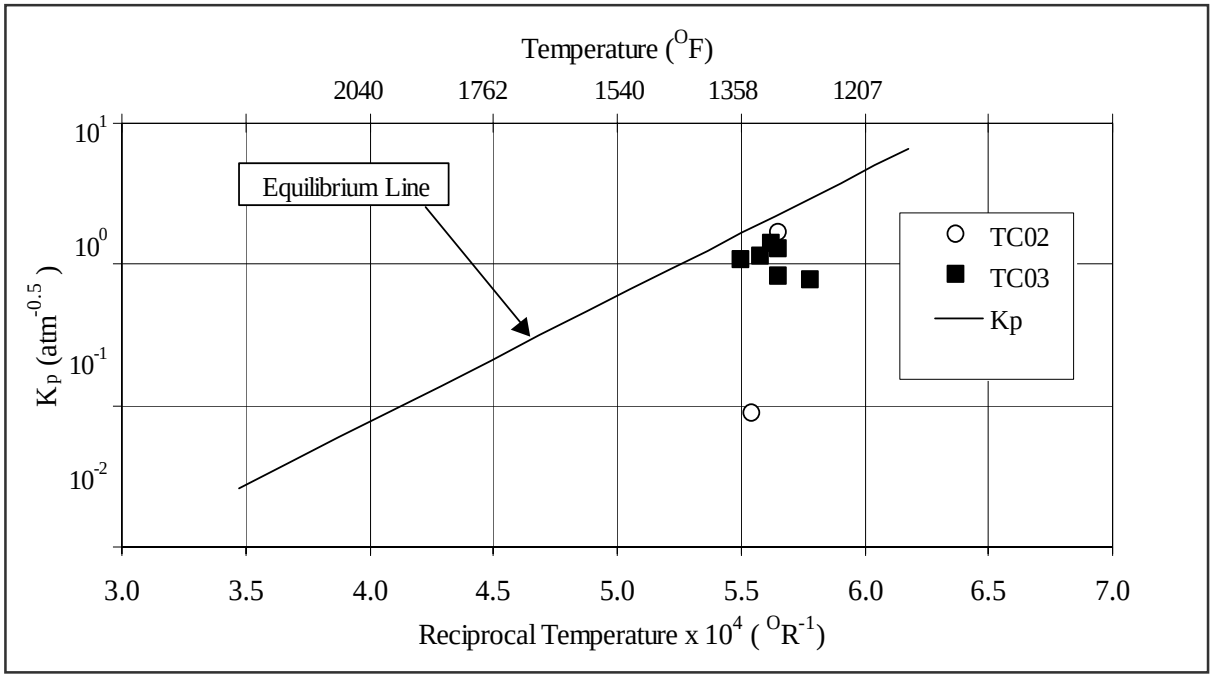


Figure 4.3-33 TC02 and TC03 $SO_2$-$SO_3$ Equilibrium

## 4.4 $NO_X$ EMISSIONS

Reactor operating conditions during test run TC03 were varied to study their effects on $NO_X$ formation as measured by a $NO_X$ analyzer downstream of the PCD. These variables included:

- Different feedstocks. (See Tables 4.1-2 and -3 for detailed analyses.)
- Coal feed rate.
- Excess air.
- Temperature.
- Sorbent feed rate.

This section will present the data collected and observations made as to the effect that these operating conditions had on $NO_X$ emissions.

Figure 4.4-1 is a schematic of the transport reactor loop that shows the air distribution locations, coal feed nozzle location, and the flue gas sample point. The combustion air can be staged, with primary air being added into the mixing zone in a lower and upper level and with secondary air added into the riser in three levels. Air added into the reactor J-leg and combustor heat exchanger (HX0203) J-leg for solids circulation is also available for the combustion reactions. In some cases, additional air that will be available for the combustion reactions may be added through the start-up burner (BR0201) J-leg and bottom of the mixing zone. Air is also added into other locations downstream of the combustion zone, such as the cyclone dipleg and reactor standpipe. Much of this aeration air moves down with the solids into the mixing zone. It should be noted that this aeration air is included in the flue gas measurements since the sample point is downstream of the PCD.

Figure 4.4-2 shows a plot of the $NO_X$ emissions given in pounds of $NO_X$ per million Btu of fuel fired (lb/MBtu) versus the oxygen concentration in the flue gas in volume percent of total flow (percent) with the Alabama and Kentucky coal and Plum Run dolomite as feed. Two data sets are plotted for the Kentucky coal from data collected during different steady-state periods. All data plotted in this figure are based on 5-minute averages due to variance in coal feed rate and, therefore, reactor temperature and oxygen concentration in the flue gas. Reactor operating conditions for this period are listed as data sets A through C in Table 4.4-1. For the Alabama coal with dolomite (data set A), the $NO_X$ varied from 0.14 lb/MBtu at 4.7-percent oxygen content in the flue gas to around 0.22 lb/MBtu at 7-percent oxygen content. For the Kentucky coal with dolomite (data set B), the $NO_X$ varied from 0.14 lb/MBtu at 4.7-percent oxygen content in the flue gas to around 0.19 lb/MBtu at 5.7-percent oxygen content. For the Kentucky coal with dolomite (data set C), the $NO_X$ varied from 0.07 lb/MBtu at 4.9-percent oxygen content in the flue gas to around 0.11 lb/MBtu at 6.0-percent oxygen content. Since data set B is from the time period immediately following the transition to Kentucky coal, the significant difference between data set B and C could be due to the time needed to reach steady state. The plot also shows a slight increase in $NO_X$ emissions as the oxygen content increases for all three data sets. For this data, the percent conversion of fuel-bound nitrogen to $NO_X$ ranged from 3 to 8 percent.

Figure 4.4-3 plots the $NO_X$ emissions versus the oxygen concentration in the flue gas for different limestones at similar Ca/S molar ratios. All data plotted in this figure are based on 5-minute averages due to variance in coal feed rate and, therefore, reactor temperature and oxygen concentration in the flue gas. The reactor operating conditions for this period are listed as data sets D through F in Table 4.4-1. The $NO_X$ emissions with the Florida and Longview limestones were similar, varying from 0.10 to 0.14 lb/MBtu as the oxygen content in flue gas varied from 7.9 to 9.0 percent but were slightly higher than the $NO_X$ emissions with the Bucyrus limestone, which varied from 0.07 to 0.10 lb/MBtu as oxygen content in flue gas varied from 7.3 to 8.4 percent. The $NO_X$ emissions with the limestones and Eastern Kentucky coal were in the same range as the $NO_X$ emissions with Plum Run dolomite steady-state data set C.

Figure 4.4-4 shows plots of the real-time data for the $NO_X$ analyzer (ppm), oxygen concentration in the flue gas (percent), coal feeder speed (rpm), and riser temperature (°F) versus time from 05:10 to 06:40 on June 12, 1998. As the coal feed rate was gradually increased from 1,350 lb/hr at 05:45 to 1,430 lb/hr at 05:50 on June 12, 1998, the temperature increased by 30°F, the oxygen content dropped by 0.6 percent, and the $NO_X$ decreased by 20 ppm. Average operating conditions from 05:10 to 06:40 on June 12, 1998, are shown as data set G in Table 4.4-1. This plot shows that the $NO_X$ emissions decreased as the coal feed rate increased. It should be noted that it is difficult to change the coal feed rate independently of the temperature and oxygen in the transport reactor. The figure also shows that as the coal feed rate was increased, the oxygen in the flue gas decreased and the temperature increased, since in this testing time the air flow rate and solids circulation rate were kept fairly constant. Since several reactor conditions varied simultaneously, it is difficult to determine the sole cause of the $NO_X$ emissions decrease. As previously noted, the $NO_X$ emissions decreased as the temperature increased. This is shown again in Figure 4.4-5, which plots data sets A through C as $NO_X$ emissions (lb/MBtu) versus the reactor temperature (°F). Other variations such as excess oxygen may have had a larger influence than temperature.

The instantaneous effect of increasing coal feed can be seen in Figure 4.4-6, which shows plots of the real-time data for the $NO_X$ analyzer (ppm), oxygen concentration in the flue gas (percent), riser temperature (°F), and dispense vessel top spheri valve position versus time from 07:00 to 08:00 on June 8, 1998. Average operating conditions for this time period are shown as data set H in Table 4.4-1. When the valve opened and coal was transferred into the dispense vessel, a small amount of coal was blown into the reactor through the rotary feeder due to pressure fluctuations. This blowing of material increased the coal feed rate about 80 to 100 lb/hr. The system responded to the higher coal feed rate as follows: the temperature increased 30 to 50°F, oxygen concentration in the flue gas dropped 1.4 percent, and the $NO_X$ emissions dropped 40 to 50 ppm.

Figures 4.4-7 to -9 show the plots for the $NO_X$ emissions versus the oxygen concentration in the flue gas for the different limestones at different limestone feed rates. All data plotted in these figures are based on 5-minute averages due to variance in coal feed rate and, therefore, reactor temperature and oxygen concentration in the flue gas. Average operating conditions for these time periods are shown as data sets I, J, K, L, M, and N, respectively, in Table 4.4-1. The plots show that the $NO_X$ emissions are higher when the Ca/S molar ratio is higher, independent of the sorbent type. The difference is more notable when comparing data without sorbent addition

to data with sorbent addition at some rate. These figures show little influence of oxygen concentration in the flue gas on the $NO_X$ emissions.

To show the response time of $NO_X$ emissions to the varying of the sorbent feed rate, Figure 4.4-10 shows the plots of the $NO_X$ analyzer reading and sorbent feeder speed versus time. Average operating conditions are shown as data set O in Table 4.4-1. The figure shows that the $NO_X$ emissions started increasing 1 minute after the sorbent feeder speed was increased. As the Ca/S molar ratio was increased from 2.1 to 11.1, the $NO_X$ emissions increased from 75 to 210 ppm (0.22 to 0.35 lb/MBtu). The initial-step change in sorbent feed rate affected $NO_X$ emissions more significantly than subsequent step changes. Figure 4.4-11 plots the $NO_X$ analyzer reading and sorbent feeder speed versus time during a time period when the sorbent feeder speed was decreased. Average operating conditions are shown as data set P in Table 4.4-1. The $NO_X$ emissions started to decrease gradually after the sorbent feeder speed was decreased. As the Ca/S molar ratio was reduced from 1.3 to zero, the $NO_X$ emissions decreased from about 60 to 40 ppm. This figure also shows the effects of instantaneous increases in sorbent feed rate. When sorbent was blown into the reactor, indicated by the high-differential pressure reading between the sorbent feed system dispense vessel and discharge line, the $NO_X$ analyzer indication increased by about 20 ppm.

In summary, the $NO_X$ emissions were as low as 0.04 lb/MBtu and varied up to 0.55 lb/MBtu when excess sorbent was added to the system as bed material. The $NO_X$ emissions using the Kentucky and Alabama coal were similar, with the $NO_X$ emissions from the Kentucky coal being lower after a certain period of time than the Alabama coal. The $NO_X$ emissions with the Florida and Longview limestone were similar, ranging from 0.10 to 0.14 lb/MBtu, but they were slightly higher than the $NO_X$ emissions with the Bucyrus limestone which ranged from 0.07 to 0.10 lb/MBtu. It was noted that as the coal feed rate was gradually increased from 1,350 to 1,430 lb/hr, the temperature increased by 30°F, the oxygen content dropped by 0.6 percent, and the $NO_X$ decreased by 20 ppm. In addition, it was observed that there was a significant increase in $NO_X$ emissions when sorbent was added to the system for all sorbent types. For example, with Bucyrus limestone, the $NO_X$ emissions increased by 40 percent as the Ca/S molar ratio was increased from 0 to 1.0.

Table 4.4-1 (Page 1 of 2)

Reactor Operating Conditions

| **Data Set** | **A** | **B** | **C** | **D** |
|---|---|---|---|---|
| Coal type | AL | KY | KY | KY |
| Sorbent type | Plum Run dolomite | Plum Run dolomite | Plum Run dolomite | Bucyrus limestone |
| Reactor temperature (°F) | 1,565 | 1,562 | 1,567 | 1,453 |
| Reactor pressure (psig) | 200 | 200 | 200 | 150 |
| Coal feed rate (lb/hr) | 1,517 | 1,364 | 1,346 | 1,131 |
| Ca/S molar ratio in feed | 2.1 | 1.4 | 1.7 | 1.0 |
| Staged air (%) | 40 | 40 | 37 | 4 |
| Start time | 6/09/98 04:00 | 6/11/98 08:00 | 6/12/98 18:00 | 7/31/98 10:00 |
| End time | 6/10/98 08:15 | 6/12/98 06:00 | 6/13/98 15:00 | 8/02/98 16:55 |
| **Data Set** | **E** | **F** | **G** | **H** |
| Coal type | KY | KY | KY | AL |
| Sorbent type | Longview limestone | Florida limestone | Plum Run dolomite | Plum Run dolomite |
| Reactor temperature (°F) | 1,454 | 1,457 | 1,566 | 1,574 |
| Reactor pressure (psig) | 165 | 167 | 200 | 200 |
| Coal feed rate (lb/hr) | 1,065 | 1,072 | 1,350-1,430 | 1,464 |
| Ca/S molar ratio in feed | 1.2 | 0.8 | 1.4 | 2.0 |
| Staged air (%) | 4 | 4 | 38 | 39 |
| Start time – 1 | 8/05/98 10:00 | 8/06/98 16:00 | 6/12/98 05:10 | 6/08/98 07:00 |
| End time – 1 | 8/05/98 11:45 | 8/07/98 08:00 | 6/12/98 05:40 | 6/08/98 08:00 |
| Start time – 2 | 8/05/98 18:00 | 8/07/98 12:25 | 6/12/98 05:50 | |
| End time – 2 | 8/06/98 06:00 | 8/08/98 18:00 | 6/12/98 06:40 | |

Table 4.4-1 (Page 2 of 2)

Reactor Operating Conditions

| **Data Set** | **I** | **J** | **K** | **L** |
|---|---|---|---|---|
| Coal type | KY | KY | KY | KY |
| Sorbent type | Bucyrus limestone | Bucyrus limestone | Longview limestone | Longview limestone |
| Reactor temperature (°F) | 1,431 | 1,456 | 1,442 | 1,471 |
| Reactor pressure (psig) | 145 | 150 | 155 | 157 |
| Coal feed rate (lb/hr) | 1,082 | 1,130 | 1,115 | 1,120 |
| Ca/S molar ratio in feed | 0 | 1.0 | 0.6 | 1.5 |
| Staged air (%) | 4 | 4 | 4 | 4 |
| Start time – 1 | 7/30/98 00:10 | 7/31/98 08:50 | 8/03/98 19:20 | 8/03/98 14:55 |
| End time – 1 | 7/30/98 13:25 | 8/01/98 06:55 | 8/04/98 00:55 | 8/03/98 18:50 |
| Start time – 2 | | | | 8/04/98 05:00 |
| End time – 2 | | | | 8/04/98 14:20 |
| Start time – 3 | | | | 8/04/98 16:05 |
| End time – 3 | | | | 8/04/98 17:10 |
| **Data Set** | **M** | **N** | **O** | **P** |
| Coal type | KY | KY | AL | KY |
| Sorbent type | Florida limestone | Florida limestone | Plum Run dolomite | Bucyrus limestone |
| Reactor temperature (°F) | 1,455 | 1,477 | 1,555 | 1,459 |
| Reactor pressure (psig) | 165 | 165 | 200 | 145 |
| Coal feed rate (lb/hr) | 1,071 | 1,092 | 947 | 1,099 |
| Ca/S molar ratio in feed | 0.8 | 1.8 | 2.1 to 11.1 | 0 to 1.3 |
| Staged air (%) | 4 | 4 | 38 | 4 |
| Start time – 1 | 8/06/98 22:00 | 8/07/98 07:10 | 6/04/98 11:00 | 7/29/98 23:15 |
| End time – 1 | 8/07/98 07:00 | 8/07/98 12:15 | 6/04/98 11:50 | 7/30/98 00:12 |
| Start time – 2 | 8/07/98 12:25 | 8/08/98 18:15 | 6/04/98 12:15 | 7/30/98 00:20 |
| End time – 2 | 8/08/98 18:10 | 8/09/98 04:50 | 6/04/98 12:30 | 7/30/98 01:15 |

Notes:

1 The staging percent was defined as the amount of secondary air flow divided by the total air flow to the reactor that is available for the combustion reactions.

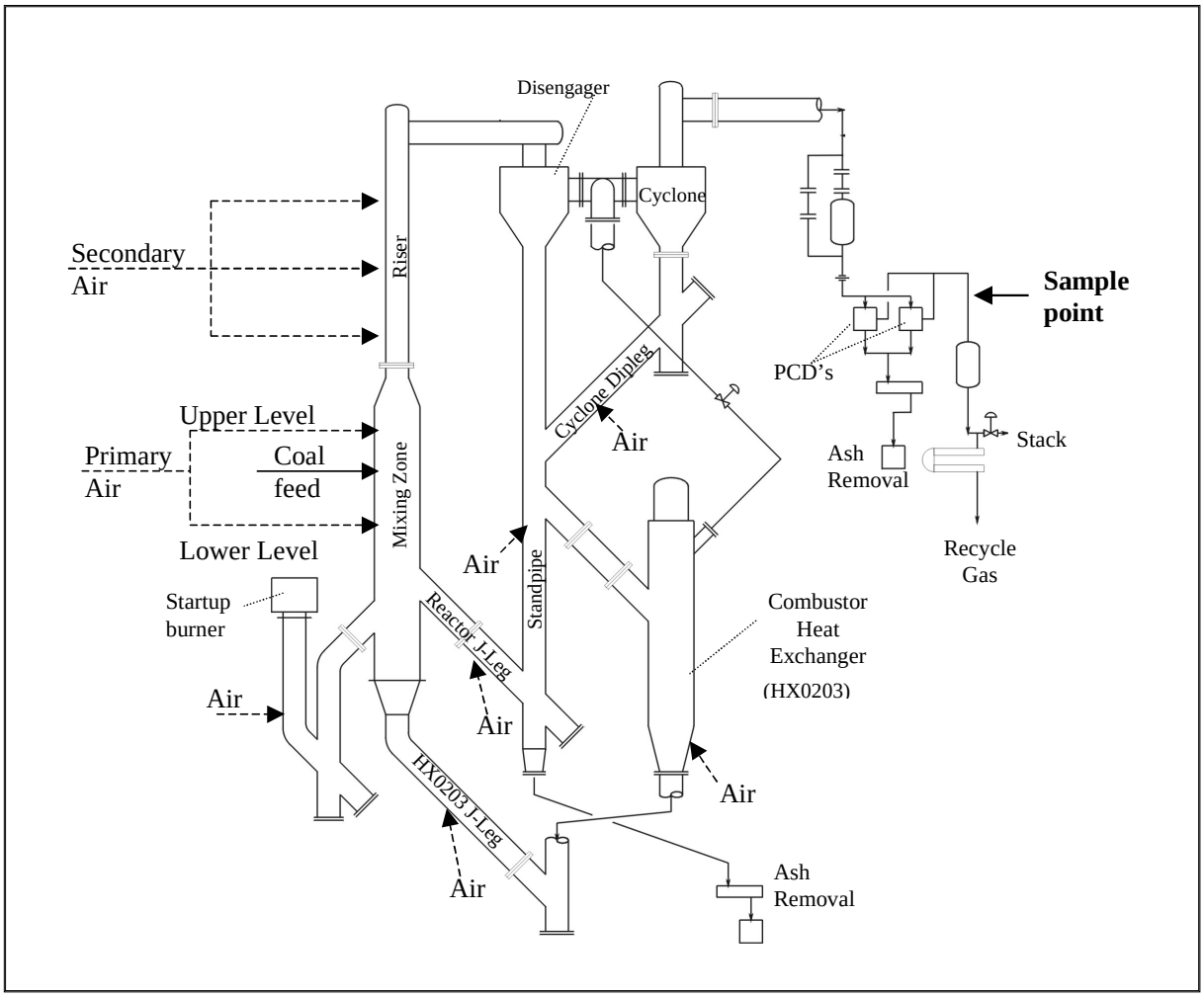


Figure 4.4-1 Transport Reactor Train Loop Schematic

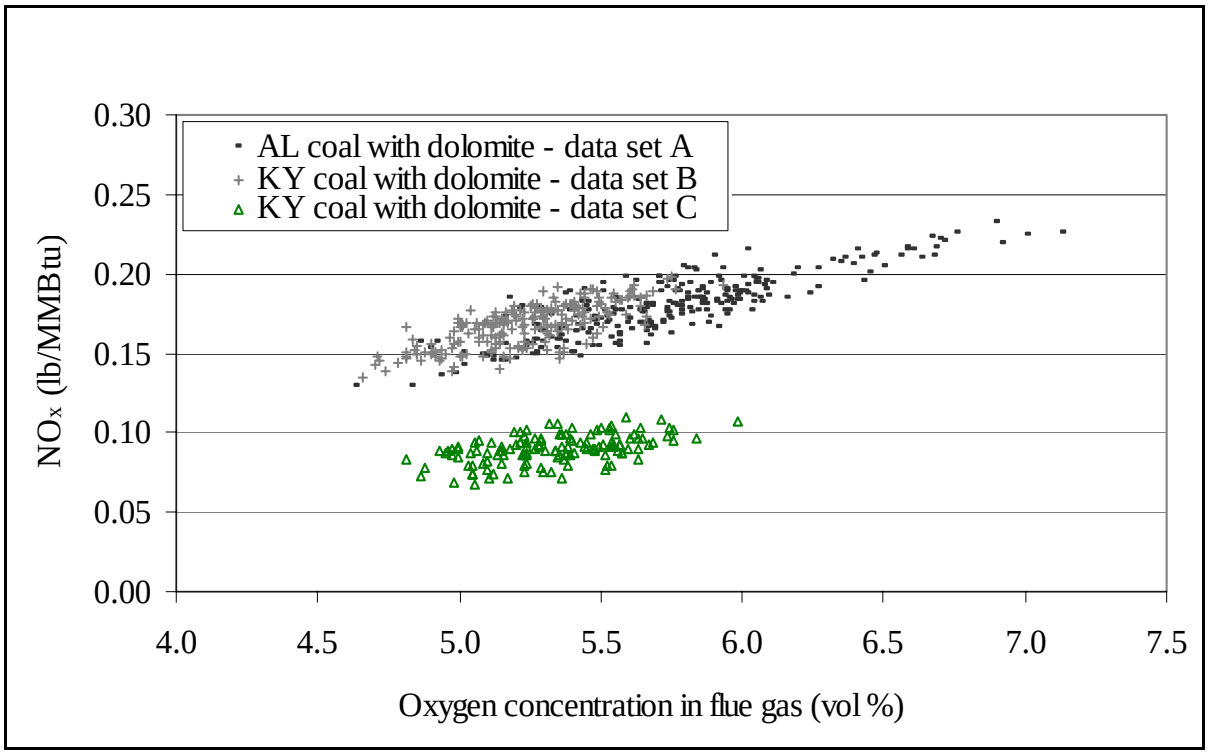


Figure 4.4-2 Effect of Different Coal Feeds on NOx Emissions

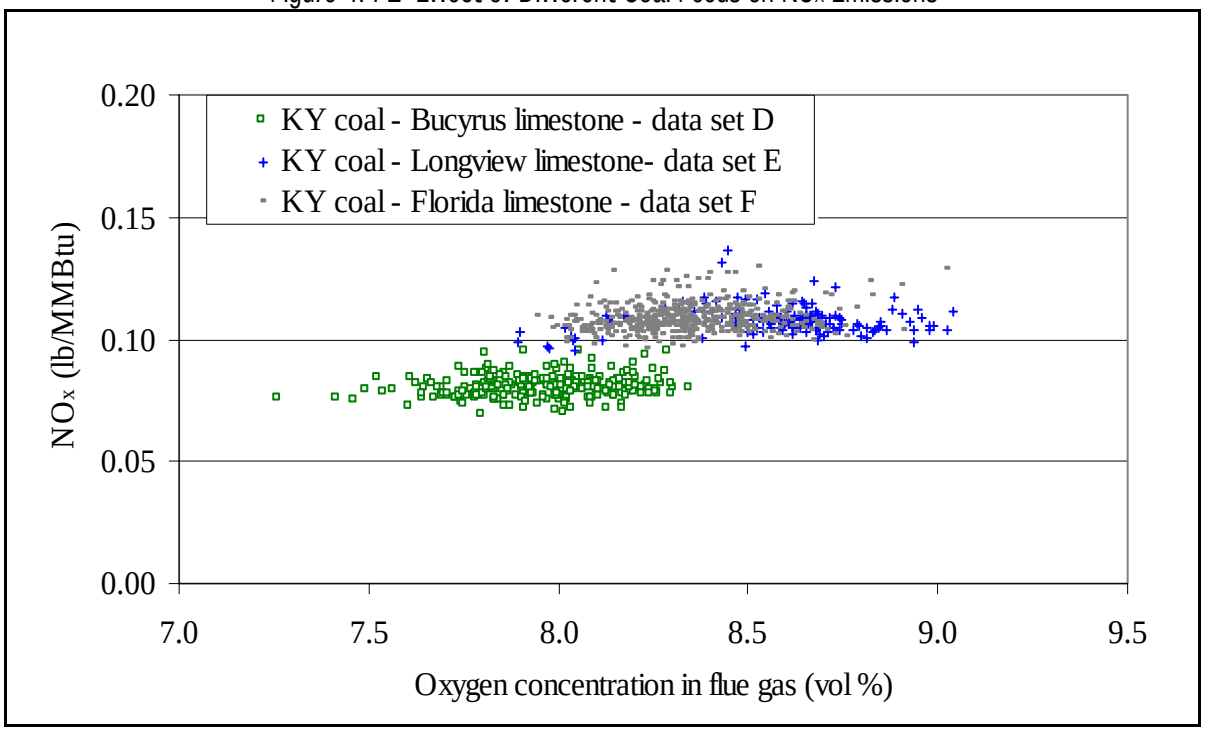


Figure 4.4-3 Effect of Different Sorbents on NOx Emissions

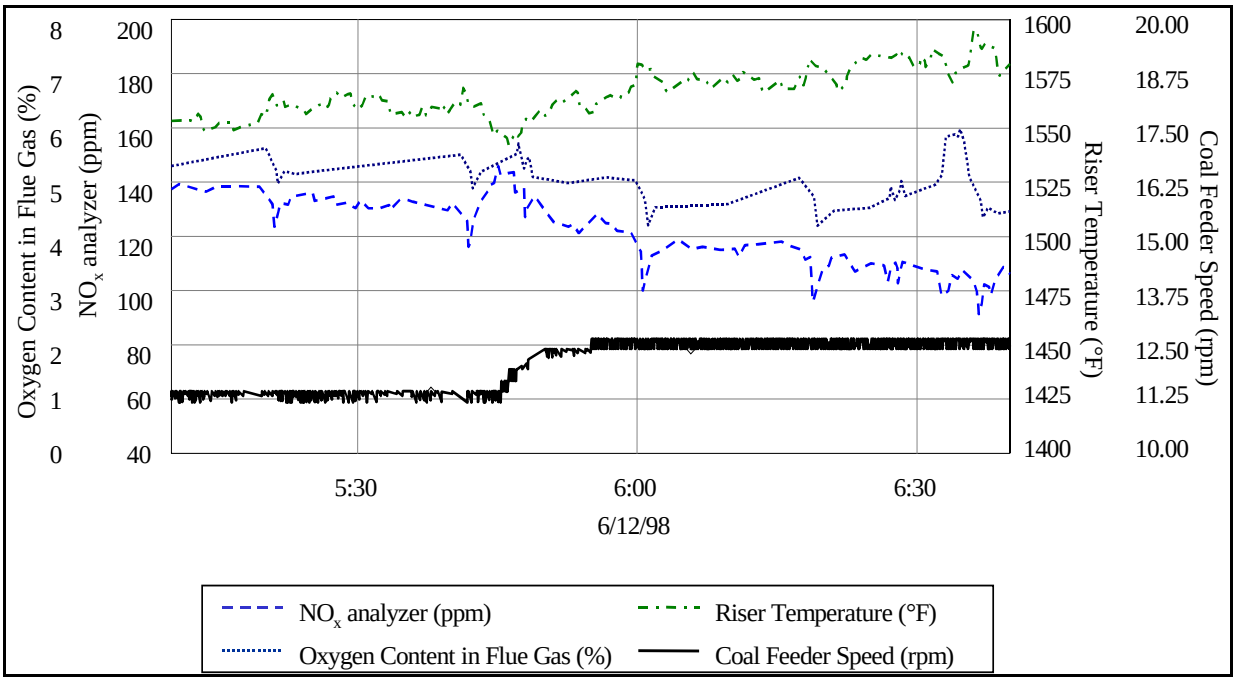


Figure 4.4-4 Effect of Increasing Coal Feed Rate on NOx Emissions (Data Set G)

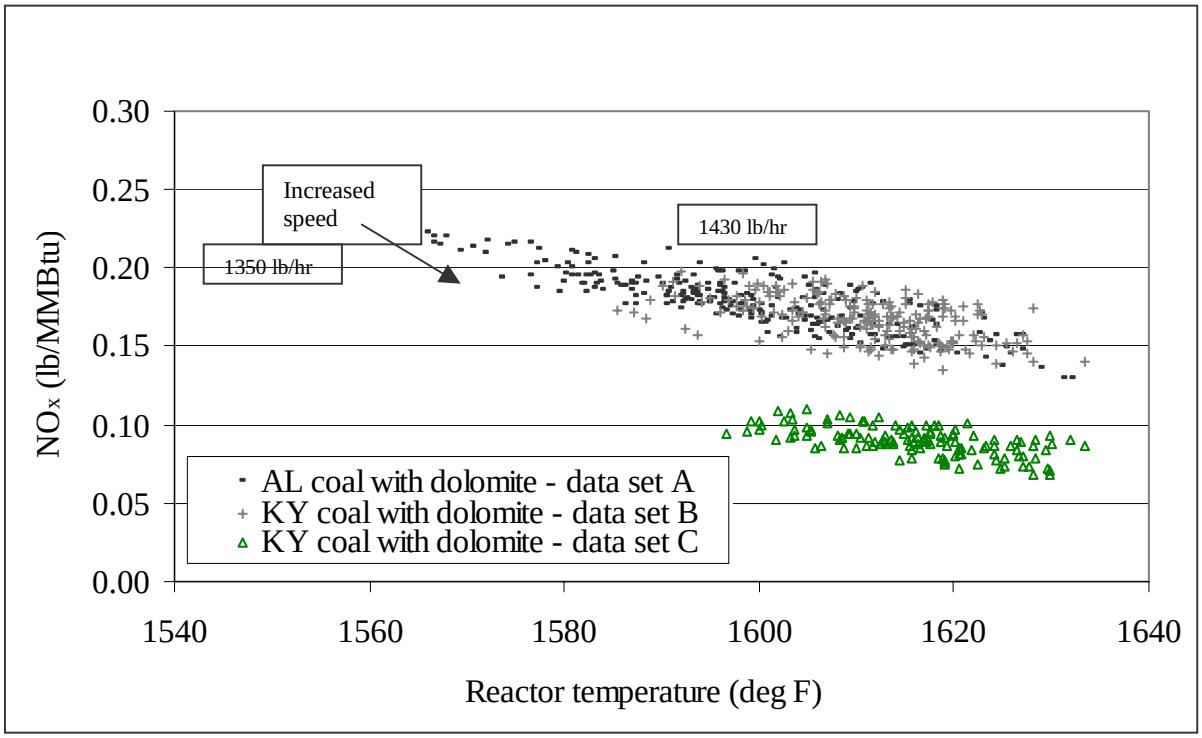


Figure 4.4-5 Effect of Reactor Temperature on NOx Emissions

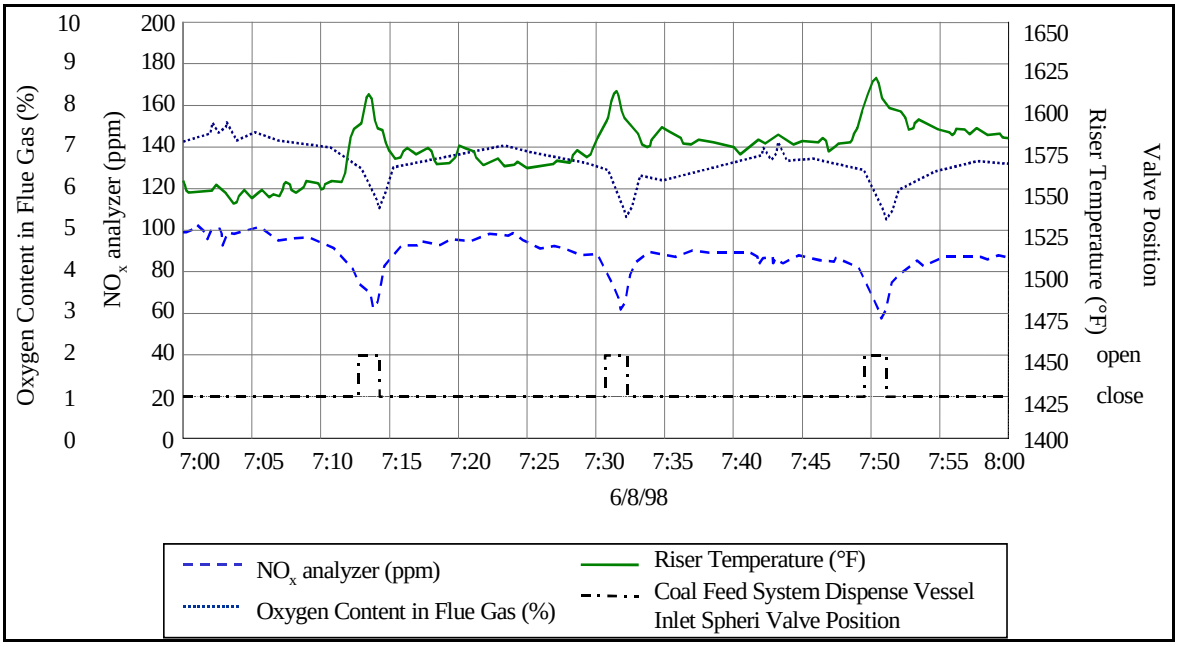


Figure 4.4-6 Effect of Coal Feed System Cycles on NOx Emissions (Data Set H)

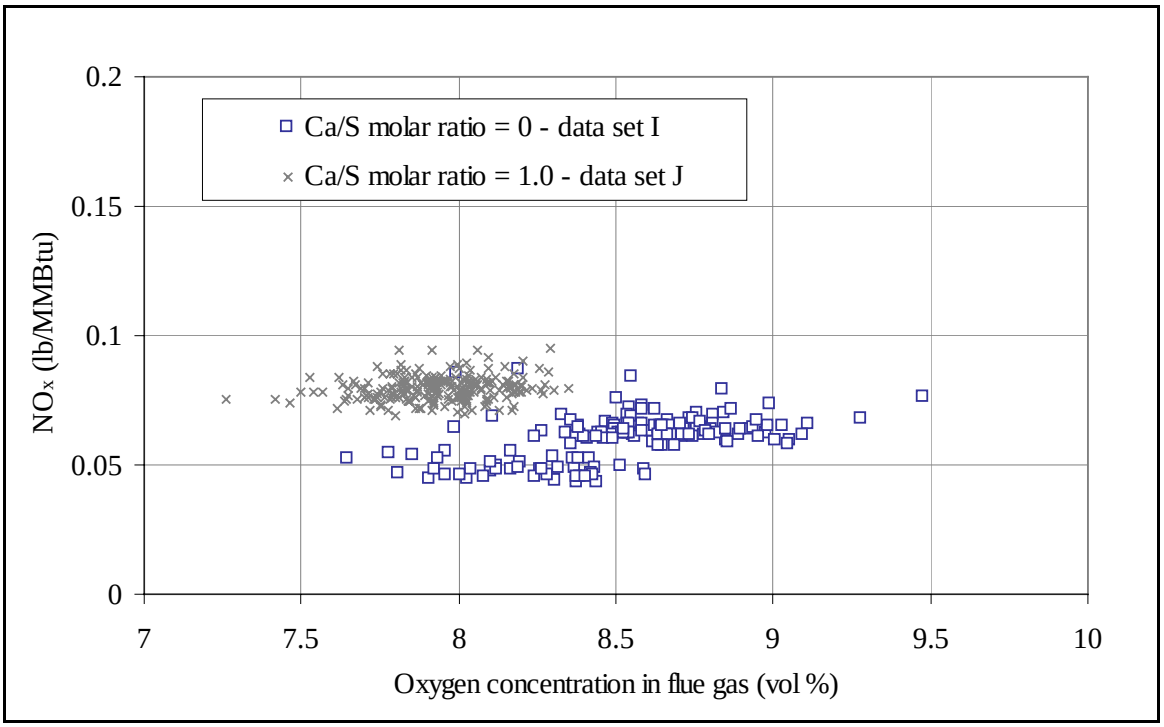


Figure 4.4-7 Effect of Bucyrus Limestone Feed Rate on NOx Emissions

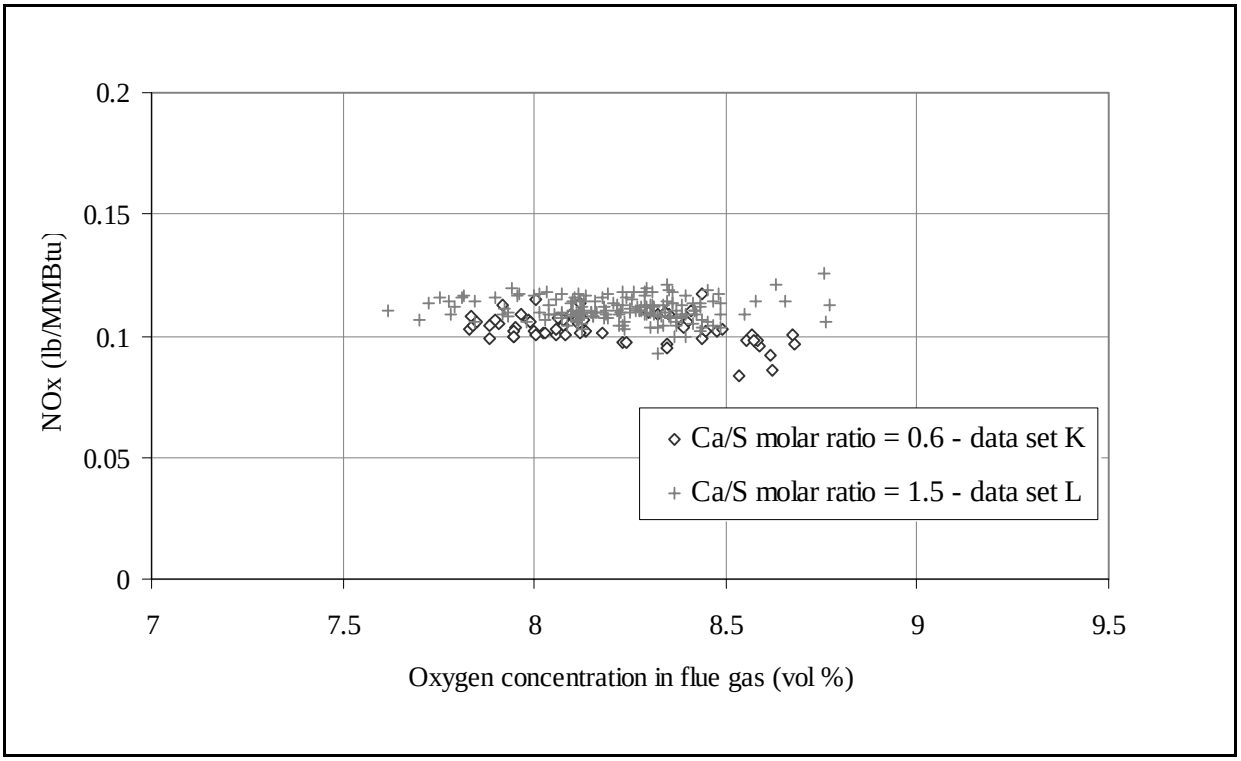


Figure 4.4-8 Effect of Longview Limestone Feed Rate on NOx Emissions

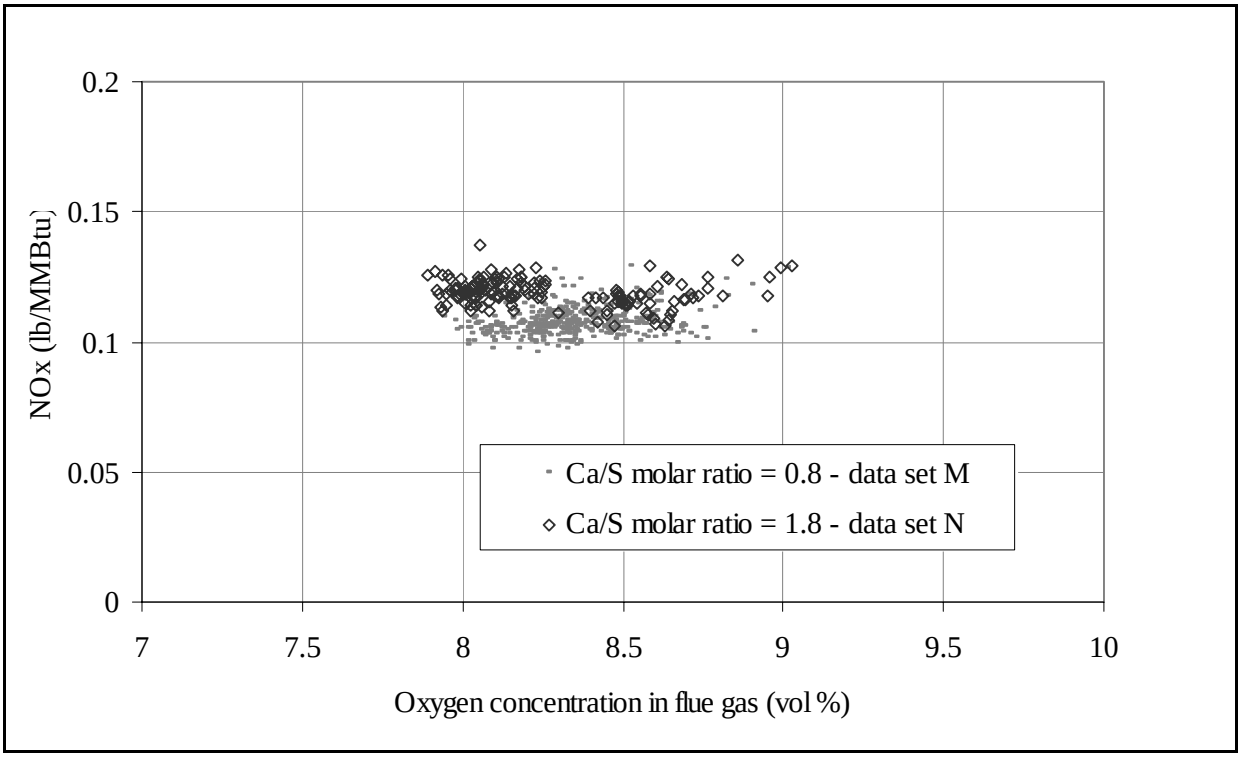


Figure 4.4-9 Effect of Florida Limestone Feed Rate on NOx Emissions

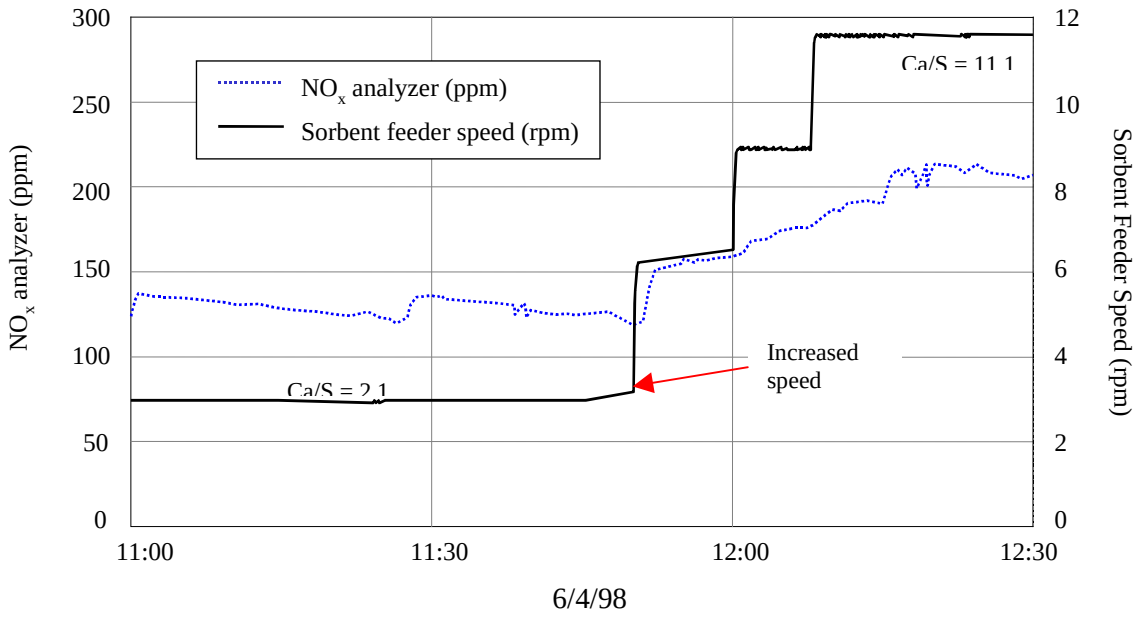


Figure 4.4-10 Response Time of NOx Emissions to Increasing Dolomite Feed Rate (Data Set O)

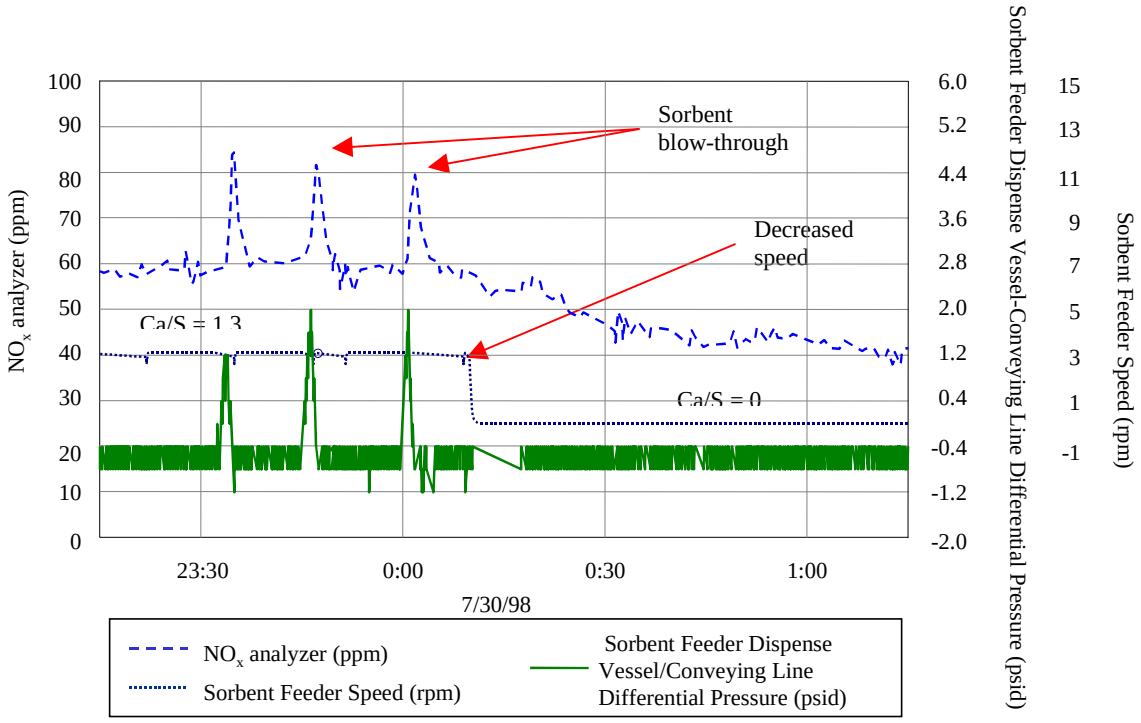


Figure 4.4-11 Response Time of NOx Emissions to Decreasing Bucyrus Limestone Feed Rate and Effect of Sorbent "Blow-Through" on NOx Emissions (Data Set P)

## 4.5 TC03 TEMPERATURE PROFILE

The temperature profile in the transport reactor was investigated to determine the differences between an Alabama bituminous coal and a higher reactive Kentucky bituminous coal. A brief comparison of the coals is found in Table 4.1-2.

The time periods were selected because each had similar operating conditions, including solids level in the standpipe and combustion heat exchanger, aeration rates, and pressure. The period using the Kentucky bituminous coal had about a 10-percent higher circulation rate than the period using the Alabama bituminous coal. The periods were selected with the same temperature entering the riser.

Figure 4.5-1 shows the temperature profile in the mixing zone and J-legs when feeding the Alabama bituminous coal and when feeding the Kentucky bituminous coal. The two mixing zone profiles show almost identical trends. The temperature profiles for the standpipe, dipleg, and combustion heat exchanger are shown in Figure 4.5-2. The profiles for these regions are very similar, with the only significant difference being that the Kentucky coal temperature profile is 5 to 10°F higher despite starting at the same temperature in the mixing zone. This is explained by the higher heat content of the Kentucky coal. The temperatures are the same once the material returns to the mixing zone because the higher circulation rate in the case of the Kentucky coal allows more heat to be removed in the combustion heat exchanger.

The temperature profiles do differ in the riser section, as shown in Figure 4.5-3. The shape of the profiles is the same, but the higher Btu content and higher reactivity of the Kentucky coal lead to higher peak temperatures in the riser despite higher circulation rates. The peak riser temperature is measured with TI360 about 10 feet from the top of the riser. The riser temperature then decays from this point to the top of the riser, through the crossover, and into the disengager. An interesting feature of both riser profiles is the second temperature peak in the secondary crossover between the disengager and cyclone. Once the bulk of the solids is removed in the disengager, a second, higher temperature peak is measured before the gas enters the primary cyclone. It has been suggested that heat transfer to the bed material prevents all of the volatile components from completely combusting.

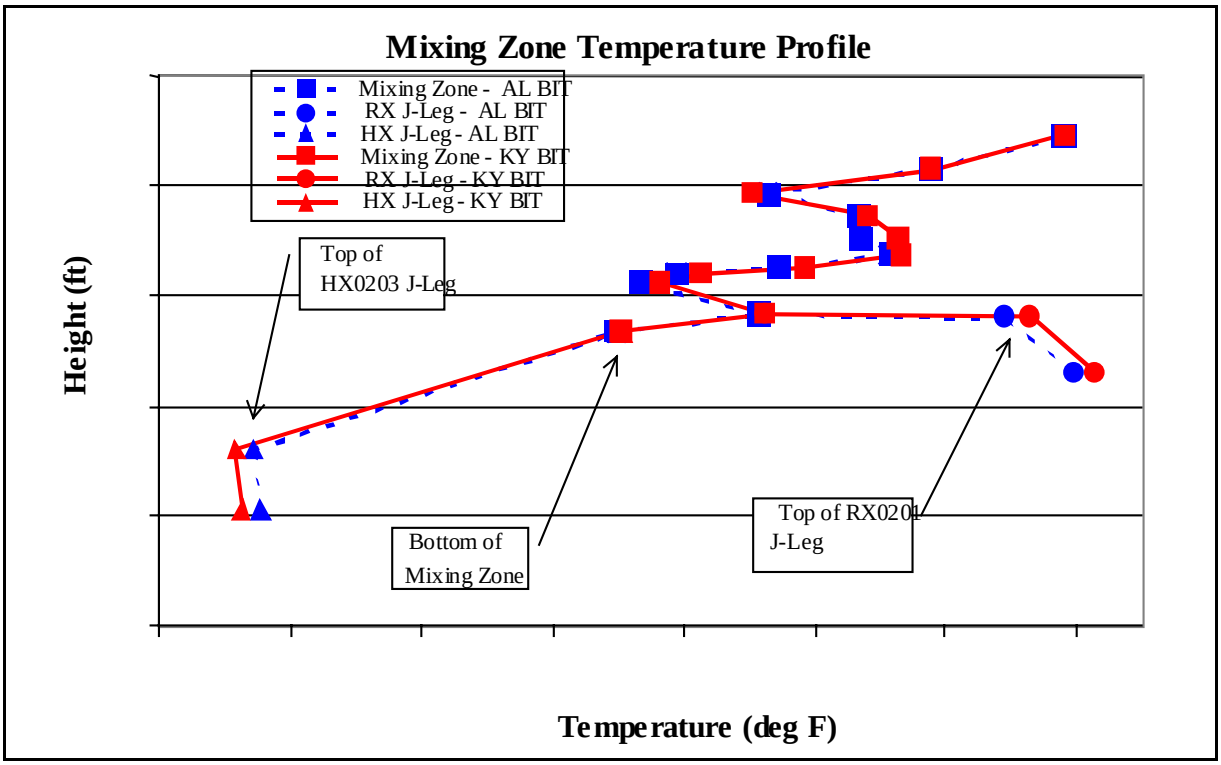


Figure 4.5-1 Mixing Zone Temperature Profile

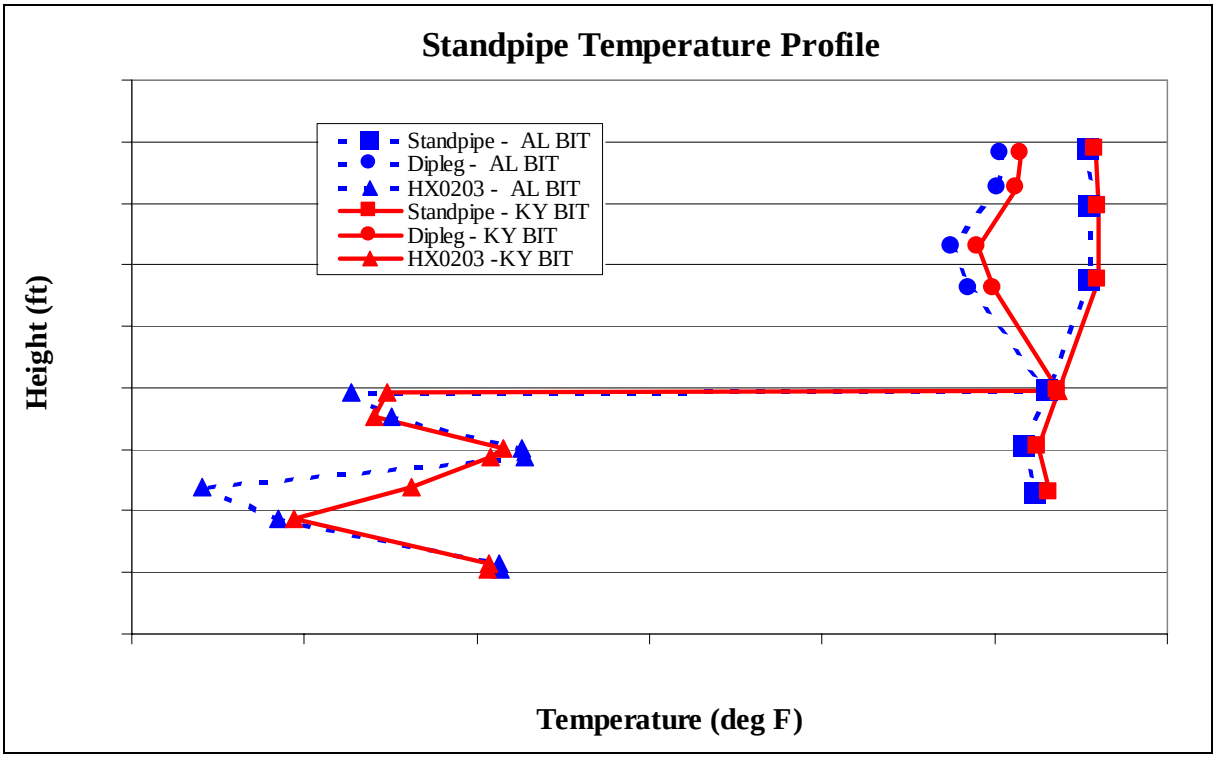


Figure 4.5-2 Standpipe, Dipleg, and HX0203 Temperature Profile

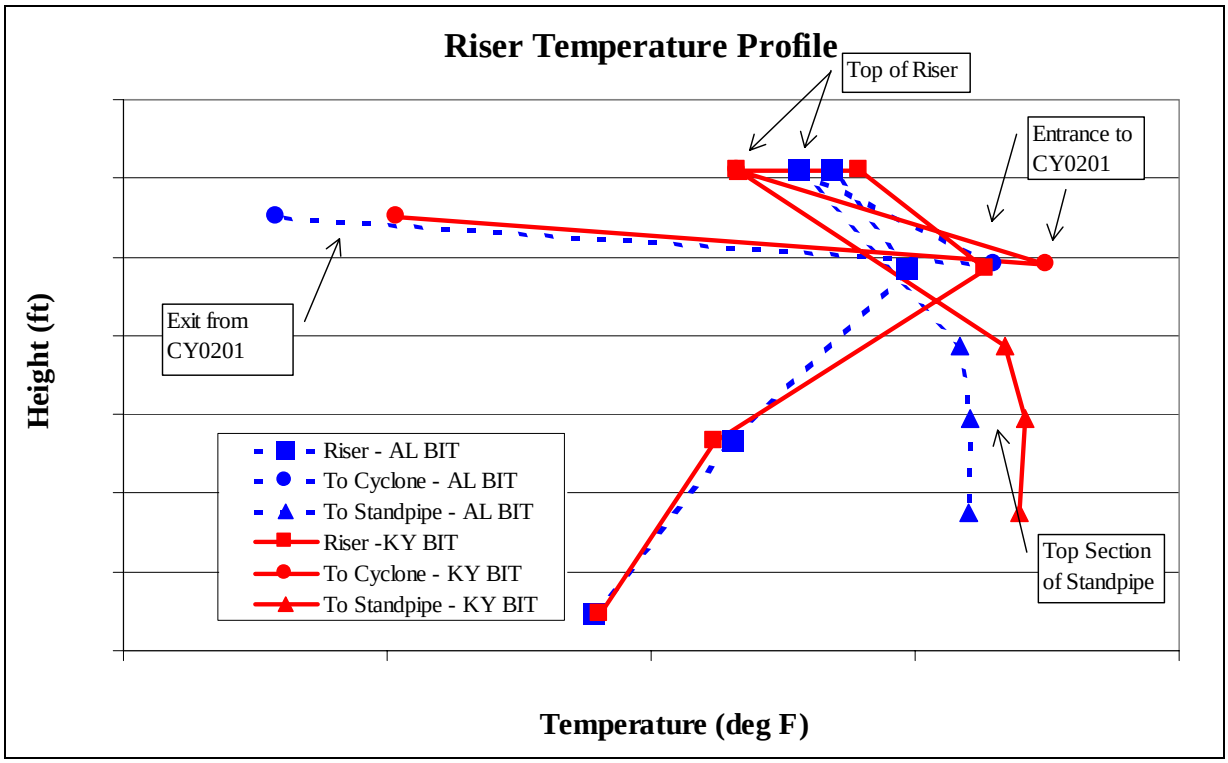


Figure 4.5-3 Riser Temperature Profile

# TERMS

## Listing of Abbreviations

| | |
|---|---|
| AAS | Automated Analytical Solutions |
| ADEM | Alabama Department of Environmental Management |
| APC | Alabama Power Company |
| APFBC | Advance Pressurized Fluidized-Bed Combustion |
| ASME | American Society of Mechanical Engineers |
| AW | Application Workstation |
| BFI | Browning-Ferris Industries |
| BFW | Boiler Feed Water |
| BMS | Burner Management System |
| BOC | BOC Gases |
| BOP | Balance-of-Plant |
| BPIR | Ball Pass Inner Race, Frequencies |
| BPOR | Ball Pass Outer Race, Frequencies |
| BSF | Ball Spin Frequency |
| CAD | Computer-Aided Design |
| CEM | Continuous Emissions Monitor |
| CFB | Circulating Fluidized Bed |
| CFR | Code of Federal Regulations |
| CHE | Combustor Heat Exchanger |
| CPC | Combustion Power Company |
| CPR | Cardiopulmonary Resuscitation |
| DC | Direct Current |
| DCS | Distributed Control System |
| DOE | U.S. Department of Energy |
| E & I | Electrical and Instrumentation |
| EERC | Energy and Environmental Research Center |
| EPRI | Electric Power Research Institute |
| FCC | Fluidized Catalytic Cracker |
| FETC | Federal Energy Technology Center |
| FFG | Flame Front Generator |
| FI | Flow Indicator |
| FIC | Flow Indicator Controller |
| FOAK | First-of-a-Kind |
| FTF | Fundamental Train Frequency |
| FW | Foster Wheeler |
| GBF | Granular Bed Filter |
| GC | Gas Chromatograph |
| GEESI | General Electric Environmental Services, Inc. |
| HP | High Pressure |
| HRSG | Heat Recovery Steam Generator |
| HTF | Heat Transfer Fluid |
| HTHP | High-Temperature, High-Pressure |

| | |
|---|---|
| I/O | Inputs/Outputs |
| ID | Inside Diameter |
| IF&P | Industrial Filter & Pump |
| IGV | Inlet Guide Vanes |
| IR | Infrared |
| KBR | Kellogg Brown & Root |
| LAN | Local Area Network |
| LIMS | Laboratory Information Management System |
| LOC | Limiting Oxygen Concentration |
| LOI | Loss on Ignition |
| LPG | Liquefied Propane Gas |
| LSLL | Level Switch, Low Level |
| MAC | Main Air Compressor |
| MCC | Motor Control Center |
| MS | Microsoft Corporation |
| NDIR | Nondestructive Infrared |
| NFPA | National Fire Protection Association |
| NOx | Nitrogen Oxides |
| NPDES | National Pollutant Discharge Elimination System |
| NPS | Nominal Pipe Size |
| OD | Outside Diameter |
| OSHA | Occupational Safety Health Administration |
| OSI | OSI Software, Inc. |
| P&IDs | Piping and Instrumentation Diagrams |
| PC | Pulverized Coal |
| PCD | Particulate Control Device |
| PDI | Pressure Differential Indicator |
| PDT | Pressure Differential Transmitter |
| PFBC | Pressurized Fluidized-Bed Combustion |
| PI | Plant Information |
| PLC | Programmable Logic Controller |
| PPE | Personal Protection Equipment |
| PRB | Powder River Basin |
| PSD | Particle Size Distribution |
| PSDF | Power Systems Development Facility |
| $\Delta P$ | Pressure Drop |
| PT | Pressure Transmitter |
| RFQ | Request for Quotation |
| RO | Restriction Orifice |
| RSSE | Reactor Solid Separation Efficiency |
| SCS | Southern Company Services, Inc. |
| SMD | Sauter Mean Diameter |
| SRI | Southern Research Institute |
| SUB | Start-up Burner |
| TCLP | Toxicity Characteristic Leaching Procedure |
| TR | Transport Reactor |
| TRDU | Transport Reactor Demonstration Unit |

| | |
|---|---|
| TSS | Total Suspended Solids |
| UND | University of North Dakota |
| UPS | Uninterruptible Power Supply |
| UV | Ultraviolet |
| VFD | Variable Frequency Drive |
| VOCs | Volatile Organic Compounds |
| WPC | William's Patent Crusher |
| XXS | Extra, Extra Strong |

## Listing of Units

| | |
|---|---|
| acfm | actual cubic feet per minute |
| Btu | British thermal units |
| °F | degrees fahrenheit |
| ft | feet |
| FPS | feet per second |
| gpm | gallons per minute |
| $g/cm^3$ | grams per cubic centimeter |
| hp | horsepower |
| hr | hour |
| inWg | inches, water gauge |
| MB | megabytes |
| MW | megawatts |
| m/s | meters per second |
| $m^2/g$ | square meters per gram |
| μ or μm | microns or micrometers |
| $dp_{50}$ | particle size distribution at 50 percentile |
| ppm | parts per million |
| ppm (v) | parts per million (volume) |
| ppm (w) | parts per million (weight) |
| lb | pounds |
| pph | pounds per hour |
| psia | pounds per square inch |
| psig | pounds per square inch gauge |
| ΔP | pressure drop |
| rpm | revolutions per minute |
| s or sec | seconds |
| scf | standard cubic feet |
| scfm | standard cubic feet per minute |
| V | volts |